Cellular Mechanisms of Myofibroblast Differentiation and Dysfunctions in Wound Healing

Adam Christopher Midgley BSc MSc

Thesis presented for the degree of Philosophiae Doctor

2014

Institute of Molecular and Experimental Medicine (IMEM)
Cardiff Institute of Tissue Engineering and Repair (CITER)
Institute of Nephrology
School of Medicine
Cardiff University
Heath Park
Cardiff
CF14 4XN

DECLARATION

This work has not previously been accepted in substance for any degree and is not concurrently submitted in candidature for any degree.

Signed…… (candidate) Date ……

STATEMENT 1

This thesis is being submitted in partial fulfilment of the requirements for the degree of ……(insert MCh, MD, MPhil, PhD etc., as appropriate)

Signed…… (candidate) Date ……

STATEMENT 2

This thesis is the result of my own independent work/investigation, except where otherwise stated.

Other sources are acknowledged by explicit references.

Signed…… (candidate) Date ……

STATEMENT 3

I hereby give consent for my thesis, if accepted, to be available for photocopying and for inter-library loan, and for the title and summary to be made available to outside organisations.

Signed…… (candidate) Date ……

STATEMENT 4: PREVIOUSLY APPROVED BAR ON ACCESS

I hereby give consent for my thesis, if accepted, to be available for photocopying and for inter-library loans **after expiry of a bar on access previously approved by the Graduate Development Committee.**

Signed…… (candidate) Date ……

Dedication

To my family, friends, and all those closest to me – this thesis is dedicated to you, your unrelenting support, and irreplaceable friendship. Thank you.

Acknowledgements

Predominantly, I'd like to express my appreciation and thanks to my two supervisors, Dr. Robert (Bob) Steadman and Professor Aled Phillips. Bob has kept me encouraged, and full of enthusiasm since day one, I am indebted to his supervision and support. If the project ever went down speed bump riddled paths, Aled would be there to rein it in and set it back onto smoother ground. I'm inspired by, and extremely grateful to have worked with, both.

Of course, everyone at the Institute of Nephrology deserves a mention and have each helped me in their own way. Many thanks to Dr. Donald Fraser, Dr. Tim Bowen and Dr. Soma Meran for vital advice and welcomed guidance. The excellent scientists: Dr. Rob Jenkins and Dr. John Martin, both have been invaluable for their knowledge, experimental expertise, and mentorship. Everyone based in the study office has provided me with ideas and advice, great memories, intelligent conversation, and witty banter! Many thanks to those brilliant people; Tanya Bodenham, Cristina Beltrami, Melisa Lopez-Anton, Emma Woods, Dr. Chris Carrington, Dr. Alexa Wonnacott, Dr. Kate Simpson, Chantal Colman, and Dr. Usman Khalid. I should probably thank you all for encouraging me to go running, the motivation to race has certainly kept me in (some sort of) shape! A massive thank you to Dr. Ruth MacKenzie, Cheryl Ward, and Kim Abberley – the assistance and support of whom, definitely keeps things running smoothly at the Institute.

Over the past few years I have met many different people and have expanded my network of contacts. I am grateful to have met them all: students I've taught, past members of the Institute, and the experts across Cardiff University whom have taught me new techniques and dispensed their wisdom.

The project itself was made possible thanks to the funding from AgeUK and Research Into Ageing – it was a pleasure to have met everyone at the annual conferences, and fascinating to learn about the extent of the scope of research that these organisations fund, they truly make a difference in advancing scientific and clinical pursuits for improving quality of life.

Finally, my family and friends for their physical and psychological support, and for all the good times we have shared and will share in the future.

Thesis Summary

In wound healing and tissue repair, the presence of α-smooth muscle actin (α-SMA) containing myofibroblasts leads to wound closure and collagen-rich scar formation. This thesis investigated mechanisms of transforming growth factor-β1 (TGF-β1)-mediated differentiation and the dysfunctions involved in age-associated loss of differentiation. The loss of epidermal growth factor receptor (EGFR) and hyaluronan (HA) production, and diminished interaction of HA with its receptor CD44 (compromising its function) were the principal contributors to aged fibroblast resistance to differentiation.

In response to TGF-β1, CD44 relocated to EGFR held in cholesterol-rich membrane-bound lipid rafts. This was HA-dependent, as hyaluronidase or 4-methylumbelliferone treatments restricted CD44 motility and prevented CD44-EGFR co-localisation. Additionally the intracellular signalling cascade was found to be a sequential phosphorylation of extracellular signal regulated kinase 1 & 2 followed by Ca^{2+}/calmodulin kinase II. The activation of both proteins was required for differentiation.

Elevated microRNA-7 (miR-7) expression was found in aged fibroblasts. Overexpressing miR-7 in young fibroblasts attenuated the expression of EGFR and inhibited differentiation. When miR-7 was inhibited, EGFR and hyaluronan synthase 2 expression, CD44 membrane motility, and TGF-β1-mediated differentiation in aged fibroblasts were restored. Activation of EGFR drove miR-7 promoter activity and expression in a JAK/STAT1 dependent manner. Treatments of aged fibroblasts with 17β-estradiol (E2) resulted in decreased miR-7 expression and, when TGF-β1 was added, restored the α-SMA-positive phenotype. E2 treatments had no impact on STAT1 phosphorylation; leading to the hypothesis that E2 regulation of inflammatory mediators may be involved.

The data demonstrated different points of intervention for the promotion or prevention of TGF-β1-regulated myofibroblast differentiation. The interactions between HA-CD44 and EGFR were crucial elements in the differentiation process and the importance of miR-7 was apparent. The mechanisms shown here may have direct implications for modifying the wound healing response, particularly for developing therapeutic strategies to improve healing in the elderly.

Publications and Presentations Arising From This Thesis

Publications

Midgley A.C., Rogers M., Hallett M.B., Clayton A., Bowen T., Phillips A.O., Steadman R., (2013). TGF-β1-stimulated fibroblast to myofibroblast differentiation is mediated by HA-facilitated EGFR and CD44 co-localisation in lipid rafts. J Biol Chem 288(21):14824-38.

Midgley A.C., Bowen T., Phillips A.O., Steadman R., (2013). MicroRNA-7 inhibition rescues age-associated loss of EGFR and HA-dependent differentiation in fibroblasts. Aging Cell, DOI: 10.1111/acel.12167 [In Press].

Presentations

Midgley A., Phillips A.O., Steadman R., Epidermal Growth Factor Receptor and Hyaluronan Receptor CD44 are Co-localised to Myofibroblast Membrane Lipid Rafts. 1st Inaugural South West Regional Regenerative Medicine Meeting, Bristol, UK, 2011 (Poster).

Midgley A., Phillips A.O., Steadman R., Epidermal Growth Factor Receptor and Hyaluronan Receptor CD44 Co-localise in Membrane Lipid Rafts to Promote Myofibroblast Differentiation. Research Into Ageing Grantholder's Conference, Nottingham, UK, 2011 (Poster).

Midgley A., Phillips A.O., Steadman R., Epidermal Growth Factor Receptor and Hyaluronan Receptor CD44 Co-localise in Membrane Lipid Rafts to Promote Myofibroblast Differentiation. 26th Annual Life Sciences Postgraduate Research Day, Cardiff, UK, 2011 (Poster).

Midgley A., Phillips A.O., Steadman R., The Cellular Mechanisms of Myofibroblast Induced Fibrosis. European Renal Cell Study Group, Arnhem, NL, 2012 (Oral) (Prize Awarded).

Midgley A., Phillips A.O., Steadman R., TGF-β1-Stimulated Fibroblast to Myofibroblast Differentiation is Mediated by Hyaluronan Facilitated EGFR and CD44 Co-localisation in Lipid Rafts. 2nd Inaugural South West Regional Regenerative Medicine Meeting, Bristol, UK, 2012 (Poster).

Midgley A., Phillips A.O., Steadman R., TGF-β1-Stimulated Fibroblast to Myofibroblast Differentiation is Mediated by Hyaluronan Facilitated EGFR and CD44 Co-localisation in Lipid Rafts. Research Into Ageing 1st International Grantholder's Conference, Lancaster, UK, 2012 (Poster).

Midgley A., Phillips A.O., Steadman R., TGF-β1-Stimulated Fibroblast to Myofibroblast Differentiation is Mediated by Hyaluronan Facilitated EGFR and CD44 Co-localisation in Lipid Rafts. 27th Annual Life Sciences Postgraduate Research Day, Cardiff, UK, 2012 (Poster) (Commended).

Midgley A., Bowen T., Phillips A.O., Steadman R., Age-associated Loss of Fibroblast Differentiation is Rescued Through MicroRNA-7 Inhibition and Restoration of EGFR and HAS2. Tissue and Cell Engineering Society, Cardiff, 2013 (Poster) (Prize Awarded).

Contents

Glossary of Abbreviations

4MU	4-methylumbelliferone
α-SMA	α-Smooth muscle actin
ADAM	A disintegrin and metalloproteinase
ANOVA	Analysis of variance
bFGF	Basic-fibroblast growth factor
BM-derived	Bone marrow-derived
BMP-7	Bone morphogenic protein-7
BSA	Bovine serum albumin
CAGE	Cap analysis gene expression
CaMKII	Ca^{2+}/calmodulin kinase II
Cav-1	Caveolin-1
CD44E	CD44 epithelial isoform
CD44s	CD44 standard isoform
CD44v	CD44 variant isoform
cDNA	Complementary DNA
CFU-Fs	Colony-forming unit-fibroblasts
CSGAGs	Chondroitin sulphate glycosaminoglycans
CTGF	Connective tissue growth factor
CTX-B	Cholera toxin subunit-B
CXCR4	C-X-C chemokine receptor type 4
dCT	Difference in cycle threshold
DMEM	Dulbecco's modified eagle medium
DMSO	Dimethyl sulphoxide
DNA	Deoxyribonucleic acid
dNTPs	Deoxyribonucleotide triphosphates
E2	17-β estradiol
ECL	Enhanced chemiluminescence
ECM	Extracellular matrix
EDA-FN	Extra domain-A-fibronectin
EDTA	Ethylenediamine tetraacetic acid
EEA1	Early endosome antigen 1
EGF	Epidermal growth factor
EGFR	Epidermal growth factor receptor
EMT	Epithelial to mesenchymal transition
ERα	Estrogen receptor α
ERβ	Estrogen receptor β
ERK1/2	Extracellular signal-regulated kinase (MAPK)
FAK	Focal adhesion kinase
FAs	Focal adhesions
FCS	Foetal calf serum
FGF	Fibroblast growth factor
FI	Fluorescent intensity
FITC	Fluorescein isothiocyanate
FRAP	Fluorescent recovery after photobleaching

GAGs	Glycosaminoglycans
GAPDH	Glyceraldehyde 3-phosphate dehydrogenase
GFP	Green fluorescent protein
GTPase	Guanosine triphosphatase
H3K4me3	Trimethylation of Lysine-4 of histone-3
H3K9/14Ac	Acetylation of Lysine-9/14 of histone-3
HA	Hyaluronan / Hyaluronic acid
HAS	Hyaluronan synthase
HGF	Hepatocyte growth factor
HRP	Horseradish peroxidase
HS	Heparin sulphate
HB-EGF	Heparan-bound epidermal growth factor
HSCs	Hepatic stellate cells
HSGAGs	Heparan sulphate glycosaminoglycans
HYAL	Hyaluronoglucosaminidase
IαI	Inter-α-trypsin inhibitor
ICA	Intensity correlation analysis
ICAM-1	Intercellular adhesion molecule-1
ICQ	Intensity correlation quotient
IFNγ	Interferon γ
IgG	Immunoglobulin G
IL	Interleukin-1
IL-1β	Interleukin-1β
IL-6	Interleukin-6
IPF	Idiopathic pulmonary fibrosis
ISGF3G	Interferon-stimulated transcription factor 3-γ
ISRE	Interferon-stimulated response element
JAK	Janus kinase
kDa	Kilodalton
KS	Keratan sulphate
LAP	Latency associated peptide
LNA	Locked nucleic acid
mAb	Monoclonal antibody
MAPK	Mitogen activated protein kinase
MβCD	Methyl-β-cyclodextrin
MCP-1	Monocyte chemotactic protein-1
MDC	Metalloproteinase-like disintegrin-like cysteine-rich
MF	Mobile fraction
MIP-1α	Macrophage inflammatory protein-1α
miR	MicroRNA
miR-16	MicroRNA-16
miR-7	MicroRNA-7
miR-RT	MicroRNA reverse transcription
MMPs	Matrix metalloproteinases
mRNA	Messenger RNA
MSCs	Mesenchymal stem cells

mTOR	Mammalian/mechanistic target of rapamycin
pAb	Polyclonal antibody
PAI-1	Plasminogen activator inhibitor-1
PBS	Phosphate buffered saline
PDGF	Platlet derived growth factor
PDL	Population doubling level
PE-R	Phycoerythrin-red
PGs	Proteoglycans
PI3K	Phosphoinositide 3-kinase
PKC	Protein kinase C
Pol. III	Polymerase III
pre-miR	Precursory microRNA
pri-miR	Primary transcript of microRNA
PSE	Proximal sequence element
PTC	Proximal tubular cells
RIPA	Radio-immunoprecipitation assay
RISC	RNA-induced silencing complex
RNA	Ribosomal nucleic acid
RNase	Ribonuclease
ROS	Reactive oxygen species
Rr	Pearson's correlation coefficient
rRNA	Ribosomal RNA
RT-PCR	Reverse transcription polymerase chain reaction
RT-QPCR	Real time quantitative polymerase chain reaction
s.e.m.	Standard error of mean
SDS-PAGE	Sodium dodecyl sulphate polyacrylamide gel electrophoresis
siCD44	siRNA targeting CD44
siHAS2	siRNA targeting HAS2
siRNA	Small interfering RNA
SMCs	Smooth muscle cells
STAT	Signal transducer and activator of transcription
TF	Transcription factor
TGF-α	Transforming growth factor-α
TGF-β	Transforming growth factor-β
TGF-β1	Transforming growth factor-β1
TGF-βR	Transforming growth factor-β receptor
TIMPs	Tissue inhibitors of metalloproteinases
TLR4	Toll like receptor 4
TNF-α	Tumour necrosis factor-α
TRITC	Tetramethylrhodamine isothiocyanate
TSG-6	TNF-stimulated gene-6
TSS	Transcription start site
UTR	Untranslated region
VEGF	Vascular endothelial growth factor
VSMCs	Vascular smooth muscle cells
vWF	Von Willebrand Factor

Chapter 1

General Introduction

1.1 Wound Healing Overview

Wound healing is a natural and complex process in which tissue repairs itself after injury or trauma. In the context of skin, normally cellular shedding from the epidermis exists in steady-state equilibrium with the proliferation of the dermis, in order to form and maintain a protective barrier against the external environment. When the protective barrier is damaged the process of wound healing is immediately set in motion. Following injury and a breach in tissue structure, a series of intricate cellular and biochemical events take place in an orchestrated cascade to repair the damage and work towards restoration of tissue function. The classic model of wound healing can be divided into four sequential, yet overlapping, phases: inflammation, proliferation, contraction and maturation/remodelling.

The rate at which a wound heals is influenced by many factors which alter the condition of the wound environment, including moisture, the presence of foreign bodies or bacterial infection [7], the levels of hormones, cytokines, and glucocorticoids present in the blood and surrounding tissue [8-10]. The initial stages of wound healing, which begin immediately following injury, involve cascading molecular and cellular events leading to haemostasis, clot formation and production of an early, provisional fibrin-based extracellular matrix (ECM) providing structural support for cellular adhesion and proliferation [11]. Subsequently, multiple cell types work together to mount an inflammatory response, synthesise granulation tissue, restore the epithelial layer and contract the wound. The late stages include collagen realignment and tissue remodelling, leading to recovery of tissue function [12-14].

1.1.1 Inflammation

Inflammation consists of the clotting cascade, vasoconstriction and vasodilation, and the influx of immune cells into the wound area. Shortly after injury, platelets aggregate at the site of trauma to form a fibrin clot, which acts to control haemostasis [11, 15-17]. Formation of

the clot signals that the inflammatory phase has been initiated. Bacteria and debris are phagocytosed and removed by macrophages attracted and activated by various chemokines and cytokines. Growth factors are released and maintained that later promote the proliferative phase, the production of ECM, and wound contraction; notably, vascular endothelial growth factor (VEGF), platelet-derived growth factor (PDGF), epidermal growth factor (EGF), interleukin-1-β (IL-1β), and transforming growth factor-β (TGF-β) [10, 16].

The clotting cascade begins with coagulation; when tissue is first wounded, collagen binds to the plasma glycoprotein Von Willebrand factor (vWF) as it becomes exposed to the bloodstream due to endothelial cell damage. Activated platelets are attracted and attach to collagen-vWF to begin thrombus (clot) formation. First forming a mass, the platelets then begin to secrete inflammatory factors (IL-1β, interleukin-6 (IL-6), and macrophage inflammatory protein-1α (MIP-1α)) and clotting factors (including Factors V and VII). Blood plasma proteins, such as Factors X and V, and thrombin, lead to the conversion of fibrinogen into fibrin. Fibrin cross-links with fibronectin to form a clot that prevents excessive protein and blood loss. The fibrin-fibronectin plug becomes the main structural support during the early stages of wound healing. Various cell types utilise it for adherence and migratory purposes [18-20]. Platelets and monocytes arriving at the wound site also adhere to the fibrin-fibronectin clot and continue to secrete ECM proteins, chemokines and growth factors [21, 22]. These growth factors (VEGF, PDGF, epidermal growth factor (EGF), TGF-β, IL-1β) help to stimulate surrounding cells, inducing proliferation and phenotypic changes.

Immediately after blood vessel and endothelial cell rupture, vasoconstriction - the constriction of adjacent blood vessels - occurs to staunch further blood loss. Damaged cell membranes release thromboxanes causing blood vessel constriction, assisting in the aggregation of platelets and promoting the coagulation cascade [17, 23]. Shortly after

vasoconstriction, vasodilation and the widening of blood vessels caused by the release of histamine from platelets, helps to increase the flow of plasma proteins and increase the number of cells that can access the wound site [23].

Within an hour of the initial wounding, neutrophils arrive at the wound site, attracted by fibronectin and various chemokines secreted by platelets and the surrounding tissue. Neutrophils phagocytose debris and bacteria, secrete proteases that break down damaged tissue, and release free radicals to help further eliminate bacteria [24]. Helper T-cells also infiltrate the wound site, secreting cytokines to increase inflammation and the activity of macrophages [25]. Macrophages are essential for wound healing, their main role is to phagocytose bacteria and cell debris, and to release proteases to debride damaged tissue [25]. The growth factors secreted by macrophages attract cells involved in the proliferation and angiogenesis stages of healing to the area [24]. Macrophage secretions also stimulate cells that cause reepithelialisation, the creation of granulation tissue, and the production of new ECM [24, 26]. It is widely accepted that the ability of the macrophage to secrete these activating factors means that they are large contributors to promoting the next phase of the wound healing process and therefore prolonged macrophage presence at the wound site may be beneficial.

However, *in vitro* evidence has suggested that the presence of macrophages may in fact delay wound contraction and thus the timely disappearance of macrophages from the wound may be essential for later phases to occur [27]. Inflammation is a necessary part of healing, however, it can lead to tissue damage if it lasts too long [28]. The presence of foreign bodies can extend the inflammatory phase for too long, leading to a chronic wound. Thus the reduction of inflammation is frequently a goal in therapeutic settings. As inflammation declines, numbers of neutrophils and macrophages are reduced at the wound site. These

changes indicate that the inflammatory phase is ending and the proliferative phase is underway.

1.1.2 Proliferation

Angiogenesis, collagen deposition, granulation tissue formation, and the beginning of re-epithelialisation characterise the proliferative phase. In angiogenesis, vascular endothelial cells form new blood vessels. In fibroplasias and granulation tissue formation, fibroblasts grow and form a new, provisional ECM by secreting collagen and fibronectin. Concurrently, re-epithelialisation of the epidermis occurs, in which epithelial cells proliferate and migrate across the wound bed, providing cover and protection for the new tissue. Approximately 48 to 72 hours after the initial wounding, fibroblasts begin to enter the wound site, marking the onset of the proliferative phase before the inflammatory phase has ended [15, 16, 29]. As in the other phases of wound healing, there are partial overlaps between phases.

Angiogenesis occurs in parallel with fibroblast proliferation, when endothelial cells migrate to the area of the wound. As the activity of fibroblasts and epithelial cells requires oxygen and nutrients, angiogenesis is imperative for other stages in wound healing, such as epidermal and fibroblast migration and proliferation [30], which in turn help to maintain neovascularisation [31].

Endothelial cells from uninjured tissue move into the wound site to establish new blood vessels. Endothelial cells are attracted to the wound area by fibronectin and angiogenic factors released by other cells: angiogenin, fibroblast growth factor (FGF), and TGF-β [17, 30, 32]. Secreted collagenases and plasminogen activators degrade the platelet-fibrin-fibronectin clot, releasing growth factors (VEGF, PDGF, TGF-β, etc.) from the degranulating platelets. Matrix metalloproteinases (MMPs) digest the cell basement membrane and ECM to allow cell migration, proliferation and angiogenesis [33, 34]. Once the wound site obtains

adequate perfusion, the migration and proliferation of endothelial cells in and around the wound site gradually reduces [16, 24].

Fibroplasia and granulation tissue formation is simultaneous with angiogenesis; fibroblasts begin accumulating in the wound site as the inflammatory phase is ending. Within the first two or three days post-injury, fibroblasts mainly migrate to and proliferate with in the wound site; the origins of these fibroblasts are thought to be from the adjacent uninjured cutaneous tissue. About one week post-wounding, fibroblasts are the most abundant cell type in the wound [20, 23]. Recent evidence suggests that blood-borne circulating cell precursors known as fibrocytes or epithelial differentiated cells may contribute to the fibroblast population [35-37]. Initially fibroblasts utilise the fibrin cross-linking fibers to migrate across the wound, subsequently adhering to fibronectin [18, 20]. Fibroblasts then deposit further ECM proteins into the wound bed; and later collagen, promoting adhesion and migration [38]. Granulation tissue consists of new blood vessels, fibroblasts, inflammatory cells, endothelial cells, myofibroblasts, and the components of a new provisional ECM [39, 40]. The new ECM consists of components including: fibronectin, hyaluronan (HA), collagen, glycosaminoglycans (GAGs), elastin, glycoproteins, and proteoglycans (PGs) [41, 42]. Later, this provisional matrix is replaced with an ECM that more closely resembles that found in non-injured tissue [12, 16, 41, 42]. Fibroblasts also secrete growth factors that encourage proliferation and attract epithelial cells to the wound site. Hypoxia also contributes to fibroblast proliferation and secretion of growth factors, although failure of angiogenesis and too little oxygen will inhibit their normal growth and result in unbalanced deposition of ECM components; leading to excessive scarring.

Fibroblasts have the important duty of collagen production [12, 15]. Collagen deposition increases the strength of the wound, replacing the fibrin-fibronectin clot. Collagen provides extra resistance to future injury and allows cells involved in inflammation, angiogenesis and

connective tissue construction to attach, grow and differentiate on the collagen matrix [43, 44]. Fibroblast deposition of type III collagen and fibronectin are the predominating tensile substances until the later phase of maturation, in which they are replaced by type I collagen fibres, which have greater tensile strength [45, 46]. Granulation gradually ceases and fibroblast numbers are reduced in the wound once the ECM has been produced. Fibroblasts undergo apoptosis, converting granulation tissue from an environment rich in cells to one that consists mainly of collagen [46]. This signals the onset of the later maturation phase.

1.1.3 Contraction

In contraction, the wound is made smaller by the action of myofibroblasts, which establish a grip on the wound edges and contract themselves using a mechanism similar to that in smooth muscle cells. Contraction is a key phase of wound healing; however, if contraction continues for too long, it can lead to disfigurement and loss of tissue function [47]. Thus, there is a great interest in understanding the biology of wound contraction [27, 48]. Contraction begins with fibroblast activity, but is more effectively completed when fibroblasts have differentiated into myofibroblasts. Myofibroblasts are responsible for contraction as they contain the same type of actin found in smooth muscle cells (α-smooth muscle actin; α-SMA) [49, 50]. Myofibroblasts are attracted by fibronectin and growth factors as they migrate over fibrin-fibronectin and the provisional ECM in order to reach the wound edges [51]. They form connections and anchor to the ECM at the wound edges, to each other, and to desmosomes along the wound edge. In addition, at an adhesion called the fibronexus, actin in the myofibroblast is linked across the cell membrane to proteins and GAGs in the extracellular matrix, including fibronectin, collagen and HA [52]. Since myofibroblasts form many adhesions, which allow them to pull the ECM when they contract, they are effective at reducing the wound size. As the actin within myofibroblasts contracts,

the wound edges are pulled together. Fibroblasts continue to support by laying down collagen to reinforce the wound as the myofibroblasts contract [16, 23]. The contraction stage ends as myofibroblasts stop contracting and begin to undergo apoptosis [47]. The breakdown of the provisional matrix leads to a decrease in HA and an increase in chondroitin sulphate GAGs, which gradually triggers fibroblasts and myofibroblasts to stop migrating and proliferating [53]. These events signal full progression into the maturation stage of wound healing.

1.1.4 Maturation and Remodelling

In the maturation and remodelling phase, collagen is realigned and any remaining redundant cells are removed by apoptosis. The primary step in wound maturation is the completion of re-epithelialisation, which starts during the latter stages of granulation tissue formation. The granulation tissue allows epithelial cells to migrate across the wound surface and form a barrier between the wound and the external environment [14-16]. Basal keratinocytes from the wound edges migrate (without first proliferating) across the granulation tissue-filled wound [41, 42]. Migration of keratinocytes over the wound site is stimulated by the lack of contact inhibition and the presence of nitric oxide [54]. Like fibroblasts, migrating keratinocytes use the fibrin-fibronectin clot that was deposited during inflammation as an attachment site [39, 41, 42]. As keratinocytes migrate, they must dissolve the clot, debris, and parts of the ECM in order to progress. This is achievable through the production of MMPs [55]. They also secrete plasminogen activator, which converts plasminogen into plasmin to dissolve the surrounding matrix and debris [56]. The growth factors released, stimulated by integrins and MMPs, cause cells to proliferate at the wound edges. Keratinocytes themselves also produce and secrete growth factors and basement membrane proteins, which aid in epithelialisation and in other phases of healing [57]. Keratinocytes continue migrating across the wound bed from either side until the wound has become reepithelialised. When they have finished migrating, the keratinocytes secrete the proteins that form the new basement

membrane and they revert to their static form through reversal of morphological changes they underwent to begin migration [16, 41, 57].

When the levels of collagen production and degradation reach equilibrium, the maturation phase of tissue repair is said to have begun. During maturation, type III collagen is replaced by type I collagen and disorganised collagen fibres are rearranged, cross-linked, and aligned along tension lines [45, 46]. The maturation phase can last for up to a year or even longer, depending on wound type [15, 16]. As the phase progresses, the tensile strength of the wound increases, with the strength approaching 50% that of normal tissue by three months after injury and ultimately becoming as much as 80% as strong as normal tissue [23].

Although the division of wound healing into phases is a useful construct, this model employs considerable overlapping among individual phases. Recently, a complementary model has been described, such that the many elements of wound healing are more-clearly delineated. In this new model, cutaneous wound healing may be described in terms of an ‘early phase’ and a ‘cellular phase.’ This description renders less overlapping of the many elements involved. In the early phase, haemostasis is accomplished and cytokines are released, initiating the inflammation process. In the cellular phase, an inflammatory response is mounted, the dermis is repopulated, wound coverage is achieved (re-epithelialisation) and a scar is formed. The importance of this new model becomes more apparent through its utility in the fields of regenerative medicine and tissue engineering [58].

1.2 Cellular Components of Wound Healing

The process of wound healing involves a wide range of cell types. However, in fibrotic disease, progressive tissue fibrosis and chronic non-healing wounds, the fibroblast and its differentiated form, the myofibroblast, play pivotal roles in the pathological outcome. These

cells contribute to the speed and efficiency of normal wound healing, the extent of scar tissue formation, and wound contraction, closure and resolution.

1.2.1 Fibroblasts

A fibroblast is a type of cell that occupies the majority of connective tissue space in most animal species. This cell provides the structural framework of tissues through the synthesis of ECM proteins (e.g. collagens, GAGs and PGs) and biochemical mediators (e.g. growth factors and proteases). Fibroblasts play a critical role in the synthesis, degradation, and remodelling of the ECM; the normal functioning of these processes is necessary for efficient wound healing. Fibroblasts are derived from the primitive mesenchyme, and therefore similarly to other connective tissue cells, express the intermediate filament protein and marker of mesodermal origin; vimentin [59, 60].

Regarding the origin of tissue fibroblasts, *in vitro* evidence for a bone marrow origin was first presented 4 decades ago [61]; colonies consisting of fibroblasts were identified through the culturing of bone marrow cells. These fibroblast colony forming units (CFU-Fs) were discovered to form fibroblast populations in a number of tissues, including bone marrow, spleen, thymus, lymph node, and peritoneal and pleural fluids. An alternative concept to the bone marrow mesenchymal stem cell (MSCs) origin of fibroblasts is the model of epithelial-mesenchymal transition (EMT); the generation of fibroblasts from epithelium [62]. EMT is thought to be a fundamental mechanism in many embryonic and developmental processes. Epithelial cells detach from surrounding cells and following a sequence of growth factor or sensory stimulations develop into mesenchymal cells. Evidence for both mechanisms of fibroblast generation has been well documented. Hepatic stellate cells, pericryptal myofibroblasts in the intestine and colon, myofibroblasts in wounded skin, and fibroblasts in pulmonary fibrosis, were found to all be derived from bone marrow [63-65]. In contrast,

fibroblasts and myofibroblasts isolated from kidney and peritoneal tissue have been identified as originating from epithelial cell sources [62, 65, 66].

The characterisation of fibroblasts relies primarily on morphological, proliferative and phenotypical characteristics. Morphologically fibroblasts are flat, elongated, narrow and spindle-shaped cells, with multiple processes originating from the cell body. Although there has been much examination of the fibroblast phenotype in various organs, no exclusively expressed marker proteins have been identified [67]. This may contribute to the fibroblast's inconspicuous persistence and presence in tissues, which could potentially result in complications such as fibrotic diseases.

The locomotion of fibroblasts involves structural membrane extensions called filopodia and lamellipodia. Where these extensions meet the surface for adherence, firm and stable focal adhesions (FAs) assemble [68]. The machinery that powers cell migration and acts as anchor points for FAs is built from the actin cytoskeleton, the largest cell organelle. Radially oriented actin filament bundles are present at the leading edge of the migrating cell. Axial bundles, called stress fibers, underlie the cell body. In addition, a network of smaller individual actin filaments fills the rest of the cell [68].

The large actin filament structure that makes up the cell cytoskeleton is able to control the shape of the fibroblast and provides a framework that supports the plasma membrane. The actin cytoskeleton can alter cell morphology through assembly or disassembly of varying lengths of actin filaments. In migratory cells, the cytoskeleton must assemble rapidly and does not always have the chance to form highly ordered structures. This allows cells, such as the fibroblast, to tailor the actin framework to perform various tasks involving motion of the entire cell or sub-cellular parts [68].

The richest area of actin filaments in a cell lies in the cortex, a narrow zone just beneath the plasma membrane. In this region, most actin filaments are arranged into a network that excludes most organelles from the cortical cytoplasm [68]. In fibroblasts, the cortical cytoskeleton of actin filaments is part of a three-dimensional network that fills the cytosol and anchors the cell to the substratum, through which sensory information, such as mechanical stress of tension, can be mechanotransduced from the adhesive surface into the cytoplasm via FA anchor points [68-70]. Mechanical stress or force-induced deformations in the surrounding ECM can lead to a cellular response, causing the production and release of excess cytokines resulting in the cell altering its morphology [71] to adapt to the conditions it is presented with. Upregulation of fibrogenic genes, involved in fibroblast to myofibroblast differentiation and excessive ECM protein production, are common responses when mechanical stress is introduced to the ECM scaffold on which fibroblasts are adhered [68, 71].

Other than mechanotransduction, the major regulator of fibroblast-myofibroblast differentiation is the stimulation of cell surface receptors (Alk5/transforming growth factor-β receptor I; TGF-βRI) by transforming growth factor-β1 (TGF-β1) [50, 72-74]. In wound healing, degranulating platelets release TGF-β1 into the surrounding tissue [14, 25, 75]. When fibroblasts become activated by TGF-β1, profibrogenic genes are activated for transcription. The fibroblast then begins to produce excessive amounts of ECM proteins, proteinases, and cytoskeletal proteins [12, 41, 46, 48]. The definitive marker of fibroblast activation is the upregulation of α-SMA [49, 74], the upregulation of which grants the cell contractile abilities and is attributed to the term ‘myofibroblast’ used to describe the activated fibroblast as an intermediate cell between a resting fibroblast and smooth muscle cells [49, 74, 76].

The successful generation of ECM components by fibroblasts is pivotal to the successful resolution and closure of a wound. The ECM proteins facilitate the attachment and migration

of many cell types and provide wound site integrity [77-79]. The production of ECM proteins is rapid as the fibroblasts proliferate to fill the wound space, creating a network within granulation tissue [76, 80]. Specific ECM components, such as fibronectin, collagens, and HA, help support the adhesion and integrity of the tissue. Fibronectin links cell surface integrins and cell adhesion molecules to collagens and ECM proteins, aiding attachment and migration of cells [81, 82]. Collagen provides tensile strength whilst HA confers tissue resistance to compression, by providing a turgor swelling force due to the binding of water molecules [83, 84].

Secretion of growth factors (bFGF, VEGF, TGF-α, TGF-β) self-stimulate fibroblasts and activate surrounding cells, signalling changes in gene expression and maintaining cell viability in the surrounding tissue, whilst attracting new cells to the wound space [16, 57, 80]. Morphological changes and phenotypic transitions occur within fibroblasts, influenced by a number of factors (as described above) and resulting in the reorganisation of the actin cytoskeleton into large bundles of fibers (parallel, terminating at the cell periphery) and an increase in the number and thickness of stress fibers [49, 74]. Changes in the distribution and composition of stress fibers can influence further alterations in FAs; the formation of super-mature FAs. These include the proteins: tensin, α-SMA, extra domain-A fibronectin (EDA-FN), and α5β1 integrin [50, 85]. TGF-β1 stimulation in particular has been described as being the major cytokine responsible for driving the differentiation of fibroblasts into an activated and contractile phenotype: myofibroblasts [22, 74]. Myofibroblasts, in addition to β- and γ-actin, express α-actin [49], synthesise excessive ECM proteins (fibronectin, collagens, elastin, GAGs, and PGs), and release remodelling enzymes (MMPs, tissue inhibitors of metalloproteinases; TIMPs) and growth factors (MCP-1, IL-1, IL-6, IL-8, TGF-β1, HGF, EGF), to increase the stability of the granulation tissue and activate the surrounding cells [16, 17, 39, 57].

The gain of contractile properties and the increased production of FA sites on the myofibroblast cell membrane grant the ability of the cell to anchor the wound edge and begin wound contraction i.e. pulling the wound closed [48, 74]. Decreasing the surface area of the wound exposed to the external environment allows the migration of keratinocytes to cover the wound for re-epithelialisation. Myofibroblasts are important cell types in the process of wound healing, however, in fibrotic disease, myofibroblasts are thought to promote the pathological process by contributing to the increased synthesis and contraction of ECM characteristic of the disorders [72, 73, 86, 87].

1.2.2 Myofibroblasts

Myofibroblasts are specialised cells within the body that aid in normal wound healing processes by exerting large contractile forces on their microenvironment with the primary job of assisting in the closure of wounds. The myofibroblast could be considered the primordial emergency cell contributing to ECM production and tissue remodelling. However, aberrant and chronic activation of myofibroblasts can lead to the development of pathological conditions including fibrosis, disease progression and the induction of the tumour stroma reaction lending to cancer invasiveness [72, 86, 88].

Myofibroblasts are important contributors to scar tissue formation and wound closure [49, 52, 74], but can severely impair organ function when they persist within the wound due to excessive contraction and ECM protein secretion. Examples of conditions central to myofibroblast activity include hypertrophic scars, scleroderma and Dupuytren's disease, as well as in heart and kidney fibrosis [76, 89, 90]. Moreover, myofibroblasts present in the stroma reaction of epithelial tumours may promote the progression of cancer invasion [88].

Morphologically, myofibroblasts have characteristic flattened, irregular shapes that are large in comparison to most cells; and well-developed cell-matrix interactions and intracellular gap

junctions [89, 91]. They can be distinguished by their increased expression of EDA-FN and in some cases, their ability to express other markers of smooth muscle cells, such as desmin, calponin and smooth muscle myosin [92].

Myofibroblast differentiation is a complex phenomenon that follows a distinct pattern and effect in many different organs. To therapeutically counteract the organ dysfunction caused by myofibroblasts, it is crucial to understand the cellular events and signalling pathways regulating their commencement and function, to distinguish the mechanisms common to all situations from those specific to a given organ or disease.

The origins of myofibroblasts may be very heterogeneous (Figure 1.1). However, the transformation of cells into a myofibroblastic phenotype follows a well-documented cascade of events, resulting in upregulation of pro-fibrotic genes and proteins. The fibroblast is a definitive source of myofibroblasts [48-50, 74, 93]. Following tissue injury, activated fibroblasts migrate into the damaged tissue and to upregulate the synthesis of ECM components, triggered by locally released cytokines from inflammatory or resident cells. Another important stimulus for this phenotypic activation is the change of the mechanical microenvironment. Fibroblasts in intact tissue are stress-shielded by the crosslinked ECM, however in injured tissue, the continuous remodelling of the wound environment and ECM results in a loss of protective function against stress [29, 47, 68, 71]. In response to mechanical challenge, fibroblasts acquire contractile stress fibers that are first composed of cytoplasmic actins, hallmarking the “protomyofibroblast.” Stress fibres can connect to fibrous ECM proteins at sites of integrin-containing, cell-matrix junctions and adherens junctions [47, 52]. These features where identified when cultured fibroblasts were mechanically activated by the rigid plastic substrate, whereas stress fibers did not form on soft culture substrate hydrogels or in compliant collagen gels [47, 89].

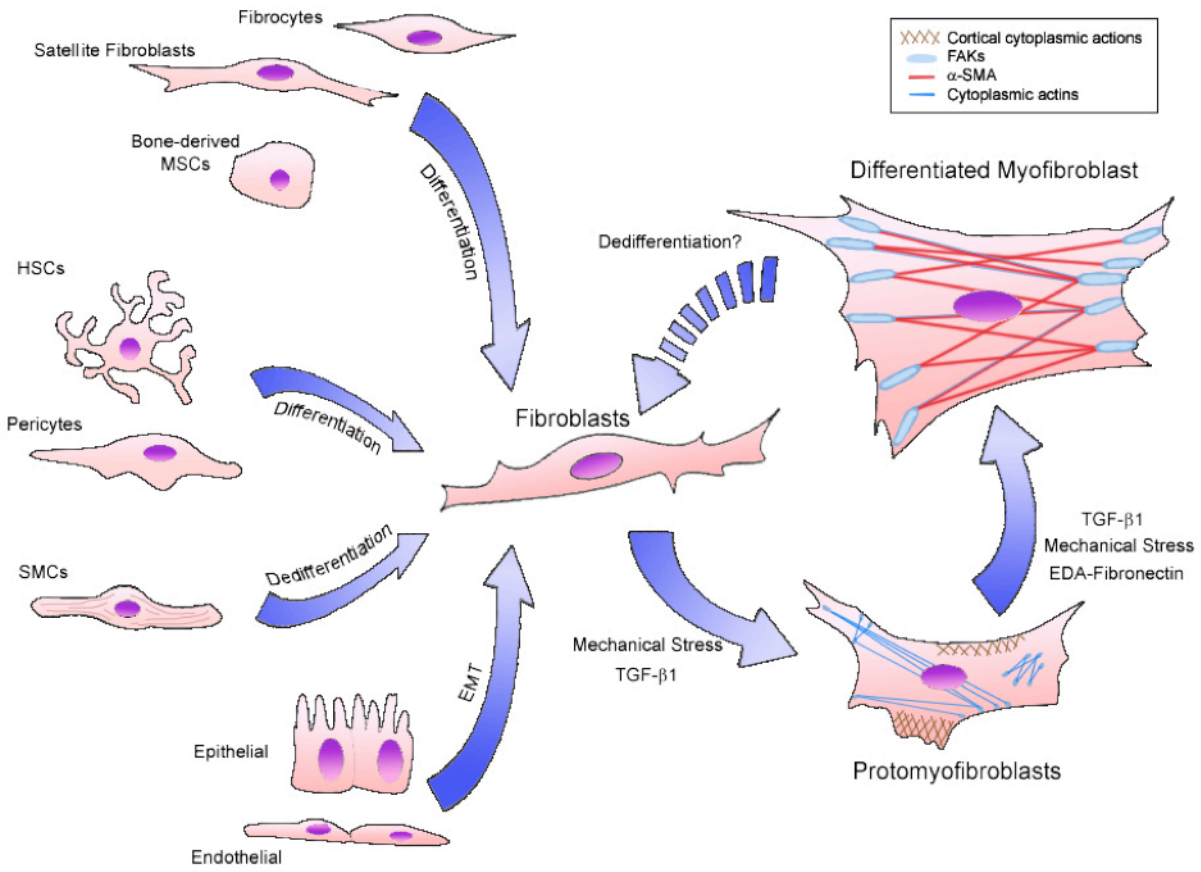

Figure 1.1. Various sources of fibroblasts derive from processes such as differentiation (circulating blood fibrocytes, satellite fibroblasts, bone-derived mesenchymal stem cell (MSCs), hepatic stellate cells (HSCs), and kidney pericytes), dedifferentiation of smooth muscle cells (SMCs), and epithelial to mesenchymal transition (EMT) of epithelial and endothelial cells. With the stimuli of mechanical stress or TGF-β1, fibroblasts transform into protomyofibroblasts (morphological change, focal adhesion kinase (FAK) and cortical and cytoplasmic actin generation). Further mechanical stress, TGF-β1, and EDA-fibronectin stimuli can drive protomyofibroblasts toward the terminally differentiated myofibroblasts (expressing α-smooth muscle actin; α-SMA, and large FAKs). Whether or not fully differentiated myofibroblasts can dedifferentiate into fibroblasts is not known. Image was adapted from Hinz et al. 2007 [127], and Tomasek et al. 2002 [130].

In culture, the 'protomyofibroblast' is a stable phenotype [89], representing an intermediate step in most *in vivo* conditions that is proceeding towards the fully differentiated myofibroblast. Expression of α-SMA in stress fibres of myofibroblasts confers at least a twofold stronger contractile activity, compared with α-SMA-negative fibroblasts in culture [94]. At least three local events have been shown to generate α-SMA-positive differentiated myofibroblasts: the accumulation of biologically active TGF-β1, the presence of specialised ECM proteins (e.g. EDA-FN) and high extracellular mechanical stress [40, 47, 50, 74].

Mechanoperception is mediated through specialised cell-matrix junctions, the fibronexus *in vivo*, or supermature FAs *in vitro* [47, 52]. With regards to myofibroblast contractile ability, ECM rigidity determines the size of the cell's anchors, which in turn limits the level of tension generated within stress fibres [47, 89]. Only when substrate stiffness permits formation of supermature FAs (8-30μm long) and the generation of approximately fourfold greater stress compared with usual FAs (2-6μm long), does α-SMA become incorporated into pre-existing cytoplasmic β-actin stress fibers [95]. Hence, α-SMA can be considered a mechanosensitive protein. The myofibroblast cytoskeleton can function as a mechanotransducer, translating mechanical tension into biochemical signals involving tyrosine phosphatase and kinase pathways – as shown in force-induced p38 phosphorylation [96, 97]. Cell adhesion signalling via FA kinase (FAK) represents another pathway through which biochemical and biophysical ECM signals as well as soluble growth factor signals are integrated [69, 70]. The main myofibroblast inducer, TGF-β1, up-regulates expression of fibronectin and its integrin receptors in fibroblasts; this is linked to activation of FAK [98-100]. At the end of tissue repair, the reconstructed ECM resumes control over the mechanical load, this stress release is a powerful promoter of myofibroblast apoptosis *in vivo* [101]. Therefore, interrupting the mechanical feedback loop of myofibroblast contraction and gradually increasing ECM tension at the level of stress perception (i.e. cell-ECM contacts) is one promising strategy to prevent tissue contracture.

To prevent myofibroblast formation in the first place and help prevent the subsequent propagation of fibrosis, knowledge of the origins of myofibroblasts is required. Depending on the type of tissue to be remodelled, myofibroblast precursor cells are recruited from different sources; among these, locally residing fibroblasts seem to be the most common [102]. Other mesenchymal cells sources suggested include pericytes and SMCs [103]; SMCs have been suggested to contribute to fibrosis in scleroderma [104]. In addition, bone marrow (BM)-

derived circulating cells known as fibrocytes (cells expressing CD45, CD34, collagen I and CXCR4 markers) [105] have been suggested as a myofibroblast source during wound healing of skin, liver, lungs, and kidneys [106-109]. Finally, myofibroblasts have been shown to derive from EMT [110, 111]. Damaged organs seem to recruit myofibroblast precursors from several sources to satisfy the temporarily high demand of tissue remodelling cells; however the two latter cases have been subject to much debate.

Examples of mixed fibroblast and myofibroblast origins can be seen in early studies in lung injury and fibrosis. The perivascular and peribronchiolar adventitial fibroblasts have been suggested as precursors [112], whereas other studies have demonstrated that BM-derived fibrocyte progenitors gave rise to lung fibroblasts [63, 113]. However, BM-derived fibroblasts to myofibroblast differentiation could not be demonstrated in some studies [63, 114]. Thus, the evidence for BM-derived myofibroblasts in organ fibrosis is controversial, suggesting instead that there are potentially multiple origins. Additional possibilities include EMT; as has been demonstrated in studies *in vitro* and *in vivo* [110, 111, 115, 116]. However, again there are studies where EMT could not be demonstrated [117]. Therefore the relative contribution by these different potential sources of myofibroblasts requires further study.

The fate of recruited and activated myofibroblasts in injured tissues may ultimately determine whether normal healing occurs or progression to end-stage fibrosis ensues. Resolution with myofibroblast apoptosis would terminate progression, however, persistence of TGF-β1 expression, ECM deposition and accumulative stress-induced FAK, promote pro-survival and anti-apoptotic phenotypes [118-120]. Selective susceptibility of myofibroblasts to nitric oxide-induced apoptosis has been reported *in vitro* [120]. Therefore, a reduction in growth factor expression, increased ECM turnover and nitric oxide generation may set the stage for triggering myofibroblast apoptosis during resolution of tissue repair and remodelling. Future

studies into the physiological triggers for myofibroblast apoptosis could potentially lead to identification of novel, more effective therapies for chronic fibrotic diseases.

In the liver, the most accepted myofibroblast progenitors are hepatic stellate cells (HSCs), which become activated and differentiate into myofibroblasts, in response to various factors including reactive oxygen species (ROS) and growth factors [121, 122]. Concomitantly, HSCs up-regulate the expression of key inflammatory receptors, including intercellular adhesion molecule-1 (ICAM-1) and toll-like receptor 4 (TLR4) [123]. Paracrine and autocrine-produced TGF-β1 is the most potent pro-fibrogenic cytokine capable of activating HSCs [124]. In addition to HSCs, other resident cells of organs have recently been described as sources of myofibroblasts: portal fibroblasts, parenchymal cells and second-layer fibroblasts in liver fibrosis [122, 125, 126]; and pericytes in kidney fibrosis [127].

Dedifferentiation of SMCs and the questions of their potential myofibroblastic nature have been raised [103]. Presently, it is well accepted that myofibroblasts share with SMCs the expression of α-SMA, which is considered an early differentiation marker of vascular SMCs [128]. Unlike SMCs, however, myofibroblasts express relatively low amounts of smooth muscle myosin heavy chain and do not express smoothelin, a late marker of SMC differentiation [129]. SMC-to-myofibroblast transition becomes relevant in view of recent work indicating that during fibrotic situations, myofibroblasts develop the capacity of producing a long-lasting tension essentially regulated at the level of Rho/Rho kinase-mediated inhibition of myosin light chain phosphatase, compared with the usual contraction-relaxation activity depending on Ca^{2+}-induced phosphorylation of myosin light chain kinase taking place in SMCs [130].

Less is known about the role of myofibroblasts during embryological development. Early embryological and scarless wound healing indicates an absence of myofibroblasts. The

transition from scarless tissue repair to healing with scar formation that occurs during late gestation has been shown to be accompanied by an increased presence of myofibroblasts in the wound environment [131].

Although it seems that TGF-β1 together with mechanical stress play important roles in fibrosis development, much less is known about factors inhibiting myofibroblast activities and the control of fibrosis. Interferon-γ (IFNγ), bone morphogenic protein-7 (BMP-7), and hepatocyte growth factor (HGF) have been shown to exert such actions, possibly through anti-TGF-β1 effects [115, 132-134]. The α-SMA N-terminal peptide AcEEED reduces force generation by the myofibroblast and exerts an anti-fibrotic activity through its capacity to displace α-SMA from stress fibers [135]. Utilisation of these tools and the discovery of novel methods to control myofibroblast function will be useful for studying mechanisms regulating tissue remodelling and the invalidating diseases characterised by the development of fibrosis. Delineating the mechanisms of myofibroblast activation seems indispensable for designing rational therapeutic strategies to inhibit the fibrogenic processes of organ fibrosis or to promote effective wound healing in chronic non-healing wounds.

1.3 Wound Repair Versus Regeneration

An injury is the disturbance of morphology and functionality of a tissue. When injury and the associated inflammatory response have resulted in the death (necrosis) of specialised cells and damage to the surrounding ECM, steps must be taken to replace dead cells with healthy tissue. This response is referred to as healing and comprises two processes. The first involves the replacement of specialised tissue by proliferation of surviving cells or infiltration of precursor cells. The second response is a reparative process and entails a connective tissue synthesis response characterised by the formation of granulation tissue and its subsequent maturation into fibrous tissue. The relative roles of both processes vary depending on tissue

type, with some tissues showing increased propensity to heal through either regeneration or repair.

The difference between wound repair and regeneration is subtle. Repair refers to the physiologic adaption of a tissue to injury in an attempt to restore structural continuity without regards to exact replacement of lost or damaged specialised tissue. True tissue regeneration is defined as the replacement of lost or damaged tissue with an exact copy, i.e. morphologically and functionally restored into the exact condition of the original tissue. In some instances such as with the skin, partial regeneration may be induced through the use of biodegradable (collagen-GAG) scaffolds [136, 137]. These scaffolds are structural analogues of the ECM found in uninjured dermis. In addition to providing support for fibroblast and endothelial cell attachment, biodegradable scaffolds inhibit wound contraction, thereby granting the time needed for the healing process to proceed towards a regenerative and scarless pathway. One other such method to prevent wound contraction may be in disabling myofibroblast differentiation, which has been investigated through the use of pharmaceutical agents [93, 138]. However, dermal tissue is also capable of healing with excessive and unregulated scarring, such as that found in hypertrophic and keloid scars. Injuries, such as burns, can occur over very important flexural joint surfaces, leading to contractures resulting in severe restriction of movement and functional disability. The liver best illustrates another example of partial regeneration. In experimental animal models, it was shown that when large amounts of the liver were removed surgically, the remaining parenchyma regenerated to a normal and sufficient mass, structure, and function [139]. In acute liver injury, there may be mass necrosis of hepatocytes, however, in most cases complete regeneration occurs with almost full restoration of liver architecture [139-141]. In contrast, repeated insults in chronic liver injury lessen the regenerative ability of hepatocytes, resulting in the substantial accumulation of fibrous tissue constituting hepatic cirrhosis [134, 142, 143].

In tissues such as lung, kidney and cardiac tissue, the healing process is dominated by a connective tissue response. Production of fibrous tissue leads to pathological scarring of the implicated organ or tissue. This is a sub-optimal response, although healing may have restored structural defect of the tissue, it has impaired function as specialised cells have been replaced with dense ECM and fibrous tissue. The outcome is also affected by the nature, severity, and duration of the injury. Interestingly, fundamental conditions required for tissue regeneration often oppose conditions that favour efficient wound repair; including the inhibition of platelet activity, low levels of inflammatory cells and their mediators (IL-6, IL-8), and prevention of wound contraction. These conditions are present in the early-gestation foetus, which heals skin wounds without scar formation [144]. This observation was confirmed in both animal models and human foetuses [145, 146]. Additionally, foetal fibroblasts display unique patterns of intracellular signalling and demonstrate differences in the composition and generation of ECM components, such as collagens and hyaluronan [147, 148]. The only tissue in adults that demonstrates what can be definitively classed as regeneration is the oral mucosa. In addition to healing in a scarless manner, oral mucosal wounds heal rapidly, comparable to foetal wounds [149, 150]. However, whilst regeneration of all tissues would be preferable, the absent conditions listed above that may contribute toward regeneration, are very important in the wound healing process and the prevention of the formation of chronic wounds.

1.3.1 Chronic Disease in Wound Healing

As the average lifespan of the general population increases, the problems of some diseases are shifting toward association with the ageing population - from communicable disease to chronic diseases. Chronic conditions have become the leaders in world mortality rates; with approximately 63% of all deaths attributed to chronic conditions; and only 25% of those deaths being in individuals under the age of 60 [151]. Chronic diseases have become the

major contributor to disability, affecting the quality of life of sufferers and their relatives. Another problem arises in the costs of healthcare; the annual cost for overall management of chronic wounds in the US alone is greater than $20 billion, not including the additional costs to society in terms of lost workdays or productivity [152]. Prevalent forms of chronic disease associated with wound healing include chronic non-healing wounds and progressive fibrosis; both pose a challenge for therapeutic treatments.

1.3.2 Non-healing Chronic Wounds

Chronic wounding occurs when the phases of wound healing, which normally progress in a predictable and timely manner, become dysfunctional. Healing may progress inappropriately to a chronic wound such as venous or diabetic ulcers, peripheral arterial disease, or pressure ulcers. Since wound healing consists of complex phases with several steps to each, it is susceptible to interruption or failure of scar formation, leading to the formation of non-healing chronic wounds. Factors which may contribute to this include diabetes, venous or arterial disease, old age and chronic infection [153-155].

Non-healing chronic wounds result from wound healing becoming detained in one of the earlier phases; commonly, wounds remain within the inflammatory phase for too long [23]. Since chronic wounding often lasts months or years, treatment and management of the pain associated usually takes priority over the treatment of the underlying problems [156]. The molecular causes of chronic wounds can be multiple; rapid degradation of ECM components or dysregulated collagen synthesis by fibroblasts can lead to an inadequate matrix to support angiogenesis, cell adhesion, and migration [23, 157]. The persistence of bacterial infection and the release of their toxins and proteases can severely inhibit the activity and function of surrounding cells and proteins [154]. Suppression of the immune system can result in chronic infection and insufficient removal of cellular debris leading to cytotoxicity [25, 158]. Loss of

cellular function through ageing or senescence can play a large role in the inability of wounds to heal [13]. In the context of ageing, the skin of older people is more easily damaged due to weakened matrix integrity. Aged cells become slow to proliferate and have increased resistance to growth factor stimulation; this in turn leads to insufficient gene upregulation and protein synthesis [159, 160]. The advances in treating age-related chronic wounds are lagging behind other fields of disease research, one of the contributing factors to this is that animal models of age-related chronic wounding are difficult to generate. Animal models usually have life spans that are too short to develop chronic disease naturally [161]. Therefore, cell-based models of age-related wound healing are a useful method for studying the underlying cellular mechanisms and dysfunction that arise from chronic non-healing wounds. An inadequate supply of growth factors can also contribute to chronic wounding. Growth factors are essential for timely wound healing; an inadequate supply can lead to dysfunctions in fibroblast ECM secretion and differentiation as well as keratinocyte re-epithelisation [80]. Diabetic ulcers are often attributed to the inability of fibroblasts to respond to growth factors, due to the conditions of the wound environment [162]. The longer the chronic wound persists, the more generations of fibroblasts are cycled through, thus senescence and debilitated growth factor responses become a more evident and real problem. Replacement of the inadequate supply of growth factors may help speed the healing process, through increased stimulation of the cells in the surrounding healthy tissue, e.g. fibroblasts [13, 57, 80, 153].

1.3.3 Fibrosis

Progressive tissue fibrosis arises due to failure of the normal wound healing response to terminate and resolve [46, 50]. Progressive and excessive fibrosis is a key component of numerous chronic diseases and can result in an array of clinical conditions. Fibrosis is defined as the formation of excess fibrous connective tissue and its contraction in an organ or

tissue, during a reparative or reactive process. Scarring is confluent fibrosis that obliterates the architecture and heavily impairs functionality of the underlying organ or tissue.

Less severe fibrosis forms cosmetically undesirable or disfiguring scars. However, more severe cases of fibrotic disease lead to tissue destruction, dysfunction and/or death from organ failure. Many clinical conditions are a result of progressive fibrosis, including pulmonary fibrosis, chronic kidney disease, liver cirrhosis, biliary atresia, retinopathy, macular degeneration, congestive cardiac failure, scleroderma, hypertrophic or pathological scarring, such as a keloid scars [85-87, 163-167]. In progressive organ fibrosis, the initial injury is responded to as normal with the activation of resident cells and the inflammatory cytokine release. The infiltrating inflammatory cells produce ROS, and fibrogenic and inflammatory cytokines [168, 169]. Fibroblasts migrate into the wound site, proliferate and undergo phenotypic activation. A large amount of ECM is synthesised and deposited by the activated fibroblasts and myofibroblasts. Resolution of the granulation tissue and the wound, however, does not occur. Therefore, fibroblasts persistently produce excessive ECM leading to qualitative changes in its composition, i.e. more collagen type III and I. Generation of components that would not usually be found in the wound space are also produced, including splice variants of fibronectin and laminin [170]. Over time, the disorganised ECM becomes cross-linked and resistant to degradation, cell penetration, and may prevent growth factors functioning correctly [88]. It is not completely clear as to why the usually self-limiting normal healing response fails and instead the progressive fibrotic response is presented.

Fibrosis can be driven by many fibrogenic factors; their release contributes to the progressive nature of fibrosis. These include TGF-β1, connective tissue growth factor (CTGF), VEGF, angiotensin II, FGF, PDGF and IL-1 [76, 171-176]. TGF-β1 is the most widely implicated in tissue fibrosis and its aberrant expression is a universal finding in virtually every type of

fibrotic disease [50, 72, 73, 171, 177]. However, TGF-β1 has many functions; it is able to stimulate its own production, stimulate differentiation, and ECM synthesis and deposition. Understanding the cellular factors involved in ECM generation and turnover is crucial in determining the pathogenic mechanisms underlying progressive fibrosis and may provide novel insights into developing new therapeutic strategies.

1.4 Transforming Growth Factor-β1

Cytokines and growth factors are important regulators of wound resolution and tissue repair. The cytokine that is central to both initiation and termination of tissue repair is TGF-β. In mammals, TGF-β exists in three isoforms with almost identical biological properties and targets. Encoded by different genes, the three isoforms: TGF-β1, TGF-β2, and TGF-β3, activate similar receptors and intracellular signalling pathways [178-180]. Although important for successful wound healing, persistent expression of TGF-β1 can promote the development of tissue fibrosis and progression. TGF-β1 is the isoform most extensively studied and has the highest expression in fibrosis, correlating with the severity of progressive fibrosis [178].

TGF-β1, a member of the transforming growth factor-β super-family is a secreted protein that performs many cellular functions, including the control of cell growth, proliferation and differentiation. In humans, the TGF-β1 gene encodes TGF-β1. Dysregulation of TGF-β1 activation and signalling may result in apoptosis [181]. Many cells synthesise TGF-β1 and have specific receptors on their cell surface for this peptide. TGF-β1 was first identified in human platelets as a protein with a molecular mass of 25 kilodaltons (kDa), and an important role in wound healing. It was later characterised as a large protein, synthesised as an inactive 390 amino acid precursor that is secreted as a large latent complex, covalently bound with latency associated peptide (LAP); and stored in an inactive form in the matrix. The inactive

form of TGF-β1 is proteolytically processed to produce a bio-active mature peptide of 112 amino acids [179].

TGF-β binds to at least three membrane receptor proteins, TGF-β receptor (TGF-βR) I, II, and III. They can exist in homo- or heterodimers. The type I and II receptors are transmembrane serine-threonine kinases that typically interact with one another to form a heterodimer in order to facilitate signalling [182]. The type III receptor, also known as betaglycan, is a membrane anchored PG with no signalling structure but can act to present TGF-β to the other receptors on the cell surface [183]. When TGF-β interacts with these receptors, a cascade of intracellular signalling results in altered gene transcription profiles. The principal route of activation is through the Smad signal transduction pathway [184]. However, TGF-β has also been described to recruit alternative pathways including the epidermal growth factor receptor (EGFR), mitogen-activated protein kinase 1 and 2 (MAPK; ERK1/2), Rho-GTPase, protein kinase B, and the Akt/mTOR pathway [160, 185-187].

TGF-β1 shows a diverse range of different activities on different types of cell depending on biological context, or cells at different developmental stages. Many cells secrete TGF-β1 including fibroblasts, myofibroblasts and most immune cells (leukocytes) [188, 189]. The TGF-β family also play important roles in controlling the immune system, the inflammatory response and foetal development [190, 191]. Specifically TGF-β1 is a known promoter of fibroblast terminal differentiation and EMT; upregulating α-SMA expression *in vitro* and *in vivo* [192]. The production and secretion of fibronectin, collagens, and matrix turnover proteins (MMPs and TIMPs) are also processes regulated by TGF-β1 signalling [193].

The traditional TGF-β signalling cascade involves the binding of TGF-β1 to TGF-βRI otherwise known as Alk5, which upon activation forms an active heterodimer with TGF-βRII [182]. The subsequent phosphorylation of targets follows a well-documented cascade event,

first through the phosphorylation of Smad2 and Smad3. When bound to co-Smad4, this Smad-signalling complex translocates to the nucleus where in it acts as a transcription regulator, binding target sites on gene promoters and either enhancing or suppressing gene transcription [184]. A classic gene target of TGF-β1 signalling includes SERPINE1, which encodes for the protein plasminogen activation inhibitor 1 (PAI-1), the expression of which is often used as a marker of TGF-β1 activity [194].

TGF-β-Smad signalling is an essential phase in the differentiation of fibroblasts to myofibroblasts. The signalling mechanism underlying the genesis of the myofibroblast is complex; with respect to the TGF-β1-Smad signalling pathway, the presence of the Smad3-binding element is important for myofibroblast differentiation and oral mucosal fibroblast proliferation [195, 196]. Despite shared expression, the regulation of the α-SMA gene in fibroblasts is more complex and in many respects different from that in SMCs [197]. In addition to transcriptional inducers, suppressors may have a higher basal activity in fibroblasts, compared to SMCs; and serve to keep the fibroblast in an undifferentiated state under normal homeostasis.

Dysregulation of TGF-β1 action has been implicated in a variety of pathological processes, including cancer and autoimmune diseases; and its involvement in progressive tissue fibrosis has been confirmed in human disease and in numerous models of animal disease [72, 73, 178, 198]. Its fibrotic actions have been attributed to its combined abilities to induce fibroblast differentiation, epithelial cell trans-differentiation and to promote accumulation of matrix proteins, including collagens, fibronectin and PGs. As discussed above, TGF-β1 also induces production of TIMPs and inhibits some MMPs and plasmin protease generation, thereby preventing matrix degradation and contributing to the fibrotic process [168]. Furthermore, it modulates expression of FA molecules that contribute to intracellular signalling,

mechanotransduction, stress generation; and facilitate cell-matrix adhesion and matrix deposition [77, 119].

Additional evidence supporting the pro-fibrotic role of TGF-β1 was shown *in vivo*, where treatment of foetal wounds with exogenous TGF-β1 promoted scarring [131, 145]. Additionally, incisional rat wounds treated with anti-TGF-β1 antibodies or anti-sense nucleotides were shown to suppress ECM synthesis and scarring [199]. However, TGF-β1 knock-out mice models have been shown to have a high rate of intra-uterine death [200], indicating the important role of TGF-β1 in development and cell survival. The few that survived to birth later died of a multi-focal inflammatory syndrome [201], signifying a TGF-β1 role in modulating immune and inflammatory cell types. Furthermore, mice heterozygous for TGF-β1 deletion, although demonstrated a normal phenotype at birth had a greatly increased frequency of carcinoma formation, when challenged with carcinogens [202]. These studies highlighted the potential challenges relating to the direct targeting of TGF-β1 in anti-fibrotic treatments. Therefore, further detailed characterisations of responses involved in the modulation of TGF-β1 actions are necessary to develop more selective, clinically appropriate, anti-fibrotic therapies.

1.5 The Extracellular Matrix

The ECM is the non-cellular, structural complex present within all mammalian tissues and organs. The ECM provides essential physical scaffolding for cellular constituents and can initiate crucial biochemical and biomechanical signals that are required for tissue morphogenesis, homeostasis, cell differentiation, migration and adhesion.

ECM components are synthesised by a variety of mesenchymal and parenchymal cells. Its extracellular distribution can be in the form of cell-associated pericellular matrices and structures that surround the periphery of cells; or in the form of a more extensive intracellular

matrix, which surrounds, connects and adheres to the connective tissue cells. The principal components that make up the ECM are collagens, elastin, structural glycoproteins, PGs and GAGs. The formation of ECM is an important event during both tissue repair and fibrosis; and an understanding of how various constituents may be involved in the regulation of cellular processes may provide valuable insights into the pathological mechanisms underlying progressive tissue disease and fibrosis. The importance of the ECM is vividly illustrated by the wide range of syndromes with varying degrees of severity that can arise from genetic abnormalities in ECM proteins [203]. Although fundamentally, the ECM is composed of water, proteins and polysaccharides, each tissue has an ECM with unique composition and topology that is generated during tissue development through a dynamic and reciprocal, biochemical and biophysical dialogue between the various cellular components (e.g. epithelial, fibroblast, adipocyte, endothelial elements); and is adapted to suit the specific cellular and protein microenvironment functionality [204].

1.5.1 ECM Turnover

The tissue remodelling enzymes, MMPs and ADAMs (a disintegrin and metalloproteinases), are endopeptidases central to the degradation and remodelling of the ECM. These proteases can also exhibit regulatory activity in cell signalling pathways, under normal conditions and in many diseases [205]. The process of connective tissue remodelling is an important mechanism contributing to tissue homeostasis and morphogenesis in development; and when in unbalance, can lead to disease states including progressive tissue fibrosis.

MMPs were discovered because of their role in amphibian metamorphosis, yet they have attracted more attention because of their roles in disease. Despite intensive scrutiny *in vitro* in cell cultures and *in vivo* in animal models, the normal physiological roles of MMPs remain elusive. Recent studies in mice and flies point to essential roles of MMPs as mediators of

change and physical adaptation in tissues, whether developmentally regulated, environmentally induced, or disease associated. An example of how MMPs contribute to disease progression is through the upregulation of MMP-2 and MMP-3. These can promote tissue fibrosis through the processing of pro-MMP-9, an enzyme involved in the activation of pro-fibrotic cytokine activity [206].

The MMPs are inhibited by specific endogenous TIMPs, which comprise a family of four protease inhibitors: TIMP1, TIMP2, TIMP3 and TIMP4. Overall, all MMPs are inhibited by TIMPs once they are activated, except the gelatinases (MMP-2 and MMP-9), which can form complexes with TIMPs [207] when the enzymes are in the latent form. However, the roles of MMP/TIMP complexes are largely unknown. TIMP activity has been implicated in promotion of tissue fibrosis through mechanisms, in response to TGF-β1-stimulated invasiveness and proliferation of pro-fibrotic cells. For example, the imbalance of TIMP-2 expression to MMP-2 and MMP-4 in the liver can lead to dysregulation of tissue turnover and progressive liver cirrhosis [208]. Therefore, TIMPs and MMPs can fine-tune the outcome of healing and fibrosis; and identification of their activation and inhibitions mechanisms could help reveal potential routes for fibrotic disease management.

The ADAM family of peptidase proteins, also known as the adamalysin family or MDC family (metalloproteinase-like, Disintegrin-like, cysteine rich) are classified as “sheddases,” because they shed extracellular portions of transmembrane proteins [209]. For example, ADAM10 can remove part of the HER2 receptor, resulting in its activation [210]. Studies in mouse models have shown that ADAM-TS1 is upregulated with collagen accumulation in myocarditis and is involved in collagen metabolism. Thus, dysregulation can lead to the development of myocardial fibrosis [211]. Development of therapeutic ADAM inhibitors could potentiate anti-fibrosis and anti-cancer therapy [34, 212].

Hyaluronidases are a family of enzymes that degrade HA. In humans, there are six associated genes, the main genes being HYAL1, HYAL2 and HYAL3 [213]. By catalysing the hydrolysis of HA, hyaluronidase lowers the viscosity of HA thereby increasing tissue permeability. Hyaluronidases are therefore implicated in bacterial pathogenesis, the spread of toxins and venoms, the acrosomal reaction/ovum fertilisation, and cancer progression [214-218]. Hyaluronidases are typically expressed alongside high expression of HA and are thought to maintain and regulate hyaluronan chain length, deposition and function.

Hyaluronidases are known to be involved in physiological and pathological processes, ranging from fertilisation to ageing. Depolymerisation of HA adversely affects the role of the ECM as a reservoir of growth factors, cytokines and various enzymes involved in signal transduction [219]. Hyaluronidase inhibitors are potent ubiquitous regulating agents that are involved in maintaining the balance between the anabolism and catabolism of HA. Hyaluronidase inhibitors can also serve as contraceptives, anti-tumour agents, and could possibly have antibacterial activities [220].

The role of hyaluronidases in cancers is controversial. Limited data support a role in metastasis, while other data support a role in tumour suppression [214]. Hyaluronidases are also thought to have a role in angiogenesis, although most hyaluronidase preparations are contaminated with large amounts of angiogeneic growth factors [215, 219]. Some bacteria, such as *Staphylococcus aureus*, *Streptococcus pyogenes* and *Clostridium perfringens*, produce hyaluronidase as a means of using HA as a carbon source. It is often speculated that *Streptococcus* and *Staphylococcus* pathogens use hyaluronidase as a virulence factor to destroy polysaccharides that hold animal cells together, making it easier for the pathogen to spread through the tissues of the host organism [216, 217], but no valid experimental data are available to support this hypothesis. In most cases of mammalian fertilisation, hyaluronidase is released by the acrosome of the sperm cell after it has reached the oocyte, digesting the

concentrated HA in the corona radiata. Once this occurs, the sperm is capable of binding with the zona pellucida; and the acrosome reaction can occur [218].

1.5.2 Collagens

The most abundant of the matrix proteins are the collagens, a large family of closely related but genetically distinct proteins. Collagens contain, at least in part, polypeptide α-chain triple helical structures. Collagens are widespread throughout the body and are important for a broad range of functions including tissue scaffolding, cell adhesion and migration, angiogenesis, tissue morphogenesis, and tissue repair. Collagen is best known as the principal tensile element of vertebrate tissues, such as tendon, cartilage, bone and skin; where it occurs in the ECM as elongated fibrils [221].

Some collagen types (e.g. I, III, and V) form fibrils by virtue of lateral cross-linking of the triple helices; and form a major proportion of the connective tissue in healing wounds. Other collagens (e.g. IV) are non-fibrillar and become components of basement membranes – for example, in the kidney glomerulus, where it contributes to functions in molecular filtration. The predominant type of collagen differs in different tissues. In those tissues exposed to shear and tensile forces, such as skin, tendons, bone, and cartilage, the predominant collagens present are types I, II, III, V and XI [222]. These collagens assemble into highly orientated aggregates. In scar tissue, the proportions of type I and III collagen are significantly increased and changes in the ratio of these collagens are thought to be involved in conferring resistance to matrix degradation in fibrous tissue [223]. The identification of transmembrane collagens on the surfaces of a variety of cells, and collagens that are precursors of bioactive peptides (BCPs) with paracrine function, has resulted in a revival of interest in collagen research.

1.5.3 Glycoproteins

Glycoproteins are high molecular weight, structurally diverse proteins, which function as matrix adhesion molecules. They include fibronectin, laminin, entactin and thrombospondin. The most abundant and best characterised is fibronectin, which exists in two forms: plasma and tissue fibronectin. It has binding sites for several other matrix proteins, such as collagens; and can also attach to cell surface integrins [20, 42]. This property allows fibronectin to act as a link between cells and the matrix. Therefore it is involved in regulating the structure of the ECM and is able to influence cellular processes, such as migration, growth and differentiation. Specifically, expression of EDA-FN is upregulated in cells treated with the pro-fibrotic cytokine, TGF-β1; and is demonstrated to be marker of myofibroblastic differentiation and necessary for the upregulation of α-SMA expression [50, 170].

1.5.4 Elastin

Elastin is a connective tissue protein that is composed of cross-linked tropoelastin molecules, producing a large, insoluble and durable protein. It confers elastic properties to connective tissues, allowing resumption of original shape following stretching or contraction. It specifically serves an important function in arteries, large blood vessels (e.g. the aorta) and is also important in the structure and function of cartilage, ligaments, lung tissue, the bladder, and the skin [203].

1.5.5 Proteoglycans

The proteoglycan (PG) super-family contains over 30 hydrophillic, heavily glycosylated glycoproteins, that fulfil a wide variety of biological functions. PGs consist of a protein core, the variation of which is responsible for the biosynthesis of PGs with different molecular

constructions and functions [203, 224]. Attached to the protein core are one or more covalently linked GAGs, which provide unique functions to various PGs [225].

PGs act as tissue organisers, influence cell growth and the maturation of specialised tissues, play a role as biological filters, modulate growth-factor activity, regulate collagen fibrillogenesis and skin tensile strength, affect tumour cell growth and invasion; and influence corneal transparency and neurite outgrowth [225]. Additional roles derived from studies of mutant animals, indicate that certain PGs have functions essential to life whereas others might be redundant [226, 227]. PGs vary in molecular organisation of the protein core, the utilisation of protein modules, and transcriptional control. PGs have been grouped into distinct gene families and sub-families offering a simplified nomenclature, based on their protein core design [228]. The structure-function relationship of some paradigmatic PGs has been discussed in depth and novel aspects of their biology have been examined [225, 228].

1.5.6 Glycosaminoglycans

Glycosaminoglycans (GAGs), otherwise known as mucopolysaccharides, are long unbranched polysaccharides consisting of repeating disaccharide units. The repeating unit (with exception for keratin sulphate), consists of an amino sugar (*N*-acetylglucosamine or *N*-acetylgalactosamine) along with uronic acid (glucuronic acid or iduronic acid) or galactose [224]. GAGs have high degrees of heterogeneity with regards to molecular weight, disaccharide construction, and sulphation, due to the fact that GAG synthesis, unlike proteins or nucleic acids, is not template driven but dynamically modulated by processing enzymes [224].

Based on core disaccharide structures, GAGs are classified into four groups. Heparin/heparan sulphate (HSGAGs) and chondroitin/dermatan sulphate (CSGAGs) are synthesised in the Golgi apparatus, where protein cores made in the rough endoplasmic reticulum are post-

translationally modified with *O*- and *N*-linked glycosylations by glycosyltransferases, forming a proteoglycan [229]. Unlike HSGAGs and CSGAGs, the third class - keratan sulphate (KSGAGs), are driven towards biosynthesis through particular protein sequence motifs. The fourth class of GAG, HA, is not synthesised by the Golgi, but instead by three transmembrane synthases that exist in three isoforms: HA synthase (HAS) 1, 2, and 3. These synthases immediately secrete the dynamically elongated disaccharide chain [229].

The functions of GAGs vary greatly. For example, highly negatively charged endogenous heparin functions to electrostatically retain and store histamine within mast cells [230]. Heparan sulphate (HS) has numerous biological activities and functions, including cell adhesion, growth and proliferation, developmental processes, cell binding of lipoprotein lipase and other proteins, angiogenesis, viral invasion, and tumour metastasis [231].

CSGAGs interact with heparin binding proteins, specifically dermatan sulphate interacts with FGF-2 and FGF-7, implicating it in cellular proliferation and wound repair [232], while interactions with HGF activate the c-Met signalling pathway and generating an anti-fibrotic effect. Other biological functions include inhibition of axonal growth and regeneration in central nervous system development, brain development, neuritogenic activity, and pathogen infection [231, 232].

One of the main functions of KSGAGs is the maintenance of tissue hydration [233]. In disease states such as macular corneal dystrophy, in which keratan sulphate (KS) levels are altered, loss of hydration within the corneal stroma is believed to be the cause of corneal haze, supporting the hypothesis that corneal transparency is dependent on KS levels [234]. KSGAGs are found in many other tissues, where they regulate macrophage adhesion, contain neurite growth, regulate embryo implantation, and affect the motility of endothelial cells

[233]. In summary, KS plays an anti-adhesive role, which suggests very important functions in cell motility and attachment.

1.6 Hyaluronan

The fourth class of GAG, HA, is a major component of synovial tissues and fluid, and soft tissue ECMs; endowing their environments with remarkable properties [235]. For example, solutions of HA are known to be viscoelastic; viscosity changes with sheer stress levels. At low sheer stress, HA viscosity can be 10^6 times that of the solvent, while under high sheer stress, viscosity may drop by 10^3 times [236]. This property of HA in solution makes it ideal for cartilage and joint lubrication. *In vivo*, HA has a stiff helical structural configuration that gives the molecule an overall random hydrated coil structure, which entangles with other HA molecules to form a network. HA networks retard diffusion by forming a barrier that regulates transport of substances through intercellular spaces [235]. For example, HA partitions plasma proteins between vascular and extravascular spaces; this excluded volume phenomenon affects the solubility of macromolecules in the interstitium, changing chemical equilibria, and stabilising collagen fibers [237].

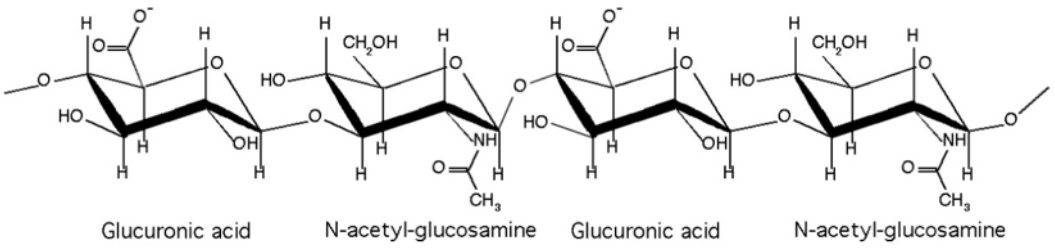

Figure 1.2. The molecular structure of HA, a polymer made of repeated sequences of the disaccharides *N*-acetylglucosamine and *D*-glucuronic acid, linked together by alternating β-1,4 and β-1,3 glycosidic bonds.

HA is a multifunctional, high molecular weight polysaccharide, classed as a non-sulphated negatively-charged GAG; and is distributed widely throughout connective tissue, epithelial and neural tissues [235]. First characterised from the vitreous of bovine eyes, its exact

chemical structure was determined in 1954 as a polymer made of repeated sequences of the disaccharides, *N*-acetylglucosamine and *D*-glucuronic acid, linked together by alternating β-1,4 and β-1,3 glycosidic bonds [235] (Figure 1.2). The number of disaccharide unit repeats varies between tissues and can approach 30,000 in some tissues, giving a molecular mass of $10x10^6$Da [238]. However, smaller HA fragments and oligosaccharides have also been described under certain physiological and pathological conditions. HA is thought to participate in many biological processes and has elevated levels during embryogenesis, cell migration, wound healing, malignant transformation, fibrosis, and tissue turnover [239, 240].

Other functions include matrix interactions with HA binding proteins (hyaladherins) such as hyaluronan binding protein (HABP), collagen VI, TNF-stimulated gene-6 protein (TSG-6), and inter-α-trypsin inhibitor (IαI) [237, 241, 242]. Cell surface interactions involving HA include its well-known coupling with CD44, which has been linked to tumour progression as well as regulation of cell interactions; and also with RHAMM (receptor for hyaluronan-mediated motility), which has been implicated in developmental processes, tumour metastasis and pathological reparative processes [240, 243]. Fibroblasts, myofibroblasts, mesothelial cells and certain types of stem cells surround themselves in a HA pericellular coat (varying in structure, size and HA content), in order to shield themselves from bacteria, red blood cells, matrix molecules, or to grant unique properties and lend to cellular adhesion and other functions [244, 245]. For example, HA helps to form the stem cell pericellular shield, protecting from the effects of growth factors. During progenitor division, the daughter cell moves outside of this pericellular shield where it can then be influenced by growth factors to further differentiate [246].

1.6.1 Hyaladherins and TSG-6

HA binding proteins or hyaladherins are proteins that bind, interact and modulate the function of HA. Several types of hyaladherins exist (Table 1.1), as either cellular receptors or extracellular hyaladherins [247, 248]; and have specific roles in cellular functions. One notable hyaladherin recently described as having a role in cellular differentiation and modulation of HA function is TSG-6, which in humans is encoded by the TNFAIP6 gene [249]. TSG-6 is a ~35kDa secreted protein containing a HA-binding LINK domain A, grouping it with the hyaladherin family of proteins [249]. The HA-binding domain is known to be involved in ECM stability and cell migration. This protein has been shown to form a stable, covalent complex with IαI; enhancing the serine protease inhibitory activity of IαI, which has importance in inflammation [249]. The expression of this gene can be induced by a number of signalling molecules, principally tumour necrosis factor-α (TNF-α) and IL-1 [250]. TSG-6 expression can also be induced by mechanical stimuli in vascular smooth muscle cells, and is found to be correlated with PG synthesis and aggregation [249].

TSG-6 interacts with a plethora of matrix-associated molecules, such as aggrecan, versican, thrombospondin-1 and -2, pentraxin-3, and fibronectin. Its role in HA-binding is important in key steps of inflammation and ovulation [247, 249]. TSG-6-mediated cross-linking of HA has been proposed as a functional mechanism (e.g. regulating leukocyte adhesion and creating HA networks). Full-length TSG-6 binds to and can cross-link HA at physiologically relevant concentrations. The co-operative binding of full-length TSG-6 arises from HA-induced protein oligomerisation, with TSG-6 oligomers acting as cross-linkers. Although the HA-binding domain of TSG-6 can bind regardless of whether the full-length protein is present, only when the LINK module and full-length TSG-6 bind and cross-link HA together can condensed and rigidified HA films form, implying that the full-length TSG-6 protein is required for assembly of functional cross-linked HA networks. Therefore, TSG-6 can be

described in whole as a potent HA cross-linking agent [251]. In the case of fibroblast differentiation, TSG-6 activity was found to be upregulated and a necessary component of TGF-β1 and HA-mediated myofibroblast generation, as small interfering RNA targeting TSG-6 abolished HA-pericellular coat formation and prevented successful myofibroblastic transformation [244, 252].

Hyaladherin	Protein Size (kDa)	Type
HABP	34	Extracellular
Aggrecan	210-250	Extracellular
Brevican	140	Extracellular
Neurocan	130	Extracellular
Versican	200-400	Extracellular
TSG-6	30-35	Extracellular
HAPLN1	40-50	Extracellular
HAPLN2/BRAL1	36	Extracellular
Iαi	225	Extracellular
CD44	80-95	Cell Surface
LYVE-1	40-60	Cell Surface
Stabilin-1	270	Cell Surface
Stabilin-2	80	Cell Surface
HYAL	45-60	Cell Surface
RHAMM	70-85	Cell Surface
CDC37	44-45	Cell Surface
CD38	120	Cell Surface

Table 1.1. Hyaladherin chart displaying well documented hyaladherins, including the size and location of each protein. Note that hyaladherins can be divided into extracellular and cell surface hyaladherins. Extracellular hyaladherins are mostly structural, binding and fortifying HA networks. Cell surface hyaladherins can act to anchor HA to the cell surface, but some can also signal through intracellular protein kinases. Chart was adapted from Day and Prestwich 2002 [241].

1.6.2 HA in Wound Healing

HA plays an important role throughout the process of wound healing. The long chain, high molecular weight HA polymers (4000–20,000kDa or 1000–5000 saccharide units) seen in wound healing create long, twisting hydrophilic chains [83]. The water attracting properties of HA grants characteristic elastic and cushioning properties, illustrated by its concentration in skin and cartilage. High concentrations of HA in this form create porous scaffolding networks, allowing for select diffusion of cells and proteins, and creating pathways for cell

migration. This is a key feature of HA, as cell migration and proliferation are essential to successful wound healing [83, 253]. Smaller molecular size HA fragments also encourage cell migration and receptor organisation and movement. These very short, low-weight (four saccharides) HA fragments are capable of inducing chemotaxis, whilst medium sized HA chains (1000–1250 saccharides) can stimulate inflammatory cytokine expression [83, 253].

As HA is required in various shapes and weights for each wound healing phase, its catabolism and synthesis are vital for normal wound healing. HA is manufactured on the cell surface by three membrane bound enzymes called HA synthases (HAS1, HAS2, HAS3) [160, 195]. While other GAGs, such as HS, are manufactured within the cell and then released by exocytosis, HAS production of HA on the outside of the cell membrane, enables it to interact readily with the extracellular environment, other cells and hyaladherins [229, 238].

The properties, catalytic rate and mode of regulation for each of the three HAS isoenzymes are different and may underlie physiologically distinct functions. Moreover, many biological and physiological roles of HA have been related to its molecular weight [238, 254]. The molecular sizes of HA synthesised by the different HAS isoforms have, therefore, also been determined. HAS1 is demonstrated to be the least active and drives the synthesis of high molecular weight HA (up to $2x10^6$Da), suggesting low constitutive levels of synthesis. HAS2 is more catalytically active and generates high molecular HA polymers of more than $2x10^6$Da in size. HAS3 is expressed late in embryonic development and in many adult tissues. It shows the highest constitutive activity of the three isoforms and drives synthesis of large amounts of lower molecular weight HA chain ($2x10^5$-$3x10^5$Da) [255]. Studies have demonstrated the importance of HAS2 in development [256], the progression of fibrosis [257], cell differentiation and proliferation [160, 195, 244, 252]. Recently, HAS2 has also been described in an anti-cancer mechanism, where exceptionally high-molecular-weight HA is synthesised in the skin of the naked mole rat, conveying resistance to tumour formation [258].

HA catabolism primarily occurs in two main ways, through hyaluronidases/HYALs and ROS [83, 220, 259]. Hyaluronidases are responsible for altering HA size for specific functions needed during each of the wound healing phases. The significance of the functions of HA polymers and their antioxidant and free-radical scavenging properties have been demonstrated with the emergence of various HA-based wound dressings [7, 44].

The cell surface interactions of HA are crucial in understanding its role in wound healing, as the size and shape of HA dictates its differing roles and interactions at each wound stage. During the inflammatory phase of wound healing, platelet synthesis of heavy molecular weight HA increases rapidly [83]. These HA fragments bind to fibrinogen to commence the clotting pathway. The large amounts of hydrophilic HA released at wounding saturates the wound site with fluid, leading to oedema of the surrounding tissue and creating a porous framework for cells to migrate to the injury site [83]. Additionally, oedema allows for the chemotaxis of inflammatory cells, which release cytokines (TNF-α, IL-1β, IL-8) triggered by the high concentrations of HA, increasing cellular recruitment. The HA-cytokine release loop continues to regulate HAS expression, although this appears to be cell type and tissue specific [253]. For example, oral and dermal fibroblasts exhibit different HAS isoform expression patterns in response to TGF-β1, with HAS2 preferentially expressed and at higher levels in dermal fibroblasts [244, 260].

Conversely, HA can also reduce and moderate the inflammatory response, through its interaction with TSG-6 [251]. TSG-6 is stimulated by inflammatory cytokines IL-1, TNF-α, and TGF-β1, causing fibroblasts and other inflammatory cells to increase expression of the TSG-6 protein [250]. Once expressed by cells, TSG-6 proteins are retained in HA-rich environments, associating with IαI and binding to high molecular weight HA polymers, which form heavy chains [261]. These heavy HA chains prevent inflammation by inhibiting

neutrophil migration and inhibition of plasmin through negative feedback loops [249, 261]. As the classic inflammatory signs recede, granulation tissue begins to form in preparation for the proliferative phase. This phase is also heavily influenced by HA's multifaceted properties. Following on from the late inflammatory phase, the proliferative phase of wound healing marks the arrival of fibroblast migration. These cells are drawn to wound tissue by small HA fragments (6–20 saccharides) and growth factors [83]. Fibroblasts synthesise collagen and GAGS (including HA), for the construction and anchoring of the newly formed ECM.

Differing HA lengths stimulate the production of specific collagen types, which can promote or inhibit scar formation. One important function that fibroblasts exert on the developing ECM is collagen synthesis, providing tensile strength to the healing wound [83]. The developing ECM is visibly identifiable as granulation tissue, with collagen and elastin providing the fibrous scaffolding. HA influx forms a cushioning gel-like structure, which upon saturation, displays elastic recoil properties similar to cartilage [235, 250]. This malleability is an important clinical feature of granulation tissue, as wound healing often occurs in areas of high movement or pressure (e.g. joints and plantar surface of feet). Without hydrophilic and porous HA networks, the macroscopic granulation tissue would not be able to hold its shape to allow for normal wound healing [83].

HA contributes to angiogenesis through short chain oligomers (6–20 molecules in length). These oligomers bind to CD44, stimulating MMPs, which break down the basement membrane of the wound allowing neovascularisation and capillary sprouting [83, 253]. The final component of the proliferative phase is re-epithelialisation. The skin contains most of the body's HA concentrated in the deeper stratum basale of the epidermis and dermis. The main cell type in the basal layer is the keratinocyte, which expresses CD44 in large amounts [262]. In the skin, HA mainly functions to hydrate and provide elasticity, but also to create the aforementioned porous structures for nutrient channelling [83].

Upon wounding, damaged keratinocytes and their HA bound matrices are ruptured, releasing HA fragments and commencing the inflammatory phase of wound healing. During re-epithelialisation, newly formed HA scaffolds promote keratinocyte migration to the wound edge and over the wound space, through interactions with CD44 displayed on the cell surface. Early studies highlighted HA presence as a requirement for effective re-epithelialisation; without its signalling and physiochemical properties, excessive scarring and delayed wound healing may occur [220, 253, 263].

Gradually, during wound resolution the wound-specific cells, structures, and HA are degraded and replaced by an avascular collagenous scar. Clinically, minimal scar tissue occurs with advanced age because of HA being primarily located in the upper dermis, as seen in foetal subjects [147, 223]. This might lead to the assumption that HA skin concentrations change at various ages. A study by Meyer and Stern in 1994 found that the polymer size and concentration of HA remains consistent throughout a lifetime. However, tissue association did change, suggesting that although the amount of HA remains the same, the amount of extractable HA changes with age because of hyaladherin binding or reorganisation [264]. This shows that while HA is present in human skin of all ages, its location and the extent of potential hyaladherins could affect its function, binding and contribution to effective wound healing or scarring.

1.6.3 HA in Fibrosis

Although HA is an essential molecule needed for efficient wound healing, it is also implicated in tissue fibrosis and its accumulation often correlates with the severity of fibrotic disease progression; and has been detected in numerous fibrotic conditions associated with organ dysfunction [257, 265, 266]. Diseases that demonstrate elevated levels of HA include:

idiopathic pulmonary fibrosis (IPF), chronic kidney disease, liver cirrhosis, liver hepatitis, scleroderma, sarcoidosis and rheumatoid arthritis, among others [73, 85, 166, 250, 257].

Simple assays for serum HA determination makes it possible to use HA as a diagnostic marker for fibrotic diseases. For example, because HA is a component of liver fibrosis and is cleared from the blood by liver endothelial cells, most investigations found increased serum levels of HA in patients with liver diseases [265, 266]. Although the pathophysiological mechanisms involved are not fully understood, an increase in HA production as well as a decrease in removal might be involved. Observed increases in HA production may be caused by the induction of cell proliferation and ECM synthesis, via excessive cytokine release. Decreases in serum HA uptake and degradation may be caused by endothelial cell injury. The measurement of serum HA levels has therefore been suggested as a method to monitor fibrotic progression in chronic liver diseases [265].

Tissue fibrosis is a major cause of morbidity and IPF is a terminal illness characterised by unremitting matrix deposition in the lung. Myofibroblasts accumulate at sites of tissue remodelling and produce ECM components, such as collagen and HA, that ultimately impair organ function. In a murine model study by Li et al. 2011, targeted overexpression of HAS2 by myofibroblasts produced severe lung fibrosis and death after bleomycin-induced injury. Fibroblasts isolated from transgenic mice overexpressing HAS2 showed a greater capacity to invade matrix. Conditional deletion of HAS2 in mesenchymal cells abrogated the invasive fibroblast phenotype, reduced myofibroblast accumulation and inhibited development of lung fibrosis. In the absence of CD44, both the invasiveness of fibroblasts and progressive fibrosis were inhibited, highlighting the dependency of IPF progression on HAS2 and CD44 expression [257]. Understanding the mechanisms leading to an invasive fibroblast phenotype could lead to novel approaches to the treatment of disorders characterised by severe tissue fibrosis.

Aberrant expression of the HAS2 gene and the increased production of HA have also been implicated in the pathology of pulmonary arterial hypertension, osteoarthritis, asthma, thyroid dysfunction, and large organ fibrosis [267]. Renal fibrosis is associated with increased cortical synthesis of HA and correlated with interstitial fibrosis *in vivo* [267]. *In vitro* data suggested that both HAS2 transcriptional induction and subsequent HAS2-driven HA synthesis may contribute to kidney fibrosis, via EMT of the renal proximal tubular epithelial cells (PTC), driven primarily by TGF-β1 [111].

In contrast, the lack of scarring in foetal skin wounds may relate to a prolonged presence of HA, increased expression of CD44, and reduced expression of hyaluronidase [144, 268]. The major differences may be in the size of HA produced, influencing its biological action, especially in angiogenesis, which is also reduced in foetal wound healing [144]. In a foetal wound study, HA and hyaluronidase activity were determined and it was found that in adult wound fluids hyaluronidase levels were higher than in foetal wound fluids [268]. The data generated by the study suggests that lower hyaluronidase levels may underlie the different pattern of HA deposition seen in foetal wounds and influence the anti-fibrotic wound healing mechanisms in foetal wound healing.

1.7 The Differentiation Mechanism

Activation of the transmembrane epidermal growth factor receptor (EGFR) has been acknowledged to occur in response to TGF-β1 stimulation of fibroblasts. It was found that the phosphorylation of EGFR was necessary for fibroblast to myofibroblast differentiation, indicating a crossover of the two signalling pathways; the TGF-β1/Smad2/3 pathway and the EGFR/ERK pathway, signalling in parallel to drive differentiation to a myofibroblastic phenotype (Figure 1.3) [195, 269]. Inhibition of either TGF-βRI or EGFR resulted in failure of differentiation, in response to TGF-β1 treatment [160]. The loss of EGFR described in

aged fibroblast cells was partly responsible for TGF-β1 resistance and failure of differentiation [160], further supporting the necessity of both pathways in myofibroblast transformation. Interestingly, HA production by HAS2, which is essential for HA pericellular coat formation, was also a required process in fibroblast differentiation [160, 252]. It was hypothesised that the HA receptor, CD44, could co-localise with and activate EGFR in response to TGF-β1, thus illustrating a mechanism whereby TGF-β1 stimulation could activate EGFR. Removal of EGF activity (upregulated by TGF-β1 in fibroblasts) using a blocking antibody did not change EGFR activation by TGF-β1 [160], suggesting an initial ligand-independent activation of EGFR by HA-CD44.

Indeed, ligand-independent activation of EGFR has been reported [270, 271]. The mechanism of HA-CD44 activation of EGFR is largely unknown. This thesis aims to investigate and detail the co-localisation of CD44 and EGFR and to further elucidate the initiation, localisation and down-stream signalling pathways that result from the interaction.

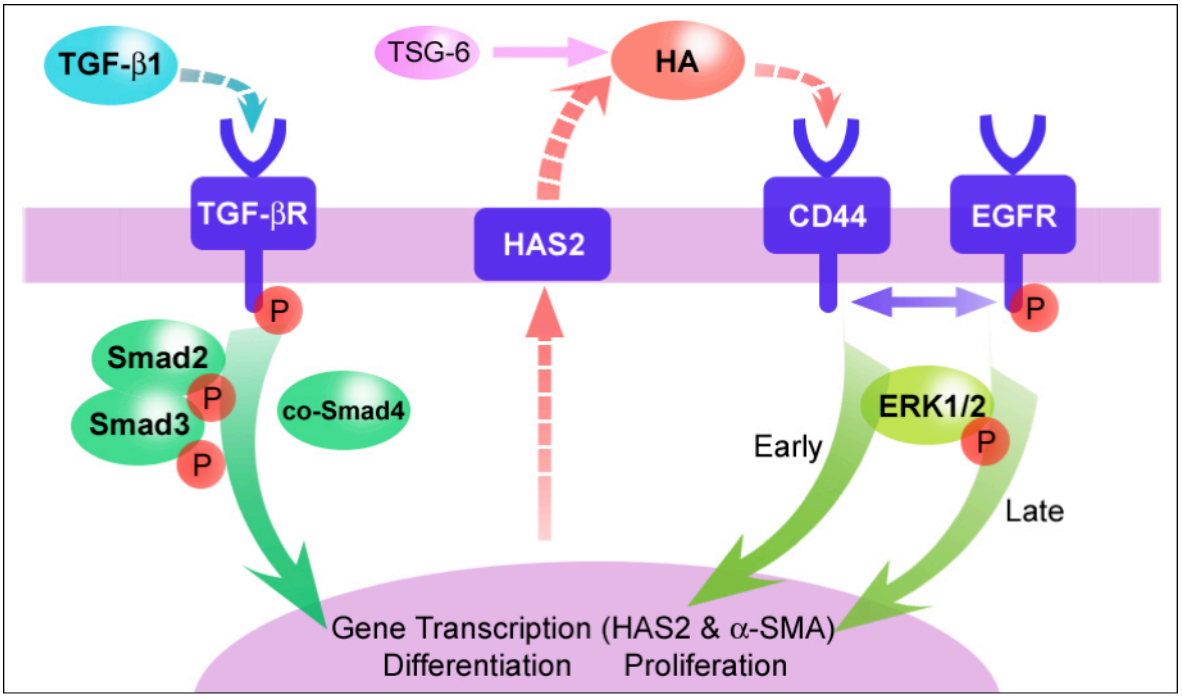

Figure 1.3. TGF-β1 stimulated and HA-mediated fibroblast to myofibroblast mechanism – when fibroblasts are stimulated by TGF-β1, TGF-βR is phosphorylated (P), signalling through Smad2/3 and co-Smad4. HA-mediated CD44/EGFR signalling is through ERK1/2. When both pathways signal in parallel the cell undergoes differentiation into a myofibroblast. Image adapted from Meran et al. 2011 [189] and Simpson et al. 2010 [79].

1.8 Project Aims and Objectives

The medical problems that stem from progressive tissue fibrosis are abundant, causing loss of organ function, tissue flexibility, or cosmetically undesirable outcomes. However, slow wound resolution, the loss of scar tissue formation and the inability to shield a wound from the external environment, can lead to chronic non-healing wounds; particularly afflicting the elderly population. The overall purpose of this thesis is to identify the mechanisms that are involved in driving fibroblast to myofibroblast differentiation; and those that are lost in aged fibroblast resistance to myofibroblast transformation. Specifically, this thesis aims to establish the role of each component of the TGF-β1 and HA-regulated pathways contributing to myofibroblast generation and fibrosis, revealing potential targets for therapeutic inhibition of scar tissue formation, but also elucidating mechanisms that could promote and restore the differentiation of aged fibroblasts and therefore, provide therapeutic benefit for chronic non-healing wounds. Through investigation of downstream signalling pathways, genetic regulation and macromolecular modulation, this thesis aims to provide potential targets for intervention.

My specific objectives were:

1. To characterise the co-localisation between EGFR and CD44, identify where in the cell that this association occurs; and also which components, growth factors, ECM proteins or receptors, are needed for co-localisation.
2. To investigate the mechanism resulting in EGFR and CD44 co-localisation, through analysis of receptor movement and how HA influences receptor association.
3. To make comparisons between young and aged fibroblasts, identify differences and pinpoint specific routes of re-establishing: a) the potential for aged fibroblasts to

differentiate into myofibroblasts; and b) targets for inhibition of myofibroblast differentiation in young fibroblasts.

4. To examine the role of genetic modulators of gene expression (e.g. microRNAs) in the age-related resistance of TGF-β1-stimulated differentiation; and how promotion of these genetic modulators are controlled.
5. To utilise potential routes for: a) the restoration of the differentiation response in aged cells through upregulation of the key differentiation components; and b) the inhibition of key regulators of differentiation in young cells, and to produce *in vitro* treatments for these purposes.

The results attained from these *in vitro* experiments could be used to identify significant points of difference between young cells, which readily differentiate into myofibroblasts, and aged cells, which resist differentiation. Those differences could reveal factors that are necessary for the initiation and progression of fibrosis or for successful wound healing; and could potentially be used in the development of therapies that target scar-free healing or the promotion of wound healing in the elderly.

Chapter 2

Materials and Methods

2.1 Materials

All general and tissue culture reagents were purchased from Sigma-Aldrich (Poole, UK), Thermo-Fisher Scientific (Roskilde, Denmark), BD Biosciences (San Jose, USA), and GIBCO/Life Technologies (Paisley, UK) unless otherwise stated. PCR and QPCR reagents and primers were purchased from Invitrogen and Applied Biosystems (Life Technologies, Paisley, UK). Cytokines used were TGF-β1, EGF and IFNγ from R&D Systems (Abingdon, UK), and 17β-estradiol (E2) from Merck Millipore (Darmstadt, Germany). Chemical treatments used were cytochalasin-B, nystatin, AG1478 and SB431542 from Merck Millipore. The sources of any other inhibitors or reagents used are described in the following sections and results chapters.

2.2 Cell Culture

Primary human lung fibroblasts (AG02262; NIA Ageing Cell Respiratory Corriel Institute, Camden, USA) were cultured in Dulbecco's Modified Eagle's Medium (DMEM) and F-12 Medium (D8062; Sigma-Aldrich), containing 2mM L-glutamine, 100 units/ml penicillin and 100μg/ml streptomycin supplemented with 10% foetal calf serum (FCS) (Biologic Industries Ltd., Cumbernauld, UK). The cells were maintained at 37°C in a humidified incubator in an atmosphere of 5% CO_2; and fresh growth medium was added to the cells every 3-4 days, until confluence. Once confluence had been attained, cells were sub-cultured. Prior to experimentation, all cells were growth-arrested in serum-free medium for 48h to allow cell-cycle synchronisation (arrest at G0). All experiments, unless otherwise stated, were performed in serum-free medium to avoid any influence of serum factors. Furthermore, all experiments were performed on approximately equivalent cell numbers.

2.2.1 Sub-culture

Once fibroblast confluence was attained, the cell populations were sub-cultures at a ratio of 1:3 and either utilised for experiments, cultured further, or cryopreserved as described below. In the case of a 75cm^2 culture flask (T-75; scale up or down as appropriate), confluent monolayers of fibroblasts were sub-cultured by treatment with 5mL 0.05% (w/v) trypsin and 0.53mM EDTA in phosphate buffered saline (PBS). The trypsin was evenly distributed over the base of the flask and incubated at 37°C for 1-3 minutes with slight agitation, or until cells became detached and appeared rounded, when examined under a light microscope. The resulting cell suspension was treated with an equal volume of FCS to neutralise the protease activity. The total volume was then transferred to a centrifuge tube and the suspension centrifuged at 1500×g for 6 minutes at room temperature. The cells were then re-suspended in 50mL medium supplemented with 10% FCS and seeded into fresh tissue culture flasks for continued growth, or seeded onto tissue culture plates for experimentation. Fibroblasts were cultured, sub-cultured and cryopreserved at various passages until senescence, at which point in time, senescent cells were no longer cultured and were discarded. Lung fibroblast senescence was determined to be at ~passage 16.

2.2.2 Cryostorage and Revival

At sub-culture, if deemed necessary, fibroblasts were harvested for cryogenic preservation. For one T-75 flask of confluent cells, following trypsin treatment and neutralisation, the cells were resuspended in a 4.5mL solution containing 10% dimethyl sulphoxide (DMSO), 10% FCS and 80% DMEM/F12 medium. 1.5mL was transferred into each of 3 cryogenic vials (Thermo-Fisher Scientific). Vials were initially placed in a -80°C freezer for 24h and then subsequently transferred to liquid nitrogen (-196°C) for long-term storage. Cryopreserved cells were revived by rapid thawing at 37°C, using a water bath. Upon complete defrosting of

contents, the cell solution from each cryogenic vial was transferred directly into a T-75 tissue culture flask, containing pre-warmed 37°C medium supplemented with 10% FCS.

2.2.3 Cell Counting and Population Doubling Level Calculations

For assessment of cell numbers, fibroblasts in culture were sub-cultured, as above, using trypsin. Upon cell resuspension in 10% FCS medium and prior to cell seeding, three 20μL volumes of cell-suspension were taken and each added to 20mL of sterile isotonic water in Coulter Counter compatible sample cups. The average cell counts of three readings were taken for each sample using a Coulter Z2 Series cell counter (Beckman Coulter Inc., Indianapolis, USA). The formulae shown below were used to calculate the total number of cells in the resuspension solution:

$$\textbf{Cells/mL} = \textbf{(Average cell number)} \times \textbf{2000}$$

$$\textbf{Total cell count} = \textbf{(Cells/mL)} \times \textbf{(Volume resuspension solution)}$$

In order to determine the PDL at the end of each passage number, the following equations were used:

$$\textbf{Total seed number [1:3 ratio sub-culture]} = \frac{\textbf{Total cell number}}{\textbf{3}}$$

$$\textbf{PDL} = 3.32 \times (\log_{10}(\textbf{Total cell count}) - \log_{10}(\textbf{Total seed number}))$$

Cumulative population doubling levels were calculated by adding the derived increase to the previous PDL. Fibroblasts were received at passage 3 and at a population doubling level (PDL) of 11.9.

2.2.4 Determination of Young and Aged Cell Groups

Using the cell counts PDL determination as described above, fibroblast growth curves were used to identify which passage numbers to assign to young and aged fibroblast groupings. Cellular senescence was found to occur at ~ passage 16, as PDL did not increase beyond the sub-culture of passage 15 fibroblasts (Figure 2.1). Using total seed number and total cell counts; a graphical representation of the fibroblast growth rate was produced (Figure 2.2). For the young fibroblast range, passages between 6 and 9 were used, as the seed number and end of passage cell counts remained approximately constant. For the aged fibroblast group, cells between passages 13 and 15 were used, as these were still pre-senescent cells capable of growth and proliferation. Note the number of days in culture needed before confluence increased two to three-fold, when compared to the young cell group. Beyond passage 16, cells became senescent and did not increase in PDL.

2.3 Cytokine Stimulations

Following growth arrest, the medium was removed and the cells washed with PBS. Stimulations were performed by incubation of fibroblasts with the desired stimuli (TGF-β1, E2, IFNγ and EGF) in serum-free medium for appropriate times and concentrations, before analysis. All cytokine treatments were determined by dose response experiments and cytotoxicity assessed by alamarBlue assay (Biosource International, Camarillo, USA). The specific details of the cell-stimulations performed for each experiment are covered in the subsequent results chapters.

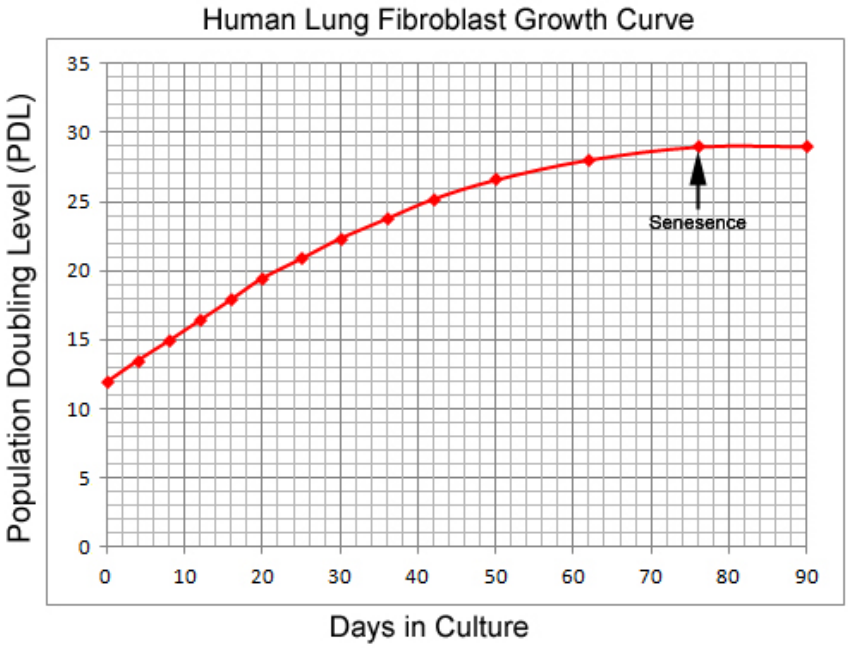

Figure 2.1. Human lung fibroblast growth curve over 90 days, the state of cellular senescence is indicated by the black arrow at approximately 76 days in culture, as the PDL did not increase after this. Red markers indicate the PDL at each passage sub-culture.

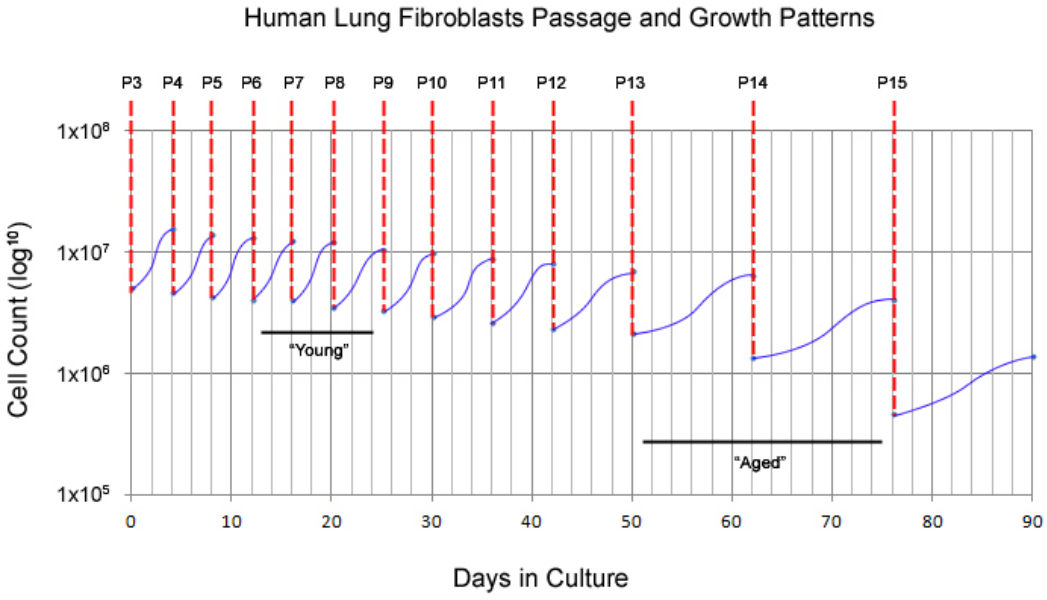

Figure 2.2. A graphical representation of human lung fibroblast growth curves detailing cell numbers (log_{10} scale) and days in culture (0-90). At each passage, total cell numbers were counted and total seed numbers were calculated. Blue curves represent the growth phase from cell seeding to sub-culture. Red dashed lines indicate passage divisions. Young and aged groupings used for experimentation are indicated on the graph.

2.4 Chemical Treatments and Cytotoxicity Testing

Cytochalasin-B and nystatin were used to breakdown the cell cytoskeleton and membrane-bound lipid rafts, respectively. Both of these mycotoxins were used to identify localisation of cell receptors, EGFR and CD44. In eukaryotic cells, cytochalasin-B acts to inhibit network formation and the polymerisation of actin filaments, nystatin acts as a cholesterol-sequestering agent, disrupting cholesterol-rich lipid rafts of the cell membrane. As these chemicals disrupt cell infrastructure and membranes, there is potential of cell death. Therefore, the cytotoxicity of cytochalasin-B and nystatin was assessed.

Cytotoxicity was assessed using the commercially available alamarBlue assay (Biosource International), which is designed to measure cell numbers and viability. The assay utilises an oxidation-reduction indicator that fluoresces in response to the reduction of growth medium resulting from cell growth and metabolism; demonstrating a linear relationship between fluorescent intensity and cell numbers and viability. Continued growth maintains a reduced environment, while inhibition of growth maintains an oxidised environment. Reduction related to growth causes the REDOX indicator to change colour; from oxidised non-fluorescent blue to reduced fluorescent red.

For this assay, following growth arrest, sub-confluent fibroblasts were incubated for 24h in serum-free medium alone or serum-free medium containing 5μM, 10μM, and 20μM of cytochalasin-B (Figure 2.3A) or 10μg/mL, 50μg/mL, and 100μg/mL of nystatin (Figure 2.3B). Then, 10% (v/v) alamarBlue was added to the medium for 1h and incubated at 37°C, 5% CO_2. Aliquots were removed from each treatment and added in 100μL triplicates to a MicroFluor-2 Black, 96-well plate (Thermo-Fisher Scientific). Subsequently, fluorescence was measured in a FluorStar Optima plate reader (BMG Labtech, Ortenburg, Germany), at an excitation wavelength of 540nm and an emission wavelength of 590nm.

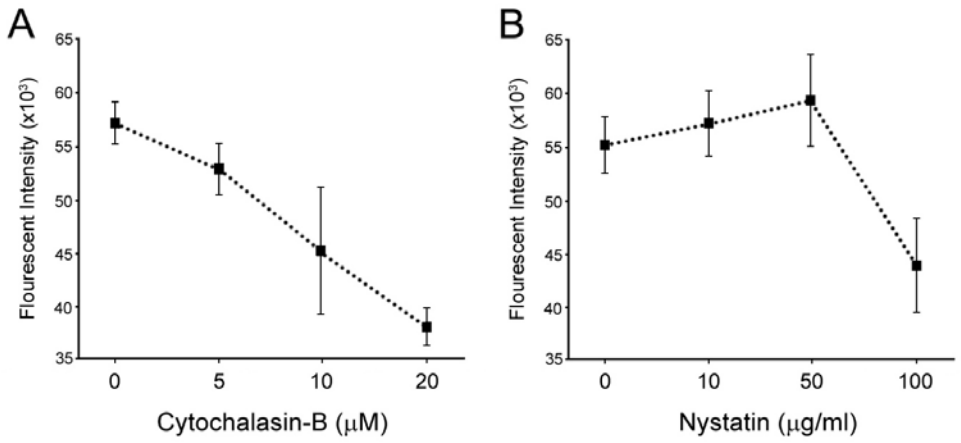

Figure 2.3. Cytotoxcity tests using the alamarBlue assay for cell viability and numbers. **A.** Fluorescent intensity is shown for each of the given concentrations of cytochalasin-B; 5μM was determined to be suitable for cell treatments. **B.** Fluorescent intensity is shown for each of the given concentrations of nystatin; 50μg/ml was determined to be suitable for cell treatments.

2.5 Immunocytochemistry

Indirect immuno-fluorescent identification of α-SMA was used as confirmation of myofibroblastic differentiation. Immuno-fluorescent visualisation of EGFR and CD44 were used to analyse receptor expression and interaction. All immunocytochemistry was performed on cells grown on 8-well glass chamber slides (Nunc; Thermo-Fisher Scientific). Cells were grown to 70% confluence, growth arrested for 48h, and then stimulated under serum-free conditions.

Following stimulation, cells were fixed in cold 4% paraformaldehyde for 15 minutes and then washed thoroughly in PBS. For visualisation of α-SMA, cells were permeabilised with 0.1% Triton X-100 for 5 minutes and then washed with PBS. Non-specific binding was blocked with 1% (w/v) bovine serum albumin (BSA) (Sigma-Aldrich) in PBS (herein referred to as BSA-PBS), for 1h at room temperature and on a STR6 platform shaker (Stuart Scientific, Stone, UK). The cells were washed thoroughly in 0.1% (w/v) BSA-PBS. Cells were incubated with the appropriate primary antibody (Table 2.1), diluted in 0.1% (w/v) BSA-PBS

overnight at 4°C on a plate Gyro-Rocker (Stuart Scientific). The cells were washed repeatedly in 0.1% (w/v) BSA-PBS, then incubated with the appropriate secondary horse-radish peroxidise (HRP) conjugated antibody (Table 2.2), diluted in 0.1% (w/v) BSA-PBS for 1h at room temperature, on a platform shaker in darkness. The cells were washed extensively with 0.1% (w/v) BSA-PBS, before incubation with Hoechst nuclear stain (Sigma-Aldrich; dilution 1:2000 in 0.1% (w/v) BSA-PBS) for 30 minutes at room temperature in darkness. Following further thorough washes with 0.1% (w/v) BSA-PBS, the slides were mounted with FluorSave mountant (Merck Millipore) and examined under fluorescent UV-light on a Leica Dialux 20 Fluorescent Microscope (Leica Microsystems UK Ltd, Milton Keynes, UK).

Table 2.1. Primary Antibodies for Immunocytochemistry

Antibody	Type	Host	Dilution
Anti-α-SMA (Dako, Cambridgeshire, UK)	Monoclonal	Mouse	1:25
Anti-EGFR (528) (Merck Millipore)	Monoclonal	Mouse	1:200
Anti-CD44 (A020) (Merck Millipore)	Monoclonal	Rat	1:200

Table 2.2. Secondary Antibodies for Immunocytochemistry

Antibody	Type	Host	Dilution
Anti-Mouse-IgG AlexaFluor 488 (FITC) (Merck Millipore)	Polyclonal	Goat	1:5,000
Anti-Rat-IgG AlexaFluor 555 (TRITC) (Merck Millipore)	Polyclonal	Goat	1:5,000

2.6 RNA Extraction and Reverse Transcription Polymerase Chain Reaction (RT-PCR)

Fibroblasts were grown to confluence in 35mm dishes and washed with PBS, prior to lysis with 500µL TRIzol reagent (Ambion; Life Technologies). RNA was purified from the samples according to the manufacturer's protocol. Briefly, 100µL of chloroform was added to the sample and agitated by inversion for 15 seconds. The sample was incubated at room temperature for 5 minutes and then centrifuged at 12,000×g for 15 minutes, at 4°C. The transparent aqueous phase was transferred to fresh eppendorfs and mixed with 250µL of isopropanol. The mixture was incubated at room temperature for 10 minute, briefly vortexed and then centrifuged at 12,000×g for 10 minutes, at 4°C. The supernatant was removed and the pellet washed with 500µL of 75% (v/v) ethanol, briefly vortexed and then centrifuged at 7,500×g for 8 minutes, at 4°C. The supernatant was removed and the pellet air-dried at room temperature for 15 minutes. The pellet was then dissolved in 16µL of RNase-free distilled H_2O (MilliQ; Merck Millipore). The absorbance was measured at 260nm and 280nm, using a Beckman UV-DU64 Spectrophotometer (Beckman Instruments Ltd, High Wycombe, UK), through the addition of 1µL sample to 49µL of RNase-free distilled H_2O. The ratio of 260:280 gave an indication of protein contamination (>1.8 was considered to indicate sufficiently pure RNA for further analysis). The concentration of RNA was calculated from the absorbance at 260nm:

$$\frac{\mathbf{ABS_{260} \times \text{dilution factor (50)} \times \text{RNA coefficient (40)}}}{\mathbf{1000}} = \mathbf{RNA\ in\ \mu g/\mu L}$$

The RT was performed using the random primer method. The RT was carried out in a final volume of 20µL per reaction, containing 1µg of RNA sample (in 10µL RNase-free distilled H_2O), 2µL of 10x RT random primers, 2µL of 10x RT buffer, 0.8µL of 25x 100mM dNTPs (deoxynucleotide triphosphates; mixed nucleotides: dATP, dCTP, dGTP, and dTTP), 1µL of Multiscribe reverse transcriptase, and 1µL of RNase inhibitor. All reagents used were

supplied as a high-capacity cDNA reverse transcriptase kit (Applied Biosystems). The RT was performed using a PTC-225 Peltier Thermal Cycler (Bio-Rad Laboratories Inc., Berkeley, USA). As a negative control, RT was performed with sterile H_2O replacing the RNA sample. The solution was incubated at 25°C for 5 minutes, to allow the random hexamer primers to anneal to the RNA. The primers were then extended using the reverse transcriptase in the presence of the dNTPs by heating to 37°C for 2h, generating cDNA. The cDNA was then heated to 85°C for 5 minutes, to separate the hybridised complexes consisting of the RNA template and the newly synthesised cDNA, deactivating the reverse transcriptase in the process. The resulting single stranded complementary DNA (cDNA) was stored at -20°C until further use.

2.7 Real Time Quantitative Polymerase Chain Reaction (RT-QPCR)

2.7.1 TaqMan Gene Expression QPCR

Following RT-PCR, cDNA samples were made up to 80µL by the addition of 60µL of RNase-free distilled H_2O (MilliQ, Merck-Millipore). QPCR was carried out in a final volume of 20µL per reaction, containing 4µL of cDNA, 10µL of TaqMan Fast Universal PCR Master Mix (20X) (Applied Biosystems), 5µL of H_2O, and 1µL of a TaqMan gene expression assay primer and probe mix (Applied Biosystems) (Table 2.3). A negative control was prepared with H_2O substituted for the cDNA. QPCR was simultaneously performed for 18S ribosomal RNA (Applied Biosystems), as a standard reference gene.

2.7.2 Power SYBR Green QPCR

Following RT-PCR, cDNA samples were made up to 80µL by the addition of 60µL of RNAse-free distilled H_2O (MilliQ, Merck-Millipore). QPCR was carried out in a final volume of 20µL per reaction, containing 4µL of cDNA, 10µL of Power SYBR Green PCR

Master Mix (Applied Biosystems), 4.8μL of H_2O, 0.6μL of 10μM custom-designed forward primer, and 0.6μL of 10μM custom-designed reverse primer (Table 2.4). A negative control was prepared with H_2O substituted for the cDNA. PCR was simultaneously performed for GAPDH (Table 2.4), as a standard reference gene.

2.7.3 QPCR and Relative Quantification (RQ)

QPCR was performed using the ViiA-7 Real Time PCR System (Applied Biosystems), using either TaqMan Universal or Power SYBR Green PCR Master Mixes (Applied Biosystems) following the manufacturer's instructions. Following completion of the QPCR run, the comparative CT method was used for relative quantification of gene expression. The CT (threshold cycle where amplification is in the linear range of the amplification curve) for the standard reference gene (rRNA or GAPDH) was subtracted from the target gene CT, to obtain the delta CT (dCT). The mean dCT for the experimental control group was then calculated. The expression of the target gene in experimental samples relative to the expression in control samples was then calculated using the formula:

$$\mathbf{2^{-(\,dCT(Experimental\ Sample)\ -\ dCT(Mean\ Control\ Group)\,)}}$$

Table 2.3. TaqMan Gene Expression Assays*

Target	TaqMan Gene Expression Assay
18S rRNA	Catalog #: 4319413E
α-SMA (ACTA2)	Hs00426835_g1
EGFR	Hs01076078_m1
CD44	Hs01075861_m1
HAS2	Hs00193435_m1
TSG-6 (TNFAIP6)	Hs01113602_m1
STAT1	Hs01013996_m1

*Applied Biosystems do not supply sequences of their QPCR primers.

Table 2.4. Custom Designed Primers for SYBR Green Assays*

Target	Custom Primer Sequences
GAPDH	Forward: 5'-CCTCTGACTTCAACAGCGACAC-3' Reverse: 5'-TGTCATACCAGGAAATGAGCTTGA-3'
EDA-Fibronectin (EDA-FN)	Forward: 5'-GCTCAGAATCCAAGCGGAGA-3' Reverse: 5'-CCAGTCCTTTAGGGCGATCA-3'

*Primer efficiency was checked using 10-fold dilution series (90-100% efficiency accepted).

2.8 Western Blot Analysis

Cells were grown to confluence in 35mm dishes and were scraped and collected in ice-cold PBS. The samples were then centrifuged at 10,000×g for 10 minutes at 4°C and the supernatant discarded, the cell pellet was then resuspended in RIPA lysis buffer, containing 1% protease cocktail inhibitor, 1% phenylmethylsulfonyl fluoride and 1% sodium orthovanadate (Santa Cruz Biotechnology Inc., Heidelberg, Germany). The samples were thoroughly vortexed and kept on ice for 5 minutes, before being centrifuged at 10,000×g for 10 minutes at 4°C. The resulting supernatant was collected and transferred to fresh eppendorfs. Protein concentrations were determined by Bradford assay (Bio-Rad Laboratories Inc.); and the samples were stored at -80°C until further use. Equal amounts of protein were mixed with equal volumes of 1x reducing buffer and boiled for 5 minutes at 99°C, before being vortexed, briefly centrifuged and allowed to cool on ice for 5 minutes. The samples were then loaded alongside a protein ladder onto 7.5% SDS-PAGE gels. Electrophoresis was carried out at 100V for 20 minutes, followed by 150V for 40 minutes; using the Mini-PROTEAN II system (Bio-Rad Laboratories Inc.). The separated proteins were then transferred at 100V for 1h to a nitrocellulose membrane (GE Healthcare, Hatfield, UK). The membrane was blocked with PBS containing 0.1% (v/v) Tween-20 (herein referred to as Tween-PBS) and 5% (w/v) non-fat powdered milk for 1h; and incubated with the appropriate primary antibody (Table 2.5) diluted in Tween-PBS on a plate rocker, at 4°C

overnight. The blots were subsequently washed with Tween-PBS, prior to incubation with the appropriate HRP-conjugated secondary antibody (Table 2.6), for 1h at room temperature on a plate shaker. Proteins were visualised using enhanced chemiluminescence (ECL) reagent (GE Healthcare), exposed to HyperFilm X-ray film (GE Healthcare), and developed using a Curix-60 developer (AGFA Healthcare, Greenville, USA) according to the ECL manufacturer's protocol.

2.9 Immunoprecipitation

Immunoprecipitation was used to examine total protein co-localisation of CD44 with EGFR. Cells were grown to confluence in 35mm dishes and total cellular protein was extracted, as described under Western Blot Analysis (Section 2.8). Approximately 10μg of anti-EGFR antibody (Table 2.5) was conjugated to 200μL MagnaBind Goat Anti-Mouse IgG magnetic beads (Thermo-Fisher Scientific), by incubation for 2h at 4°C, whilst on a constant mix. The beads were then washed with PBS, using a magnetic strip to separate beads from solution. Equal amounts of each of the cell protein samples were incubated with the anti-EGFR antibody-conjugated MagnaBind beads, overnight at 4°C. Following three washes with Nonidet P-40 buffer (Sigma-Aldrich), the beads were resuspended in PBS and transferred to clean microcentrifuge tubes. The bead-antibody-protein complex was boiled with 1x reducing buffer for 5 minutes, before brief centrifugation. The supernatant was transferred into gel lanes for SDS-PAGE (as in Section 2.8). Western Blotting with rat anti-CD44 primary antibody (Table 2.5) was used for further analysis (secondary HRP antibody in Table 2.6). The specificity of immunoprecipitation was confirmed by negative control reactions performed with mouse serum IgG.

Table 2.5. Primary Antibodies and Dilutions used in Western Blot Analysis

Antibody	Type	Host	Dilution
Anti-EGFR (528) (Merck Millipore)	Monoclonal	Mouse	1:1,000
Anti-Phospho-EGFR (Y1068) (Cell Signaling Technology, Beverly, USA)	Polyclonal	Rabbit	1:5,000
Anti-CD44 (A020) (Merck Millipore)	Monoclonal	Rat	1:5,000
Anti-Phoshpo-p44/42 MAPK (ERK1/2) (T202/Y204) (Cell Signaling Technology)	Monoclonal	Rabbit	1:10,000
Anti-p44/42 MAPK (ERK1/2) (Cell Signaling Technology)	Polyclonal	Rabbit	1:10,000
Anti-Phospho-CaMKII (T286) (Cell Signaling Technology)	Polyclonal	Rabbit	1:2,000
Anti-CaMKII (pan) (Cell Signaling Technology)	Polyclonal	Rabbit	1:5,000
Anti-Caveolin-1 (Sigma-Aldrich)	Polyclonal	Rabbit	1:500
Anti-EEA1 (BD Biosciences)	Monoclonal	Mouse	1:5,000
Anti-TGF-βRI (Santa-Cruz Biotechnology Inc.)	Polyclonal	Rabbit	1:1000
Anti-Phospho-STAT1 (Cell Signaling Technology)	Monoclonal	Rabbit	1:2,000
Anti-STAT1 (Cell Signaling Technology)	Monoclonal	Mouse	1:2,000
Anti-Phospho-Smad2 (S465/467) (Cell Signaling Technology)	Polyclonal	Rabbit	1:5,000
Anti-Smad2 (Cell Signaling Technology)	Monoclonal	Mouse	1:5,000
Anti-GAPDH (Abcam, Cambridge, UK)	Polyclonal	Rabbit	1:5,000

Table 2.6. Secondary Antibodies and Dilutions used in Western Blot Analysis

Antibody	Type	Host	Dilution
Anti-Mouse-IgG HRP (Abcam)	Polyclonal	Goat	1:5,000
Anti-Rat-IgG HRP (Abcam)	Polyclonal	Goat	1:5,000
Anti-Rabbit-IgG HRP (Cell Signaling Technology)	Polyclonal	Goat	1:5,000

2.10 Laser Confocal Microscopy and Fluorescent Recovery After Photobleaching (FRAP) Analysis

Cells were grown to 70% confluence on sterilised 22mm diameter glass coverslips, in 35mm dishes. Following appropriate experimental methods, the coverslip was removed from the medium and mounted on a microscope stage heated at 37°C. After ensuring a watertight seal between stage and coverslip was made, 500μL of medium was placed onto the coverslip and the appropriate primary fluorophore-conjugated antibodies/ligands were added (Table 2.7). Analysis was performed by laser confocal microscopy and FRAP. Briefly, an approximately 10μm area of the cell membrane was chosen for photobleaching with high intensity laser light of appropriate wavelength (Table 2.7), for 5-10 seconds or until the antibody fluorophore diminished. A time-lapse video was recorded, clips were recorded for >500 frames over 5 minutes.

Co-localisation data were analysed using ImageJ (NIH Software) and Intensity Correlation Analysis (ICA), including the following statistical tests: Mander's Co-localisation Coefficient (percentage of FITC co-localisation with TRITC), Pearson's Correlation Coefficient (Rr); where perfect correlation = 1; and Intensity Correlation Quotient (ICQ), where with random staining ICQ = ∼0 and for dependent staining $0 < ICQ \leq +0.5$ [272].

Leica Confocal Software (Leica Microsystems, Hamburg GmbH) was used to assess FRAP data and generate fluorescence intensity ratios (FI ratio); defined as FI ratio=F_z/F_o, where F_z is the intensity of the photobleached zone and F_o is the intensity of the control region taken from outside of the photobleached zone. Average diffusion constants (D) were calculated from the $D=(w^2/2t_{½})\gamma_D$ equation, where w is the radius of the photobleached area, $t_{½}$ is the half time of fluorescent recovery, and γ_D is a constant that is dependent on experimental conditions [273]. Mobile fractions (MF) represent the fraction of receptors that had the ability to recover into the photobleached zone, over the observed time.

Table 2.7. Antibodies/Markers and Dilutions used in Confocal Laser Microscopy and FRAP

Antibody	Wavelengths (nm)		Dilution
	Excitation	Emission	
Anti-EGFR FITC (Abcam)	488	525	1:500
Anti-CD44 FITC (Abcam)	488	525	1:500
Anti-CD44 PE-R (Abcam)	528	578	1:500
CTX-B AlexaFluor 555 (Life Technologies)	555	565	1:500

2.11 Flow Cytometry

Fibroblasts were grown to confluence and growth arrested in serum-free medium for 48h, before treatment with serum-free medium alone or serum-free medium, containing 50μg/ml nystatin for 1h. Cells were washed with PBS and incubated with 0.01% trypsin-EDTA to lift the cells. Trypsin was subsequently neutralised with FCS and the cell solution was centrifuged at 1,500×g for 5 minutes, at 20°C. The supernatant was aspirated and the cell pellet resuspended in 1% BSA-PBS, containing anti-EGFR-FITC (1:1000) and anti-CD44-

PE-R (1:1000) or CTX-B AlexaFluor 555 (1:1000) (Table 2.7); and incubated on ice for 30 minutes. Cells were then centrifuged at 1,500×g for 5 minutes at 4°C; and washed with ice-cold PBS, before resuspension in 1% (w/v) BSA-PBS. Flow cytometry was then performed using a FACSCanto II Flow Cytometer (BD Biosciences) and data was analysed using FlowJo, version 7 (Tree Star, Olten, Switzerland).

2.12 Plasmid Generation

2.12.1 EGFR Promoter Luciferase Reporter

A 247bp insert encoding the EGFR promoter was PCR amplified, using the Phusion DNA polymerase system (New England Biolabs, Hitchin, UK) from the forward primer, 5'-ACTCCCGCCGGAGACTAGGT-3'; and the reverse primer, 5'-CCGCGTCGGGCGCTCACACC-3', with the addition of KpnI and XhoI endonuclease restriction sites, respectively. Amplified promoter inserts were PCR purified, digested with the appropriate endonuclease restriction enzymes (New England Biolabs), for 2h at 37°C, electrophoresed; and extracted from 1% agarose gel, according to Qiagen Gel Extraction Kit protocol (Qiagen, Barcelona, Spain). Inserts were then ligated together with KpnI and XhoI digested pGL3Basic (pGL3b) Vector using the T4 DNA Ligase System (New England Biolabs), overnight at 16°C. The pGL3b plasmid, containing the 247bp EGFR promoter insert (pGL3b-EGFR), was then transformed using the 42°C heat-shock method into one-shot competent *Escherichia coli* (New England Biolabs); and grown overnight on ampicillin containing agar. Single colonies were extracted, cloned and DNA purified according to the Miniprep Kit protocol (Sigma-Aldrich). Cloned pGL3b-EGFR Vector uptake of insert was confirmed with DNA sequencing (BIOCore Sequencing, Cardiff University, UK).

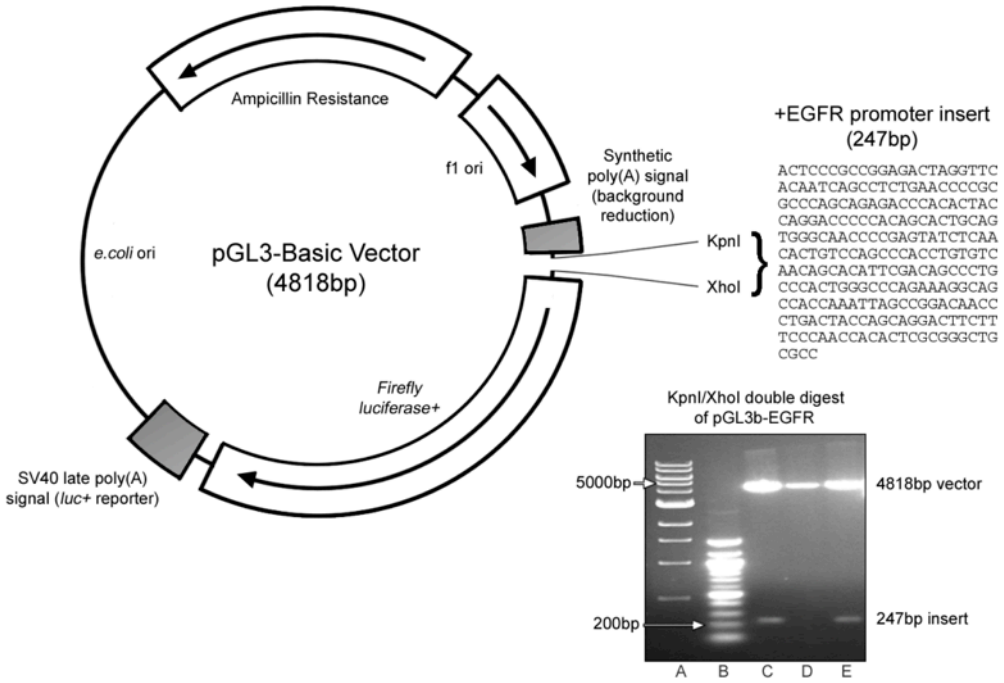

Figure 2.4. Diagram of pGL3-Basic Vector (pGL3b), indicating size (4818bp) and layout of the components within the vector, note the restriction endonuclease sites; KpnI and XhoI were used to first digest the plasmid and inserts, before ligation into a plasmid of approximately 5065bp. Test digestion of ligated pGL3b-EGFR plasmid resulted in two bands with correct sizes, in relation to the empty vector (4818bp) and the EGFR promoter insert (247bp). Lanes: 10kb DNA ladder (A), 1kb DNA ladder (B), pGL3b-EGFR digest (C), empty pGL3b digest (D), pGL3b-EGFR digest (E).

2.12.2 miRNA-7 Promoter Luciferase Reporter

A 424bp insert encoding the miR-7 promoter was PCR amplified using the Phusion DNA Polymerase System (New England Biolabs), from the forward primer, 5'-CTTGACAGGTTTAGGGAGCGT-3'; and the reverse primer, 5'-AGGTCCCCAAAAGGTTGAGAC-3', with the addition of KpnI and XhoI endonuclease restriction sites, respectively. Amplified promoter inserts were PCR purified, digested with the appropriate endonuclease restriction enzymes (New England Biolabs), for 2h at 37°C, electrophoresed; and extracted from 1% agarose gel, according to Qiagen Gel Extraction Kit protocol (Qiagen). Inserts were then ligated together with KpnI and XhoI digested pGL3Basic (pGL3b) Vector using the T4 DNA Ligase System (New England Biolabs), overnight at 16°C. The pGL3b plasmid, containing the 424bp miR-7 promoter insert (pGL3b-miR-7), was then transformed using the 42°C heat-shock method into one-shot competent

Escherichia coli (New England Biolabs); and grown overnight on ampicillin containing agar. Single colonies were extracted, cloned and DNA purified, according to the Miniprep Kit protocol (Sigma-Aldrich). Cloned pGL3b-miR-7 Vector uptake of insert was confirmed with DNA sequencing (BIOCore Sequencing).

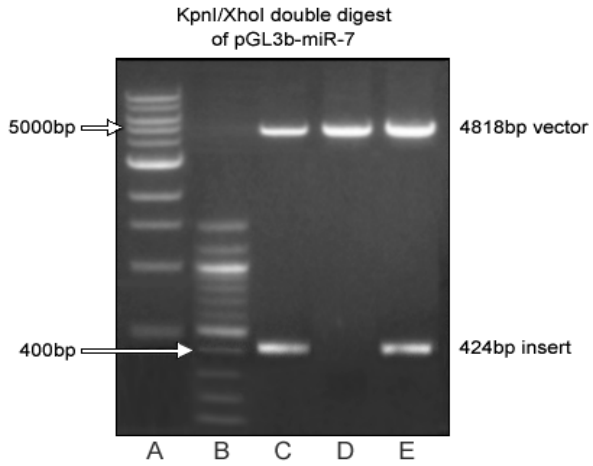

Figure 2.5. Test digestion of ligated pGL3b-miR-7 plasmid (approximately 5242bp), resulted in two bands with correct sizes in relation to the empty vector (4818bp) and the miR-7 promoter insert (424bp). Lanes: 10kb DNA ladder (A), 1kb DNA Ladder (B), pGL3b-miR-7 digest (C), empty pGL3b digest (D), pGL3b-miR-7 digest (E).

2.12.3 HAS2 Overexpression Vector

The HAS2 open reading frame [244] was inserted into the Vector pCR3.1, using a standard ligation reaction with T4 DNA Ligase (New England Biolabs). Amplification of the cloned vector was performed via bacterial transformation into one-shot competent *Escherichia coli* (New England Biolabs); and grown overnight on ampicillin containing agar. Single colonies were extracted, cloned and DNA purified, according to the Miniprep Kit protocol (Sigma-Aldrich). Cloned pCR3.1-HAS2 Vector uptake of inserts was confirmed with DNA sequencing (BIOCore Sequencing). Negative RT experiments were performed alongside HAS2 mRNA QPCR, to ensure that pCR-3.1-HAS2 Vectors weren't conveying false-positive overexpression.

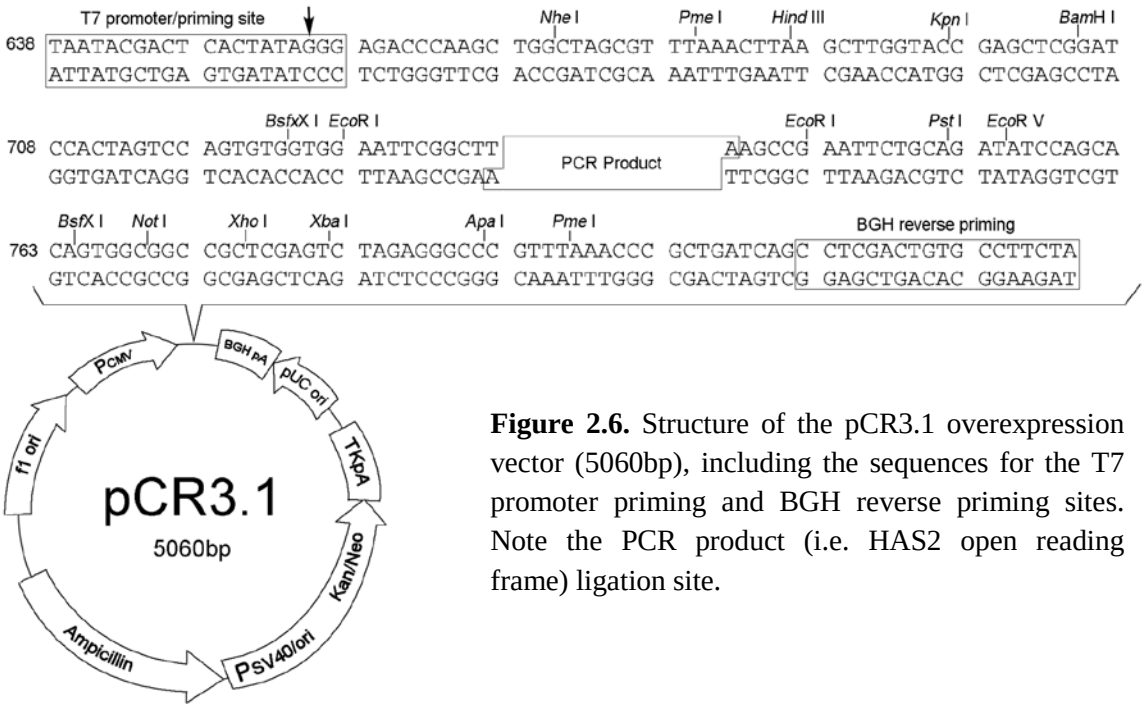

Figure 2.6. Structure of the pCR3.1 overexpression vector (5060bp), including the sequences for the T7 promoter priming and BGH reverse priming sites. Note the PCR product (i.e. HAS2 open reading frame) ligation site.

2.13 Transient Transfection

Plasmids pGL3b-EGFR/miR-7 and pCR3.1-HAS2, and miRCURY LNA (Exiqon, Vedbaek, Denmark) transfections were completed using the Lipofectamine LTX system (Invitrogen; Life Technologies), according to manufacturer's protocol, following optimisation of transfection. Pre-miR-7 (Ambion; Life Technologies) and small interfering RNA (siRNA) (Applied Biosystems) transfections were completed using the Lipofectamine 2000 system (Invitrogen; Life Technologies), according to manufacturer's protocol, following optimisation. Transfection optimisation and efficiency for luciferase reporter plasmids were determined by co-transfection of a Renilla luciferase reporter. Transfection optimisation and efficiency for overexpression vectors were determined by co-transfection of pmaxGFP vector (Amaxa, Cologne, Germany) (Figure 2.7). Pre-miR-7, siRNA and LNA transfections were optimised according to the manufacturers' protocols. All transfections were performed on 60-70% confluent cell monolayers. Cells were incubated for 24h following transfection, prior to continuation of experiments.

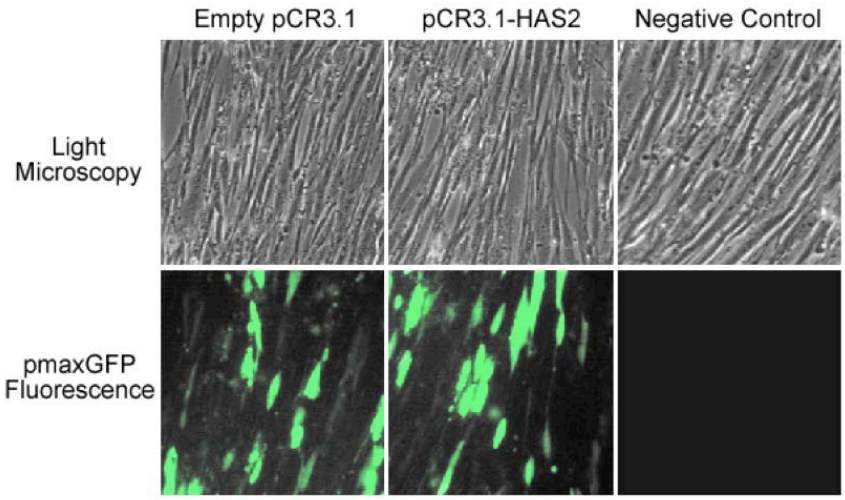

Figure 2.7. Transfection efficiency of empty pCR3.1 and pCR3.1-HAS2 overexpression vectors was optimised through the co-transfection of pmaxGFP nucleofector vector (Amaxa), as described in section 2.13.2. The cells were imaged using light (top row; total cell number) and fluorescent microscopy (bottom row; cells successfully transfected), at 48h post-transfection. The transfection efficiency of empty pCR3.1 and pCR3.1-HAS2 was 68% and 66%, respectively. Non-transfected cells were used as a negative control for pmaxGFP expression.

2.13.1 Luciferase Reporter Transfection

Transfections of luciferase reporter plasmids were performed on cells grown on 22mm dishes (12-well tissue culture plates), according to the Lipofectamine LTX transfection reagent protocol (Life Technologies). Briefly, 1μg of plasmid DNA (empty pGL3b, pGL3b-EGFR, or pGL3b-miR-7) and 1μL PLUS-reagent were added to 100μL of OPTIMEM transfection medium. Following 5 minutes incubation at room temperature, 2μL of Lipofectamine LTX transfection reagent was added, mixed well and left to incubate at room temperature for 40 minutes. Renilla luciferase was co-transfected with pGL3b plasmids at a ratio of 1:4 (0.25μg:1μg) and used as a control for transfection efficiency and for the normalisation of data. Reporter analysis was performed 24h after transfection using the Dual-Luciferase Reporter Assay Kit (Promega, Southampton, UK); and detected with a FLUOstar OPTIMA plate reader (BMG Lab Technologies).

2.13.2 Overexpression Vector Transfection

Overexpression vectors using the pCR3.1 plasmid were transfected with the Lipofectamine LTX Transfection Kit according to the manufacturer's protocol (Life Technologies). Briefly, for two 22mm cell culture dishes, 750ng plasmid DNA, 0.75µL PLUS reagent and 4µL Lipofectamine LTX were added to 400µL OPTIMEM transfection medium, mixed well and incubated at room temperature for 40 minutes. Following incubation, 200µL of transfection solution was then added to each 22mm cell culture dish containing DMEM/F-12 growth medium with 10% FCS. Cells were incubated for 24h, before the medium was replaced with serum-free growth medium for further cell experimentation or analysis. To ensure transfection efficiency was optimum, 750ng pmaxGFP (Amaxa) was co-transfected with the pCR3.1 plasmid and GFP fluorescence was visualised 48h post-transfection, using a UV light microscope (Axiovert 135; Zeiss, Jena, Germany). As a negative control, an empty pCR3.1 plasmid (containing no open reading frame sequence) was transfected into cells.

2.13.3 Small interfering RNA (siRNA) Transfection

Transient transfection of fibroblasts was performed with specific siRNA nucleotides targeting CD44 (I.D.: 4390824, Applied Biosystems) and HAS2 (I.D.: 4392420, Applied Biosystems). Transfection was performed in 35mm dishes using Lipofectamine 2000 transfection reagent (Invitrogen), in accordance with the manufacturer's protocol. Briefly, for transfection of a single 35mm well: two solutions were made, the first consisted of the target siRNA (final transfection concentration of 30nM) in 100µL OPTIMEM transfection medium. The second solution consisted of 4µL Lipofectamine 2000 transfection reagent in 100µL OPTIMEM transfection medium. The solutions were mixed together and incubated for 40 minutes, at room temperature. Following incubation, an additional 800µL of OPTIMEM was added to the transfection solution. The cells were washed with OPTIMEM medium and the 1mL

transfection solution was incubated with the cells for 5-7 hours, after which an additional 1mL of cell culture medium containing 20% FCS was added to the well. Following 24h of incubation, the medium was removed and replaced with serum-free media, in preparation for further cell treatments or analysis. As a negative control, cells were transfected with negative control siRNA (a scrambled sequence that bore no homology to the human genome) (I.D.: AM17110, Applied Biosystems).

2.13.4 Pre-MicroRNA-7 Transfection

Following growth arrest, pre-miR-7 (I.D.: PM10047; Ambion) was transfected into cells using the Lipofectamine 2000 Transfection System (Life Technologies). Two solutions were prepared; the first consisted of pre-miR-7 (final working concentration of 125nM) in 100μL OPTIMEM transfection medium; and the second consisted of 5μL Lipofectamine 2000 transfection reagent in 100μL OPTIMEM. Solutions were mixed and incubated for 40 minutes at room temperature. Solutions were then made up to 1mL by the addition of OPTIMEM. Cells were washed with OPTIMEM and the 1mL solution was added to the 35mm cell culture dish. After 5-7 hours, 1mL of DMEM/F-12 growth medium containing 20% FCS was added to the cell culture dish, which was then incubated for a further 24 hours. As a negative control, a scrambled pre-miR (I.D.: AM17110; Ambion) was transfected into cells (a sequence that codes for no known pre-miR). Medium was then removed and replaced with serum-free medium for further experimentation.

2.13.5 miRCURY miR-7 Inhibitor LNA Transfection

MicroRNA-7 locked nucleic acid (LNA) (I.D.: 410428-00; Exiqon) transfection was performed using the Lipofectamine LTX transfection reagent (Life Technologies). A solution of 1μL PLUS reagent, 2.5μL Lipofectamine LTX and miR-7 LNA (final working

concentration of 125nM) in 400µL OPTIMEM transfection medium was prepared. The transfection solution was incubated for 40 minutes and then added to the 35mm cell culture dish containing 2mL of DMEM/F-12 growth medium with 10% FCS. The cells were incubated in the transfection solution and growth medium mix for 24 hours, before the medium was replaced with serum-free DMEM/F-12 growth medium for further cell treatments or analysis. As a negative control, the commercially available Negative Control A LNA (I.D.: 199004-00; Exiqon) was used in place of the miR-7 LNA (a LNA sequence of similar length with no known miR targets).

2.14 MicroRNA RT-PCR

RNA was extracted and purified according to the methods described in conventional RT-PCR (Section 2.6). The RNA sample was diluted to 10ng and RT was performed for each miR, according to the instructions provided with TaqMan miR Gene Expression Assay Kits (Applied Biosystems). Briefly, a master mix containing 3µL TaqMan looped miR RT primer, 0.15µL 100mM dNTPs, 1µL MultiScribe reverse transcriptase, 1.5µL 10x RT buffer, 0.19µL RNase inhibitor, 4.16µL nuclease-free H_20 was made. Each RT-PCR reaction had a final volume of 15µL, consisting of 10µL master mix and 5µL RNA sample. The RT used the following parameters: 30 minutes at 16°C to allow looped RT primer to anneal to the target miR, 30 minutes at 42°C to allow random dNTP and transcriptase extension of the cDNA strand; and 5 minutes at 85°C to dissociate the looped RT primer from the miR/cDNA strands. The RT was performed on a PTC-225 Peltier Thermal Cycler (Bio-Rad Laboratories Inc.). Samples were cooled to 4°C and then transferred to -20°C, until further use.

2.15 MicroRNA RT-QPCR

MicroRNA RT-QPCR was performed, according to the TaqMan MicroRNA Gene Expression Assay Kit protocol (Applied Biosystems). A master mix solution was made consisting of 1μL TaqMan MicroRNA Assay (20X), 10μL TaqMan 2X Universal PCR Master Mix, and 7.67μL nuclease-free H_2O. Analysis was performed in triplicate on a 96-well plate with a final reaction volume of 20μL, consisting of 1.33μL of cDNA and 18.67μL of master mix solution. The plate was briefly centrifuged and the QPCR was performed using the ViiA-7 Real Time PCR System (Applied Biosystems), using TaqMan 2X Universal PCR Master Mix (Applied Biosystems), following the manufacturer's instructions. Following the completion of the QPCR run, the data was calibrated against a house-keeping miR, with no expression change under any experimental conditions performed (miR-16), using the comparative CT method as described in Section 2.7.3.

Table 2.8. TaqMan miR Expression Assays

Target	TaqMan miR Expression Assay
miR-16	hsa-miR-16 (UAGCAGCACGUAAAUAUUGGCG)
miR-7	hsa-miR-7-5p (UGGAAGACUAGUGAUUUUGUUGU)
miR-7-1-3p	hsa-miR-7-1-3p (CAACAAAUCACAGUCUGCCAUA)
miR-7-2-3p	hsa-miR7-2-3p (CAACAAAUCCCAGUCUACCUAA)

2.16 Biochemical Isolation of Lipid Rafts

All procedures were carried out on ice. Fibroblast or myofibroblast monolayers were washed twice with ice-cold PBS; and cells from two 35mm confluent dishes were then scraped into 1mL of ice-cold lysis buffer, containing 1% Triton X-100 and 1% protease inhibitor mixture (Sigma-Aldrich). Samples were vortexed thoroughly and left to incubate on ice for 30 minutes, before centrifugation (1500×*g* for 5 minutes, at 4°C). The sample supernatants were

placed at the bottom of a 5mL ultracentrifuge tube. Discontinuous OptiPrep gradients (35–20% and 0%) (Sigma-Aldrich) were made according to the manufacturer's protocol; and added to the ultracentrifuge tube, containing the sample by overlaying. The gradients were centrifuged at 200,000×*g* for 14 hours with 2 hours of gentle acceleration and deceleration on either side in an Optima-Max ultracentrifuge (Beckman Coulter). Centrifugation time was sufficient to gain a continuous gradient, from which ten 500μL fractions were carefully collected, starting from the top of each tube.

2.16.1 Fraction Analysis

The collected fractions were subjected to SDS-PAGE and transferred to a nitrocellulose membrane, as described by Western Blot Analysis (Section 2.8). The presence of proteins of interest was examined using specific antibodies. The presence of caveolin-1 (Cav-1) and early endosomal antigen-1 (EEA1) was used to determine whether the fraction represented lipid raft or non-raft proteins, respectively. Following transfer of proteins to the nitrocellulose membrane, the membrane was blocked with 5% non-fat powdered milk in 0.5% Tween-PBS for 1 hour; and then incubated with rabbit anti-caveolin-1 or mouse anti-EEA1 (Table 2.5) in 1% BSA, 0.1% Tween-PBS, at 4°C overnight. The blots were subsequently washed with 0.1% Tween-PBS and then incubated with the appropriate secondary antibody, and visualised using ECL reagent (GE Healthcare). Cholera Toxin subunit B-HRP conjugate (CTX-HRP) (Sigma-Aldrich; dilution 1:500) was incubated with cell monolayers on ice for 1 hour, prior to lysis. CTX-HRP bound samples were used for dot-blot analysis, to confirm the presence of lipid rafts. 5μL of each fraction was pipetted onto a pre-washed nitrocellulose membrane and allowed to dry, the membrane was washed briefly with PBS and visualised with ECL reagent (GE Healthcare).

2.17 *In Silico* Analysis

In silico analysis was performed to determine promoter start sites, transcription factor binding regions, miR protein or pathway target analysis, and for primer design. Putative transcription start sites were analysed using miRStart (National Chiao-Tung University, Hsinchu, Taiwan) and Genomatix MatInspector (Genomatix Software GmbH, Munich, Germany). Potential transcription factor binding regions were analysed using Genomatix MatInspector (Genomatix Software GmbH). TargetScan v6.2 (Whitehead Institute, Cambridge, USA), miRBase (Manchester University, UK) and GoDAVID v6.7 (National Cancer Institute, Frederick, USA) software were used to analyse potential miR protein and pathway targets, including details of conserved miR binding sites on the 3'UTR of targets. UCSC Genome Browser and PrimerBLAST (UCSC Genome Bioinformatics Group, Santa Cruz, USA) were used to design custom primers for use in QPCR or for PCR product amplification, for ligation into plasmids.

2.18 Statistical Analysis

Western blot images were densitometrically analysed by ImageJ (NIH Software). Graphical data are expressed as averages ± standard error mean (s.e.m.). To test for normal distribution of data and variances, the One-Way ANOVA, followed by Anderson-Darling and Bartlett's Test, was used. The unpaired two-tailed Student's *t* test was used for pairwise comparisons (excluding time course experiments), to identify statistical significance. Data were analysed using the software MiniTab version 15.0 (Minitab Solutions) and $*P=<0.05$ or $**P=<0.01$ were considered significant.

Chapter 3

Characterisation of Cellular Receptor Mechanisms Involved in Myofibroblast Differentiation

3.1 Introduction

3.1.1 The HA Receptor CD44

The CD44 antigen is a glycoprotein and the major cell surface receptor for HA, essential for many HA-regulated intracellular influences. In humans, the CD44 antigen is encoded by the CD44 gene on chromosome 11 and is expressed in a large number of mammalian cell types [262, 263]. The standard isoform, designated CD44s, comprising exons 1–5 and 16–20, is expressed in most cell types. Alternative splicing of CD44 results in several splice variants containing variable exon regions, these are designated CD44vN (where N = 1 to 10). Some epithelial cells also express a larger isoform (CD44E), which includes exons v8–10 [274]. It is not yet clear whether or not certain CD44 variants have specific roles in cellular function. However, it has been suggested that higher expression of CD44v3 and v6 may be related to tumour metastasis [275, 276].

Although CD44 is the main receptor for HA, it can also interact with other ligands, such as osteopontin, collagens, MMPs; and other cell surface or transmembrane receptors, such as TGF-βRI and EGFR [160, 252, 262, 263]. CD44 function is controlled by post-translational modifications. One critical modification involves discrete sialofucosylation of glycan regions present on CD44v isoforms that have been noted to be involved in the migration of human hematopoietic and mesenchymal stem cells, but also in cancer cell metastasis [277, 278]. CD44 glycosylation also directly controls its binding capacity to fibrin and immobilised fibrinogen. Acylation through palmitoylation has recently been described as a mechanism of directly regulating CD44 endocytosis, lipid raft association and signal transduction [279]. The cellular functions of CD44 are diverse with participation in actions, including lymphocyte activation, cell-cell and cell-ECM interactions, migration, proliferation, differentiation, haematopoiesis, and tumour metastasis [262, 263].

3.1.2 HA-CD44 Binding

The extracellular domain of CD44 contains a HA binding site referred to as the Link domain which shares a 100-amino acid region of homology with other hyaladherins. However, CD44 differs in important ways from other HA-binding proteins. Whilst the Link module of TSG-6 can bind HA on its own, HA binding by CD44 requires sequences outside the link module, regulated by cell-specific factors; and requires multiple CD44/HA engagements to achieve a functional avidity. Depending on the type and activation state of the cell in which it is expressed, CD44 may be inactive (unable to bind HA), inducible (able to bind HA upon treatment with certain CD44-specific mAb or with inducers of cell activation), or constitutively active (able to bind HA without any treatment). The activation state seems to be determined, at least in part, by post-translational modification (especially glycosylation) of the CD44 molecule itself [262, 263].

The most significant feature that distinguishes CD44 from other HA-binding proteins is that CD44 binding to HA takes place at the cell surface, where multiple, clustered or closely arrayed CD44 receptor molecules, interact with the highly multivalent repeating disaccharide chain of HA [254]. The affinity of a single CD44 HA-binding domain for HA is likely to be very low. Thus, binding of a CD44-positive cell to an HA substrate, or of a soluble HA molecule to the surface of a CD44-positive cell, involves multiple weak receptor-ligand interactions. This is a feature common to cell surface adhesion receptor-ligand interactions, but is especially important in the case of CD44, because of the highly repetitive nature of its ligand HA [263].

3.1.3 CD44 in Fibrosis and Myofibroblast Differentiation

The functional relationship between HA and CD44 is of significant importance during TGF-β1 stimulated differentiation, as the HA composition on the cell surface is modified. The

network of HA chains, bound to the cell surface by CD44, surrounding the cell; and linked together by heavy chain transfer from IαI – a process facilitated by and reliant on TSG-6 [280] – forms what is known as the HA pericellular matrix or coat. The HA pericellular coat is pivotal for myofibroblast differentiation, as knockdown of either CD44 or TSG-6 using siRNA transfection, resulted in a loss of pericellular coat formation and failure of differentiation in response to TGF-β1 stimulation [244, 252]. The functional significance of HA pericellular coat formation on the cell-surface or the intracellular interactions of CD44, its localisation and function as a co-receptor; and how the CD44 receptor properties are affected by HA-binding, remains unclear. Recent evidence suggests that other cell surface receptors, such as EGFR, can be activated in a CD44-dependent manner, leading to signal transduction via the MAPK/ERK pathway [160, 281]. Clusters of CD44 receptors appear to have the potential to surround, co-localise with and activate EGFR. Whether this is due to direct binding motif association, growth factor shuttling by CD44 (some CD44 variants are reportedly able to bind growth factors to 'handle domains' or able to bind and present HB-EGF to cell surface receptors) [275, 276], or direct phosphorylation of EGFR by CD44, is unknown. This complex activation mechanism has also been suggested to be an essential step in driving both proliferation and differentiation in fibroblasts, in response to TGF-β1 stimulation [160, 195]. Therefore, the roles of CD44 in both wound healing and the development of fibrosis are apparent. The invasive qualities gained from fibroblast and myofibroblast expression of HA and CD44 have been described as being necessary for the progression of severe lung fibrosis. Treatment with a CD44 blocking antibody abrogated the development of lung fibrosis in mice *in vivo* [257]; and *in vitro* work has demonstrated the importance of CD44 in the differentiation mechanism, as blocking CD44 activity prevented myofibroblast formation in response to TGF-β1 treatments [160].

3.1.4 CD44 Localisation

CD44 exists as a transmembrane receptor that has association with different cellular components, including both cytoskeletal and membrane-bound lipid rafts [282-285]. Through interaction with the cortical cytoskeleton [285], CD44 has been shown to have involvement in cytoskeletal reorganisation; and direct association with and activation of cytoskeletal bound proteins, such as ankyrin and cortactin, both of which are involved in structural cytoskeletal changes [282]. CD44 association with the cytoskeleton has been described as a means of signalling transduction from extracellular HA and could be a means of cell adaption to the extracellular environment [286]. However, previous research has reported a strong association between CD44 and cholesterol-rich membrane-bound lipid rafts, micro-domains of the membrane composed of a combination of glycosphingolipids and receptors. These specialised regions can compartmentalise and regulate cellular processes, by serving as organising centres for the assembly of signalling receptors and protein trafficking [287]. It has been reported that the localisation of CD44 in lipid rafts serves as a means of both restricting CD44 protein-protein interactions, in the case of the pro-migratory protein ezrin [283]; and promotion of protein-protein interactions, such as with integrin-β1, leading to endocytosis of CD44 and bound HA [284]. Since EGFR has been reported to exist both inside and outside of lipid raft domains [288, 289], the localisation of the TGF-β1-dependent association between CD44 and EGFR has not yet been pinpointed to a specific location in fibroblasts. It also remains unknown whether EGFR moves to localise with CD44 at either the cytoskeleton or lipid raft domains, or whether CD44 re-localises to areas of EGFR expression. Identification of the cellular location where CD44 and EGFR association and signalling occurs could therefore build upon what components of the differentiation mechanism have previously been shown [160, 195, 196, 244, 252, 260]; and reveal novel targets for intervention of myofibroblast differentiation and progressive fibrosis.

3.1.5 Intracellular Signalling

Intracellular signalling through MAPK (ERK1/2) and Ca^{2+}/calmodulin-dependent kinase II (CaMKII) has been previously shown to be activated by TGF-β1, as well as EGFR and CD44 [187, 195, 290]. Whether these activators are independent or co-dependent, as part of the differentiation mechanism, has not yet been investigated. ERK1/2 has important cellular functions including the promotion of cell survival, proliferation, differentiation and migration [291-293]; and has been shown to be activated rapidly following TGF-β1 stimulation and crucial for myofibroblast differentiation [195]. Although CaMKII has been shown to be involved in cytoskeletal reorganisation, actin bundling and actin formation [290, 294-296], the information regarding CaMKII activity in myofibroblast differentiation is limited. Due to the nature of the function of CaMKII and its reported involvement in HA-CD44 mediated signalling [290], investigation into its role in the differentiation response is warranted. Investigation into the TGF-β1-induced or HA-CD44/EGFR activation of ERK1/2 and CaMKII signalling in fibroblast to myofibroblast differentiation, would provide insight into the mechanism of activation and a hierarchy of signalling; whether through TGF-β1 directly or through CD44 interaction with EGFR; and whether or not activation of one is dependent on the other.

3.1.6 Summary of Aims

The work outlined in this Chapter aimed to further describe the TGF-β1-dependent myofibroblast differentiation mechanism and expand upon previous findings [160, 195, 196, 244, 252, 260]; and to investigate the hypothesis that compartmentalisation of CD44 with EGFR within a specific cellular location is necessary for activation of intracellular signal cascades, leading to myofibroblast differentiation. Specifically, the aim of this Chapter was to characterise the role of CD44 in the myofibroblast differentiation response in relation to:

i. Co-localisation with EGFR.

ii. The affect of differentiation on membrane receptor dynamics.

iii. The localisation of CD44-EGFR association.

iv. Downstream intracellular signalling pathways:

    a. Characterisation of ERK1/2 and CaMKII signalling responses.

    b. Determination of hierarchy of signalling.

v. HA-regulation of CD44 interaction, function and signalling.

The results from this Chapter will detail the role of CD44, its interactions with EGFR, its receptor behaviour, its intracellular actions; and help to characterise its relationship with HA in the myofibroblast differentiation mechanism.

3.2 Results

3.2.1 Characterisation of the Phenotypic Changes Associated With Terminal Myofibroblast Differentiation

Fibroblasts were grown to 70% confluence for immunocytochemistry, or 100% confluence for QPCR analysis. Cells were deprived of serum for 48 hours, before the addition of recombinant TGF-β1 (10ng/ml) in serum-free medium, for 72 hours. To assess the phenotypic changes associated with myofibroblast differentiation, the expression of the myofibroblastic marker, α-SMA, was visualised using immunocytochemistry. In comparison to untreated control fibroblasts (average width approximately 5μm ± 1μm), the myofibroblasts displayed larger morphology (average width approximately 11μm ± 2μm). Myofibroblasts also expressed clearly defined α-SMA fibres, which were not observed in untreated cells (Figure 3.1A). In addition, QPCR analysis showed a TGF-β1 induced increase in α-SMA of approximately 42-fold (Figure 3.1B); and an increase in the myofibroblastic marker EDA-FN of approximately 32-fold (Figure 3.1C).

Components contributing to the formation of the HA pericellular coat were also assessed for mRNA expression and were also significantly upregulated by TGF-β1 stimulation. The HA synthase, HAS2 – previously identified as the major contributor to HA coat formation in fibroblasts [244] (with the exception of oral fibroblasts [297]), was upregulated by approximately 3-fold (Figure 3.1D). TSG-6, the hyaladherin involved in HA-cross-linking, was upregulated by approximately 15-fold (Figure 3.1E). The observations made indicate the phenotypic alterations that occur in fibroblast to myofibroblast differentiation, highlighting the key components that are upregulated, in order to alter the cell morphology through intracellular and pericellular matrix production.

3.2.2 Analysis of the Regulation of TGF-β1-dependent Differentiation by CD44 and its Co-localisation With EGFR

Confocal Laser Scanning Microscopy was used to assess the expression of EGFR and CD44 in fibroblasts and changes associated with TGF-β1-dependent differentiation (Figure 3.2A). Both receptors were expressed in fibroblasts, with strong independent staining along the cell membrane. Following TGF-β1-induced differentiation to myofibroblasts, however, CD44 (red) expression was found in areas of co-localisation with EGFR (green), visible as yellow (merged). Following lysis of myofibroblasts, CD44 was found to co-immunoprecipitate with EGFR (Figure 3.2B). Potential changes in the expression of CD44 receptor protein were examined and no significant changes were found (Figure 3.2C). Both transfection of siRNA targeting CD44 (siCD44) and treatment with the chemical inhibitor of EGFR activation, AG1748, inhibited phosphorylation of EGFR and of the down-stream signalling proteins, ERK1/2 (Figure 3.3A-C). CD44 knockdown was confirmed by QPCR (Figure 3.3D) and the effect of each treatment on differentiation was assessed by QPCR (Figure 3.3E). These data highlight the importance of both EGFR and CD44 and their active roles in the differentiation and signalling response.

3.2.3 Analysis of Cellular Membrane Dynamics of CD44 and EGFR in Fibroblasts

CD44 membrane dynamics change following differentiation. Fluorescence Recovery After Photobleaching (FRAP) was used to investigate receptor dynamics in the plasma membrane of fibroblasts and myofibroblasts (Figure 3.4). In fibroblasts, EGFR was bound in clusters, within discrete areas of the cell membrane (Figure 3.4A); and did not diffuse into the bleached zone (Figure 3.4B). CD44, however, diffused rapidly (<100 seconds) into the bleached area (Figure 3.4C). In myofibroblasts, EGFR was also found in static membrane domains (Figure 3.4D). In contrast to fibroblasts, however, CD44 on the surface of

myofibroblasts had a reduced mobility, with a diffusion constant of only 10% of that in fibroblasts (Figure 3.4E). The mobile fraction (MF) of CD44 receptors was also reduced from approximately 60% in fibroblasts to 15% in myofibroblasts. These results suggest that the loss of CD44 mobility in the membrane may be an important factor in the mechanism of myofibroblast induction.

3.2.4 Determination of the Cellular Localisation of CD44 and EGFR

The transmembrane receptor EGFR has been described to exist within lipid raft domains in tumour cells and neuronal cells [298, 299]; and can have ligand-independent activation outside of raft domains [288, 289, 300] – a possible mechanism through which CD44 may be responsible. CD44 itself has been documented to associate with different cellular structures, such as the cytoskeleton [282, 286] and membrane bound lipid rafts [279, 283]. To determine the cellular location where CD44 and EGFR co-localisation occurs, the chemicals cytochalasin-B (5μM), an inhibitor of actin formation; or nystatin (50μg/ml), a cholesterol sequestering agent and inhibitor of cholesterol synthesis, were used to pre-treat growth arrested cells for 1 hour, prior to incubation with TGF-β1 (10ng/ml) in serum-free medium for 72 hours. To assess each chemical's action on α-SMA stress-fibre formation, immunocytochemistry was used to visualise α-SMA (Figure 3.5A). In cells treated with either cytochalasin-B or nystatin, the ability for the cells to produce α-SMA fibres was abolished. To determine whether this effect was due to the loss of EGFR (green) and CD44 (red) co-localisation, fixed cells were stained using antibodies against each receptor (Figure 3.5B). It was observed that both chemical treatments resulted in loss of stress-fibre generation. The loss of receptor co-localisation was more prominent in cells treated with nystatin, with areas of co-localisation remaining following cytochalasin-B treatments. Analysis of mRNA expression of α-SMA (Figure 3.5C) and HAS2 (Figure 3.5D) was assessed to determine

changes in gene activation and transduction. Although both chemical treatments significantly down-regulated expression of both mRNAs, compared to TGF-β1 stimulated untreated cells, there remained a smaller activation of both genes with TGF-β1 in those cells pre-treated with cytochalasin-B. Nystatin pre-treatment prevented gene induction from TGF-β1 stimulation.

Assessment of total receptor and ERK1/2 signalling protein was required to determine whether chemical treatments were preventing signalling and gene induction; and hence myofibroblast differentiation, through disruption of cellular structures or through direct downregulation of proteins. Western blotting of total EGFR, CD44, and ERK1/2 proteins from whole cell lysate was performed (Figure 3.5E). Total EGFR protein remained unaltered in all experimental conditions, as shown in the densitometry graph. CD44 and ERK1/2 total protein was significantly down-regulated in cells treated with cytochalasin-B. These data suggest that the cellular location of CD44 interaction with EGFR was not the cytoskeleton, as co-localisation of the receptors persisted despite disruption of the actin cytoskeleton, suggesting lipid rafts as a potentially viable area of co-localisation. The loss of differentiation from cytochalasin-B treatment was likely not due to the loss of co-localisation, but primarily due to the nature of the chemical inhibition of actin formation and cytoskeletal disruption, with both CD44 and ERK1/2 - proteins with cytoskeletal association - reduced in pre-treated fibroblasts.

3.2.5 The Co-localisation of CD44-EGFR in Membrane-bound Lipid Raft Domains and the Role of Lipid Rafts in Differentiation

To investigate whether EGFR or CD44 were located in lipid rafts in primary human fibroblasts, Laser Confocal Scanning Microscopy was performed using cholera toxin subunit-B (CTX-B)-555 (TRITC) conjugate, which binds GM1 containing, cholesterol-rich regions of the cell-membrane (Figure 3.6). Figure 3.6A indicates that in fibroblasts, wherever EGFR

was located, there were also cholesterol-rich domains containing CTX-B (yellow merged images). In contrast, CTX-B and CD44 had areas of no co-localisation, in addition to some areas of co-localisation, as can be seen in the merged images. In myofibroblasts (Figure 3.6B), there was also co-localisation of EGFR with CTX-B at the cell surface (white arrows), although CTX-B binding was not exclusively found in areas positive for EGFR. In contrast to fibroblasts, however, CD44 on myofibroblasts was highly co-localised to areas positive for CTX-B (merged panel).

To confirm the involvement of lipid rafts, both nystatin and methyl-β-cyclodextrin (MβCD) were used independently (Figure 3.6C) to disrupt rafts. Following incubation of myofibroblasts with either compound, the co-localisation of both EGFR and CD44 with CTX-B was reduced. EGFR or CD44 expression was visible in areas absent of CTX-B binding (indicated by white arrows). The summary of results from three independent experiments, showing the degree of co-localisation and the intensity correlation quotient (ICQ), is shown in Figure 3.6D. These data indicate that there was a 4- to 5-fold decrease in EGFR association with CTX-B following nystatin treatment, before addition of TGF-β1. They also demonstrate a 3-fold increase in CD44 association with CTX-B, following myofibroblastic induction with TGF-β1, which is lost in cells pre-treated with nystatin.

To further test the hypothesis that lipid rafts serve as the primary location of EGFR and co-localisation with CD44 following differentiation, lipid rafts were biochemically isolated by ultracentrifugation and the collected fractions were examined for the lipid raft markers; Cav-1 and CTX-HRP. EEA1 was used to determine non-raft regions of the cell membrane. In fibroblasts, EGFR was primarily found in lipid raft domains (Cav-1/CTX-B positive fractions; 5 & 6) and CD44 in non-raft regions (EEA-1 positive fractions; 8, 9 & 10) (Figure 3.7A). In differentiated myofibroblasts, a proportion of CD44 was found to move into the fractions positive for lipid raft markers, demonstrating that CD44 existed in two populations, within

and outside lipid raft regions (Figure 3.7B). The quantification of receptors in lipid raft fractions (Figure 3.7C) indicated that the quantity of EGFR found in lipid raft fractions did not alter significantly between cellular phenotype. The presence of CD44 in lipid raft fractions significantly increased from approximately 10% to more than 40%, following differentiation. Cellular expression of Cav-1 (Figure 3.7D) had no significant change between fibroblasts and myofibroblasts, signifying that the increase of CD44 directed toward lipid raft fractions was a primary change as a result of differentiation, and not a consequence of an increased generation of Cav-1 positive rafts.

To investigate the degree to which lipid rafts were involved in the mechanism controlling myofibroblast induction, α-SMA expression was assessed by immunocytochemistry (Figure 3.8A). α-SMA was markedly downregulated in cells pre-treated with nystatin. QPCR (Figure 3.8B) demonstrated that this was also a transcriptional effect on α-SMA mRNA. Co-localisation of EGFR and CD44 in fibroblasts pre-treated with nystatin before the induction of differentiation with TGF-β1 was prevented, indicating that lipid rafts were key locations of the EGFR-CD44 association (Figure 3.8C). Statistical analysis showed a decrease in CD44 co-localisation with EGFR in myofibroblasts from 70% to approximately 10%, if cells were pre-treated with nystatin (Figure 3.8D). Flow cytometry and Western blot analysis showed that nystatin treatment did not alter the expression nor total protein levels of EGFR or CD44 over the course of treatment times (Supplementary Figure 3.SA). These results support the importance of lipid rafts in the TGF-β1-dependent differentiation pathway.

3.2.6 TGF-β1 Activation of the ERK and CaMKII Signalling Cascade

Previous research has shown that ERK1/2 are involved in the differentiation and proliferation of various cell types [195, 301-304]. Western blotting was used to assess the degree of phosphorylation of these kinases, following incubation with TGF-β1 (Figure 3.9A-B). Figure

3.9A shows the characteristic bi-phasic phosphorylation of ERK1/2, peaking at 10 minutes and again at 3 hours after the addition of TGF-β1.

CaMKII is a kinase that is involved in cytoskeletal remodelling and the differentiation response (44, 45). Western blotting for phosphorylated CaMKII (Figure 3.9B) showed that CaMKII was also activated and its phosphorylation had a similar bi-phasic time-dependent activation to ERK phosphorylation, implicating CaMKII in the TGF-β1-dependent signalling pathways involved in myofibroblast differentiation. Neither ERK1/2 nor CaMKII phosphorylation fluctuated over the 3 hours, if cells remained in serum-free conditions (Supplementary Figure 3.SB)

Whether ERK and CaMKII activation were independent of each other was investigated using the chemical inhibitor of ERK phosphorylation, PD98059; and the chemical inhibitor of CaMKII, KN-93. PD98059 inhibited ERK activation (Figure 3.9C) following TGF-β1 stimulation, attenuating both peaks of the bi-phasic activation profile. Similarly, KN-93 attenuated both peaks of CaMKII activation (Figure 3.9D), as expected. In addition, KN-93 had no effect on ERK1/2 signalling and the bi-phasic activation was retained (Figure 3.9E). Interestingly, PD98059 inhibited CaMKII phosphorylation (Figure 3.9F), suggesting that ERK activation was a necessary upstream mediator of CaMKII activation. Since CaMKII activation was abolished following incubation with the chemical inhibitor of ERK1/2, the results shown here suggest that following the addition of TGF-β1, ERK is activated first leading to the down-stream activation of CaMKII.

3.2.7 The Relationship Between EGFR-CD44 Co-localisation in Lipid Rafts and the Activation of Early Differentiation Signalling of the EGFR-ERK1/2-CaMKII Pathway

To confirm that it was raft-associated co-localisation that was responsible for the induction of ERK and CaMKII, nystatin was used to disrupt lipid rafts and then Western blotting was used to examine the phosphorylation of EGFR, ERK1/2 and CaMKII (Figure 3.10). Nystatin inhibited the early signalling phase of TGF-β1-dependent EGFR (Figure 3.10A), ERK (Figure 3.10B); and CaMKII (Figure 3.10C) phosphorylation, without affecting the late activation phase of either kinase. The loss of the early ERK and CaMKII signalling phases and the fibroblast resistance to differentiation following nystatin treatment, confirmed that the early signalling phase was primarily responsible for initiation of fibroblast to myofibroblast differentiation, as previously reported [267]; and that it was initiated in lipid rafts. Additionally, the expression of TGF-βRI and the activation of the Smad2 pathway remained unaffected by nystatin treatment (Supplementary Figure 3.SC).

3.2.8 The Organisation of CD44 Co-localisation with EGFR and Downstream Intracellular Signalling by HA

HAS2-regulated HA synthesis is a key mediator of TGF-β1-dependent myofibroblast differentiation and proliferation. HAS2 is the enzyme primarily responsible for upregulation of HA synthesis in fibroblasts, following TGF-β1-induced differentiation to myofibroblasts [244, 297, 305, 306]. The Institute of Nephrology has previously shown that HAS2 is an important mediator of differentiation in fibroblasts [160, 195]. Transfection with siRNA targeting HAS2 (siHAS2) reduced HAS2 mRNA expression by 4-fold and prevented HAS2 upregulation in response to TGF-β1 (Figure 3.11A). The upregulation of α-SMA mRNA by TGF-β1 was prevented by siHAS2 transfection (Figure 3.11B); and CD44 co-immunoprecipitation with EGFR was also prevented following siHAS2 transfection (Figure

3.11C). Whether HA production by HAS2 was a direct regulator of the ERK and CaMKII intracellular signalling pathways leading to phenotypic change was investigated by Western blotting for protein phosphorylation following transfection with siHAS2 or scrambled siRNA. The fibroblasts transfected with siHAS2 had attenuated TGF-β1 activation of EGFR (Figure 3.11D), ERK (Figure 3.11E) and CaMKII (Figure 3.11F). In addition, both the early and late peaks of the bi-phasic signalling pattern were lost. The loss of early ERK and CaMKII phosphorylation peaks supports previous studies that have shown that HAS2 impairment in aged cells inhibits fibroblast differentiation [160]. In addition, the attenuation of the late phosphorylation peaks supports previous findings, highlighting HAS2 and HA as necessary mediators of fibroblast proliferation [195].

3.2.9 The Role of HA in the Regulation of CD44 Membrane Dynamics

To determine whether cell-surface HA was necessary for CD44 co-localisation with EGFR and membrane dynamics and behaviour, Confocal Microscopy and FRAP analysis were used, following hyaluronidase treatment (Figure 3.12). Interestingly, CD44 co-localisation with EGFR was partially lost, following hyaluronidase treatment (Figure 3.12A-B). CD44 movement was restored in myofibroblasts incubated with hyaluronidase from both *Streptomyces* (S) and bovine testicular (BT) sources (Figure 3.12C-E). However, the MF indicated that hyaluronidase alone was not sufficient to restore mobility to the levels observed in fibroblasts. These data suggest that HAS2 production of the HA pericellular coat was partly responsible for the sequestration and anchoring of CD44 into lipid raft domains, where it co-localised with EGFR and enables the resulting differentiation signalling response.

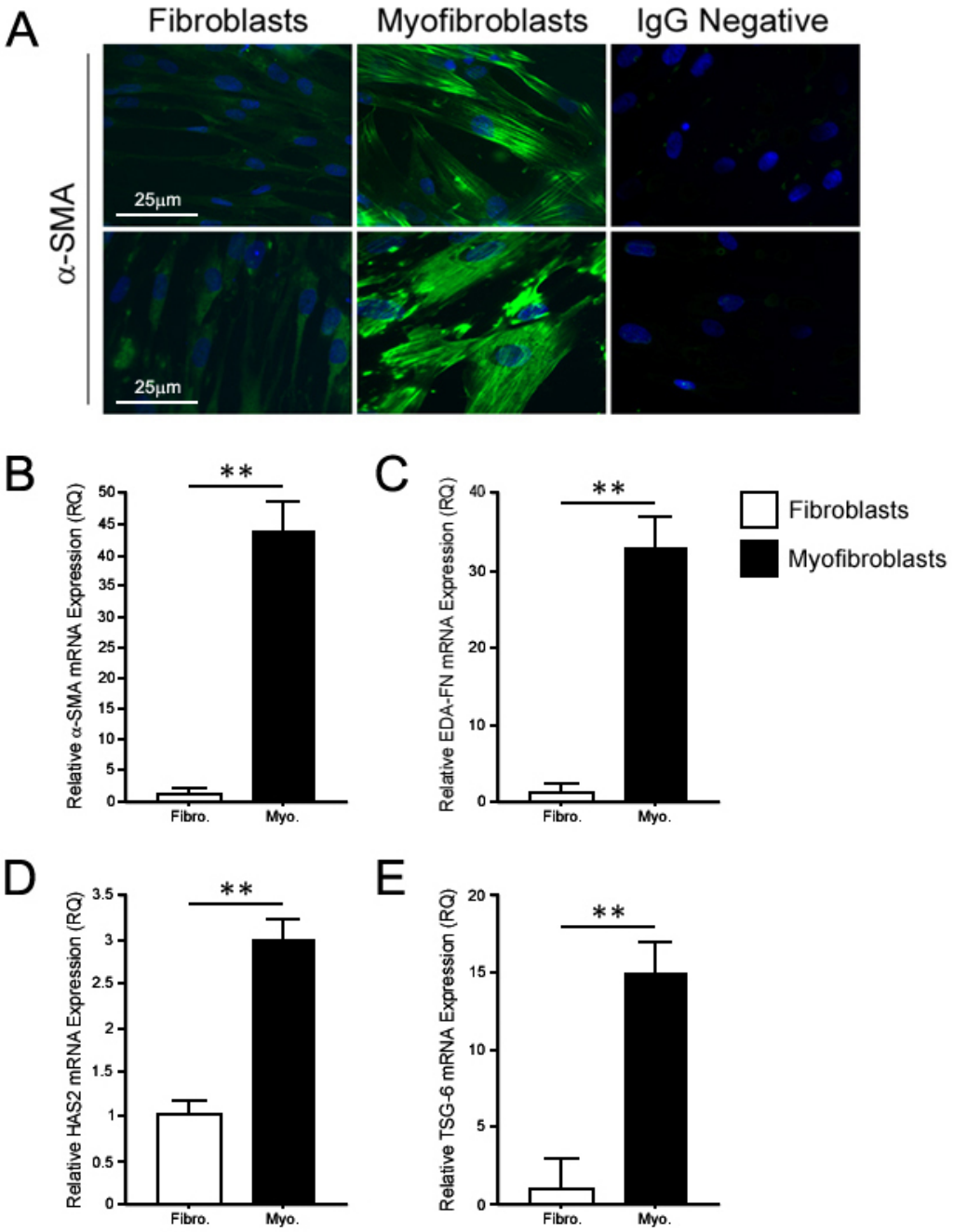

Figure 3.1. Phenotypic Changes in Myofibroblast Differentiation. A. Cells were grown to 70% confluent monolayers and growth arrested for 48 hours. Cells were then incubated in serum-free medium alone (fibroblasts) or in medium containing 10ng/ml TGF-β1 for 72 hours (myofibroblasts). The expression of α-SMA (green) was examined by immunocytochemistry, nuclei were visualised by Hoechst stain. Images shown are a representation of 5 independent experiments. Original magnification x400. The mRNA expression of **B.** α-SMA, **C.** EDA-FN, **D.** HAS2 and **E.** TSG-6, was analysed using QPCR. Results are shown as the mean ± s.e.m. of 3 individual experiments. ***P=<0.01*.

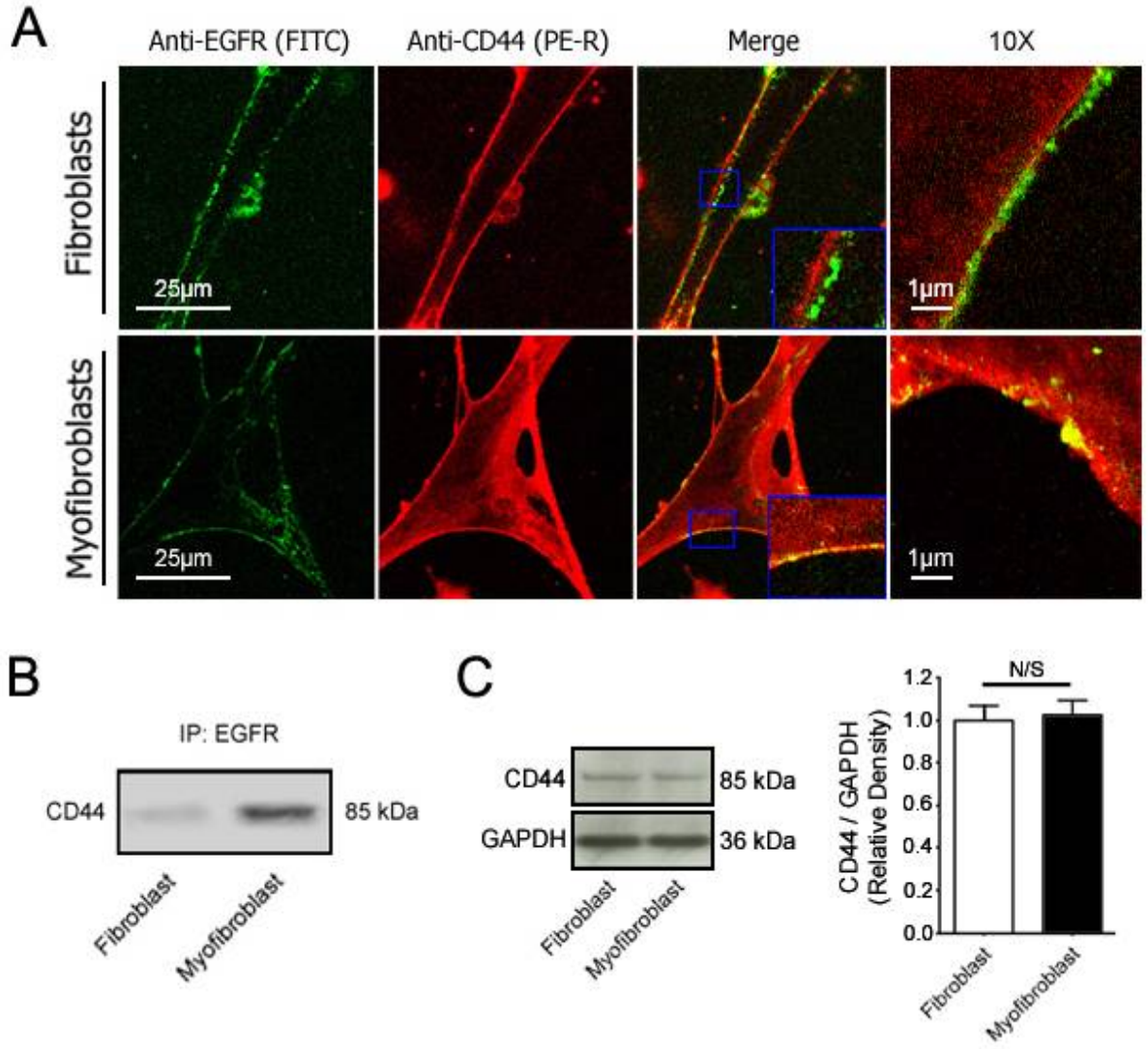

Figure 3.2. CD44 and EGFR Co-localisation in Myofibroblasts. A. Cells were grown to 70% confluent monolayers and growth arrested for 48 hours. Cells were then incubated in serum-free medium alone (fibroblasts) or in medium containing 10ng/ml TGF-β1 for 72 hours (myofibroblasts). Confocal Laser Scanning Microscopy was used to examine the expression of EGFR (green; FITC) and CD44 (red; PE-R). Areas of co-localisation are shown in the merged images (yellow; enlarged images shown in blue boxes). Images shown are a representation of 5 independent experiments. Original magnification x630. **B.** Co-localisation of EGFR and CD44 was analysed by immunoprecipitation for EGFR, followed by immunoblotting for CD44. Image shown is representative of 3 individual experiments. **C.** Western blot analysis of total CD44 protein in fibroblasts and myofibroblasts. GAPDH was used as a loading control. Representative blot is shown. Densitometry graph shown is ± s.e.m. of 3 individual experiments. *N/S* = no

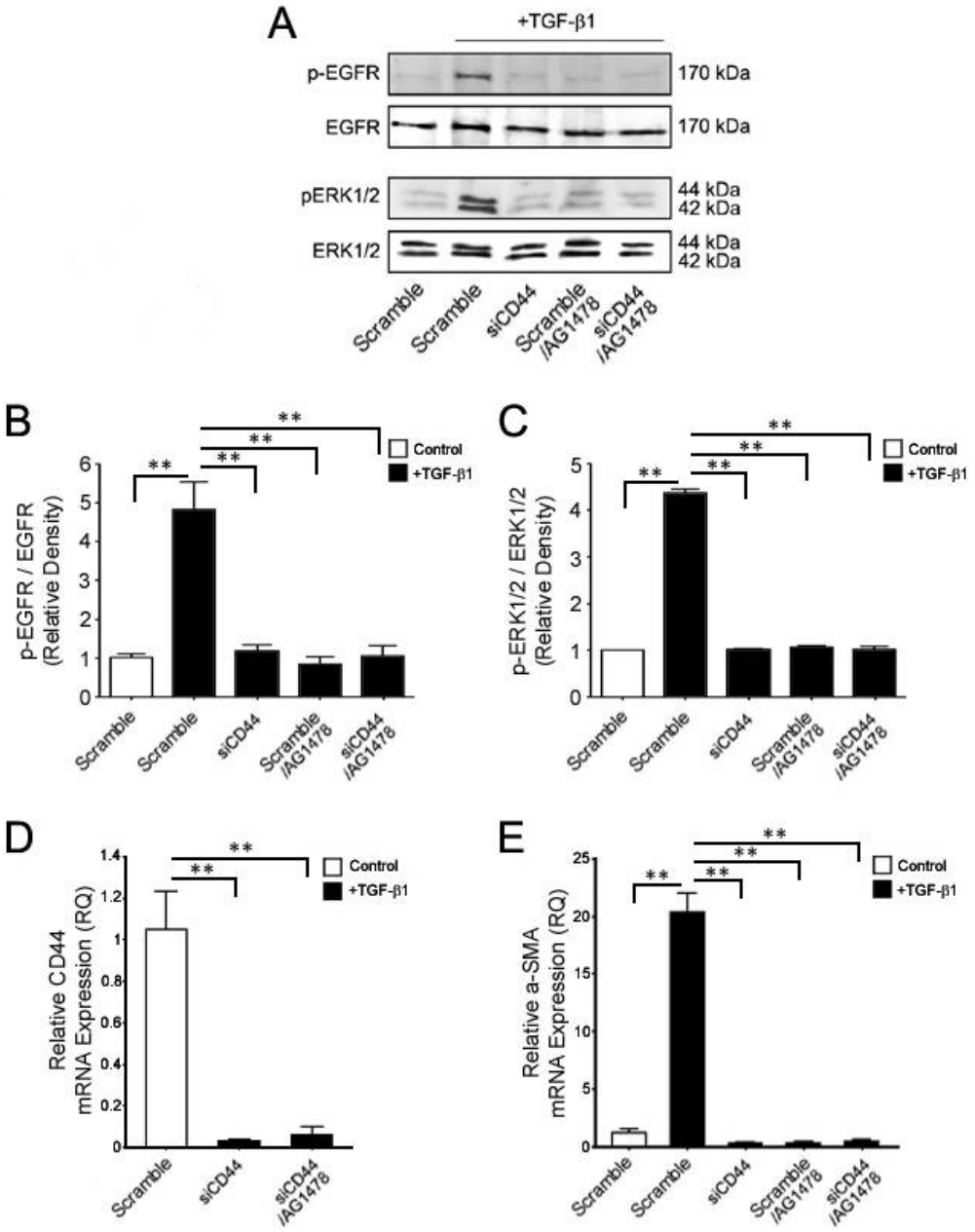

Figure 3.3. Both CD44 and EGFR are Required for Signal Transduction. A. Fibroblasts were transfected with a scrambled siRNA sequence or siRNA targeting CD44, prior to treatments with or without AG1478 for 1 hour, before TGF-β1 for 72 hours. Phosphorylation of EGFR and ERK1/2 was analysed by Western blotting. Total EGFR and ERK1/2 proteins were used as loading controls. Image shown is representative of 3 independent experiments. **B.** Densitometric analysis of p-EGFR, normalised to total EGFR. Graph shows ± s.e.m. of 3 independent experiments. **C.** Densitometric analysis of p-ERK1/2, normalised to total ERK1/2. Graph shows ± s.e.m. of 3 independent experiments. **D.** QPCR was used to confirm CD44 mRNA knockdown by siCD44. Results shown are ± s.e.m. of 3 individual experiments. **E.** QPCR was used to analyse α-SMA mRNA, following siCD44 and 10μM AG1478 cellular treatments. Results shown are ± s.e.m. of 3 individual experiments. ***P=<0.01*.

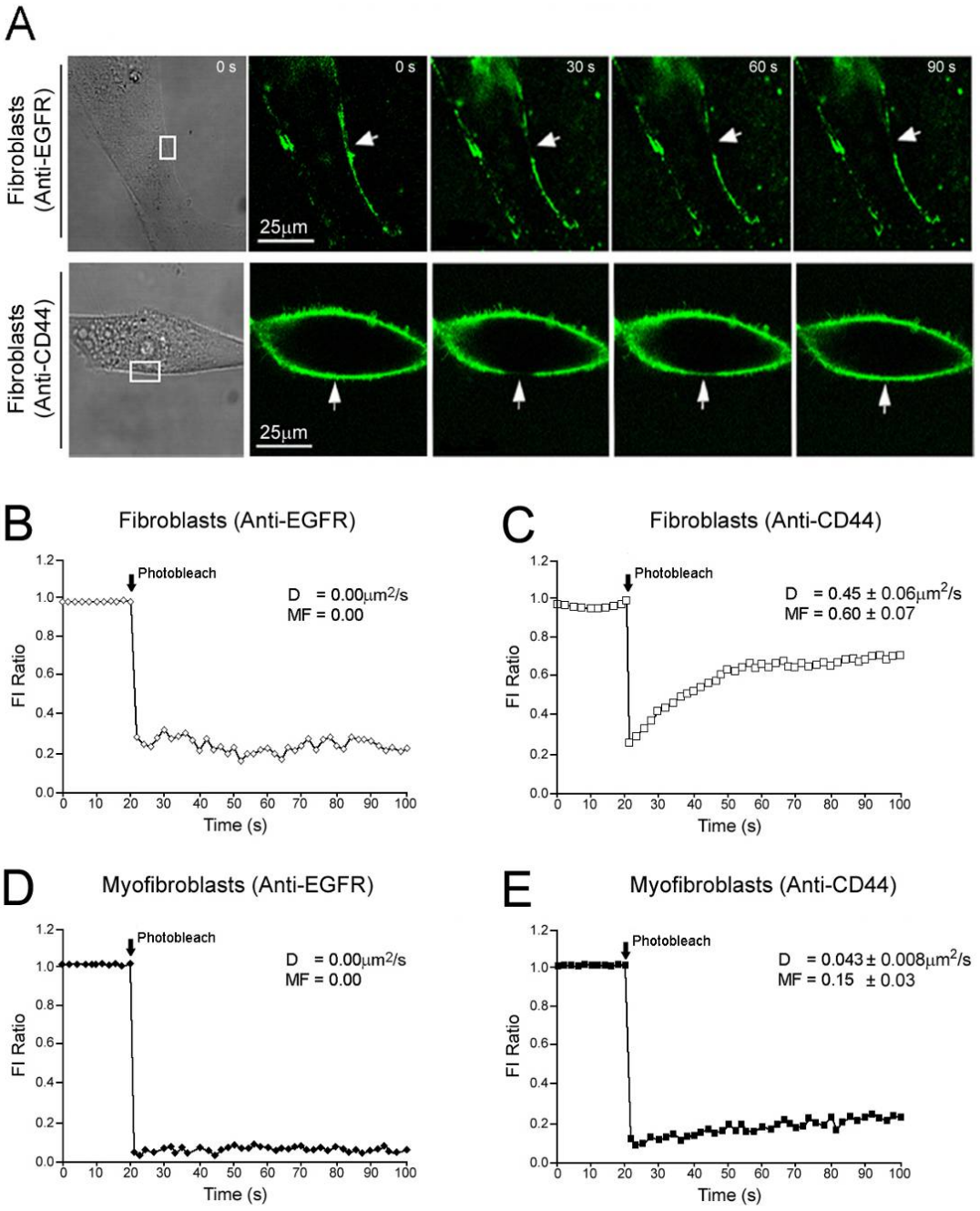

Figure 3.4. The Membrane Dynamics of CD44 and EGFR. A. Sample time-lapse series of fluorescent recovery, after photobleaching (FRAP) experiments. Original magnification x630. Fibroblasts or myofibroblasts were grown to 70% confluent monolayers on 22mm diameter glass coverslips, in 35mm 6-well tissue culture plates. Cells were growth arrested in serum-free medium for 48 hours. FRAP was performed at 37°C by photobleaching an approximately 10μm area of the cell membrane (indicated by white boxes on bright-field images). The recovery of fluorescence into this area (indicated by white arrows) was quantified and expressed as a fraction of the fluorescence intensity (FI) of a second region of membrane, outside of the photobleached area (FI Ratio). Complete quantified time-courses, average diffusion constants (D) and mobile fractions (MF) are shown for: **B.** EGFR in fibroblasts; **C.** CD44 in fibroblasts; **D.** EGFR in myofibroblasts; and **E.** CD44 in myofibroblasts. All results shown are representative of 5 independent experiments. Statistics shown are ± s.e.m. of 5 independent experiments.

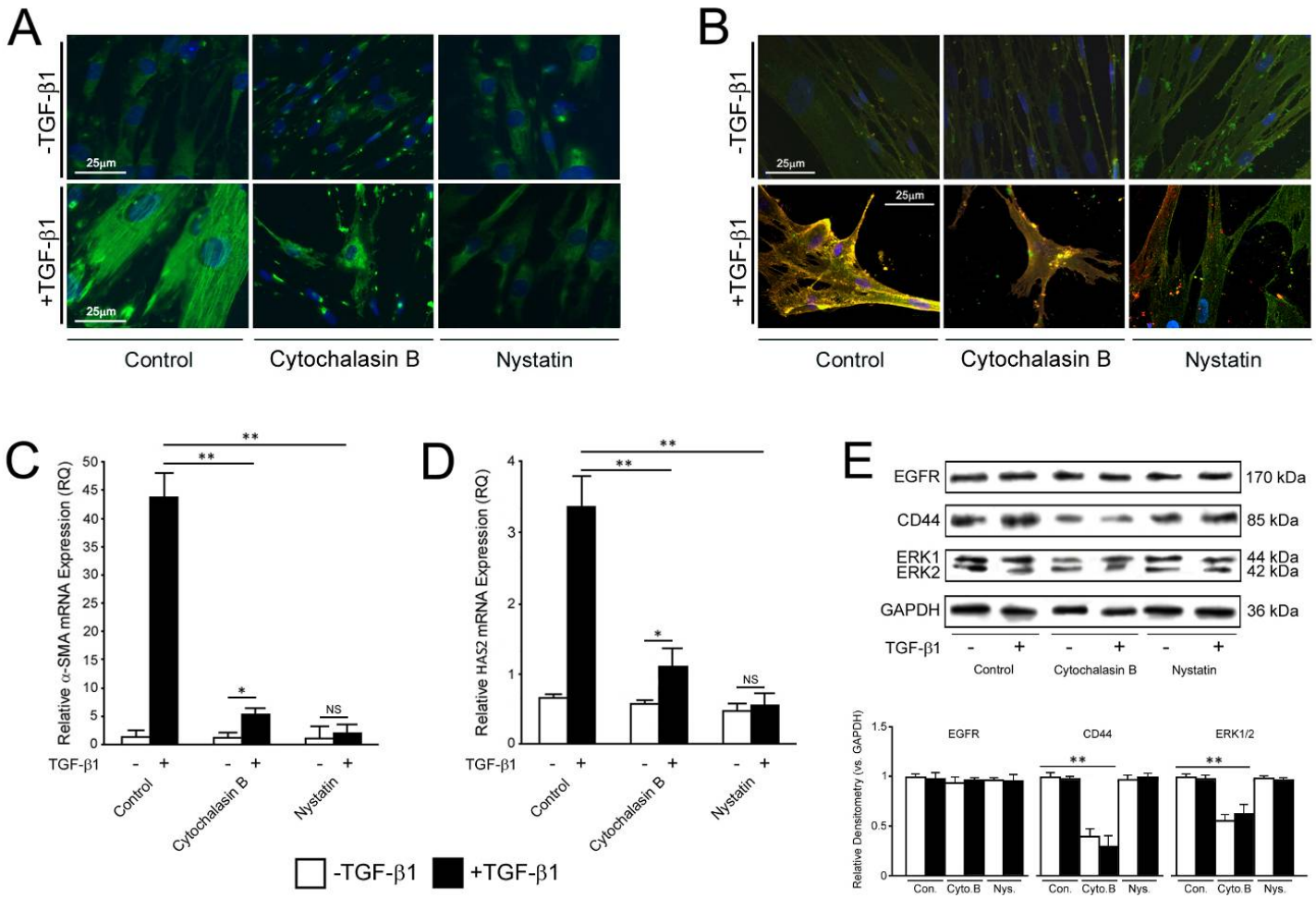

Figure 3.5. Co-localisation is Lipid Raft Associated and Not Cytoskeletal. Cells were grown to 70% confluence, growth arrested for 48 hours and treated with 5μM cytochalasin-B or 50μg/ml nystatin for 1 hour. Following 72 hours of incubation in serum-free media with or without 10ng/ml TGF-β1, cells were fixed and stained for **A.** α-SMA visualisation or **B.** EGFR (green) and CD44 (red) (areas of co-localisation in yellow). Original magnification x630. The expression of **C.** α-SMA mRNA and **D.** HAS2 mRNA, were assessed by QPCR. Results are shown as the mean ± s.e.m. of 3 individual experiments. **E.** Western blotting and densitometry analysis of total EGFR, CD44 and ERK1/2 proteins, from whole cell lysates. Immunoblots are representative of 3 individual experiments and the densitometry analysis is displayed as the mean ± s.e.m. of 3 individual experiments. *$P=<0.05$, **$P=<0.01$, *N/S* = no significance.

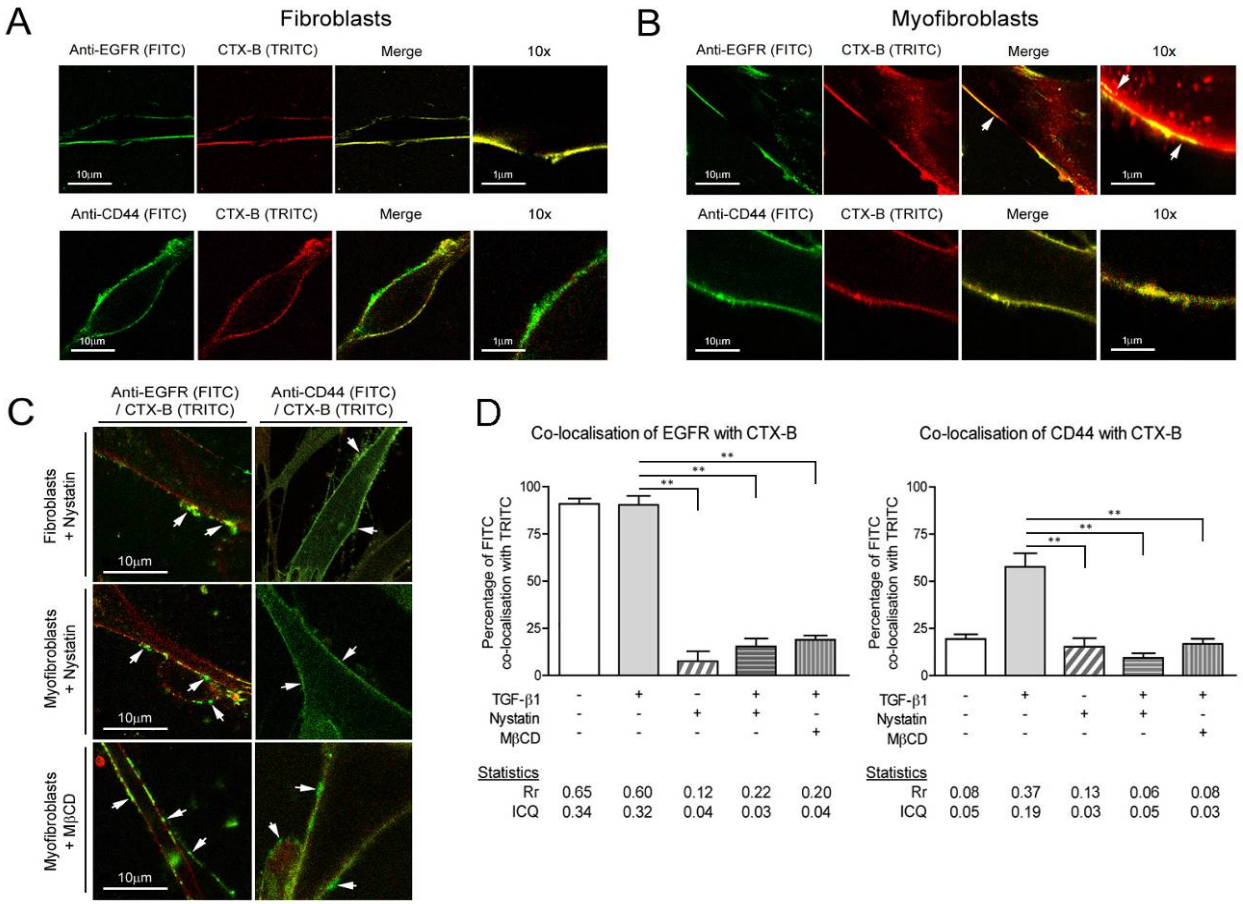

Figure 3.6. CD44 and EGFR Co-localisation with Lipid Raft Marker CTX-B. Fibroblasts or myofibroblasts were grown on 22mm diameter glass coverslips and examined for **A.** EGFR (green; FITC) and CTX-B binding (red; TRITC); and **B.** CD44 (green; FITC) and CTX-B binding (red; TRITC), using Confocal Laser Scanning Microscopy (areas of co-localisation shown in yellow; areas of CTX-B binding with EGFR marked by white arrows). Images are representative of 5 individual experiments. Original magnification x630. **C.** Cells were treated with nystatin (50μg/ml) or MβCD (10mM) for 1 hour, before examination of EGFR or CD44 expression (green; FITC) and CTX-B binding (red; TRITC), (areas of EGFR or CD44 expression without CTX-B binding marked by white arrows). Images are representative of 3 individual experiments. Original magnification x630. **D.** Co-localisation of EGFR or CD44 with CTX-B was quantified (Mander's Co-localisation Coefficient). Statistical analysis includes the average Pearson's Correlation Coefficient (Rr) and Intensity Correlation Quotient (ICQ) for each experimental condition. Results shown are ± s.e.m. of 3 independent experiments. ***P=<0.01*.

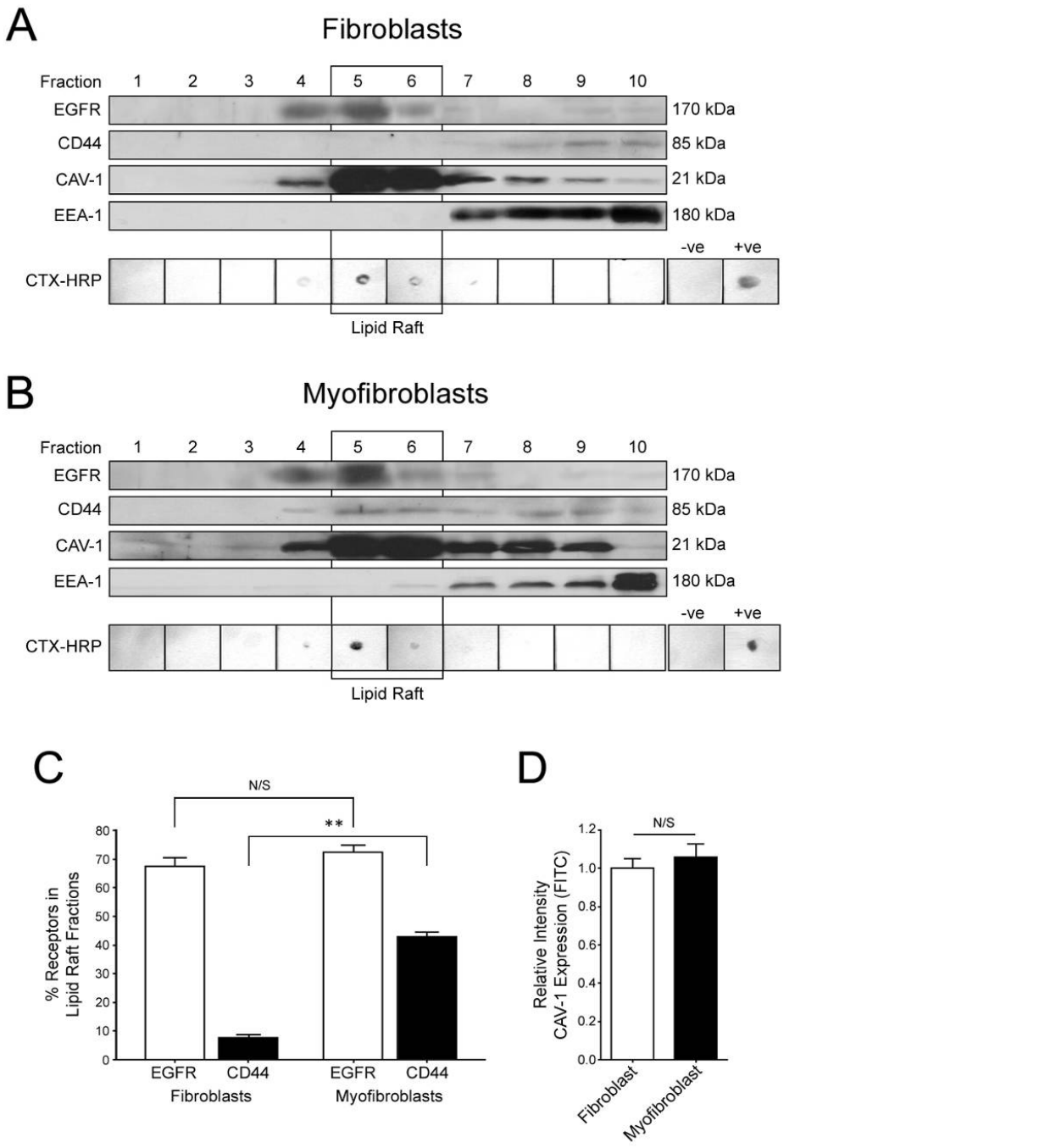

Figure 3.7. Membrane Fraction Analysis in Fibroblasts and Myofibroblasts. Cells were grown to confluence and growth arrested for 48 hours. Cells were incubated in **A.** serum-free medium alone (fibroblasts) or **B.** serum-free medium containing 10ng/ml TGF-β1 for 72 hours (myofibroblasts). Cellular membrane preparations were separated in a discontinuous OptiPrep gradient by ultracentrifugation. Fractions were analysed for the presence of EGFR and CD44. Cav-1 was used to detect fractions positive for lipid rafts, and EEA-1 for non-raft fractions. Lipid raft fractions were confirmed using CTX-HRP dot-blots for each fraction. Positive and negative control dot-blots were used to confirm the specificity of CTX-HRP. **C.** Quantification of the percentage of EGFR and CD44 found within lipid raft fractions 5-6 in fibroblasts and myofibroblasts. Results shown are ± s.e.m. of 3 independent experiments. **D.** Flow Cytometry analysis of cell surface expression of Cav-1 in fibroblasts and myofibroblasts. Unlabelled cells were used as intensity controls. Bar graph of relative intensity shown is ± s.e.m. of 3 individual experiments. *N/S = no significance*; ***P=<0.01*.

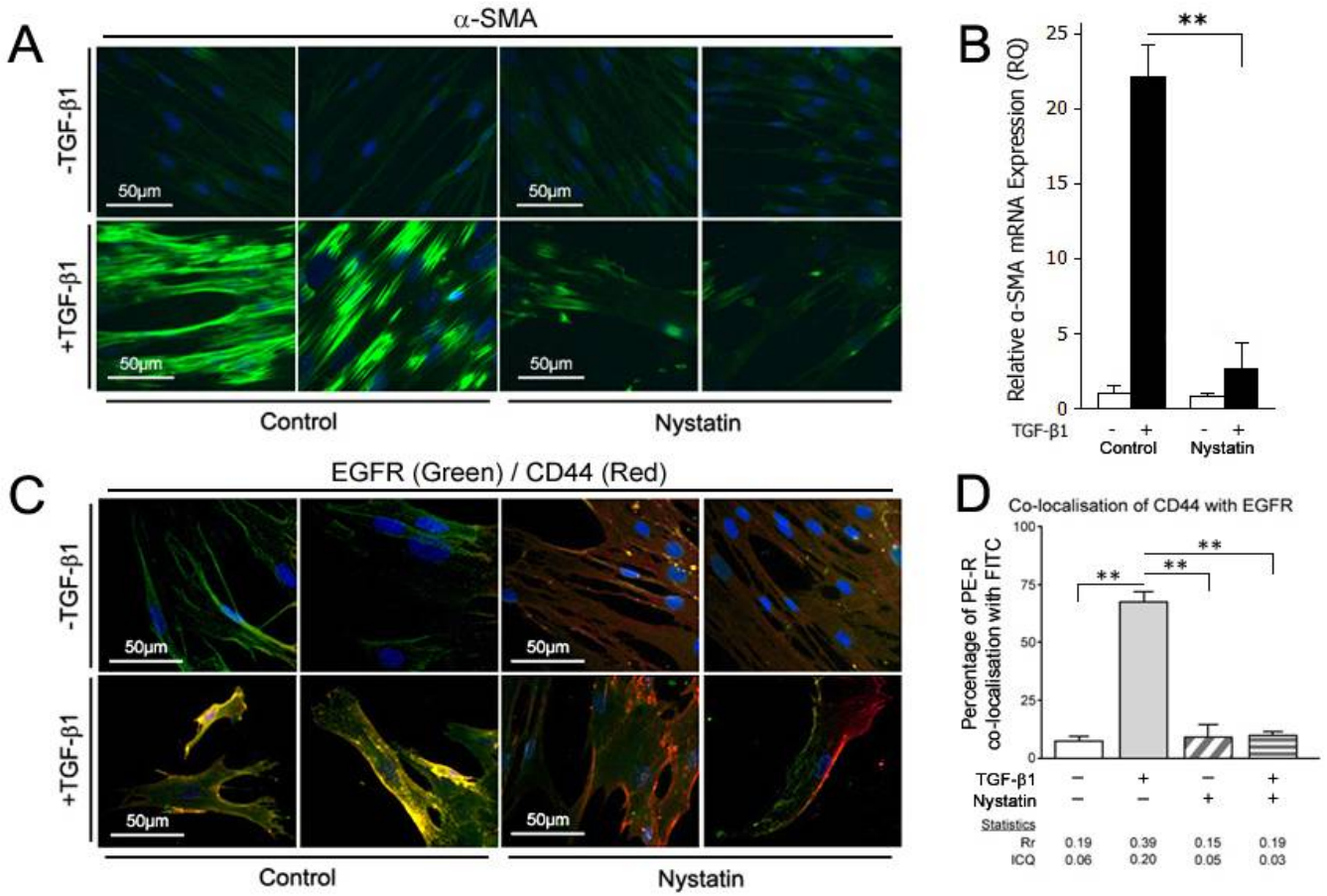

Figure 3.8. Lipid Raft Disruption Inhibits Myofibroblast Differentiation. Cells were grown to 70% confluence and growth arrested for 48 hours. Cells were incubated with 50μg/ml nystatin for 1 hour, before incubation in serum-free medium alone or containing 10ng/ml TGF-β1 for 72 hours. **A.** α-SMA expression (green) was examined by immunocytochemistry. Nuclei visualised by Hoechst stain (blue). Naïve IgG was used for negative controls. Images are representative of 3 independent experiments. Original magnification: x400. **B.** Cells were examined for α-SMA mRNA using QPCR. Results are shown as the mean ± s.e.m. of 3 individual experiments. **C.** EGFR (green; FITC) and CD44 (red; PE-R) expression was examined by immunocytochemistry. Areas of co-localisation are shown in yellow. Nuclei visualised by Hoechst stain (blue). Naïve IgG was used for negative controls. Images are representative of 5 individual experiments. Original magnification: x400. **D.** The co-localisation of CD44 with EGFR was quantified (Mander's Co-localisation Coefficient). Statistical analysis includes the average Pearson's Correlation Coefficient (Rr) and Intensity Correlation Quotient (ICQ) for each experimental condition. Results shown are ± s.e.m. of 5 individual experiments. ***P=<0.01*.

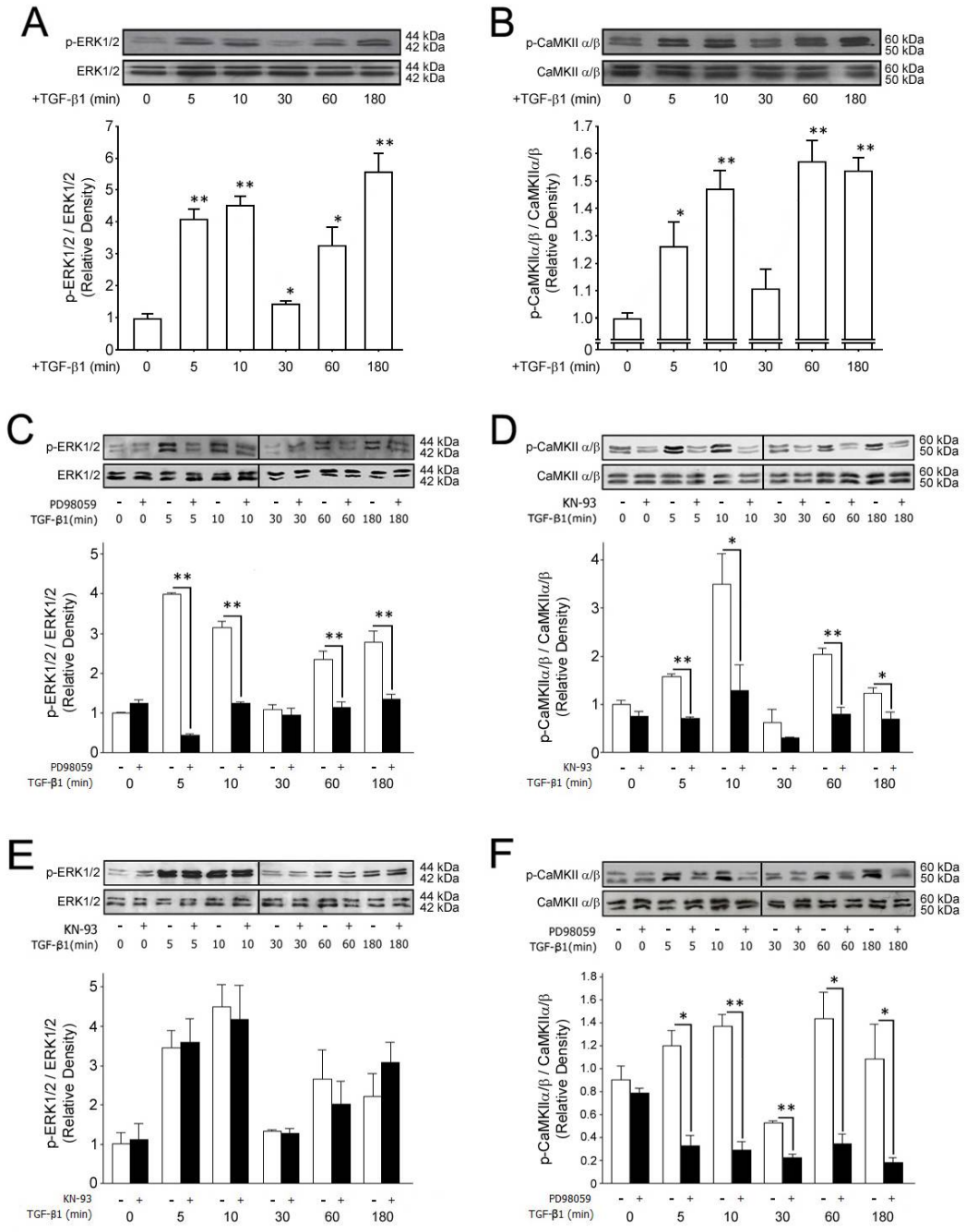

Figure 3.9. Intracellular Signalling Through ERK1/2 and CaMKII. Confluent fibroblast monolayers were growth arrested for 48 hours and were subsequently incubated with 10ng/ml TGF-β1, for up to 3 hours. The phosphorylation of **A.** ERK1/2 and **B.** CaMKII proteins was assessed by Western blot analysis at the indicated times. Western blot analysis for the appropriate total proteins was performed to ensure equal loading of protein samples. Following scanning densitometry, phosphorylated ERK1/2 and CaMKII expression was corrected for the expression of total ERK1/2 and CaMKII protein respectively; and is represented as ± s.e.m. of 3 separate experiments. Cells were pre-treated with 10μM MEK/ERK inhibitor PD98059(+) or left untreated(-) (**C.** and **F.**), or 10μM CaMKII inhibitor KN-93(+) with the inactive isomer KN-92(-) as a control (**D.** and **E.**) for 1 hour. Phosphorylation of ERK1/2 (**C.** and **E.**) and CaMKII (**D.** and **F.**) proteins was assessed by Western blot analysis at the indicated times. Western blot analysis for the appropriate total proteins was performed to ensure equal loading of protein samples. Following scanning densitometry, alterations in phosphorylated ERK1/2 and CaMKII expression were corrected for the expression of total ERK1/2 and CaMKII protein, respectively. Representative blots of 3 independent experiments are shown and densitometry graphs show ± s.e.m. of 3 separate experiments. **P=<0.05*; ***P=<0.01*.

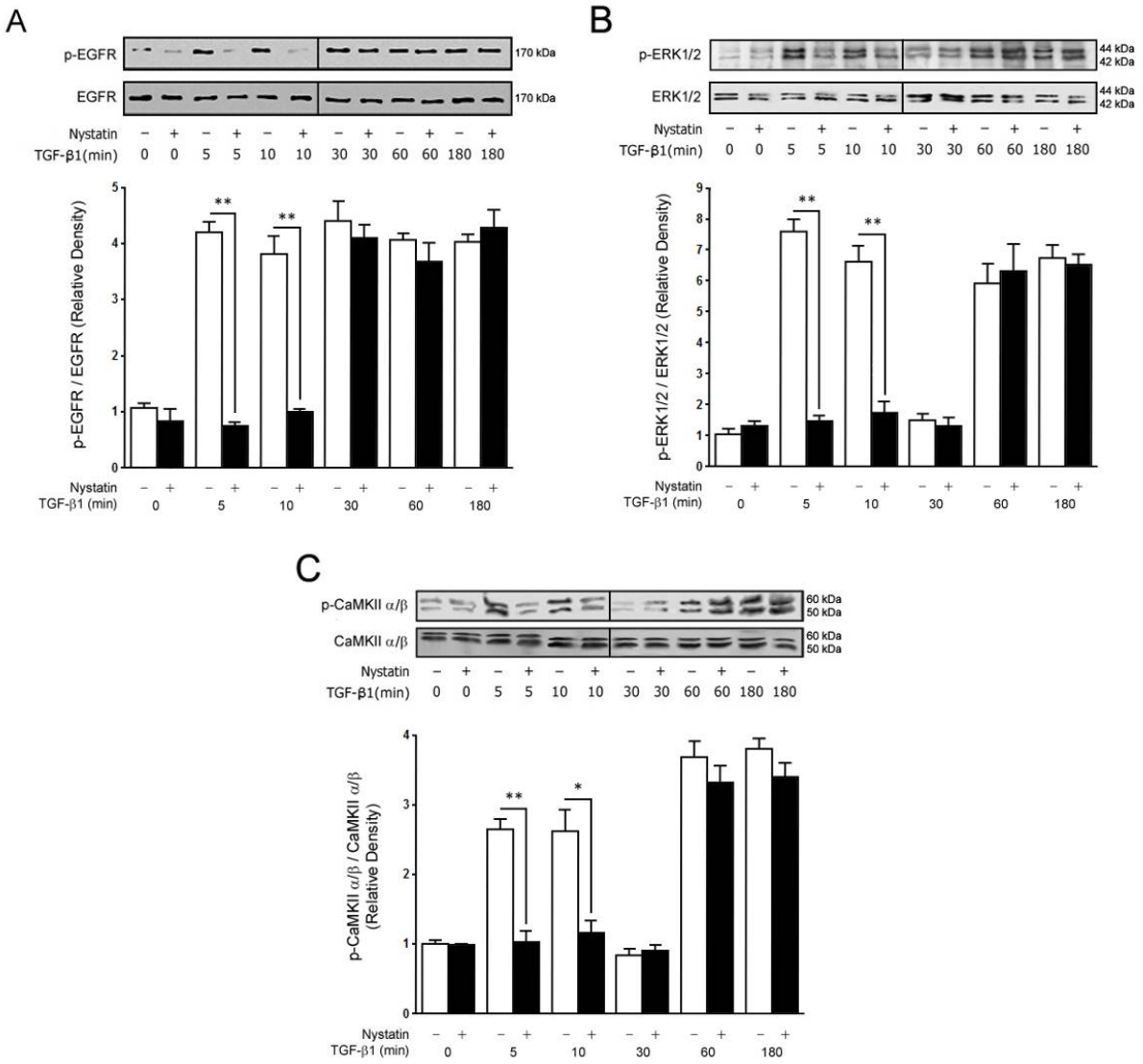

Figure 3.10. The Early Phase of Signalling is Dependent on Lipid Raft Integrity. Confluent monolayers of fibroblasts were growth arrested in serum-free medium for 48 hours. Subsequently, cells were incubated with (+) or without (-) 50μg/ml nystatin for 1 hour, before incubation with 10ng/ml TGF-β1 for up to 3 hours. **A.** Phosphorylation of EGFR was assessed by Western blot analysis at the indicated times. Western blot analysis for total EGFR protein was performed to ensure equal loading of protein samples. Densitometry graph shows ± s.e.m. of 3 individual experiments. **B.** Phosphorylation of ERK1/2 was assessed. Western blot analysis for total ERK1/2 protein was performed to ensure equal loading of protein samples. Densitometry graph shows ± s.e.m. of 3 individual experiments. **C.** Phosphorylation of CaMKII was assessed. Western blot analysis for total CaMKII protein was performed to ensure equal loading of protein samples. Densitometry graph shows ± s.e.m. of 3 individual experiments. All blots shown are representative of 3 separate experiments. **P=<0.05*; ***P=<0.01*.

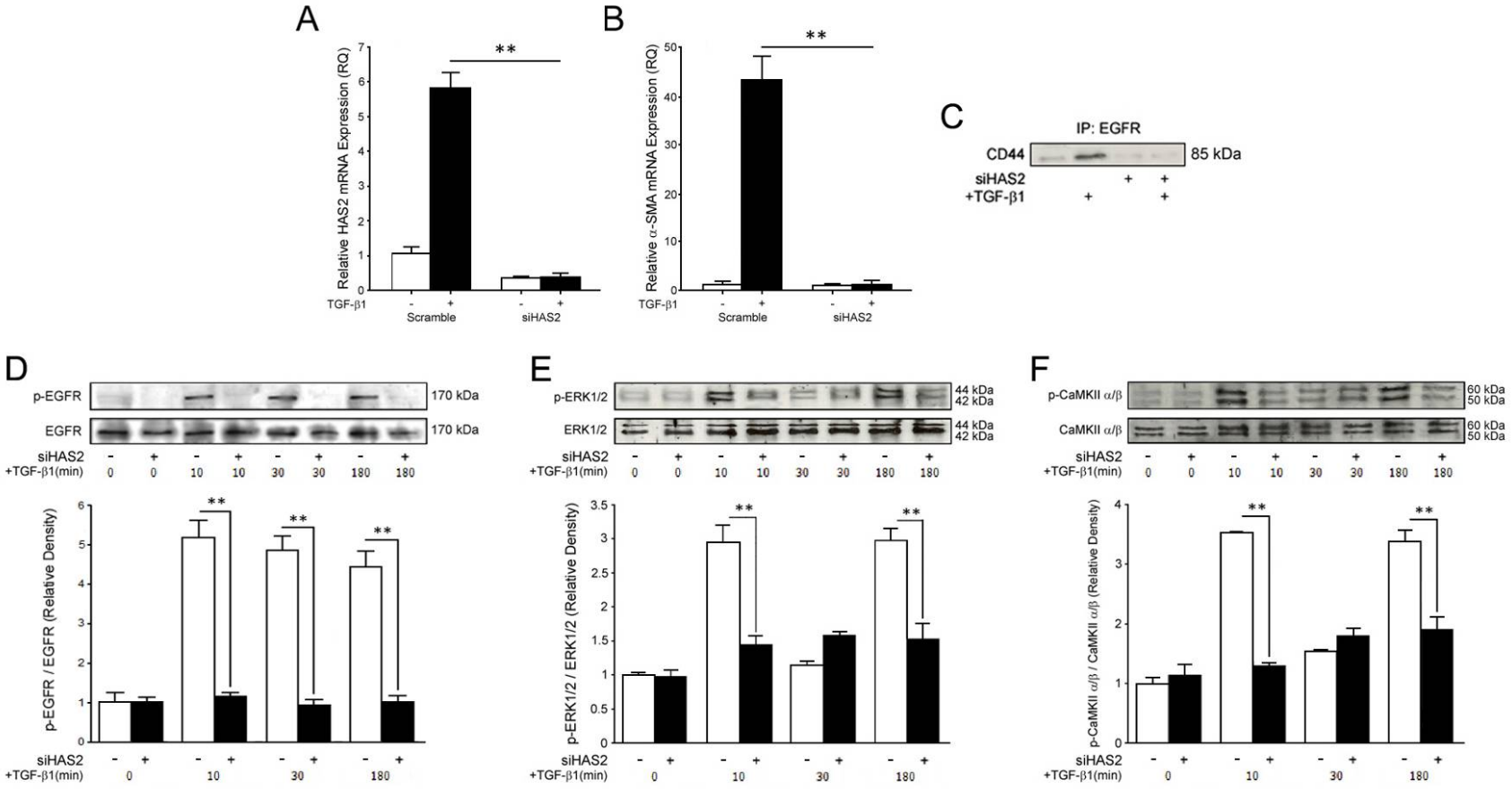

Figure 3.11. CD44-EGFR Co-localisation and Signalling is HA-regulated. Fibroblasts were grown to 70% confluence and were growth arrested in serum-free medium for 24 hours. Subsequently, cells were transfected with scrambled siRNA (control) or HAS2 siRNA for 24 hours, before incubation with 10ng/ml TGF-β1 for up to 72 hours. **A.** QPCR analysis to confirm knockdown of HAS2 mRNA. Data shown is ± s.e.m. of 3 individual experiments. **B.** QPCR was used to examine α-SMA mRNA expression. Data shown is ± s.e.m. of 3 individual experiments. **C.** Immunoprecipitation of EGFR followed by immunoblotting of CD44. Image shown is representative of 3 separate experiments. **D.** Western blot analysis of phosphorylated and total EGFR at the indicated times and corrected densitometry graph. **E.** Western blot analysis of phosphorylated and total ERK1/2 at the indicated times and corrected densitometry graph. **F.** Western blot analysis of phosphorylated and total CaMKII at the indicated times and corrected densitometry graph. All blots shown are representative of 3 separate experiments and all densitometry graphs show ± s.e.m. of 3 separate experiments. ***P=<0.01*.

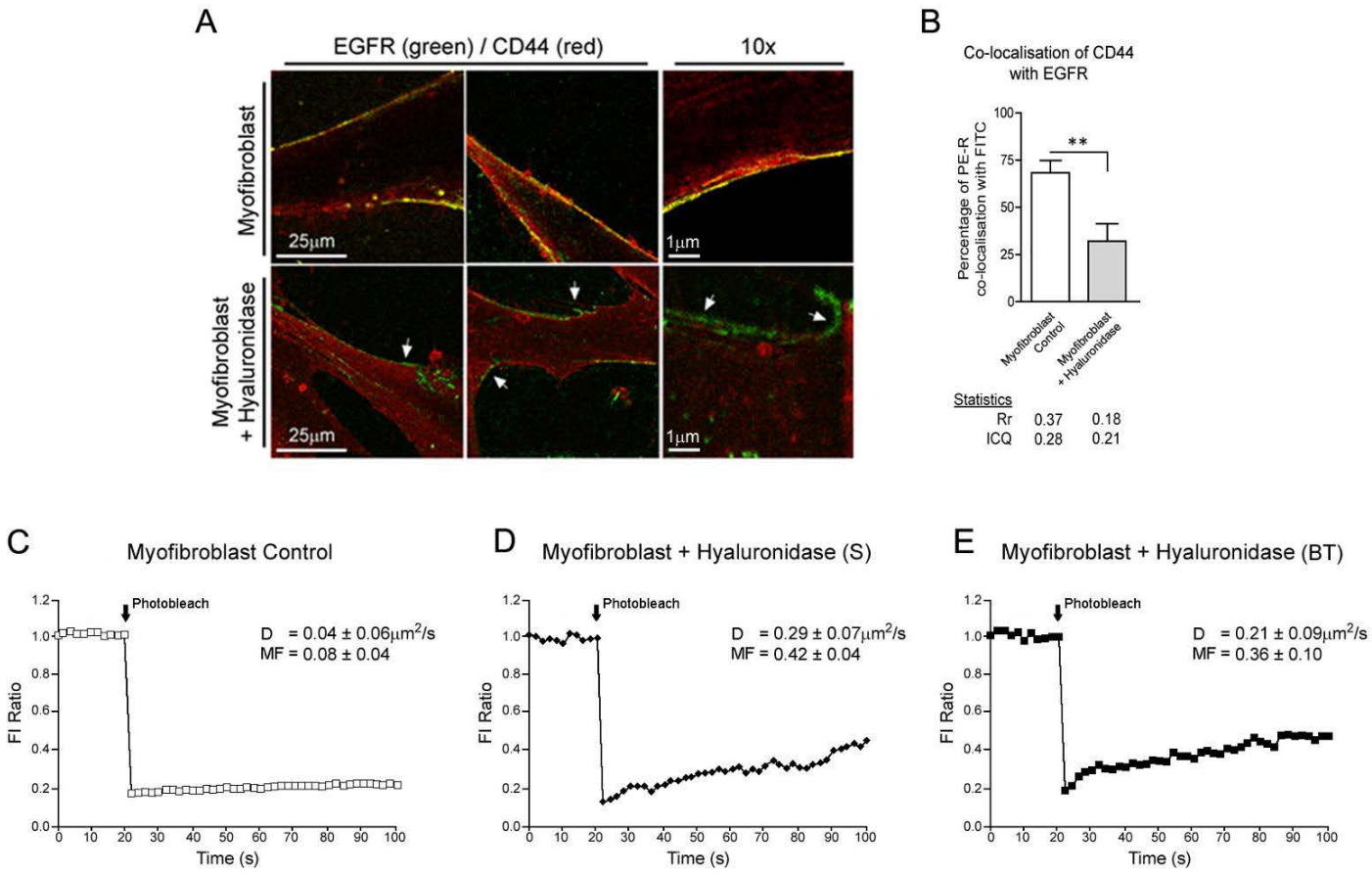

Figure 3.12. The HA Pericellular Coat Maintains CD44-EGFR Co-localisation. A. Myofibroblasts were grown to 70% confluence and Confocal Laser Scanning Microscopy was used to assess the effect of hyaluronidase treatments on EGFR (green; FITC) and CD44 (red; PE-R) co-localisation in myofibroblasts (white arrows indicate areas of no co-localisation). Images are representative of 3 individual experiments. Original magnification x630. **B.** Receptor co-localisation was quantified (Mander's Co-localisation Coefficient). Statistical analysis includes the average Pearson's Correlation Coefficient (Rr) and Intensity Correlation Quotient (ICQ) for each experimental condition. Results shown are ± s.e.m. of 3 individual experiments. The recovery of fluorescence into a photobleached area was quantified and expressed as a fraction of the fluorescence intensity (FI) of a second region of membrane, outside of the photobleached area (FI Ratio). Complete quantified time-courses, average diffusion constants (D) and mobile fractions (MF) are shown for: **C.** CD44 in myofibroblasts; **D.** CD44 in myofibroblasts treated with 1U/mL *streptomyces* (S) hyaluronidase, and **E.** CD44 in myofibroblasts treated with 100μg/ml bovine testicular (BT) hyaluronidase. Results are shown are representative of 3 independent experiments. ***P=<0.01*.

3.3 Discussion

This Chapter provides insights into the mechanisms controlling TGF-β1-dependent differentiation of fibroblasts to myofibroblasts, through the interaction of CD44 with EGFR in lipid rafts. The HA receptor, CD44, can function as a co-receptor, physically associating with several membrane-bound proteins, resulting in modulation of intracellular signal transduction pathways and facilitating the formation of specialised signalling complexes [307, 308]. In light of these reports, I sought to determine if a similar system operated during myofibroblast differentiation. The data reported here support previous findings, where following TGF-β1 stimulated differentiation, CD44 and EGFR co-localised in dermal fibroblasts [160] and also in oral fibroblasts, but only if in a HA-rich environment [195].

Although the myofibroblast phenotype is well documented, the mechanism leading to differentiation from fibroblasts has had limited detailing. Investigation into the co-localisation between CD44 and EGFR that was previously suggested [160, 195], and the cellular location of this association could characterise a differentiation-unique mechanism that results in myofibroblast generation and therefore, contributes to progressive fibrosis. The results reported here illustrate that EGFR was held static, at discrete, membrane-bound sites, whilst CD44 was free to diffuse within the plasma membrane. Following TGF-β1-induced differentiation, EGFR remained static, while the ability of CD44 to diffuse freely was attenuated as it became co-localised with EGFR. It was, therefore, determined that the co-localisation mechanism was a result of CD44 movement directed toward the cellular location of EGFR.

Analysis of the possibilities of the cellular structure where CD44 and EGFR co-localisation takes place used cellular treatments with cytochalasin-B and nystatin. The loss of α-SMA generation in cytochalasin-B treated cells was likely to be a result of cytochalasin-B

disruption of the cellular population of CD44, rather than through an inhibition of receptor association. It was also noted that there was knockdown of total CD44 and ERK1/2 protein in cytochalasin-B treated cells, compared to both untreated and nystatin treated cells, further supporting the hypothesis that inhibition of differentiation was from direct knockdown of key components involved in the response. Nystatin, on the other hand, was able to inhibit α-SMA generation and CD44-EGFR co-localisation, without attenuating total CD44 and ERK1/2 proteins. The combination of data from the chemical treatments of cells and FRAP experimentation, suggests that CD44 can exist in two populations, one with high mobility and cytoskeletal association in resting fibroblasts; and the other with restricted movement and interaction with EGFR potentially held in membrane bound lipid rafts in myofibroblasts.

Further examination to clarify the localisation of EGFR revealed that in both fibroblasts and myofibroblasts, EGFR was associated and co-localised with cholesterol-rich micro-domains or lipid rafts [309]. These findings supported previous reports of EGFR being bound in lipid raft domains in other cell systems [310]; and of lipid rafts as regulators of EGFR and other receptors [288, 311, 312]. CD44 was found to co-localise with lipid raft domains after differentiation of fibroblasts to myofibroblasts, supporting the hypothesis that CD44 re-localisation to EGFR in lipid rafts was implicated in the differentiation pathway. Co-localisation of EGFR and CD44 was lost when lipid rafts were disrupted; and these data support fibroblast lipid rafts as the areas where EGFR aggregated and to which CD44 moved to, associating with EGFR during phenotypic change. The disruption of lipid rafts also resulted in prevention of α-SMA upregulation, following TGF-β1-induced differentiation of fibroblasts at both mRNA and protein levels, antagonising the induction of myofibroblasts. The data reported here suggest that lipid rafts are essential structures for accommodation of EGFR-CD44 complexes and the subsequent differentiation signalling. As CD44 motility was reduced, but not completely abolished, in myofibroblasts and was also found in membrane

fractions positive for EEA-1, it can be concluded that CD44 is present in multiple regions of fibroblasts and myofibroblasts and indeed the cellular membrane. This coincides with previously published data, which shows CD44 as being bound to the cell cytoskeleton [290], able to move to membrane bound lipid rafts [279] and co-localise with other proteins [290, 302, 307], attributing to its repertoire of roles and cellular functions.

It is well known that TGF-β1 can induce activation of the ERK signalling pathway. Several studies have proposed a contributory role of ERK signalling in the promotion of the fibrotic response [313, 314]; and have also shown that ERK1/2 activation was required for TGF-β1-driven proliferation in both oral and dermal fibroblasts [195]. The results shown here confirm that there is a two-peak or "bi-phasic" activation profile of ERK1/2, dubbed the early and late signalling responses. In addition, the data presented in this chapter also showed a co-incident bi-phasic activation of the kinase, CaMKII, at the same time-points as ERK1/2, suggesting both may be involved and play a large role in TGF-β1-dependent responses. Previous research in cancer cell lines demonstrated that CaMKII is centrally involved in cytoskeletal reorganisation and modification [290] and that HA-CD44 interaction mediated CaMKII-dependent cellular migration, independently of ERK1/2 phosphorylation. In this chapter's investigations, inhibition of ERK phosphorylation prevented activation of CaMKII, suggesting that ERK and CaMKII are closely associated. In contrast, inhibition of CaMKII did not attenuate ERK signalling. These data demonstrate that ERK activation is upstream of CaMKII in differentiating fibroblasts and that ERK1/2 activation is a regulator of CaMKII activation with both required for the subsequent differentiation response.

I propose that the early ERK1/2 and CaMKII responses are involved in the induction of fibroblast differentiation, as abolition of membrane-bound lipid rafts with nystatin resulted in the attenuation of both ERK1/2 and CaMKII early waves of activation. In contrast, the late activation remained in cells pre-treated with nystatin, suggesting that the late signalling

response of ERK1/2 and CaMKII leading to proliferation was indicative of another originating source that was not in lipid raft domains. This has been suggested in research highlighting how EGFR can be susceptible to ligand-free activation and can produce a proliferation response, when it has been released to non-lipid raft areas of the cell membrane [287, 289]. However, it is not known whether this occurs in fibroblasts, in the absence of HA or CD44.

Several previous studies have underlined the importance of HA in fibroblast function and wound healing [241, 244, 297, 315, 316]. It was, therefore, sought to determine whether HA synthesis and upregulation through HAS2 were necessary steps leading to EGFR phosphorylation, receptor co-localisation; and both ERK and CaMKII intracellular signalling. I have also investigated whether HAS2 activity was the primary modulator of the differentiation pathway, independent of the TGF-β1-SMAD signalling pathway. Here it is shown that inhibition of HAS2 attenuated activation of EGFR and both signalling phases of ERK and CaMKII phosphorylation, confirming that HAS2 was an essential component in the TGF-β1-mediated differentiation pathway. It was also demonstrated that removal of the HA-pericellular coat with hyaluronidase released CD44 from static membrane domains, thus partially restoring the potential of movement throughout the cell membrane, indicating that there may be further changes to CD44 that have taken place to maintain its association with lipid rafts and EGFR. The data presented here highlight the importance of the HA-pericellular coat in orchestrating CD44 to enable modulation of intracellular signalling pathways. Previous work from our laboratory reported that HAS2 and EGFR overexpression could restore the differentiation potential of aged fibroblasts [160]. However, it was also demonstrated that HAS2 overexpression alone was not enough to initiate EGFR-CD44 coupling or differentiation and that TGF-β1 stimulation was also required [195]. The data presented in this chapter indicate that HAS2 activation mediates differentiation through

initiating CD44 sequestration into lipid rafts and the co-localisation with EGFR, leading to phosphorylation of EGFR and subsequently, ERK and CaMKII signalling. Therefore, HAS2-regulated HA synthesis is a major determining factor in the phenotypic activation of fibroblasts. This change in phenotype, however, also involves the simultaneous activation of the classical Smad-mediated signalling pathway, initiated by TGF-β1 binding to its receptor [160].

The data presented in this chapter provides mechanistic insights into the process of transition between scarring and scar-free tissue repair. The data also extends the findings from our laboratory that demonstrated the important regulatory role of HA-rich pericellular matrices in the co-ordination of TGF-β1-dependent fibroblast differentiation [260]. Combining previous results with the current findings suggests that stimulation of differentiation in response to TGF-β1 requires a HA-rich matrix, functionality of CD44; and EGFR associated with cholesterol-rich membrane-bound lipid rafts. HA and HA pericellular coat formation facilitates TGF-β1-dependent fibroblast differentiation through HA-CD44 binding and relocation, promoting interaction between the CD44 and EGFR within lipid rafts. This then promotes specific intracellular signal transduction through the ERK-CaMKII pathway, acting to complement the Smad pathway, resulting in myofibroblastic transformation (as summarised in Figure 3i).

In summary, the data reported in this Chapter demonstrated, in-depth, the mechanism of CD44 co-localisation with EGFR, providing a key cellular compartment for this receptor interaction and the signalling mechanisms involved in contribution to successful myofibroblast differentiation. These results may yield valuable insights into potential targets for preventative measures or therapeutic treatments for progressive fibrosis. In light of this chapter's findings and previously gathered data, the role of EGFR in the differentiation

mechanism can be described as pivotal. The following chapter will examine the dysfunctions of differentiation deriving from the age-associated loss of EGFR by investigation into the regulation of EGFR transcription and synthesis; and use experimental techniques in order to restore EGFR expression and function and therefore, myofibroblast differentiation.

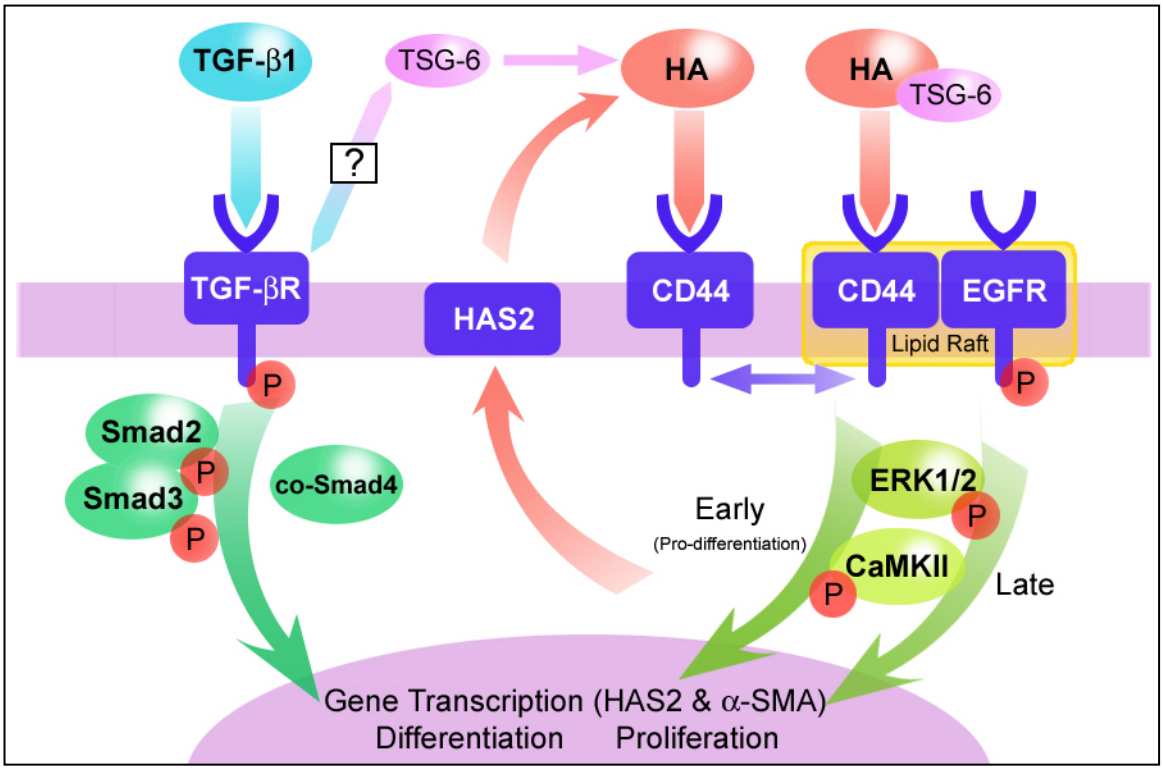

Figure 3i. Summarised and updated cell signalling mechanism for fibroblast-myofibroblast differentiation. Additional detailing includes HA-dependent CD44-EGFR co-localisation in lipid rafts (yellow), CaMKII activation downstream of ERK1/2 (light-green pathway), indication of the bi-phasic ERK1/2-CaMKII signalling with early phase association to pro-differentiation; and HAS2 gene upregulation (red arrow) dependent on the EGFR branch of the differentiation response.

Chapter 4

Factors Contributing to Dysfunction and Age-associated Loss of Myofibroblast Differentiation

4.1 Introduction

4.1.1 Loss of EGFR in Age-associated Dysfunction of Myofibroblast Differentiation

The synergistic effects between TGF-β1 and EGFR signalling have been previously demonstrated [317-319]; and were further explored in the previous results chapter. Earlier studies have also demonstrated that TGF-β1 induces the expression of high-affinity EGFR in stromal fibroblasts [320] and in epidermal cell lines TGF-β1 increased tyrosine phosphorylation of EGFR that was not dependent on protein synthesis [321]. Previous studies [322] and work from the Institute of Nephrology [160, 195] reported that TGF-β-mediated Smad phosphorylation was independent of TGF-β1-mediated EGFR signalling. This indicated that the TGF-βRI and EGFR signalling pathway were crucial, yet independent, events for TGF-β1-mediated myofibroblastic differentiation.

Furthermore, studies revealed that EGFR levels preferentially declined during cellular ageing of fibroblasts regardless of whether the cellular ageing occurred *in vivo* or *in vitro* [159]. This was highlighted by a loss in ligand binding sites per cell. EGFR mRNA levels were also diminished, in parallel with reduced surface and total EGFR protein. An age-related transcriptional control element remains to be identified, the results of the study by Shiraha *et al.* suggest that this preferential loss of EGFR was caused by a gradual loss of mRNA transcriptional activity, although the factors regulating said activity in this context are not yet fully understood.

Although age-related failure of TGF-β1-induced myofibroblast differentiation was reported to be associated with the inability to induce HAS2, a decrease in HA synthesis and a lack of pericellular coat formation; HA synthesis and coat assembly restored by forced expression of HAS2 followed by TGF-β1 stimulation [244], did not restore the myofibroblast phenotype.

Studies, including those from the Institute of Nephrology, have demonstrated that the loss of EGFR expression and its responsiveness in aged cells was central to age-related resistance to differentiation [159, 160]. Investigation into the factors limiting EGFR transcription and protein synthesis in aged fibroblasts, could help unravel a potential method for the restoration of EGFR in aged cells and thus help restore potential to undergo differentiation.

4.1.2 EGF and EGFR Signalling

Epidermal growth factor (EGF) is a 53 amino acid growth factor and cytokine involved in signalling pathways promoting cell proliferation, survival and differentiation [323]. Its cell surface receptor, EGFR (ErbB-1; HER1 in humans) is the cell-surface receptor for members of the EGF-family of extracellular protein ligands. EGFR is a member of the ErbB family of receptors, a subfamily of four closely related receptor tyrosine kinases: EGFR (ErbB-1), HER2/c-neu (ErbB-2), Her 3 (ErbB-3) and Her 4 (ErbB-4) [324].

EGFR exists on the cell surface as a transmembrane receptor and is activated by the binding of it ligands, including EGF, TGF-α, HB-EGF and more [324]. ErbB2 has no known direct activating ligand and may be in an activated state constitutively, or become active upon heterodimerisation with other family members, such as EGFR. Upon activation by its growth factor ligands, EGFR undergoes a transition from an inactive monomeric form to an active homodimer [325]. However, there is some evidence that preformed inactive dimers may also exist before ligand binding [271]; and their activity may be regulated by other proteins, receptors or lipids. An example of which includes high-density cholesterol lipid rafts (or lipid micro domains), areas within the cell membrane which have been reported to sequester and contain receptors to limit or modulate their activity [288, 311]. In addition to forming homodimers, EGFR may pair with another member of the ErbB receptor family, such as ErbB2/Her2/neu, to create an activated heterodimer [326]. There is also evidence to suggest

that clusters of activated EGFR exist, although it remains unclear whether this clustering is important for activation itself, occurs subsequent to activation of individual dimers, or that these clusters are held within specific cellular locations, such as lipid rafts; in order to regulate their signalling potential [327, 328].

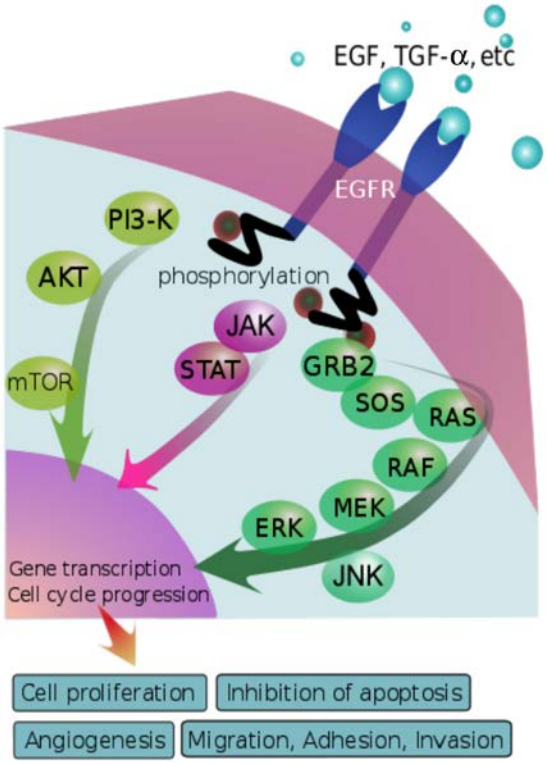

Figure 4i. EGFR intracellular signalling pathways - cytokine/ligand induced phosphorylation of EGFR leads to intracellular protein kinase cascades, among these are the Akt/mTOR, JAK/STAT, MAPK and MEK/JNK pathways. Figure compiled from Andl et al. 2004 [1], Cocoran et al. 2012 [2], Cordero et al. 2012 [3], Dobashi et al. 2009 [5], and Hashimoto et al. 1999 [6].

EGFR dimerisation stimulates its intrinsic intracellular protein-tyrosine kinase activity. As a result, auto-phosphorylation of several tyrosine residues occurs in the C-terminal domain of EGFR. This auto-phosphorylation elicits downstream activation and signalling through several other proteins that associate with the phosphorylated tyrosines, through their own phosphotyrosine-binding SH2 domains [325]. These downstream signalling proteins initiate several signal transduction cascades, including the MAPK/ERK, Akt, JNK and JAK pathways (Figure 4i) [1-3, 5, 6], leading to DNA synthesis, cell proliferation, migration, adhesion, survival, or differentiation. The kinase domain of EGFR also cross-phosphorylates tyrosine residues of other receptors with which it is aggregated with [329, 330]; and can itself be activated in that manner, as demonstrated by CD44 [259].

4.1.3 MicroRNA Regulation of EGFR and Age-associated Loss of Differentiation

A major mechanism controlling EGFR expression could be regulation by microRNAs (miRNAs). These short, single-stranded and looped, 18-24 nucleotide non-coding RNA molecules function as post-transcriptional regulators of gene expression, by binding and actively inhibiting the expression of mRNA (through affecting the stability and translation of mRNAs), to moderate cell function. In brief (summarised in Figure 4ii), miRNAs are transcribed by RNA polymerase II as part of primary transcripts (pri-miRNAs), which can be within either protein-coding or non-coding regions of genes and intronic or exonic regions of DNA. The pri-miRNA is cleaved by Drosha ribonuclease III enzyme to produce a stem-loop precursor miRNA (pre-miRNA), which is further cleaved by the cytoplasmic Dicer ribonuclease to generate a miRNA duplex, consisting of the mature miRNA (miRNA-5p) and antisense miRNA (miRNA-3p) products. The mature miRNA is incorporated into a RNA-induced silencing complex (RISC), which recognises target mRNAs (3'UTR regions) through either perfect or imperfect base pairing with the miRNA; and results in translational inhibition or destabilisation of the target mRNA.

Among the predicted miRNA targets for the EGFR 3' UTR, the one which is most commonly associated with EGFR transcriptional inhibition is miRNA-7 (miR-7). Although the mature miR-7 with predicted EGFR mRNA inhibitory action is located at the pri-miRNA locus for miR-7-1, loci exist at miR-7-2 and miR-7-3 sites within the human genome. Whether or not the pre-miRNA generated from the pri-miRNA for miR-7-2 and miR-7-3 contribute to the overall expression of active and mature miR-7, capable of inhibitory action against EGFR, is not clear and warrants investigation. Several studies highlight the activity of miR-7 in different cell systems and its role in different disease states. miR-7 has been shown to antagonise EGFR expression [331], to be involved in EGFR-related cancer progression [332,

333], and to regulate EGFR-mediated development [334]. However, whether or not miR-7 is implicated in age-associated loss of EGFR and therefore, fibroblast resistance to differentiation, has yet to be investigated and could provide key insights into the down regulation of EGFR that correlates with cellular ageing.

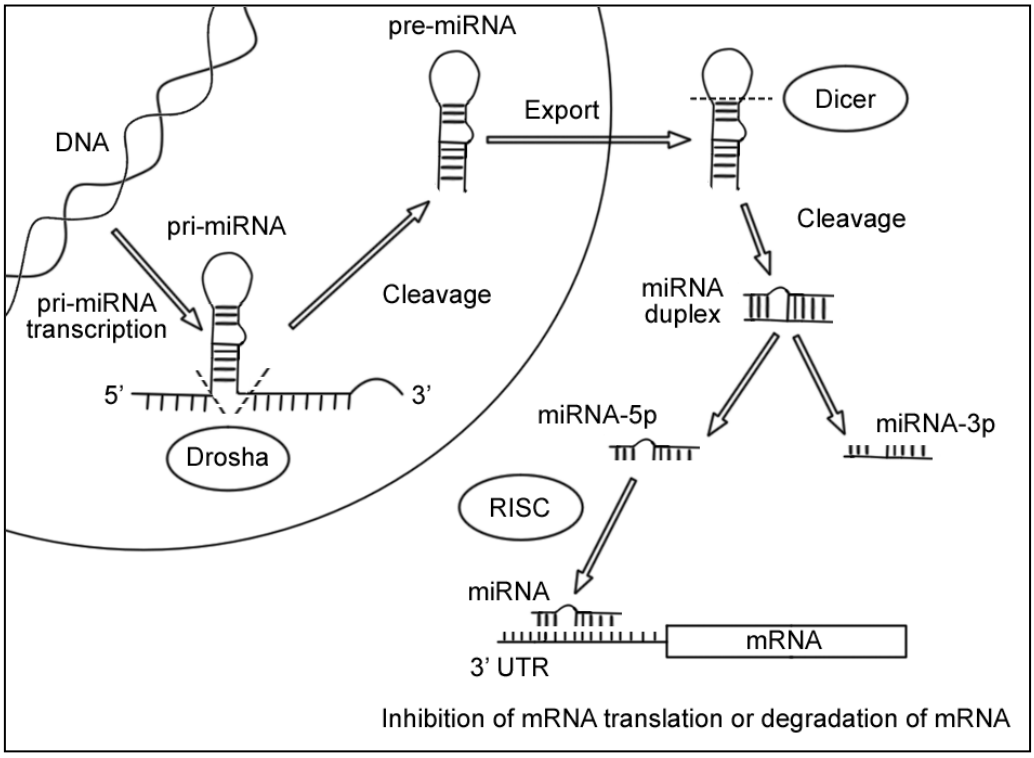

Figure 4ii. Pathway of microRNA generation – The primary transcript of miRNA (pri-miRNA) is transcribed from the cell DNA, Drosha then cleaves out the stem-looped precursor miRNA (pre-miRNA). The pre-miRNA is exported and then cleaved by Dicer into a miRNA duplex, separation of which leads to the mature miRNA (miRNA-5p), which when coupled with RNA-induced silencing complex (RISC) can bind the 3'UTR of a mRNA target, resulting in the inhibition of translation or degradation of the mRNA. Figure adapted from Catto, et al. 2011 [4].

4.1.4 Summary of Aims

The hypothesis for this results Chapter is that age-related miR-7 upregulation may be central to the loss of the HA-dependent EGFR signalling pathway. Herein, this results Chapter will aim to investigate how miR-7 affects the cellular expression and functionality of EGFR and whether there is implication of a role in the cellular resistance to differentiation; and to detail the functional consequences arising from miR-7 upregulation in young cells. In addition, this chapter aims to demonstrate that inhibition of miR-7 can rescue the differentiation response

in *in vitro* aged fibroblasts. Furthermore, once a novel mechanism in which miR-7 regulates the HA-mediated CD44/EGFR signalling pathway can be described, this chapter will then examine whether miR-7 has an influence over CD44 movement, therefore highlighting whether miR-7 can indirectly regulate HA and CD44; and the subsequent loss of differentiation in response to TGF-β1 stimulation.

Specifically the aims of this Chapter are to investigate the following areas in detail:

i. Characterisation of the age-associated loss of TGF-β1-dependent differentiation with increasing cell PDL.
ii. Investigate the loss of EGFR in ageing fibroblasts, through determination of EGFR promoter activity in aged cells.
iii. Examination and analysis of microRNA regulation of EGFR, through:
    a. *In silico* based analysis of miR seed sites on the EGFR 3' UTR.
    b. Overexpression of miR-7 in young fibroblasts.
    c. Inhibition of miR-7 in aged fibroblasts.
iv. Analysis of the indirect effects of miR-7 upregulation or inhibition on other key components of the myofibroblast differentiation mechanism.

Fulfilling the aims listed above will help to explain the loss of EGFR in ageing fibroblasts, which could potentially apply to other cell types. Additionally, it will provide insights into the regulation of the differentiation mechanisms in the ageing process, providing potential targets for the promotion of fibroblast and myofibroblast function in cases of chronic non-healing wounds. Furthermore, fulfilment of the aims could provide means for the inhibition of myofibroblast formation, in cases where prevention or treatment of fibrosis is required.

4.2 Results

4.2.1 Characterisation of Age-associated Loss of Differentiation and CD44-EGFR Co-localisation

The age-associated loss of myofibroblast differentiation can lead to the failure of wound contraction and resolution, with the potential to lead to non-healing chronic wounds in the elderly. To characterise the loss of differentiation and failure to obtain the myofibroblast phenotype, cells of increased passage or PDL were stained to visualise α-SMA stress fibre formation through the use of immunocytochemistry (Figure 4.1A). With increasing PDL, the cells' ability to generate α-SMA stress-fibres in response to TGF-β1 decreased to the point of late cell passage (PDL 29), when cells were nearing senescence. These were negative for α-SMA staining. To assess the transcriptional activity of key components of the differentiation mechanism, QPCR was used to analyse expression of α-SMA (Figure 4.1B) and HAS2 (Figure 4.1C) mRNA. Again, increasing PDL correlated with decreasing expression of both genes. The difference between young (PDL 17) and aged (PDL 29) fibroblasts was a 10-fold reduction in the expression of both mRNAs.

Additional investigation into the co-localisation potential of CD44 and EGFR in aged fibroblasts was examined by labelling EGFR (green) and CD44 (red) in live cells, using Confocal Laser Scanning Microscopy (Figure 4.2A). It was found that the co-localisation between CD44 and EGFR was lost in aged cells, as areas of the cell membrane were positive for EGFR staining independent of areas positive for CD44 staining. Quantification of receptor co-localisation (Figure 4.2B) demonstrated the loss of co-localisation in aged cells, compared to the young counterparts. The percentage of CD44 (red) with EGFR (green) was approximately 80% in young cells treated with TGF-β1, but this was reduced to less than 10% in aged cells treated with TGF-β1. The data from these findings suggest the loss of the

ability to differentiate was multi-factorial, involving decreased α-SMA and HAS2 expression and the inability of CD44 to co-localise with EGFR.

4.2.2 The Importance of EGFR in the Differentiation Response

The EGFR tyrosine phosphorylation inhibitor, AG1478, was used to determine how the inhibition of EGFR signalling affects the expression of crucial components that are usually upregulated during myofibroblast differentiation. Young fibroblasts were treated for 1 hour with 10μM AG1478, prior to incubation with serum-free medium alone and serum-free medium containing 10ng/ml TGF-β1 for 72 hours. QPCR was used to measure the expression of HAS2 (Figure 4.3A), α-SMA (Figure 4.3B) and EDA-FN (Figure 4.3C) mRNA. Results show that upregulation of HAS2, α-SMA, and EDA-FN by TGF-β1 was completely attenuated if cells were treated with AG1478, indicating the importance of TGF-β1 transactivation of the fully functional EGFR pathway in myofibroblast differentiation.

Previous studies [159, 160, 244] have demonstrated a loss of EGFR that correlates with increasing fibroblast PDL. However, the mechanism responsible for this loss of expression is not clear. To determine the extent of EGFR loss in our cell system, we analysed EGFR mRNA, total protein, cell surface expression, and constitutive EGFR promoter activity in young and aged fibroblasts. EGFR mRNA, analysed by QPCR, was found to be significantly downregulated in aged fibroblasts (Figure 4.4A). This was reflected in age-associated loss of both EGFR total protein, as determined by Western blot (Figure 4.4B); and cell surface expression, as determined by Flow Cytometry (Figure 4.4C). Interestingly, when the activity of the EGFR promoter was tested using a luciferase reporter construct, no observable differences in luminescent intensity were observed between young and aged cells (Figure 4.4D), suggesting that the down-regulation of EGFR mRNA and protein were not necessarily

a result of reduced levels of transcription factors binding to the EGFR promoter; and thus the aged-associated loss of EGFR could be a consequence of post-transcriptional activity.

4.2.3 Differences in Receptor Membrane Dynamics Between Young and Aged Fibroblasts

The loss of EGFR expression in aged fibroblasts has been reported to impact on a reduced differentiation potential through a loss of the interaction between CD44 and EGFR, an important step in driving fibroblast to myofibroblast transformation [160, 195, 335]. The previous chapter highlighted the importance of CD44 membrane motility in contribution to EGFR interaction. Here, we examined whether the receptor behaviours of EGFR and CD44 altered in aged cells by using FRAP. Representative FRAP images are shown for young fibroblast EGFR and CD44 (Figure 4.5A). EGFR was found to remain within static domains across the membrane, regardless of cellular age (Figure 4.5B-C). In contrast, while CD44 had the potential to move throughout the membrane in young fibroblasts (Figure 4.5D), this was lost in aged fibroblasts (Figure 4.5E). These data suggest that CD44 mobility could be another contributor to the age-associated loss of differentiation; and could explain why previously overexpressed EGFR alone [160] was not sufficient to fully restore aged fibroblast differentiation to myofibroblasts.

4.2.4 MicroRNA-7 Targeting of the EGFR mRNA 3'UTR and Changes With Ageing

MicroRNA-7 (miR-7) has been reported to target and prevent EGFR production in many instances, such as in cancers and during development [332-334]. *In silico* analysis revealed one highly conserved and two poorly conserved seed sites for miR-7 within the 3' UTR of EGFR mRNA (Figure 4.6A). In order to determine whether or not miR-7 was upregulated in aged fibroblasts, miR-RT followed by QPCR was used. Results showed that miR-7 was

found to have a higher expression in aged fibroblasts and in cells stimulated with TGF-β1, when compared to young untreated control cells (Figure 4.6B). These data coincide with the downregulation of EGFR mRNA and protein in aged fibroblasts, as seen in Figure 4.4. It was next sought to determine which of the miR-7 loci, miR-7-1 (Figure 4.6C) or miR-7-2 (Figure 4.6D), were predominantly responsible for mature miR-7 expression and its upregulation by TGF-β1 and in aged fibroblasts. To analyse the expression of the miR-3p (3-prime) strand of each miR-7 loci, miR-QPCR was used. The expression of miR-7-1-3p coincided with the expression of mature miR-7, whilst the expression of miR-7-2-3p showed no significant difference in cells treated with TGF-β1 or between young and aged fibroblasts, confirming that miR-7-1 was the active locus for mature miR-7 expression.

4.2.5 The Effect of Overexpressing miR-7 in Young Fibroblasts

Analysis of the effect of overexpression of miR-7 was examined through transfection of pre-miR-7 into young fibroblasts. The relative expression of miR-7 was determined by QPCR; and in cells transfected with pre-miR-7, the results showed a significantly large increase in the levels of miR-7 present (Figure 4.7A). EGFR mRNA was found to be significantly downregulated in cells transfected with pre-miR-7 (Figure 4.7B), whilst α-SMA (Figure 4.7C) and HAS2 (Figure 4.7D) mRNA failed to be induced by TGF-β1 treatment. Transfection of pre-miR-7 also prevented the upregulation of the myofibroblastic marker, EDA-FN [336] mRNA, by TGF-β1 (Figure 4.7E). These data indicated that miR-7 upregulation had the potential to negatively regulate the essential components of myofibroblast differentiation [160, 195, 196, 244]. Similarly, both total EGFR protein (Figure 4.7F) and EGFR cell surface expression (Figure 4.7G) were found to be approximately halved in the presence of pre-miR-7 transfections. To determine whether or not pre-miR-7 transfected cells were still able to differentiate following TGF-β1 stimulation, α-SMA staining was assessed using

immunocytochemistry. α-SMA fibre formation was lost in cells transfected with pre-miR-7, indicating a prevention of differentiation (Figure 4.7H).

4.2.6 The Effect of Inhibiting miR-7 Activity in Aged Fibroblasts

In order to test the hypothesis that miR-7 was effectively inhibiting the differentiation response in aged fibroblasts, transfection of miR-7 locked nucleic acids (LNA) was used to bind and inhibit free miR-7 within these cells. As predicted, EGFR mRNA was upregulated in miR-7 LNA transfected cells, compared to negative control LNA transfected cells; and did not fall when the cells were treated with TGF-β1 (Figure 4.8A). In cells transfected with miR-7 LNA α-SMA (Figure 4.8B), HAS2 (Figure 4.8C) and EDA-FN (Figure 4.8D) mRNA were significantly upregulated, following TGF-β1 stimulation. Total EGFR protein (Figure 4.8E) and cell surface expression (Figure 4.8F) were also increased. Determination of cellular differentiation was tested and in cells that had been transfected with miR-7 LNA, there was fluorescence for α-SMA intracellular fibres (Figure 4.8G), indicating that the aged fibroblasts had their ability to differentiate restored if miR-7 was prevented from acting. These data demonstrate the effectiveness of targeting miR-7 in restoring the differentiation response in aged fibroblasts, revealing a potentially valuable mechanism to target in chronic non-healing wounds in the elderly.

4.2.7 Analysis of CD44 Membrane Motility in the Presence and Absence of miR-7 or HA

The conclusions from the previous Chapter suggested that the loss of HA-dependent CD44 motility in the membrane could prevent the CD44/EGFR interaction necessary for differentiation [160, 195, 337]. Observations from the results presented in Figure 4.5 showed a loss of CD44 motility in aged fibroblasts. It was, therefore, examined whether overexpression or inhibition of miR-7 would affect CD44 membrane movement. Young

fibroblasts were transfected with either a scrambled pre-miR sequence (Figure 4.9A) or with pre-miR-7 (Figure 4.9B). Interestingly, in cells transfected with pre-miR-7, the potential for CD44 movement throughout the membrane, as highlighted by the diffusion constant (D) and mobile fraction (MF), dropped significantly (both P=<0.01), when compared to the scrambled control transfection. These data are indicative of miR-7 having an indirect action on CD44 receptor behaviour, possibly through a HA-dependent mechanism. To test this hypothesis, DMSO (0.6% v/v) control (Figure 4.9C) or 4-methylumbelliferone (4MU) (Figure 4.9D) treatments were performed on resting fibroblasts, prior to FRAP analysis. Cells treated with 4MU had significantly lower D and MF values (both P=<0.01), suggesting that cellular presence and synthesis of HA was required for CD44 membrane motility.

It was then examined whether the inhibition of miR-7 in aged fibroblasts could restore CD44 movement, through the transfection of negative control LNA (Figure 4.10A) and miR-7 LNA (Figure 4.10B). When aged cells were transfected with miR-7 LNA, the diffusion constant was increased, when compared to negative control LNA transfected cells (P=<0.05). The MF of CD44, although significantly increased (P=<0.05), was not restored to the levels shown in younger fibroblasts (P=<0.01 vs. Fig. 2D).

It was hypothesised that the reason for the restoration seen in miR-7 inhibitory experiments was due to an upregulated presence of HAS2-produced HA. To test this hypothesis, we transfected aged fibroblasts with an empty vector (Figure 4.10C) or with a HAS2 overexpression vector (Figure 4.10D). In cells overexpressing HAS2, there was an observable restoration in CD44 diffusion, compared to the empty vector control (P=<0.05). The MF was also increased (P=<0.01), but again not to the full extent of young fibroblasts (P=<0.05 vs. Figure 4.5D). These data illustrate an alternative mechanism through which miR-7 can regulate the differentiation response. When taken together with the inhibition of HAS2

mRNA shown when overexpressing miR-7 in young fibroblasts (Figure 4.7D) and the restoration of HAS2 mRNA expression shown in aged fibroblasts transfected with miR-7 LNA (Figure 4.8C), these data suggest that there may be a HA-dependent regulation of CD44 membrane motility that is operational in young, but not aged, fibroblast cells.

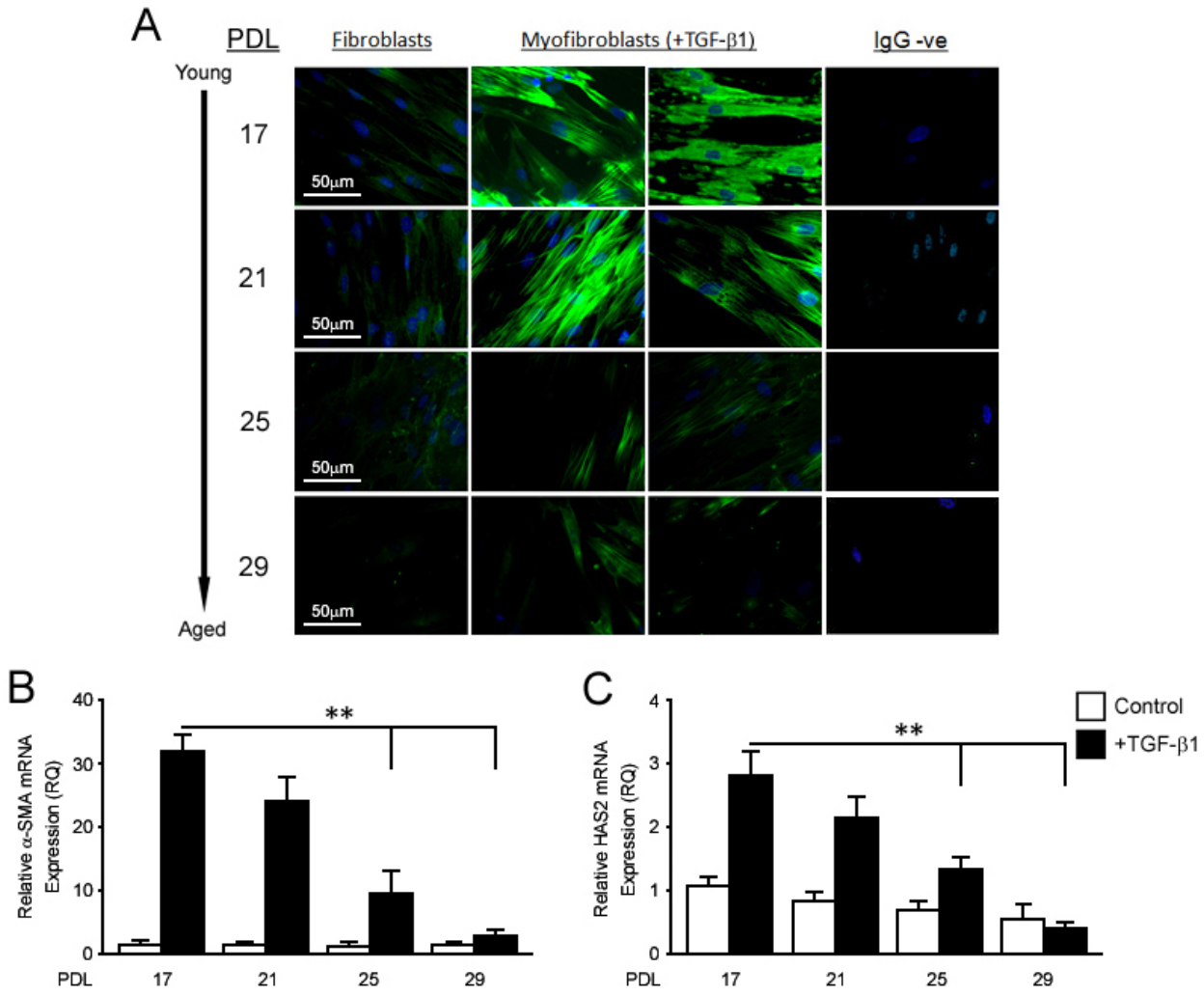

Figure 4.1. Age-associated Loss of Myofibroblast Differentiation. Young and aged fibroblasts of PDL 17, 21, 25 and 29; were grown to confluence and growth arrested for 48 hours. Cells were then incubated in serum-free medium alone or in medium containing 10ng/ml TGF-β1 for 72 hours. **A.** Cells were stained for α-SMA (green) using immunohistochemistry (Hoechst stained nuclei in blue). Images shown are representative of 3 independent experiments, naïve IgG was used in place of primary antibody for negative controls. Original magnification x400. **B.** α-SMA and **C.** HAS2 mRNA expression over the PDL range was assessed by QPCR, results are shown as the mean ± s.e.m. of 3 individual experiments, ***P=<0.01*.

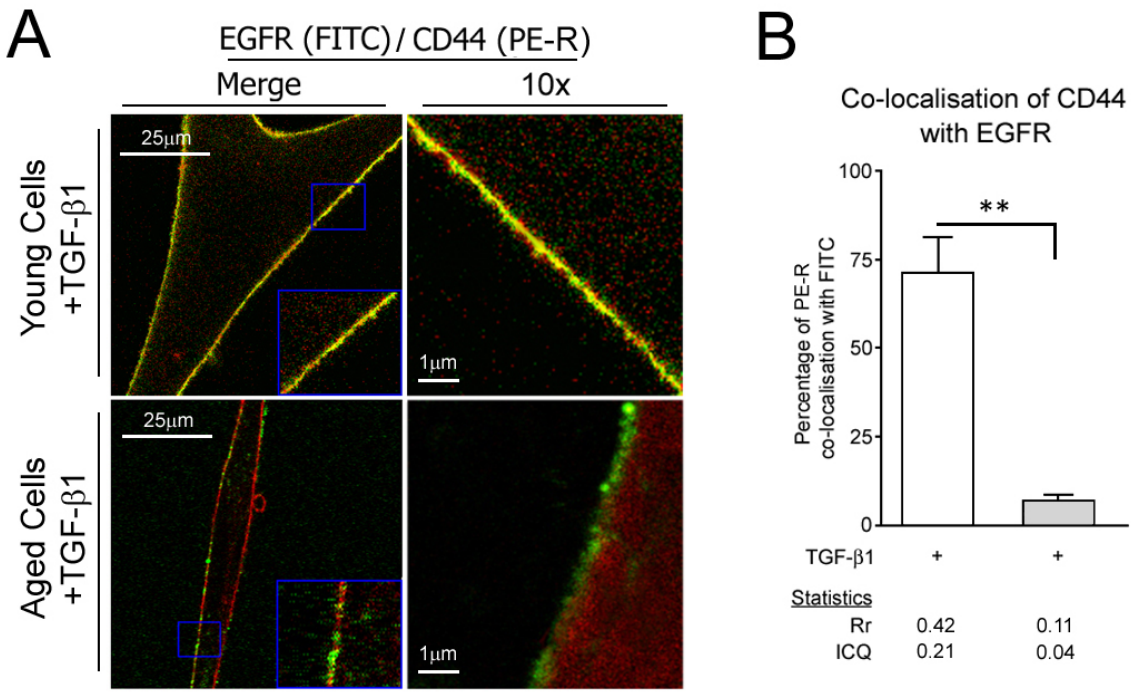

Figure 4.2. Age-associated Loss of CD44-EGFR Co-localisation. Young (PDL 17) and aged (PDL 29) fibroblasts were grown to confluence and growth arrested for 48 hours. Cells were then incubated in serum-free medium alone or in medium containing 10ng/ml TGF-β1 for 72 hours. **A.** Cells were stained for EGFR (FITC; green) and CD44 (PE-R; red) and visualised using Confocal Laser Scanning Microscopy (areas of co-localisation are shown in yellow). Images shown are representative of 3 independent experiments. Original magnification x630. **B.** Co-localisation of CD44 (PE-R) with EGFR (FITC) was quantified (Mander's Co-localisation Coefficient). Statistical analysis includes the average Pearson's Correlation Coefficient (Rr) and Intensity Correlation Quotient (ICQ) for each experimental condition. Results shown are the mean ± s.e.m. of 3 independent experiments. ***P=<0.01*.

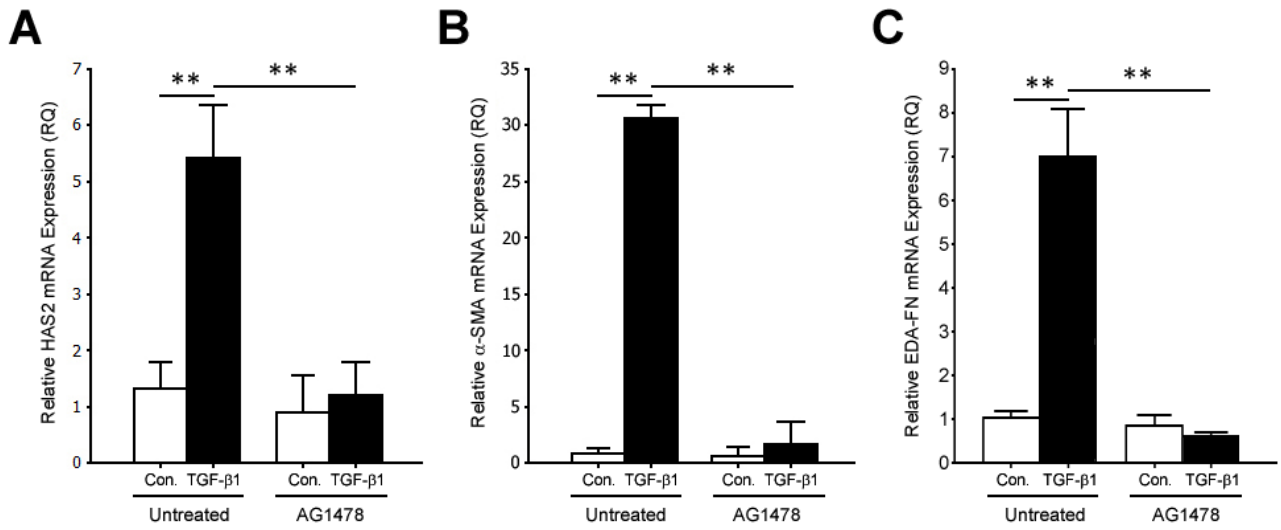

Figure 4.3. Inhibition of EGFR Signalling Prevents Differentiation. Young fibroblasts were grown to confluent monolayers and were growth arrested for 48 hours. Cells were treated with 10μM EGFR inhibitor, AG1478, for 1 hour, prior to incubation in serum-free medium alone or in medium containing 10ng/ml TGF-β1 for 72 hours. The expression of **A.** HAS2, **B.** α-SMA and **C.** EDA-FN mRNA was examined by QPCR and results are shown as the mean ± s.e.m. of 3 individual experiments, ***P=<0.01*.

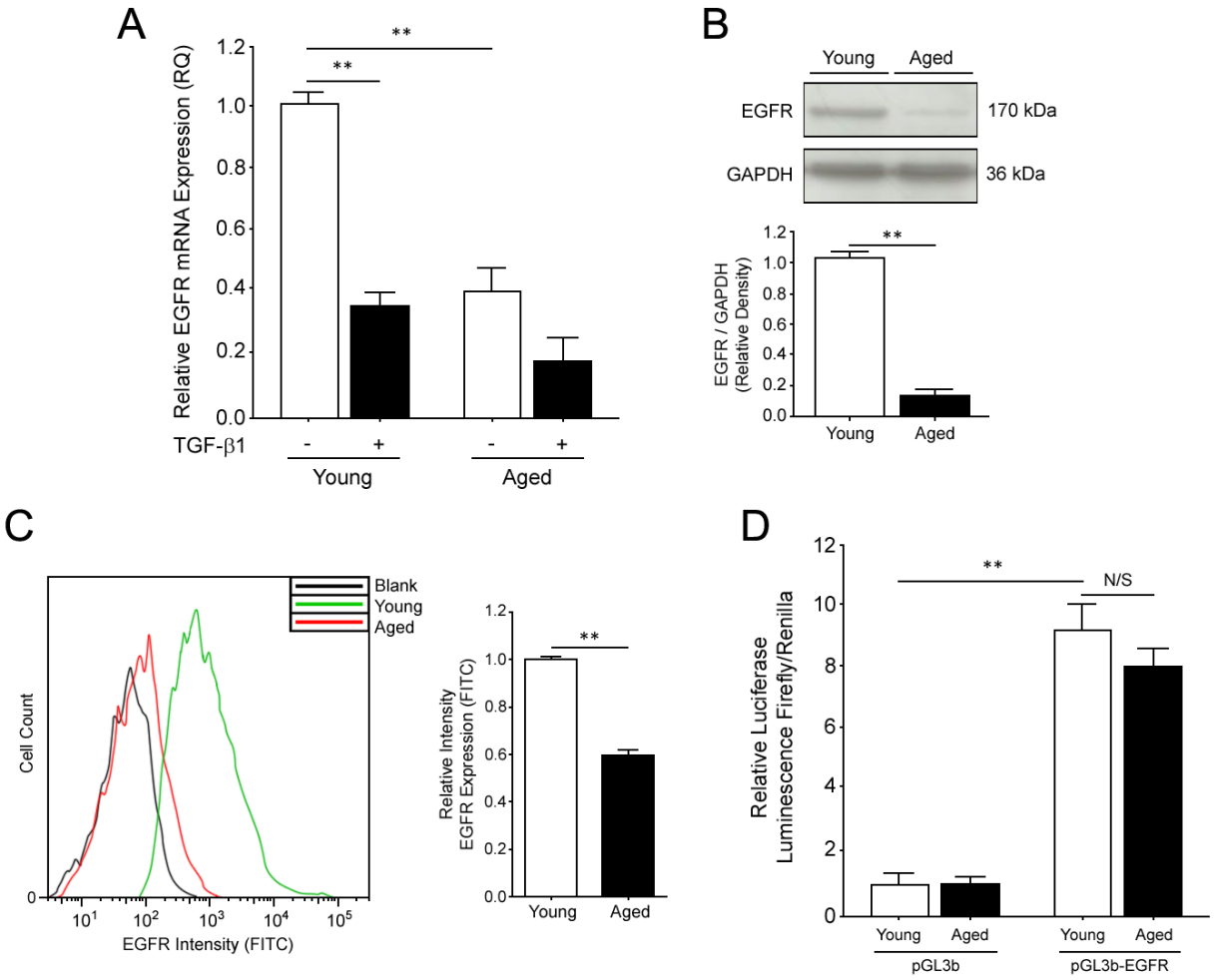

Figure 4.4. Changes in the Expression of EGFR Between Young and Aged Fibroblasts. Young and aged fibroblasts were grown to confluent monolayers and growth arrested for 48 hours. Cells were then incubated in serum-free medium alone or in medium containing 10ng/ml TGF-β1 for 72 hours. **A.** The expression of EGFR mRNA was examined by QPCR and results are shown as the mean ± s.e.m. of 3 individual experiments. **B.** Western blot analysis of total EGFR protein in young and aged fibroblasts. GAPDH was used as a loading control. Representative blot is shown and densitometry graph shown is the mean ± s.e.m. of 3 individual experiments. **C.** Flow Cytometry analysis of cell surface expression of EGFR in young (green) and aged (red) fibroblasts. Unlabelled cells (black) were used as intensity controls. Bar graph of relative intensity shown is the mean ± s.e.m. of 3 individual experiments. **D.** Young or aged fibroblasts were grown to 70% confluence and transiently transfected with either an empty pGL3b vector or pGL3b-EGFR. Luminescence was measured averaged. Cells were co-transfected with Renilla to measure efficiency and to normalise data. Graph shown is the mean ± s.e.m. of 3 individual experiments. *N/S = no significance, **P=<0.01.*

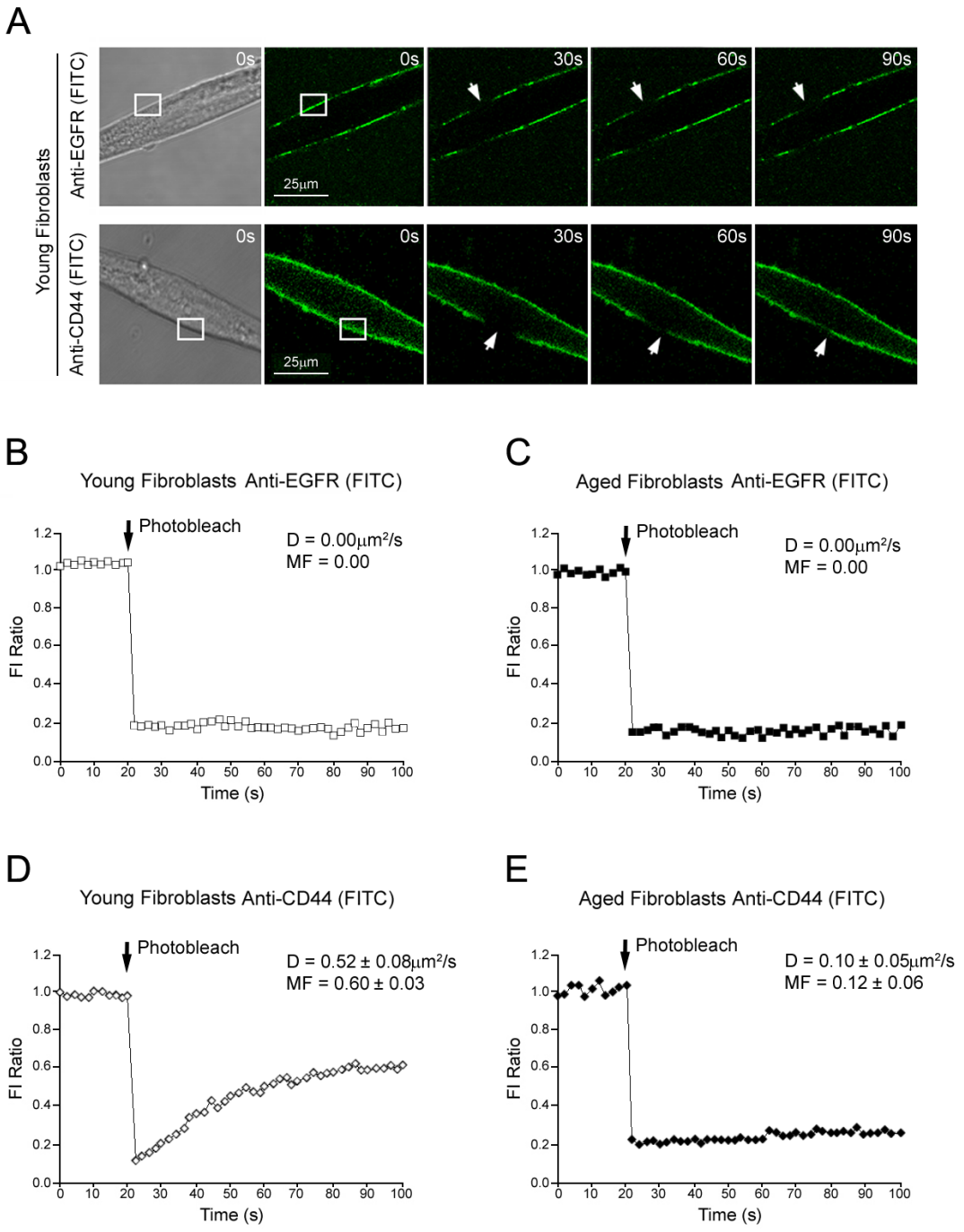

Figure 4.5. Analysis of Receptor Membrane Dynamics in Young and Aged Fibroblasts. A. Sample time-lapse series of fluorescent recovery after photobleaching (FRAP) experiments. Original magnification x630. Young or aged fibroblasts were grown to 70% confluent monolayers on 22mm diameter glass coverslips, in 35mm 6-well tissue culture plates. Cells were growth arrested in serum-free medium for 48 hours. FRAP was performed at 37°C by photobleaching an approximately 10μm area of the cell membrane (indicated by white boxes). The recovery of fluorescence into this area (indicated by white arrows) was quantified and expressed as a fraction of the fluorescence intensity (FI) of a second region of membrane, outside of the photobleached area (FI Ratio). Complete quantified time-courses, average diffusion constants (D) and mobile fractions (MF) are shown for: **B.** EGFR in young fibroblasts; **C.** EGFR in aged fibroblasts; **D.** CD44 in young fibroblasts and **E.** CD44 in aged fibroblasts. All results shown are mean ± s.e.m of 5 independent experiments.

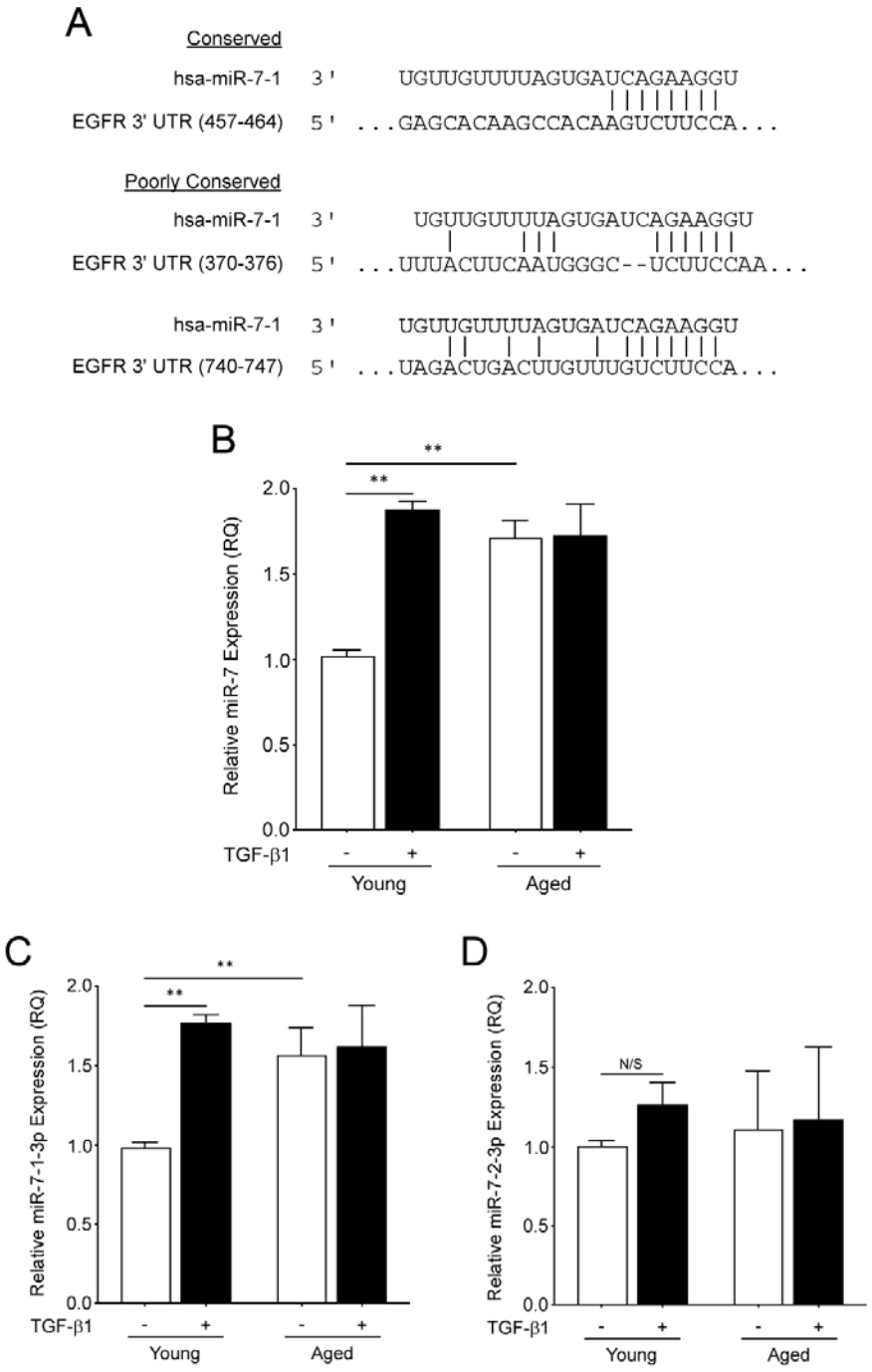

Figure 4.6. Analysis of miR-7 in Young and Aged Cells. A. Highly conserved and poorly conserved microRNA-7 (miR-7) seed sites on the 3' UTR of EGFR mRNA, as determined by *in silico* analysis with TargetScan v6.2. Young and aged fibroblasts were grown to confluent monolayers and growth arrested for 48 hours. Cells were then incubated in serum-free medium alone or in medium containing 10ng/ml TGF-β1 for 72 hours. The expression of **B.** miR-7 (miR-7-1-5p), **C.** miR-7-1-3p and **D.** miR-7-2-3p was examined by miR-QPCR. Results are shown as mean ± s.e.m. of 3 individual experiments. *N/S = no significance*, ***P=<0.01*.

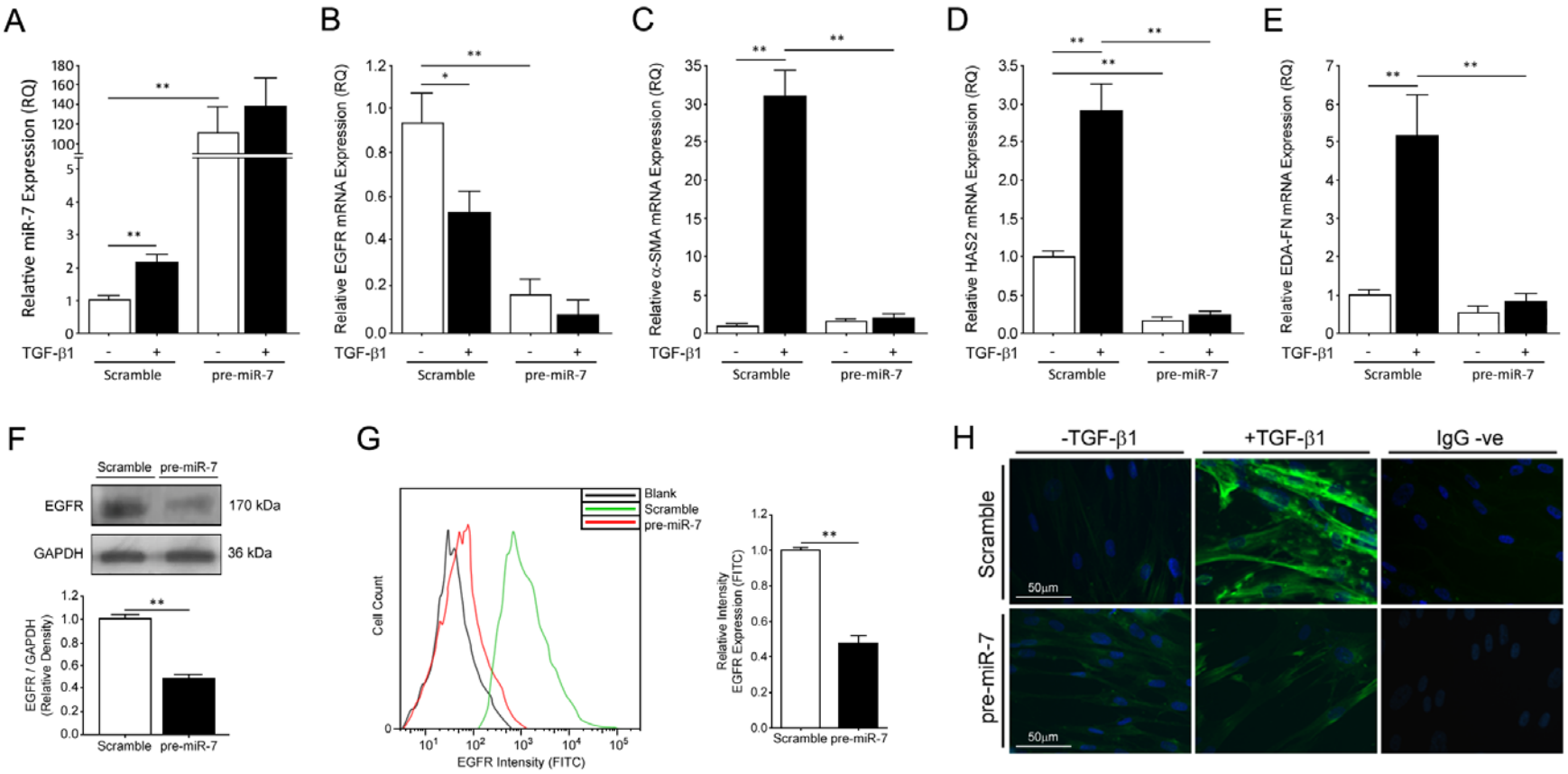

Figure 4.7. Overexpression of miR-7 Attenuates the Differentiation Response. Young fibroblasts were grown to confluent monolayers and growth arrested for 24 hours before transient transfection with either scrambled pre-miR or pre-miR-7. The relative expressions of **A.** miR-7, **B.** EGFR mRNA, **C.** α-SMA mRNA, **D.** HAS2 mRNA and **E.** EDA-FN mRNA, were examined by QPCR, following incubation in serum-free medium alone or in medium containing 10ng/ml TGF-β1 for 72 hours. Results shown are mean ± s.e.m. of 3 individual experiments. **F.** Western blot analysis of total EGFR protein in young and aged fibroblasts. GAPDH was used as a loading control. Representative blot is shown and densitometry results shown are the mean ± s.e.m. of 3 individual experiments. **G.** Flow cytometry analysis of cell surface expression of EGFR in young (green) and aged (red) fibroblasts. Unlabelled cells (black) were used as intensity controls. Bar graph of relative intensity is shown as the mean ± s.e.m. of 3 individual experiments. **H.** Cells were incubated in serum-free medium alone or in medium containing 10ng/ml TGF-β1 for 72 hours and then analysed by immunocytochemistry for α-SMA. Representative images are shown for 3 individual experiments. *$P=<0.05$, **$P=<0.01$.

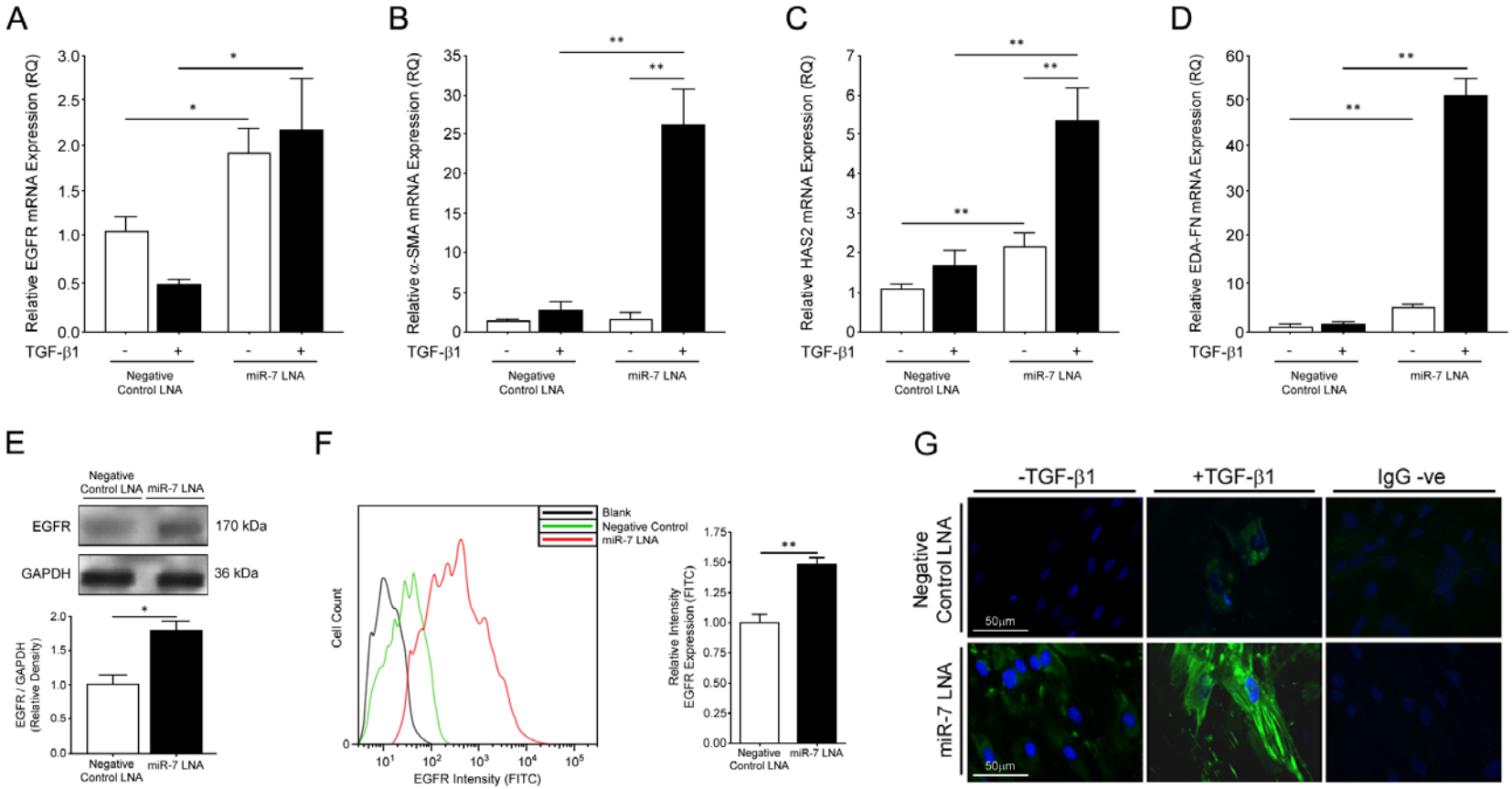

Figure 4.8. Inhibition of miR-7 Rescues the Differentiation Response in Aged Fibroblasts. Aged fibroblasts were grown to confluent monolayers and growth arrested for 24 hours, before transient transfection with either negative control LNA or miR-7 LNA. The relative expressions of **A.** EGFR mRNA, **B.** α-SMA mRNA, **C.** HAS2 mRNA and **D.** EDA-FN mRNA, were examined by QPCR, following incubation in serum-free medium alone or in medium containing 10ng/ml TGF-β1 for 72 hours. Results shown are the mean ± s.e.m. of 3 individual experiments. **E.** Western blot analysis of total EGFR protein in young and aged fibroblasts. GAPDH was used as a loading control. Representative blot is shown and densitometry graph shown is mean ± s.e.m. of 3 individual experiments. **F.** Flow Cytometry analysis of cell surface expression of EGFR in young (green) and aged (red) fibroblasts. Unlabelled cells (black) were used as intensity controls. Bar graph of relative intensity shown is mean ± s.e.m. of 3 individual experiments. **G.** Cells were incubated in serum-free medium alone or in medium containing 10ng/ml TGF-β1 for 72 hours; and then analysed by immunocytochemistry for α-SMA. Representative images are shown for 3 individual experiments. *$P=<0.05$, **$P=<0.01$.

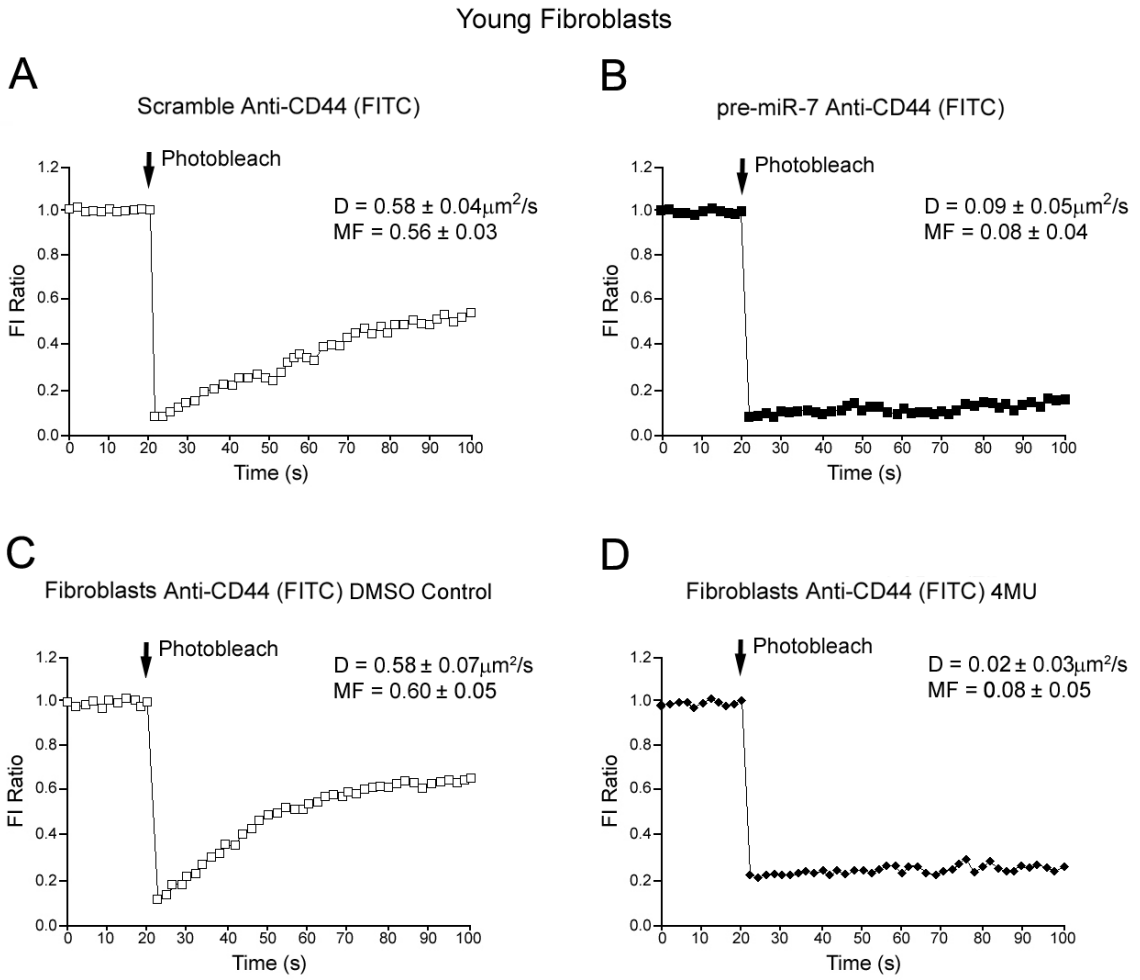

Figure 4.9. Overexpression of miR-7 Inhibits CD44 Motility in Young Fibroblasts. Young fibroblasts were grown to 70% confluent monolayers on 22mm diameter glass coverslips, in 35mm 6-well tissue culture plates. Cells were growth arrested in serum-free medium for 48 hours. FRAP was performed at 37°C by photobleaching an approximately 10μm area of the cell membrane. The recovery of fluorescence into this area was quantified and expressed as a fraction of the fluorescence intensity (FI) of a second region of membrane, outside of the photobleached area (FI Ratio). Complete quantified time-courses, average diffusion constants (D) and mobile fractions (MF) are shown for CD44 in: young cells transfected with **A.** scrambled pre-miR or **B.** pre-miR-7; and cells treated with **C.** control DMSO (0.6% v/v) or **D.** 24 hours with 0.5μM 4MU, prior to FRAP analysis. All results shown are mean ± s.e.m. of 5 independent experiments.

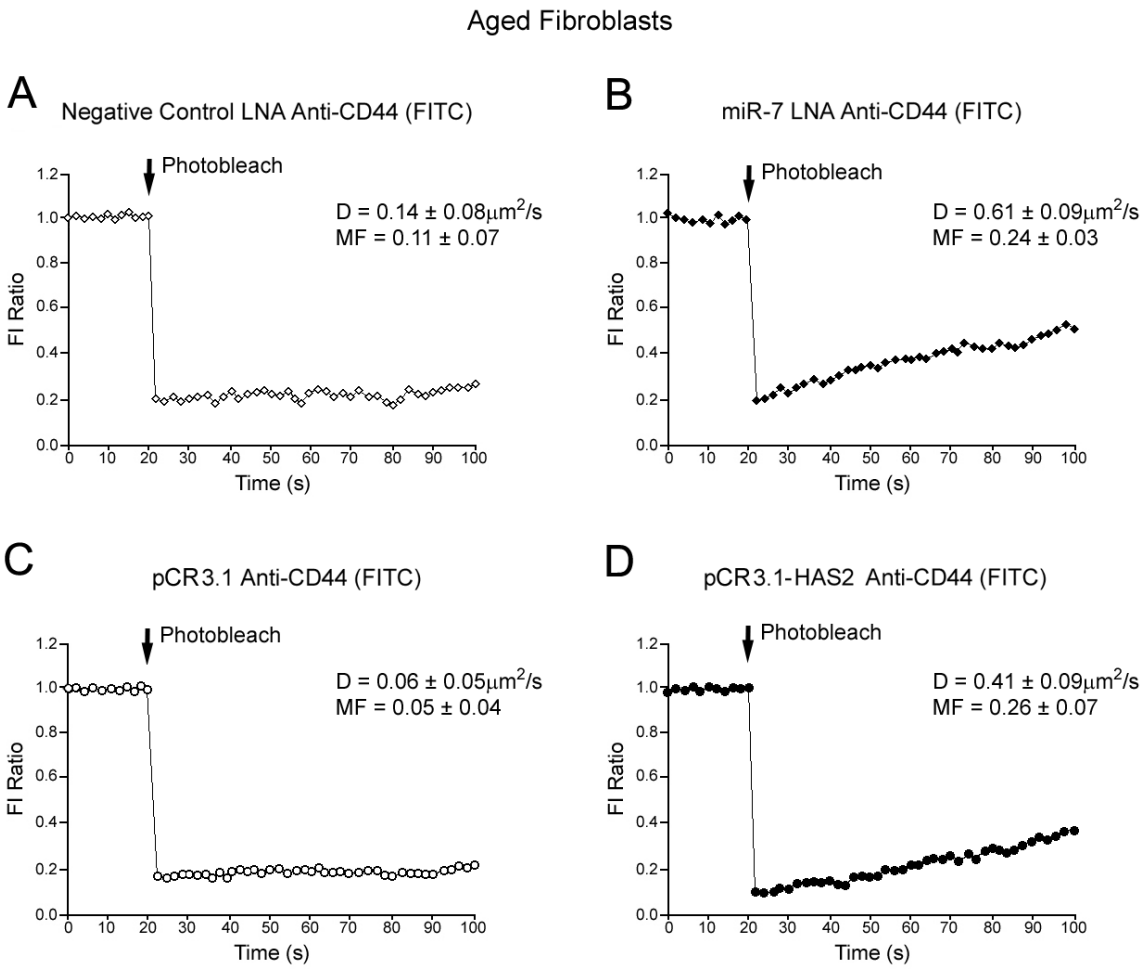

Figure 4.10. Inhibition of miR-7 Restores CD44 Motility in Aged Fibroblasts. Aged fibroblasts were grown to 70% confluent monolayers on 22mm diameter glass coverslips, in 35mm 6-well tissue culture plates. Cells were growth arrested in serum-free medium for 48 hours. FRAP was performed at 37°C by photobleaching an approximately 10μm area of the cell membrane. The recovery of fluorescence into this area was quantified and expressed as a fraction of the fluorescence intensity (FI) of a second region of membrane, outside of the photobleached area (FI Ratio). Complete quantified time-courses, average diffusion constants (D) and mobile fractions (MF) are shown for CD44 in: young cells transfected with **A.** negative control LNA, **B.** miR-7 LNA, **C.** empty pCR3.1 Vector, or **D.** pCR3.1-HAS2 overexpression Vector. All results shown are mean ± s.e.m. of 5 independent experiments.

4.3 Discussion

The data reported in this Chapter provide additional mechanisms and insights into the age-associated loss of TGF-β1-dependent, fibroblast to myofibroblast differentiation. The importance of EGFR and its loss in cellular ageing has been described recently and been shown to have a significant effect on the myofibroblast differentiation pathway [160, 297, 337], going some way towards explaining the mechanisms of resistance to TGF-β1-stimulated differentiation [159, 160]. In light of these reports and the loss of differentiation and CD44-EGFR co-localisation potential with increasing cell PDL as observed in this results Chapter, it was sought to determine the extent of the loss of EGFR in aged fibroblast cells and further detail the EGFR deficiency at multiple levels including its transcriptional, translational and cell surface expression. Figure 4.3 defined and highlighted the importance of functional EGFR signalling in the differentiation response. The data reported here support previous findings of the age-associated loss of EGFR at the mRNA and protein levels. However, the activity of the EGFR promoter was not found to be significantly different between young and aged fibroblasts. The maintenance of EGFR promoter activity indicated that the transcription factors involved in EGFR transcription were unlikely to be affected in an age-dependent manner; and that there was another factor responsible for the loss of EGFR mRNA, protein and cell-surface expression. I, therefore, hypothesised that age-associated loss of EGFR could be regulated through the presence of mRNA inhibitors, such as miRNAs.

The results in this study also illustrated an age-associated loss of CD44 receptor membrane motility, as demonstrated by FRAP Confocal Microscopy. The HA receptor, CD44, can function as a co-receptor, physically associating with several membrane-bound proteins, resulting in modulation of intracellular signal transduction pathways and facilitating the formation of specialised signalling complexes [307, 308, 338]. The ability to do so with

EGFR plays a key role in myofibroblast differentiation as demonstrated by the previous results chapter. Whilst CD44 was free to diffuse within the plasma membrane of young fibroblasts, the ability of CD44 to diffuse freely was attenuated in aged cells. Since the loss of HA production by aged cells has also been described previously [244], we determined CD44 mobility to be HA-dependent and thus, a loss of overall HA could contribute to the loss of CD44 cell membrane movement in aged fibroblasts. Cell treatments with 4MU demonstrated that removal of HA production did indeed result in a loss of CD44 membrane motility.

Multiple reports have described miR-7 as having an important role in the regulation of EGFR in cancer and development [331, 332, 334]. However, this relationship between miR-7 and EGFR has not been described in other areas of EGFR function, such as fibroblast differentiation or age-associated loss of phenotype. *In silico* analysis identified the highly conserved seed site for miR-7-1 derived mature miR-7 on the 3'UTR of the EGFR mRNA. The upregulated levels of miR-7 reflect the downregulated EGFR mRNA present in aged fibroblasts. Additionally, an interesting observation was made in the young fibroblast group, wherein miR-7 was upregulated and EGFR mRNA downregulated, in response to TGF-β1. Whether this change to miR-7; and in turn EGFR mRNA, is directly modulated by TGF-β1 stimulation is not currently known and requires further investigation. However, a possible mechanism of miR-7 activity has been shown through its upregulated expression by EGFR-dependent c-Myc activation [332].

Interestingly, through miR-7 overexpression in young fibroblasts, the outcome was able to mimic the decreased expression of EGFR observed in aged fibroblasts, further supporting a role for miR-7 in age-associated regulation of EGFR and the differentiation response. Furthermore, the inhibition of miR-7 in aged fibroblasts significantly induced EGFR mRNA, protein and cell-surface expression, together with HAS2 mRNA. Additionally, in response to

TGF-β1 treatment in the presence of miR-7 inhibition, there was successful upregulation of α-SMA fibre formation and induction of α-SMA, HAS2 and EDA-FN mRNA, indicating the restored differentiation of fibroblasts to myofibroblasts.

The importance of HA-CD44 in mediating differentiation [339, 340] and the TGF-β1-induced, myofibroblast response [160, 196, 244, 297, 337], has been previously documented. Next, the effect of miR-7 overexpression and inhibition on CD44 motility in the cellular membrane was examined. Overexpression of miR-7 in young cells resulted in diffusion rates of CD44, declining to similar levels as those found in aged fibroblasts. Similarly, knockdown of HA synthesis by 4MU treatment reduced CD44 membrane motility. In addition, the inhibition of miR-7 in aged fibroblasts restored the diffusion rates of CD44, to levels observable in young fibroblasts. Since inhibition of miR-7 with LNA was able to upregulate both EGFR and HAS2 mRNA, the hypothesis that overexpression of HAS2 in aged fibroblasts could restore CD44 movement was tested. HAS2 overexpression and miR-7 LNA transfection restored CD44 movement in aged fibroblasts to rates observable in young fibroblasts. It was proposed that HAS2 synthesis of HA was an important mechanism mediating CD44 lateral movement throughout the cellular membrane and that miR-7 could regulate HAS2 expression through the inhibition of EGFR and components of its signalling pathway, therefore indirectly affecting CD44 movement in order to prevent cellular differentiation. Indeed, miR-7 has been shown to inhibit the protein kinase B/mammalian target of rapamycin (Akt/mTOR) pathway downstream of EGFR signalling [331, 333]; and an association between Akt and HAS2 production has previously been illustrated [341, 342].

Explanation of how miR-7 inhibition could rescue age-associated loss of differentiation, whilst EGFR overexpression alone could not [160], may be a result of an effect on the other mRNA targets of miR-7. *In silico* analysis of miR-7 seed sites revealed potential targets on

neither HAS2, α-SMA nor CD44. However, there were several targets of miR-7 within the EGFR signalling pathway. The activation of these targets is necessary for HAS2 induction, the reorganisation of the actin cytoskeleton, α-SMA upregulation and myofibroblast differentiation. These targets included MAPK/ERK, CaMKII, Rho-GTPase, phosphoinositide 3-kinase (PI3K), Akt and mTOR. EGFR overexpression in aged fibroblasts [160] failed to successfully restore differentiation. It is possible that this was due to an elevated expression of miR-7 in aged cells, not only inhibiting EGFR mRNA, but also the production of its downstream targets and thus, HAS2 and α-SMA gene induction. Bypassing the EGFR pathway and also overexpressing HAS2 could restore differentiation; and this was likely through the increased production of HA, restoration of CD44 membrane motility and its interaction with EGFR, solidifying the signalling response of EGFR and providing sufficient activity to trigger the differentiation response in aged fibroblasts.

The results shown in this Chapter can be summarised through the proposition of a mechanism in which miR-7 upregulation in aged cells is able to downregulate EGFR protein and expression through targeting EGFR mRNA for breakdown. miR-7 also has additional targets within the EGFR-dependent signalling pathway that directly regulate HAS2 production. The consequence of miR-7 activity, therefore, results in the downregulation of the key cellular components, EGFR and HAS2, involved in fibroblast to myofibroblast differentiation. Additionally, as a direct result of reduced HAS2 expression, there is a reduction in HA production and binding to CD44, compromising its ability to move throughout the cellular membrane and therefore, a reduction in its interaction with EGFR in response to TGF-β1 [160, 195, 308], an essential step in driving differentiation (summarised in Figure 4iii).

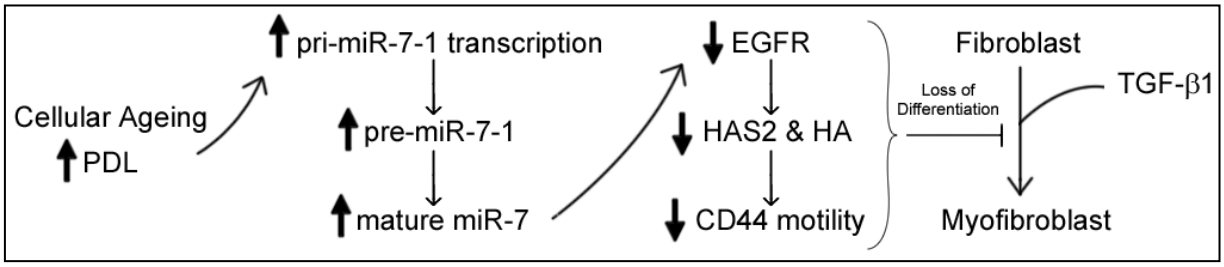

Figure 4iii. Summary of the actions of miR-7 derived from cellular ageing (increasing PDL). Increased expression of miR-7 leads to the inhibition of EGFR and its signalling, causing a decreased synthesis of HA and therefore, a reduction in CD44 motility within the cell membrane. These cumulate in the loss of TGF-β1 stimulated, fibroblast to myofibroblast differentiation.

The loss of cellular phenotype and response to stimulation is a pivotal change in cellular ageing. Age-related loss of fibroblast-to-myofibroblast differentiation is often associated with failure of normal wound healing and contraction, leading to chronic non-healing wounds in the elderly. Chronic non-healing wounds have been estimated to affect 4% of the UK population over the age of 65; and the morbidity associated with this impaired wound healing is estimated to cost the health service in excess of £1 billion annually in the UK [153] and $9 billion in the United States [343]. With the costs rising in correlation with the ageing population's ever-increasing lifespans, chronic wounds pose a real problem to present and future healthcare across the world.

The data reported in this chapter provide a novel insight into the targeting of miR-7 in aged fibroblasts, in order to rescue and promote differentiation into myofibroblasts and therefore, drive effective wound healing in the elderly. The following results chapter investigates the mechanism by which miR-7 expression is upregulated through increased transcription factor binding to its promoter region; and assessment of the impact of 17β-estradiol (E2) on the fibroblast phenotype and miR-7 expression, in light of reports of E2 interactions with EGFR and the stimulation of HAS-produced HA [344-348].

Chapter 5

The Roles of TGF-β1 and 17β-Estradiol in MicroRNA-7 Regulation and Effective Wound Healing

5.1 Introduction

5.1.1 Transcriptional Regulation of MicroRNA

The growing family of miRNAs regulate a diverse range of cellular processes and can impact on the progression of various diseases, through RNA-mediated gene-silencing mechanisms. Many current studies focus on regulatory functions of miRNAs, few are directed towards their transcriptional regulation. Although work into defining the structural features of miRNA promoters is limited, characterisation of miRNA promoter regions has gone some way to predicting miRNA transcription start sites.

Advancements in computational and biochemical methods [349-351] have revealed that many miRNAs use their own transcription start sites (TSS), whether they are located within non-protein coding DNA between genes (intergenic) or embedded within the introns of protein coding genes (intronic). However, some intragenic (within introns or exons) miRNAs use host gene TSS [352]. Recent studies of miRNA transcription have elucidated that intragenic miRNAs are co-transcribed by RNA polymerase II, or independently transcribed from their own RNA polymerase II or III initiation sites [353, 354]. It is, therefore, important when determining the TSS for miRNA, to take into consideration RNA polymerase II and III initiation sites within the promoter sequence.

Modifications to histones on promoter regions can provide some indication of where putative TSSs begin, such as trimethylation of lysine-4 of histone-3 (H3K4me3) and acetylation of lysine-9/14 of histone-3 (H3K9/14Ac). These have proven to be valuable markers of transcriptionally active promoters [355-358]. TSS identification has also been hampered by difficulty in determining start sites proximal to the mature miRNA sequence, especially when pri-miRNAs can have large and variable lengths [359, 360]. Despite this, an additional characteristic of transcriptionally active genes was observed, they were found to be

nucleosome-free within 100-130bp surrounding their TSS [361, 362]. A combination of these observations with reoccurring sequences commonly found within known TSS and at the 5' end of mRNA (TSS and cap analysis gene expression (CAGE) tags respectively), has led to the development of search engine software to help identify putative TSS of pri-miRNAs [352]. These techniques will be used in this chapter to help elucidate putative TSS for miR-7.

Several lines of evidence have recently emerged to suggest that miRNAs participate in self-regulatory loops, modulating their own expression. Recently, miR-145 was identified to be dependent on TP53 activation, which in turn could stimulate miR-145 expression [363]. It was also reported that several miRNAs regulate the expression of receptors and are themselves regulated by those same receptors in cancer cell-lines [364]. Since many miRNAs can have multiple mRNA targets, further study of the interaction between miRNAs and their regulatory factors may help illustrate their role in normal function and disease progression.

It has been previously indicated that miR-7 was a key mediator of EGFR signalling in lung cancer cells [332, 333]. It was found that c-Myc bound to the miR-7 promoter and enhanced its activity; and this was dependent on the activation of the EGFR-regulated Ras/ERK/c-Myc pathway [332]. In addition, miR-7 has been reported to target Akt and blocking the EGFR-mediated PI3K/Akt pathway also attenuated miR-7 expression [365]. These studies highlight two self-regulatory loops for miR-7 expression. However, in the cellular ageing of fibroblasts, the expression of EGFR is lost as highlighted in previous studies [159, 160] and the results of the previous Chapter, therefore suggesting the activity of Ras/ERK/c-Myc and the EGFR-dependent PI3K/Akt pathway would also be diminished. Therefore, the upregulated expression of miR-7 in aged fibroblasts is likely to be through an alternative receptor or signalling pathway, that is persistently activated through cellular ageing and can potentially activate c-Myc, Akt or additional enhancers of miR-7 expression. This results Chapter will further investigate the promoter region for miR-7 and any changes in transcription factors in

response to cytokine treatments, to help describe an alternative mechanism of miR-7 upregulation.

5.1.2 17β-Estradiol (E2)

17β-Estradiol (E2) is a derivative of the sex hormone estrogen and has the greatest potency of the estrogen by-products [366, 367]. Although E2 has greater serum abundance in females, it is also present in males as an active metabolic product of testosterone. However, the serum levels of E2 in elderly men (20-60pmol/L) are roughly comparable to those of elderly women (<35pmol/L). Therefore, in old age there is little discrepancy between gender and E2 levels [368]. E2 *in vivo* is interconvertible with estrone [367] and its main role is in reproduction. However, it also plays an important role in other organ systems and bone metabolism [369-371].

During the reproductive years, most E2 in women is produced by the granulosa cells of the ovaries, through estrone to E2 conversion by 17β-hydroxysteroid dehydrogenase [367]. Smaller amounts of E2 are also produced by the adrenal cortex and in men, by the testes. In both sexes, testosterone is converted to E2 by aromatisation [372, 373] and adipose tissues can produce active precursors of E2 [374].

E2 enters cells freely and interacts with cytoplasmic target cell receptors, estrogen receptor-α (ERα) and estrogen receptor-β (ERβ). The ER-complex can enter the nucleus of the target cell [375]; and regulate gene transcription through the modulation of additional transcription factors and binding to specific DNA sequences. This ultimately leads to modulation of gene expression and mRNA transcription, DNA replication and cellular proliferation. In plasma, E2 is largely bound to globulin or albumin and only a fraction (2.21% ± 0.04%) is free and biologically active [376].

Changes in the body shape affecting bones, joints, fat structure and deposition; and skin composition, are modified by E2 [374, 377-380]. The development and progression of cancers such as breast cancer, ovarian cancer and endometrial cancer, have also been cited as E2 driven [381-383]. Interestingly, it has also been noted that E2 treatments protect against cellular senescence [384].

5.1.3 E2 in Wound Healing

A link between estrogen and ageing has been previously established. Differences in gene expression between young and aged wound biopsies were found to be largely estrogen regulated [385]. Other studies demonstrated that both E2 and estrogen accelerated wound healing in ovariectomised mice [386].

The receptor mechanism through which E2 signals is of importance, as several studies have highlighted. E2 treatments in ERβ-null mice resulted in a negative effect on wound healing. This was also found *in vitro* in keratinocytes, with the researchers concluding that the inhibition of wound healing was via ERα activation [387]. Both human skin fibroblasts and keratinocytes have been shown to express ERα in the cytosol and ERβ in the nuclear compartment. However, in fibroblasts, ERβ had a higher basal expression, which increased when fibroblasts were treated with E2, promoting a pro-wound healing response [388-391]. Interestingly, human mammary fibroblasts and oral epithelial cells only express ERβ [390, 392]; and human lung fibroblasts preferentially express ERβ [392]. When these cells were treated with E2, an increased proliferative response was observed *in vivo* and *in vitro* [390, 392]. E2 treatments also increased secretions of HGF [391], the growth factor that is persistently expressed by oral mucosal fibroblasts and thought to potentiate their ability to rapidly proliferate and migrate. Additionally, the expression of epidermal ERβ was deemed to mediate effective skin healing [393].

Furthermore, ERα signalling caused decreases in HAS1 mRNA in VSMCs and resulted in an anti-proliferative effect [394]. E2 treatment was found to protect the HA matrix from photoageing in mice, by stimulating the upregulation of HAS3 in keratinocytes *in vitro* and *in vivo* [395]. E2 was also reported to increase the levels of HAS2 in mouse cumulus cells (granulosa cells surrounding the oocyte) [347]; and increase the HA content in the skin of mice [396].

Previous studies have indicated the co-ordinated actions of ER with EGFR [397, 398]. Changes in ER and EGFR expression followed similar profiles under E2 treatments and in inhibition studies, suggesting the two could be co-regulated [399]. Furthermore, the combined inhibition of ER and EGFR caused anti-proliferative effects in cancer cells [400]. However, it has recently been reported that in MCF-7 breast cancer cells, E2 treatments were detrimental to EGFR expression in an ERα- and miR-7-dependent manner [401]. Since the results from the previous Chapter demonstrate the regulatory effect of miR-7 in the age-associated loss of differentiation, this Chapter will investigate whether E2 treatment of fibroblasts (young and aged), regulate HAS, EGFR, miR-7, and their potential to differentiate.

5.1.4 Summary of Aims

The advantage of targeting miRNAs as therapeutic approaches is in their specificity, efficacy and markedly reduced toxicity, as compared to current treatment programmes. Previous reports have shown successful prevention of aberrantly over-expressed miRNAs with antagomirs [402, 403]. On the other hand, the effects remain transient, requiring continued treatment to maintain efficacy. Undesirable off-target effects that may arise from synthetic miRNA recognition of non-target mRNAs bearing partial homology, are also important factors for consideration. Instead, defining the processes that regulate miRNA expression could help to facilitate the discovery of novel therapeutics to correct aberrant expression,

through the targeting of disease or condition specific regulators of miRNA, which may prove more effective than direct transient inhibition of miRNAs.

Specifically this results Chapter will aim to explore the following in depth:

i. Assessment of the primary contributor from the differentiation pathway controlling the transcriptional regulation and upregulation of miR-7.

ii. Examination of the miR-promoter in detail using *in silico* analysis.

iii. The analysis of specific transcription factor regulation of miR-7 by;

    a. Determination of which pathway is responsible for the activation of transcription factors of interest.

    b. Through direct pathway inhibitor experiments.

iv. Assessment of the changes within young and aged fibroblasts, treated with E2.

v. Investigation into the changes to specific transcription factor activation with TGF-β1 and E2 treatment time-courses.

vi. To test whether combinational treatments with TGF-β1 and E2 are beneficial and can restore the differentiation potential in aged fibroblasts.

Investigation into the listed points will help to develop a detailed functional and mechanistic sequence of events that could help to explain the increased expression of miR-7 in response to TGF-β1 and cellular ageing, therefore addressing the issue of EGFR loss and age-associated loss of myofibroblast differentiation. The data generated in this Chapter could reveal specific targets for therapeutic treatment of aberrant miR-7 expression, which could potentially benefit and help restore ideal wound healing conditions for fibroblasts in chronic non-healing wounds in the elderly.

5.2 Results

5.2.1 Elucidation of the miR-7 Activating Pathway

Understanding the mechanism of regulation of miR-7 and the resultant suppression of EGFR and HAS2 mRNA, would allow specific targeting of the key elements of differentiation dysfunction, aiding the restoration of myofibroblastic properties in the chronic wounds of the elderly or to prevent the development of progressive fibrotic diseases. In order to elucidate which branch of the differentiation pathway, TGF-βRI-mediated or EGFR-mediated, was responsible for the upregulation of miR-7 and the down-regulation of EGFR, as observed in the previous Chapter, the chemical inhibitor of TGF-βRI or Alk5 receptor family activation, SB431542; and the chemical inhibitor of EGFR activation, AG1478, were used as treatments for cells, prior to TGF-β1 or EGF stimulation (Figure 5.1). Following treatments, the mRNA levels of EGFR (Figure 5.1A) and α-SMA (Figure 5.1B) were assessed by QPCR.

Treatments with SB431542 or AG1478 alone had no effect on the mRNA levels of either EGFR or α-SMA. TGF-β1 or EGF decreased the mRNA expression of EGFR. However, when SB431542 was used as a pre-treatment, only EGF reduced EGFR mRNA levels. Additionally, when AG1478 was used as a pre-treatment, the down-regulation was attenuated, suggesting that EGFR is self-regulatory and controlled through the HA-CD44/EGFR signalling arm of the differentiation response. The only treatment that was successful in the upregulation of α-SMA mRNA was TGF-β1 treatment alone, confirming that both branches of the differentiation pathway are required; and that TGF-β1 activated EGFR through the HA-CD44 mechanism, as discussed in the previous Chapters. These data also highlight that EGF stimulation of the EGFR-mediated branch alone is not sufficient enough to upregulate α-SMA levels and therefore, drive differentiation.

The expression of miR-7 was also assessed (Figure 5.1C) and where EGFR mRNA decreased (treatments with TGF-β1, EGF, or EGF+SB431542), miR-7 expression was significantly increased. These data support the findings from the EGFR mRNA assessment, in that the EGFR-mediated branch of the differentiation pathway is primarily responsible for the upregulation of miR-7. TGF-β1 is only able to upregulate miR-7, when EGFR is activated. These data indicate an EGFR-miR-7 self-regulatory loop, wherein a pathway activated by EGFR is able to upregulate miR-7 expression, which in turn can degrade EGFR mRNA.

5.2.2 Analysis of the miR-7 Promoter and Associated Transcription Factors

The miR-7 promoter has been reported to be within a -600bp to -300bp region upstream of the miR-7 coding region [332]. To further the investigation into a mechanism for miR-7 regulation, *in silico* analysis of the putative TSS for miR-7 and therefore, the promoter region, was carried out (Figure 5.2A). Using a combination of CAGE, TSS, and H3K4me3 tags, the putative TSS for pri-miR-7 was determined to be approximate to -250bp upstream of the miR-7 coding region, as indicated by the density of highly conserved CAGE and TSS tags flanked by H3K4me3 sites. Therefore, a sequence -624bp to -200bp upstream of the coding region (Figure 5.2B) was analysed *in silico* for putative transcription factor binding sites (Figure 5.2C). Interestingly, multiple signal transducers and activators of transcription (STAT) binding sites were present within the promoter sequence, including sites for STAT1, interferon-stimulated regulatory element (ISRE); and interferon-stimulated transcription factor 3γ (ISGF3G), upstream of a likely TSS location, as indicated by RNA polymerase III proximal sequence element (RNA Pol. III PSE); a strong determinant for the recruitment of RNA polymerase III. These potential transcription factor-binding sites suggest a strong possibility that STAT activation could contribute to the upregulated expression of miR-7, a plausible mechanism, especially since EGFR activation of the JAK/STAT pathway is possible [1, 3]. The underlined sequences denote the primer sequences selected for use in

miR-7 promoter luciferase reporter investigations, using TGF-β1 or EGF stimulation in the absence or presence of SB431542 or AG1478 (Figure 5.3). Fibroblasts were transfected with empty pGL3b (white bars) or miR-7-pGL3b (black bars, the chosen miR-7 promoter fragment ligated into a luciferase reporter construct). Similarly to the results from relative miR-7 expression analysis, both TGF-β1 and EGF were able to trigger the miR-7 promoter. However, when the Alk5 inhibitor, SB431542, was used as a pre-treatment, only EGF stimulation produced a luminescent response from the reporter construct. Treatment with AG1478, followed by TGF-β1 or EGF, produced luminescent responses. However, these were significantly attenuated from the treatments without the EGFR inhibitor. In light of the reported STAT and ISRE transcription factor binding sites within the miR-7 promoter, interferon γ (IFNγ) was used to test whether the upregulated promoter activity was a consequence of STAT activation. The results show that IFNγ induced the largest promoter activity. These data suggest that the activation of the miR-7 promoter is firstly EGFR-mediated in the TGF-β1-dependent differentiation response; and that this is likely through the activation of STATs.

To further examine the hypothesis of STAT-activated upregulation of miR-7, the mRNA of STAT1 was assessed by QPCR (Figure 5.4). STAT1 mRNA was upregulated approximately 4-fold in response to TGF-β1, EGF, EGF+SB431542, or IFNγ treatments (Figure 5.4A). It was also shown that STAT1 mRNA levels were increased in aged fibroblasts, when compared to their young counterparts (Figure 5.4B). Western blotting was used to assess changes in levels of phosphorylated STAT1 in the various experimental treatment conditions (Figure 5.4C). Phosphorylated levels of STAT1 were upregulated 2-fold in response to TGF-β1, 4-fold in response to EGF; and 10-fold in response to IFNγ. Treatments with AG1478 attenuated this phosphorylation. These data suggest that STAT1 is upregulated and activated following TGF-β1 stimulation, by the EGFR-mediated branch of the differentiation response.

5.2.3 The Role of the JAK/STAT Pathway in miR-7 Regulation

Investigation into the extent of the JAK/STAT pathway and its activation in the regulation of differentiation components and miR-7 was performed, by inhibiting the activation of JAK, using JAK inhibitor I, followed by QPCR analysis. The α-SMA upregulation by TGF-β1 was not affected by the inhibition of JAK (Figure 5.5A). The down-regulation of EGFR by TGF-β1 and IFNγ was prevented by JAK inhibition (Figure 5.5B). Interestingly, inhibition of JAK significantly increased HAS2 mRNA levels in both TGF-β1 and IFNγ stimulated cells, although IFNγ treatment alone did not change HAS2 expression (Figure 5.5C). Furthermore, inhibition of JAK attenuated the miR-7 upregulation by both TGF-β1 and IFNγ treatments (Figure 5.5D). The results shown here illustrate the role of the JAK/STAT pathway in miR-7 regulation, acting through a pathway that is independent of the TGF-β1-Smad pathway and the control of α-SMA expression.

5.2.4 The Effects of E2 on the Phenotype of Young and Aged Fibroblasts

The effects of E2 on fibroblasts and keratinocytes have been well documented [387-392], although whether E2 treatment has any effect on the differentiation response or the regulation of miR-7 has not yet been investigated. To determine whether E2 treatment affected the phenotype of young and aged fibroblasts, cells were incubated in serum-free media alone (white bars) or with 100nM E2 (black bars) for 72 hours. QPCR analysis of mRNA targets indicated that E2 treatment had no effect on α-SMA expression (Figure 5.6A). It did, however, significantly upregulate EGFR (Figure 5.6B) and HAS2 (Figure 5.6C) in both young and aged cells. Furthermore, E2 treatment downregulated miR-7 expression in young and aged fibroblasts (Figure 5.6D). To investigate the effect of E2 on cell proliferation, an alamarBlue assay was used (Figure 5.6E). Both the young (white boxes) and aged (black boxes) fibroblasts had significantly higher fluorescent intensity readings when incubated with E2, indicating the positive effect that E2 treatment had on proliferation. These data suggest

that E2 treatment is beneficial to fibroblasts, especially those that are nearing senescence, by restoring the levels of EGFR, HAS2 and miR-7, to those similarly observed in resting young fibroblasts, as well as increasing the potential for cells to continue to divide.

5.2.5 The Relationship Between miR-7 Regulation, TGF-β1 and E2 Stimulation

The results shown in this Chapter thus far indicate a relationship between miR-7, TGF-β1-dependent differentiation and E2 restoration of young fibroblast characteristics; all of which revolve around the EGFR-mediated branch of the differentiation pathway and the activation of the JAK/STAT1 signalling pathway. To further investigate this functional and mechanistic relationship, time-course experiments were performed and analysed by Western blotting and QPCR. TGF-β1 treatment over the course of 72 hours resulted in the gradual accumulation of phosphorylated STAT1, with no changes in the total STAT1 protein (Figure 5.7A). In contrast, phosphorylation of STAT1 decreased after 48 hours of E2 treatment; and this trend continued onto the 72 hour time-point (Figure 5.7B). Next, the mRNA expression of STAT1 was assessed. With TGF-β1 treatment, STAT1 mRNA was significantly upregulated at the 72 hour time point (Figure 5.7C), whilst E2 treatment had no significant affect on STAT1 mRNA expression (Figure 5.7D).

QPCR of EGFR mRNA and miR-7 under TGF-β1 and E2 treatments, assessed further consequences of changes in STAT1 activation. The levels of EGFR mRNA expression consistently decreased over the 72 hour time course, when cells were incubated with TGF-β1 (Figure 5.8A), the opposite was observed in cells incubated with E2 (Figure 5.8B). In contrast to EGFR expression, the expression of miR-7 was inversely correlated. miR-7 was consistently upregulated by TGF-β1, with a significantly increased 4-fold and 7-fold expression changes at 48 and 72 hours, respectively (Figure 5.8C). Additionally, miR-7 was significantly downregulated with E2, with a 2-fold and 4-fold decrease at 48 and 72 hours

respectively. (Figure 5.8D). It was therefore determined that 72 hours of treatment with E2 was sufficient to upregulate EGFR, whilst downregulating miR-7.

It was next investigated whether 72 hours of treatment with E2, followed by 72 hours of TGF-β1 was effective at restoring the differentiation response in aged fibroblasts. In cells that were treated with E2 followed by TGF-β1, expression of EGFR was maintained (Figure 5.9A) and expression of HAS2 significantly upregulated, compared to untreated controls (Figure 5.9B). The levels of miR-7 initially downregulated by E2 treatment, returned to those seen in untreated control cells, following TGF-β1 (Figure 5.9C). The myofibroblastic markers α-SMA (Figure 5.9D) and EDA-FN (Figure 5.9E), were both significantly upregulated when cells were incubated with E2, followed by TGF-β1. To test whether α-SMA stress-fibres were forming within the cells following treatments, the cells were permeabilised and stained for α-SMA (Figure 5.9F). In cells that had receieved both E2 and TGF-β1 treatments, there was a noticeable increase in the intensity of the α-SMA stain and although stress-fibres were not formed throughout the entire cell, there were bundles present. These data suggest that pre-treatment of cells with E2 can "prepare" aged cells for TGF-β1-dependent differentiation, through the upregulation of key components, EGFR and HAS2; and the down-regulation of the limiting factor, miR-7; indicating that optimisation of E2 treatments in combination with TGF-β1 could be beneficial for restoration of the differentiation response in cells nearing senescence.

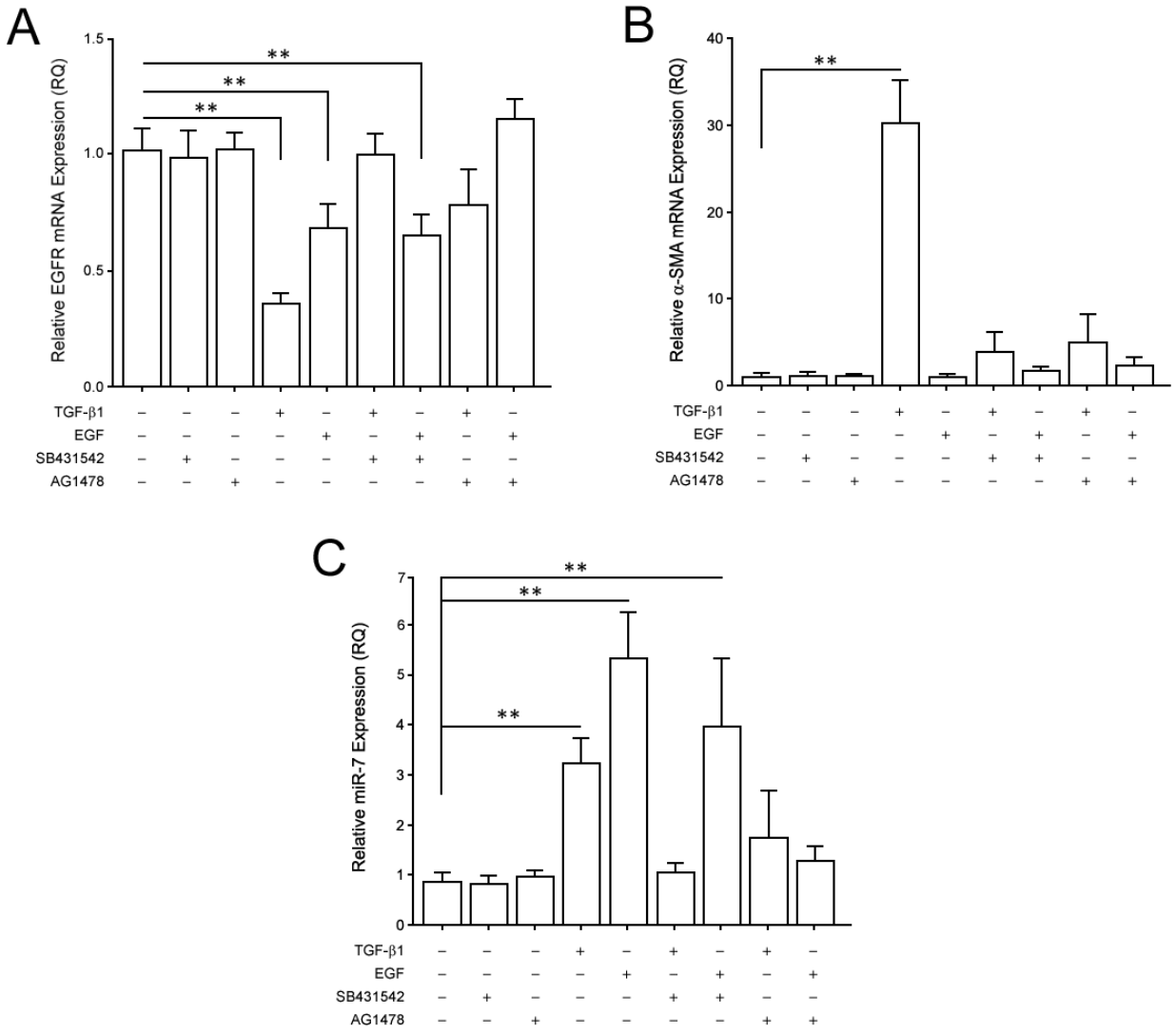

Figure 5.1. Determination of the miR-7 Upregulation Pathway. Fibroblasts were grown to confluence, growth arrested and incubated in serum-free media containing 0.6% (v/v) DMSO, 10μM SB431542 or 10μM AG1478 for 1 hour, before the media was replaced with serum-free media alone, media containing 10ng/ml TGF-β1, or media containing 10ng/ml EGF for 72 hours. RNA was extracted, purified, and reverse transcribed and then QPCR was used to analyse the mRNA expression of **A.** EGFR and **B.** α-SMA. **C.** miR-QPCR was used to analyse miR-7 expression. All results are shown as the mean ± s.e.m. of 3 independent experiments. ***P=<0.01*.

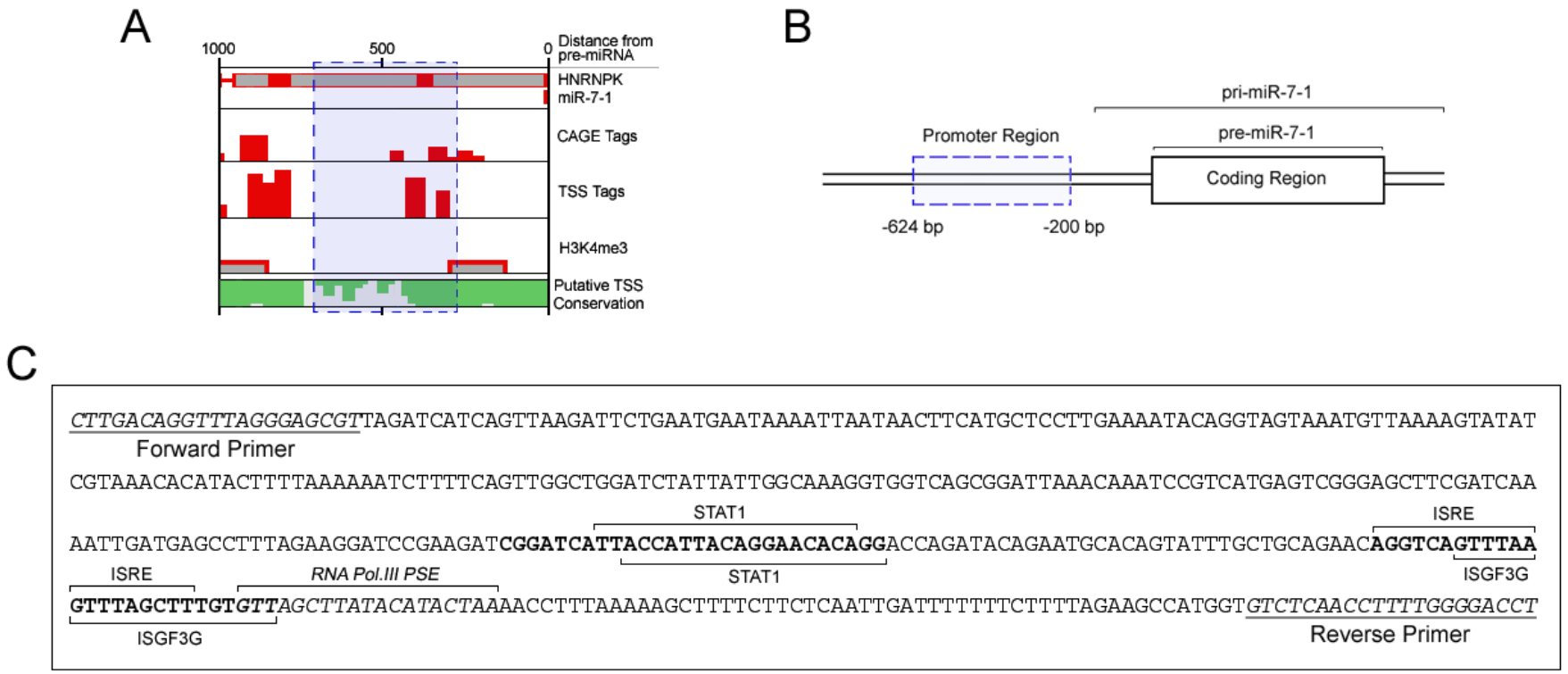

Figure 5.2. *In Silico* Analysis of the miR-7 Promoter Region. *In silico* analysis was used to determine **A.** the putative TSS for miR-7, dashed blue box indicates the region predicted to contain the TSS and upstream promoter sequence. Image was generated and analysed using miRStart computational software (Institute of Bioinformatics and Systems, National Chiao Tung University, Hsinchu, Taiwan). **B.** Diagram of miR-7 coding region and upstream promoter region used for analysis, dashed blue box indicates region used for promoter studies. **C.** The promoter region for miR-7 was analysed for recognised transcription factor binding sites. Transcription factors of interest are labelled and underlined sections indicate the primers used for promoter amplification. Promoter sequence was analysed for transcription factors using MatInspector (Genomatix Software, Munich, Germany).

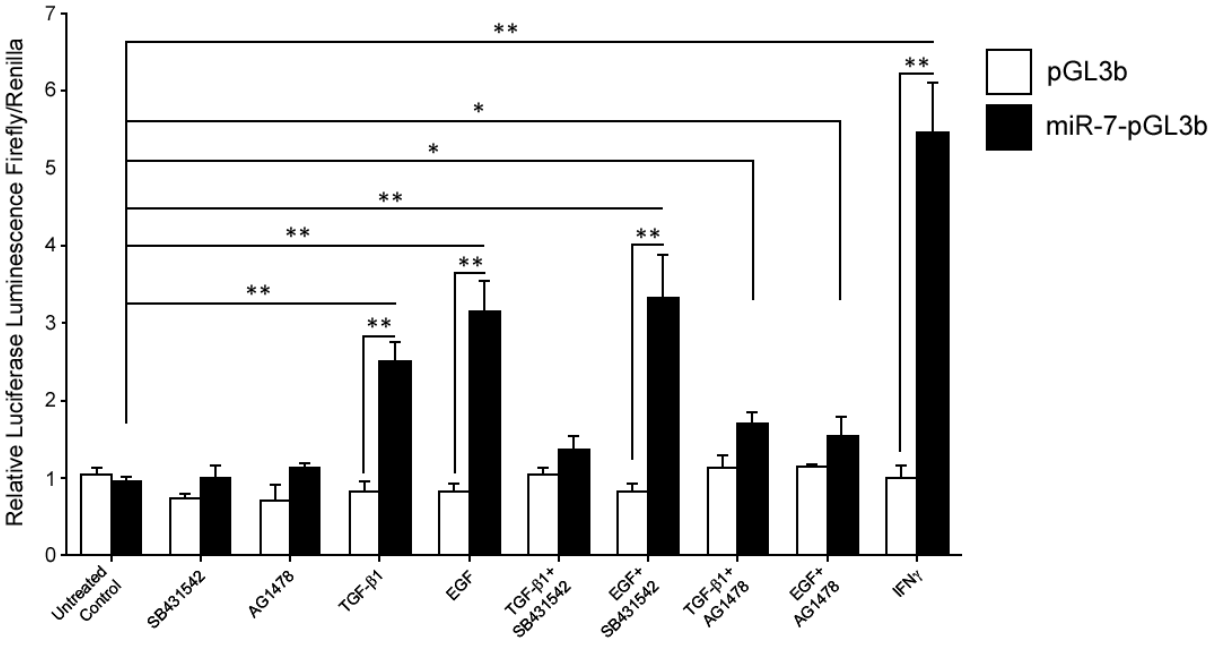

Figure 5.3. Analysis of miR-7 Promoter Activity. Fibroblasts were grown to 60-70% confluence and transfected with either empty pGL3b (white bars) or miR-7-pGL3b (black bars). The indicated cellular treatments were performed 24 hours post-transfection and the promoter activity analysed after a further 24 hours. Co-transfection of Renilla was used to measure transfection efficiency and for normalisation of data. The results shown are the means of the firefly luciferase/Renilla luciferase ratios ± s.e.m. of 3 independent experiments. *$P=<0.05$, **$P=<0.01$.

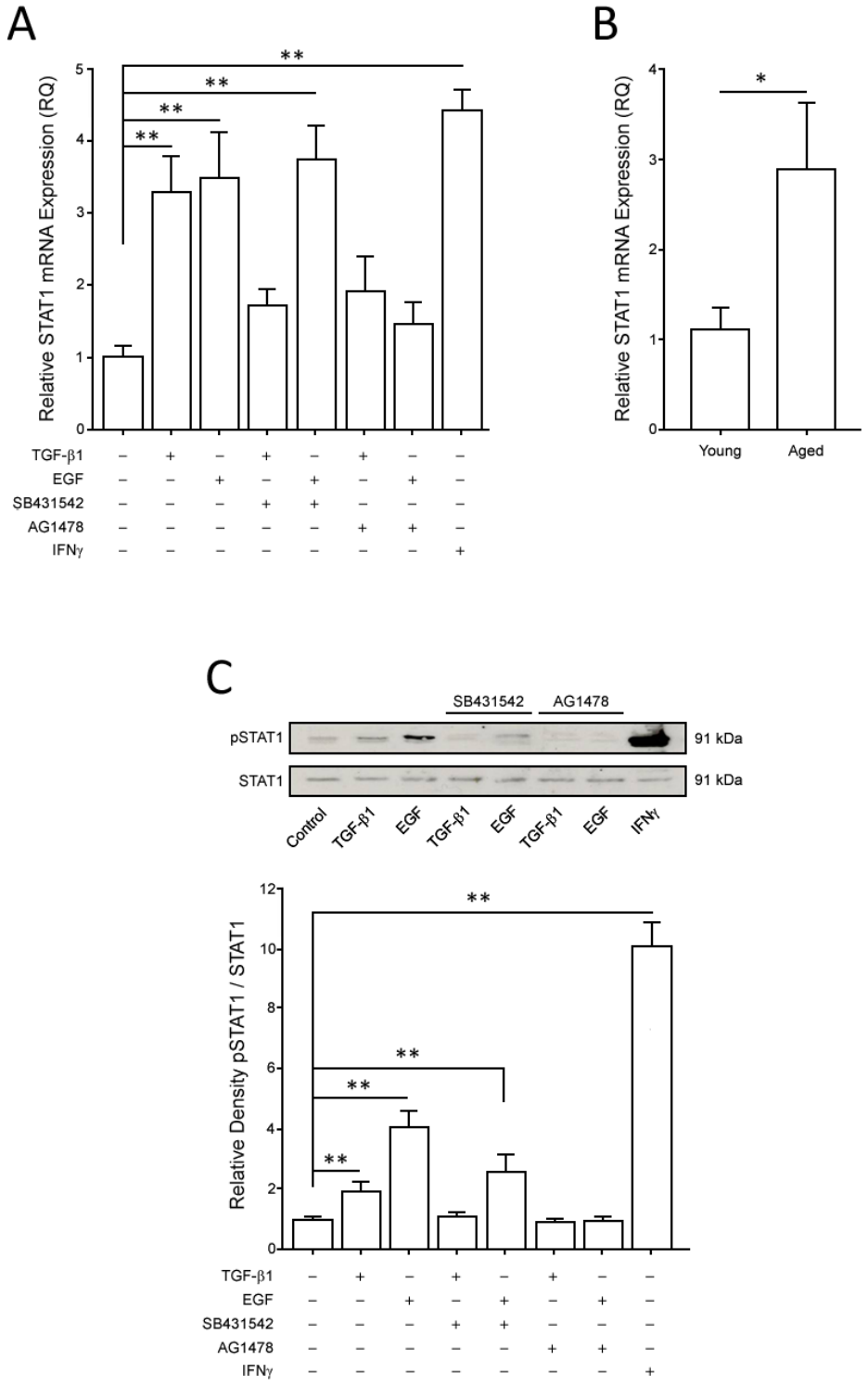

Figure 5.4. Induction of STAT1 Activation and Expression. A. Young fibroblasts were grown to confluence, growth arrested and stimulated with the indicated treatments for 72 hours, before STAT1 mRNA was assessed by QPCR. Results are shown as the mean ± s.e.m. of 3 independent experiments. **B.** Young or aged cells were grown to confluence and STAT1 mRNA was assessed by QPCR. Results are shown as the mean ± s.e.m. of 3 independent experiments. **C.** Young fibroblasts grown to confluence were growth arrested and incubated with the indicated treatments. Protein was extracted and Western blotting was used to assess the phosphorylation of STAT1. Total STAT1 protein was used as a loading control and for normalisation. The results shown are the mean ± s.e.m. of 3 independent experiments. *$P=<0.05$, **$P=<0.01$.

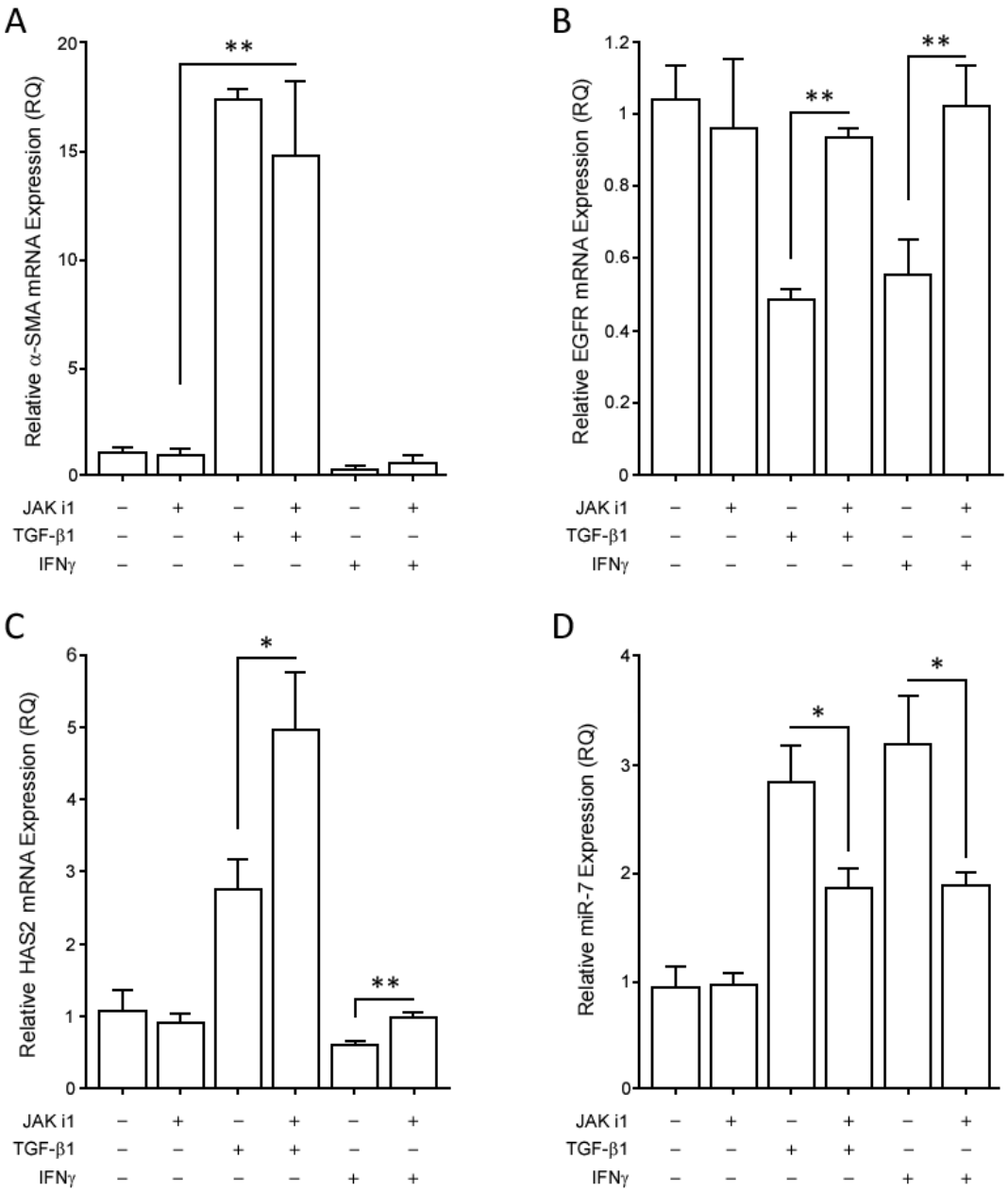

Figure 5.5. The Effects of Inhibiting the JAK/STAT Pathway. Fibroblasts were grown to confluence, growth arrested and incubated with 15nM JAK Inhibitor I for 1 hour, prior to incubation in serum-free media alone, media containing 10ng/ml TGF-β1, or media containing 10ng/ml IFNγ for 72 hours. QPCR was used to analyse the expression of **A.** α-SMA mRNA, **B.** EGFR mRNA, **C.** HAS2 mRNA and **D.** miR-7. Results are shown as the mean ± s.e.m. of 3 independent experiments. **P=<0.05*, ***P=<0.01*.

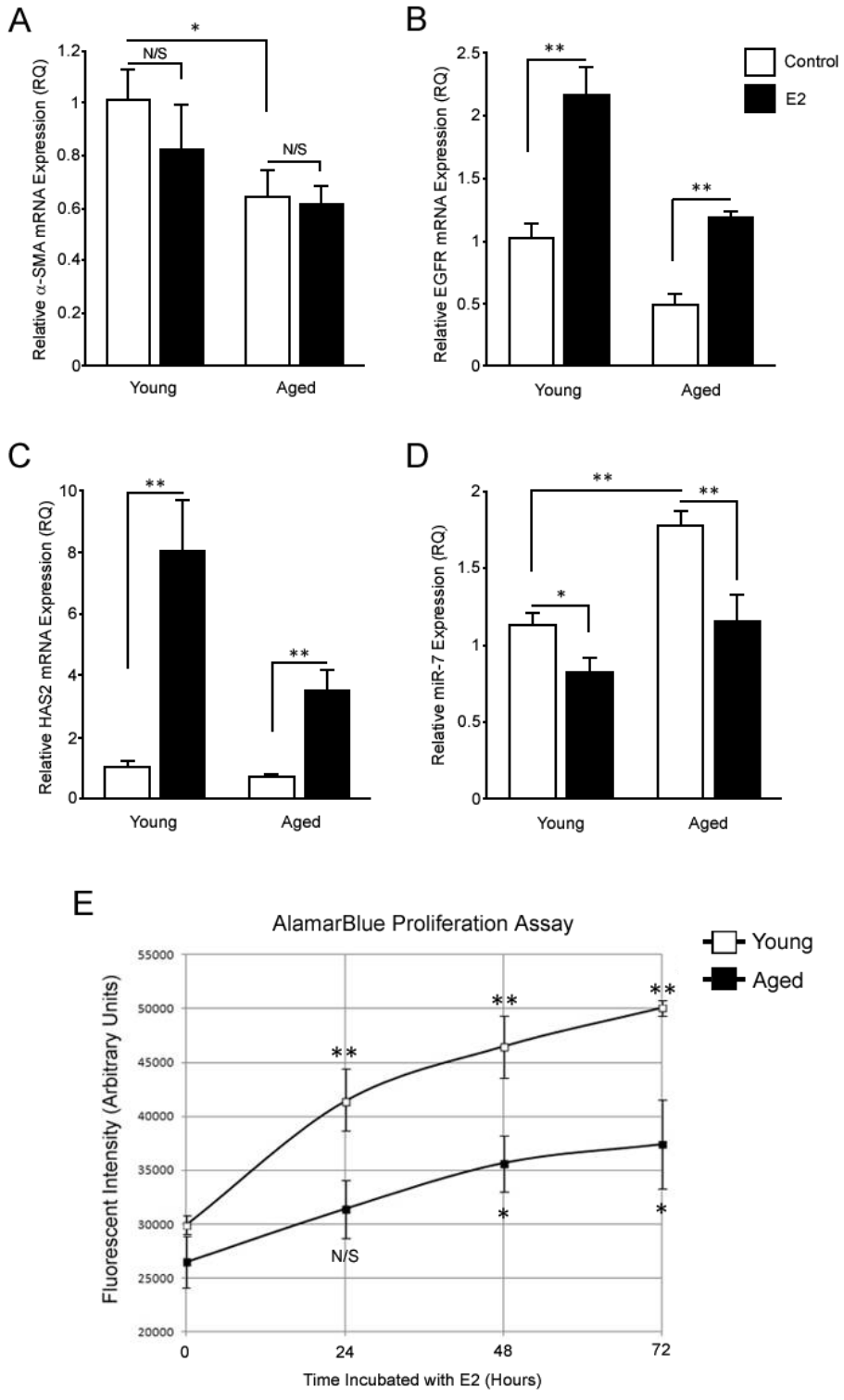

Figure 5.6. The Effects of E2 on Young and Aged Fibroblasts. Young or aged fibroblasts were grown to confluence, growth arrested and incubated with serum-free media alone (white bars) or media containing 100nM E2 (black bars), for 72 hours. QPCR was used to analyse the expression of **A.** α-SMA mRNA, **B.** EGFR mRNA, **C.** HAS2 mRNA and **D.** miR-7. Results are shown as the mean ± s.e.m. of 3 independent experiments. **E.** Young (white boxes) and aged (black boxes) fibroblasts were incubated with E2 over 72 hours. At each indicated time-point, the proliferation rates were measured by the addition of 10% (v/v) alamarBlue for 1 hour, before fluorescent intensity analysis with an optical plate reader. **P=<0.05, **P=<0.01*.

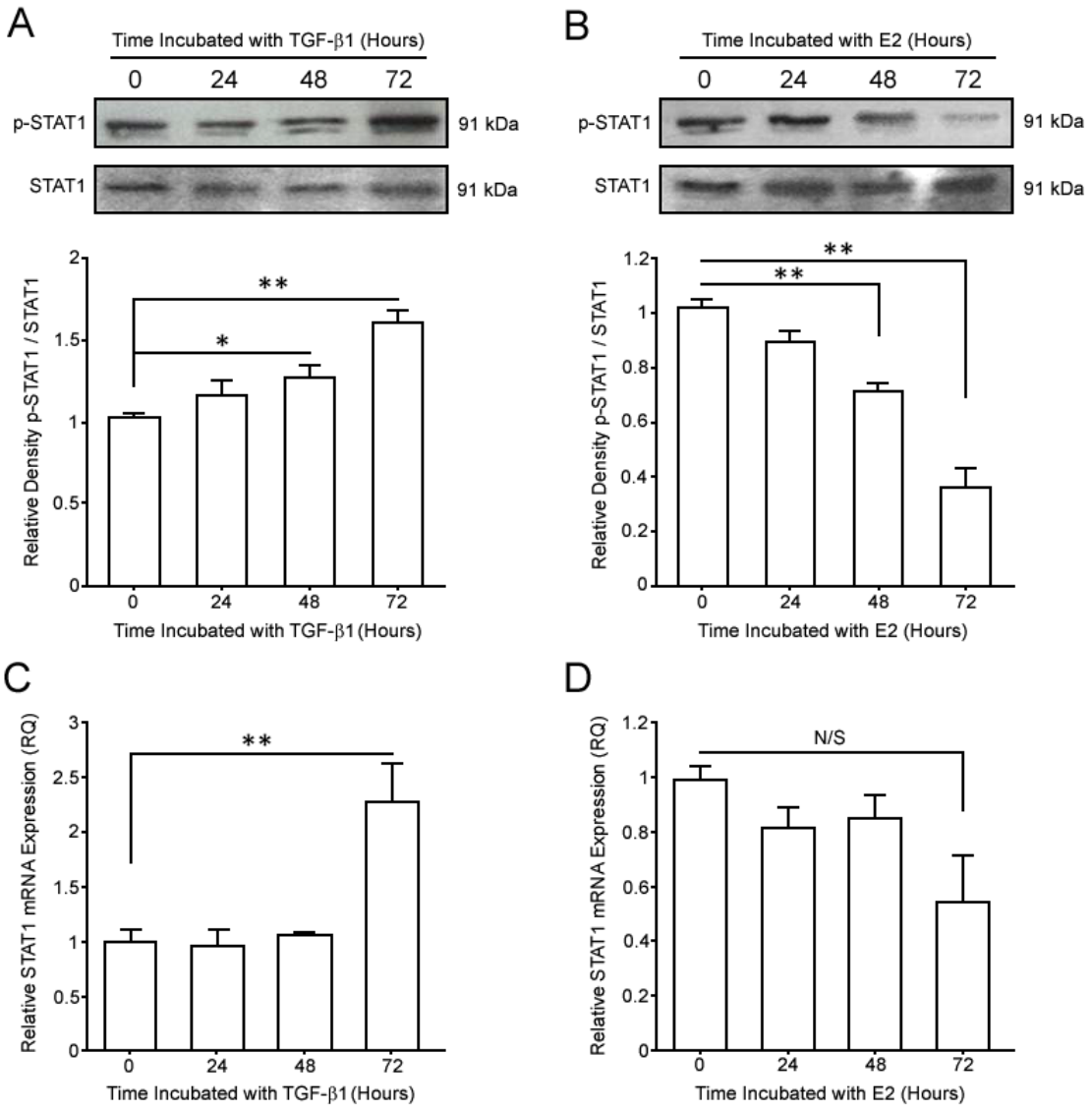

Figure 5.7. Regulation of STAT1 by TGF-β1 and E2. Fibroblasts were grown to confluence, growth arrested and incubated with serum-free media alone, media containing 10ng/ml TGF-β1, or media containing 100nM E2 over 72 hours. Protein was extracted and Western blotting was used to assess the changes in phosphorylation of STAT1 with **A.** TGF-β1 treatment and **B.** E2 treatment. Total STAT1 protein was used to ensure equal loading and for normalisation of densitometry. Results shown are the mean ± s.e.m. of 3 independent experiments. QPCR was used to analyse the expression of STAT1 mRNA with **C.** TGF-β1 treatment and **D.** E2 treatment. Results are shown as the mean ± s.e.m. of 3 independent experiments. *N/S= no significance*, **P=<0.05*, ***P=<0.01*.

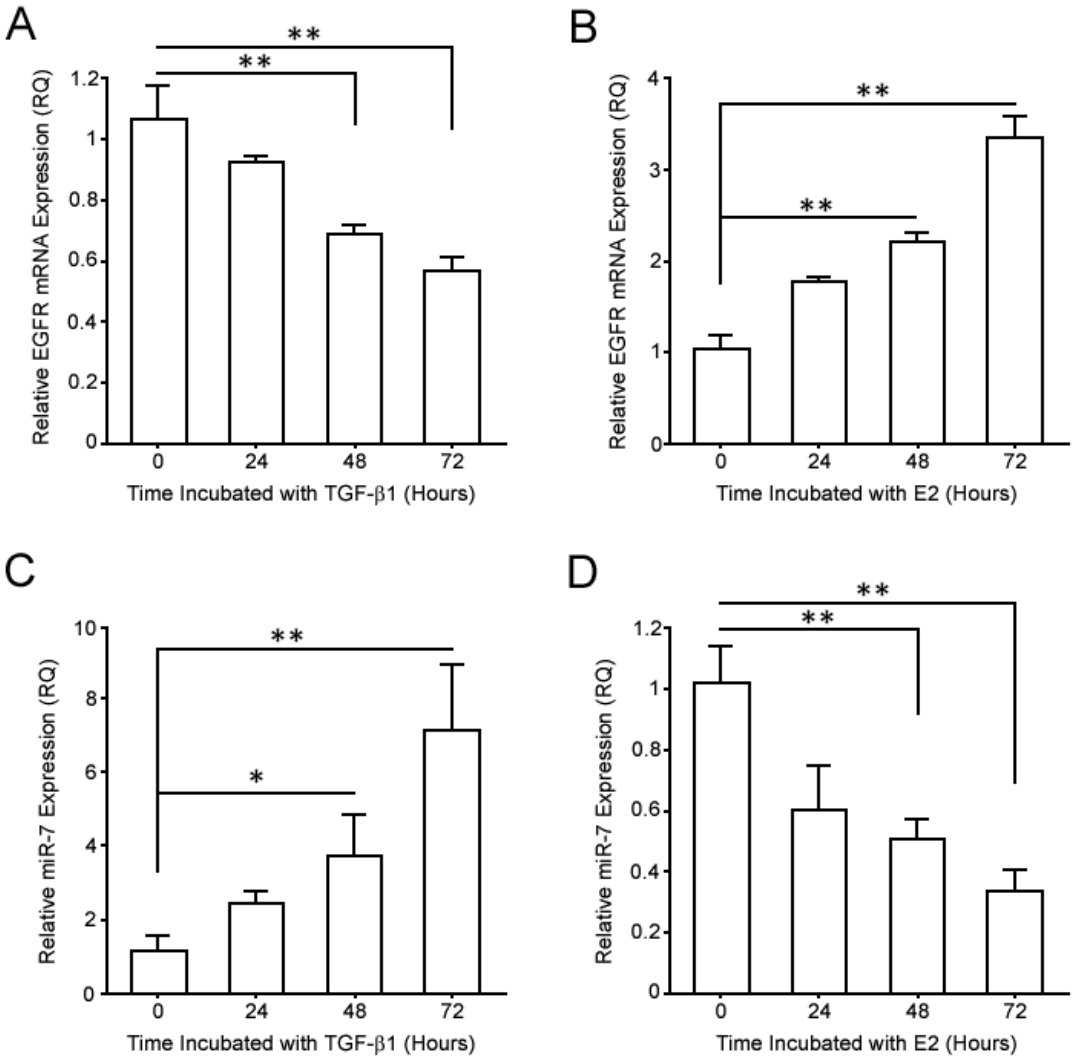

Figure 5.8. Regulation of EGFR and miR-7 by TGF-β1 and E2. Fibroblasts were grown to confluence; growth arrested and incubated with serum-free media alone, media containing 10ng/ml TGF-β1, or media containing 100nM E2 over 72 hours. RNA was extracted and purified and then QPCR was used to analyse the expression of EGFR mRNA with **A.** TGF-β1 treatment and **B.** E2 treatment, and the expression of miR-7 with **C.** TGF-β1 treatment and **D.** E2 treatment. Results are shown as the mean ± s.e.m. of 3 independent experiments. *$P=<0.05$, **$P=<0.01$.

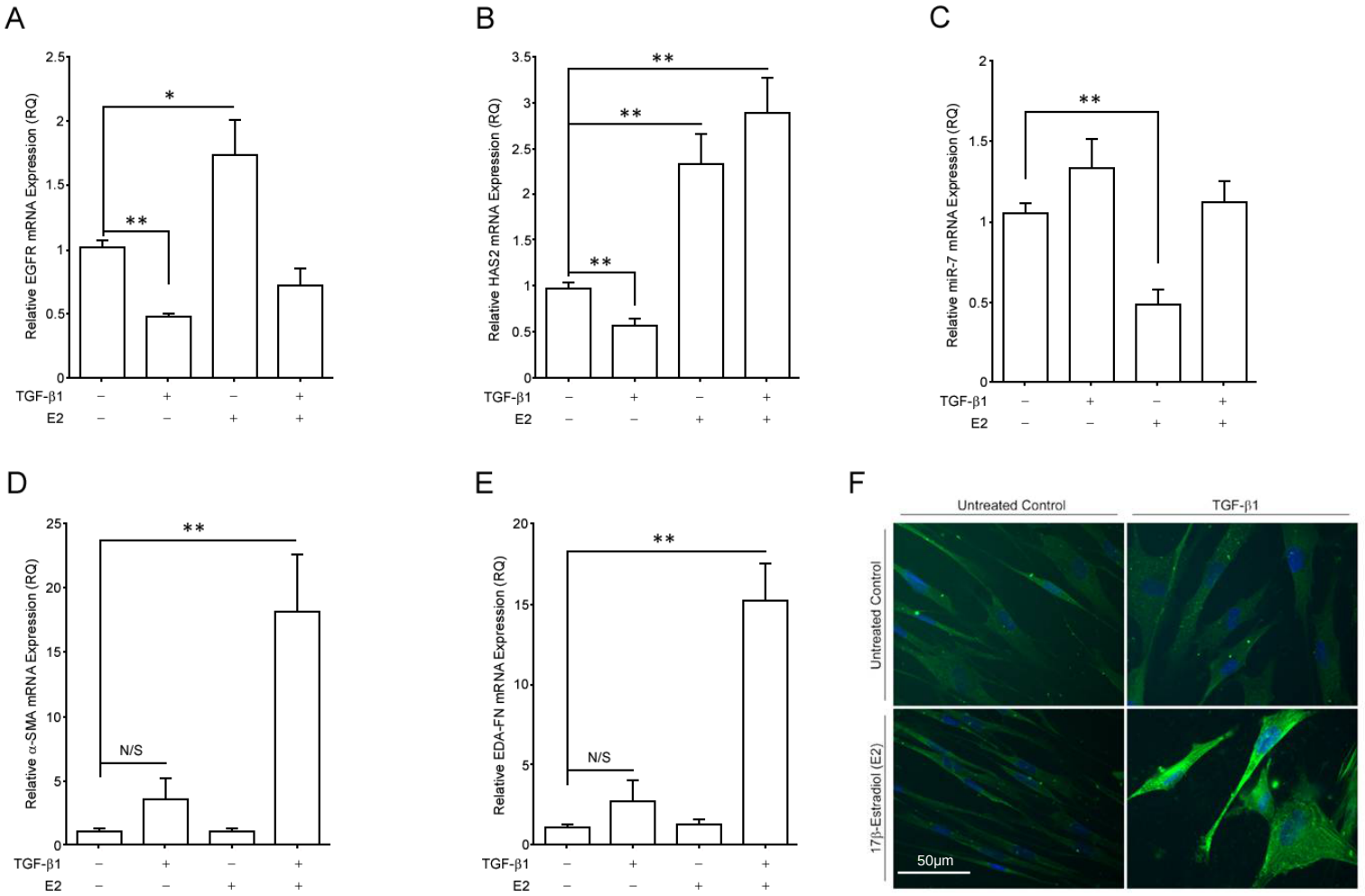

Figure 5.9. E2 and Subsequent TGF-β1 Treatment Restores Differentiation in Aged Fibroblasts. Aged fibroblasts were grown to confluence; growth arrested and incubated with either serum-free media alone, media containing 10ng/ml TGF-β1, or media containing 100nM E2 for 72 hours. An additional treatment with media containing 10ng/ml TGF-β1 was made to E2 treated cells for a further 72 hours. The expression of **A.** EGFR mRNA, **B.** HAS2 mRNA, **C.** miR-7, **D.** α-SMA mRNA and **E.** EDA-FN mRNA, was analysed using QPCR. Results are shown as the mean ± s.e.m. of 3 independent experiments. **F.** Immunocytochemistry was used for 70% confluent cells, staining for the visualisation of α-SMA protein. Images displayed are representative of 5 individual experiments. *$P=<0.05$, **$P=<0.01$.

5.3 Discussion

The data reported in this Chapter provide an important mechanistic insight into the regulation of miR-7 by STAT1 activation; and unveils novel interactions between the cytokines that directly or indirectly modulate miR-7 expression and the phenotype of fibroblasts. The role of miR-7 in the regulation of EGFR and its pathway has been reported in many instances and in different species [332-334], highlighting its conserved function. However, this Chapter and the previous results Chapter examined miR-7 expression in the context of cellular ageing and wound healing, specific studies that have not been performed before.

As shown in the previous Chapter, the activity of the EGFR promoter was not modulated by cellular ageing and a candidate for the suppression of EGFR expression, miR-7, was determined to suppress the production of EGFR protein at the mRNA level, pre-translation. Therefore, understanding the principal factor(s) in the upregulation of miR-7 transcription was an important first step of this investigation and it was determined, through the use of cell surface receptor inhibitors, that the EGFR signalling branch (HA-CD44-mediated) of the differentiation pathway was responsible for the upregulation of miR-7 expression and the suppression of EGFR mRNA; a self-regulatory loop involving the EGFR upregulation of miR-7, with miR-7 in turn, causing the downregulation of EGFR. Examination of the miR-7 promoter was ideal for furthering the investigation, as isolating transcription factors that enhance the miR-7 transcription would provide targets for interventional measures. The promoter region of miR-7 was elucidated using previous studies [332] and *in silico* analysis of TSS associated tags. Determining which transcription factors were binding to the miR-7 promoter and enhancing miR-7 transcription was the next step of the investigation; and it was noted that there was an abundance of interferon regulated elements, specifically STATs, in the putative promoter region.

To further investigate the involvement of STATs and whether the EGFR pathway was responsible for increased miR-7 promoter activity, the promoter region was ligated into a luciferase reporter plasmid. The data shown suggested that EGFR was capable of mediating the promoter activity of miR-7; and the induction by IFNγ treatment supported the hypothesis that STATs were the responsible transcription factors. These data led to the hypothesis of a potential mechanism involving EGFR activation of the JAK/STAT pathway, which has been reported previously [1, 3]; and was further supported by the EGFR-mediated phosphorylation of STAT1 as shown in Figure 5.4. However, the fluctuations in STAT1 mRNA expression did not seem to impact on the total STAT1 protein present from whole cell lysates, a change that may be seen at longer time-points. The inhibition of JAK did not alter TGF-β1 upregulation of α-SMA, providing evidence that the differentiation pathway was independent in function from the EGFR-mediated JAK/STAT pathway. However, when JAK was inhibited, EGFR mRNA did not down-regulate and HAS2 mRNA increased in the presence of TGF-β1 or IFNγ, suggesting multiple functions of STATs on the regulation of differentiation pathway components. Suppression of EGFR through miR-7 upregulation may be separate from HAS2 suppression (possibly through an alternative miRNA), a mechanism that should be investigated further.

The effects of E2 on wound healing have been an area of research that has generated much interest over recent years [346, 380, 386, 387, 395]. Although previous research has shown the changes in fibroblasts treated with E2, exploring the links between E2 and its effect on the proteins necessary for myofibroblast differentiation has had limited attention. The results in this Chapter illustrated the changes of EGFR, HAS2 and miR-7 expression in young and aged fibroblasts, by E2 treatment. Whether E2 also affects translational or post-translational changes in EGFR, HAS2 and HA synthesis is not known and warrants further investigation. The data that is shown here revealed a means by which incubation of aged cells with E2

"prepared" the cells for the subsequent TGF-β1 treatment by increasing the expression of the mRNA for key components (EGFR and HAS2), whilst decreasing the expression of the pathway limiter (miR-7). Additionally, it was shown that E2 followed by TGF-β1 treatment was able to restore the ability of aged fibroblasts to form α-SMA stress-fibres.

The *in vitro* benefits of E2 on fibroblasts described here indicate a mechanism of action that downregulates miR-7 and thereby relieves the suppression placed on EGFR mRNA, increasing its expression. Therefore, further investigation is required to elucidate the specific interactions or functional and mechanistic outcomes of direct actions by E2 treatment.

Two areas of investigation warrant further analysis, the first is to assess the direct action of E2 on the miR-7 promoter. *In silico* analysis identified a sequence motif within the promoter region used, for estrogen response elements (IR3) and estrogen receptor (ER) binding, potentially indicative of a transcriptional suppression role. Through experiments exploring E2 stimulation using either site deletions or ER inhibition, the effect of E2 on the miR-7 promoter could be explored. Additionally, it was observed that the phosphorylation of STAT1 was reduced the longer cells were incubated with E2. The second area of investigation would be examination of whether E2 has direct effects on other STAT targets (e.g. STAT3), the production of activators of STATs, such as IFNγ, the previously reported downregulation of IL-6 [105, 404-407]; and their corresponding cell surface receptors, could help detail a full mechanism of action for E2 and explain its impact on miR-7, EGFR, HAS2 and the differentiation pathway in fibroblasts.

Specifically, analysis of IL-6 would be of primary interest as the correlation between cellular ageing and IL-6 has been previously reported in a plethora of studies [408, 409]; and the serum concentrations of IL-6 have been reported to increase with progressing age [410], although one study did not observe this correlation [411]. IL-6 is also a potent activator of

STATs and stimulates increased production of STAT mRNA [412, 413], which would go some way to supporting the observations made in this results Chapter. Furthermore, a broader analysis of changes in miRNAs under TGF-β1 and E2 treatments in young and aged fibroblasts, using microarrays, could indicate other miRNAs that may be present and actively inhibiting the differentiation pathway components.

Although with direct E2 treatment *in vitro*, the fibroblasts established beneficial outcomes, the effects of circulating serum levels of E2 *in vivo* may have a limited effect on the fibroblasts within the dermis or in other organ systems. Additionally, when combined with the low levels of estrogen in men and in post-menopausal women, E2 application may only be of therapeutic significance in terms of wound healing, when used to upregulate factors lost from cellular ageing. It can be concluded from the data presented in this results Chapter that a combinational treatment of E2 and TGF-β1 to aged fibroblasts was beneficial in reversing the age-associated loss of differentiation. The initial E2 treatments had a profound effect on fibroblasts, upregulating the key components needed for successful differentiation (EGFR, HAS2) and downregulating the limiting factors (p-STAT1, miR-7). The subsequent incubation with TGF-β1 was, therefore, able to drive myofibroblast differentiation, as shown by the production of myofibroblastic markers (α-SMA, EDA-FN). However, the treatment regime of 72 hours of E2 followed by 72 hours of TGF-β1 incubation may require further optimisation in order to achieve the best results.

Chapter 6

General Discussion

The data presented in this thesis advances the knowledge of a complex cellular mechanism: fibroblast to myofibroblast differentiation. A detailed pathway of action was described, encompassing the various components of differentiation. A key finding was the alterations in behavioural dynamics of the HA receptor, CD44, within the cell membrane. The rate at which CD44 diffused throughout the membrane changed with cellular ageing and during differentiation. However, the loss of CD44 motility in each case was for different reasons. Figure 6i illustrates an explanation of the behavioural changes of CD44, under various conditions.

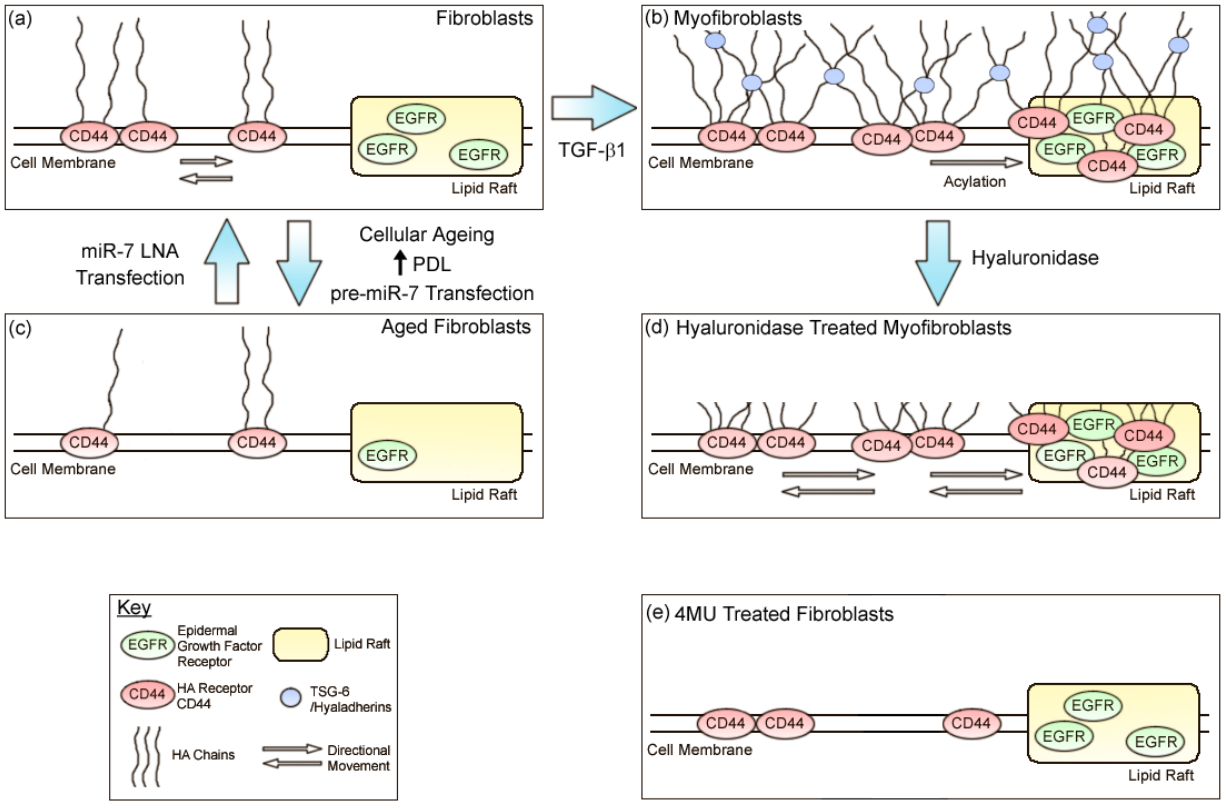

Figure 6i. Illustrated explanation of the behavioural changes in CD44 interactions and membrane motility, with cellular ageing, myofibroblast differentiation and various cellular treatments.

a) Fibroblasts – In young, resting fibroblasts, CD44 diffused rapidly throughout the cell membrane. The movement of CD44 within the membrane could be essential for its fast re-localisation and association with multiple proteins [281-283, 290], its role as a co-receptor for

rapid induction of intracellular signalling [414, 415]; and its cleavage which can drive migration in lung cancer cells [416]. A possible explanation for the motility of CD44 may lie with its biochemical properties. One CD44 receptor in itself has low affinity for binding HA, when multiple CD44 bind HA, the affinity and binding strength between CD44 clusters and HA increases [417-419]. It could be that there is constant association and disassociation of free CD44 with HA, due to a ratio of high levels of CD44 to low levels of HA. There is currently no literature on CD44 membrane dynamics and therefore, there is limited insight and revelations on the functional significance of CD44 diffusion potential. This thesis investigated CD44 movement and provides a viable hypothesis for HA-dependent CD44 movement and its requirement for co-receptor interactions.

b) Myofibroblasts – Changes in the production of HA and the HA pericellular coat are marked in myofibroblast differentiation [244, 252]. Following myofibroblast differentiation, the changes in HA production have a distinct effect on the mobility of CD44 within the cell membrane. Here, it is proposed that the loss of CD44 motility was due to strong binding to multiple HA-chains present on the myofibroblast cell surface, balancing the HA:CD44 ratio; and combined with CD44 association with EGFR in lipid rafts, following acylation or palmitoylation of CD44 [279, 315] (a possible effect of TGF-βRI activation). There is limited research on what protein or pathway is responsible for CD44 conformational and functional change. It has been reported that PKC (a downstream target of TGF-βRI phosphorylation [420]) may have a role in this [283, 421]. Strong associations with EGFR and multiple HA-chains hold CD44 in clusters. Due to hyaladherin upregulation/release following TGF-β1 stimulation; TSG-6, IαI or other hyaladherins cross-link HA chains forming a rigid network surrounding the cell; the HA pericellular coat [247, 422, 423]. This coat formation “locks” up the CD44 in the membrane and in lipid rafts. One limiting step for CD44-EGFR co-localisation and differentiation is acylation/palmitoylation of CD44, described in

chondrocytes as being a necessary step for CD44 association with lipid raft micro-domains [279]. Treatment with the palmitoylation inhibitor, 2-bromo-palmitate, inhibited CD44 association with lipid rafts and downstream signalling events [279, 424]. This modification to CD44 was found to occur on cysteine residues of the CD44 cytoplasmic tail (cys^{286} or cys^{295}). Mutation of these sites reduced palmitic acid incorporation into CD44 and prevented CD44-lipid raft association. This also prevented HA internalisation and CD44 turnover in CD44 transfected, COS-7 cells [425], indicating the important function of lipid-rafts. These reports raise questions about whether the association of CD44 with lipid rafts has regulatory effects on other CD44 related functions, such as cell signalling or co-receptor interactions. The data presented here would suggest that is the case and that targeting the protein responsible for CD44 acylation may be a useful mechanism for prevention of the TGF-β1 differentiation of fibroblast to myofibroblasts.

c) Aged Fibroblasts – The loss of HA synthesis, cell-surface EGFR and CD44 transcription, were factors identified as contributors to age-associated dysfunction of differentiation; findings supported by previous research [160, 195, 244]. The data suggests that in aged fibroblasts, CD44 had reduced membrane diffusion ultimately deemed to be HA-regulated (restored by HAS2 overexpression). As such, it could be speculated that low levels of HA present on the aged fibroblast attenuated movement of CD44 between HA binding points. The loss of HA synthesis by HAS2, a consequence of diminished EGFR levels, was found to be liable for the reduced motility of CD44. This proposal was supported through pre-miR-7 transfection into young fibroblasts, which produced an aged-like phenotype with reduced CD44 movement. These findings raise the question, how does inhibition of miR-7 result in HAS2 upregulation and HA production? Measurements of the levels of HA and activated EGFR as a result of miR-7 LNA transfection, would provide useful answers and information.

d) Hyaluronidase Treated Myofibroblasts – The hypothesis that HA was involved in regulating CD44 membrane movement was tested by using hyaluronidase, to remove the HA pericellular coat prior to FRAP analysis. The data suggest that although CD44 could remain in association with EGFR, the loss of HA released clusters of CD44 and restored their membrane motility. The results provided a key insight into the role of the HA pericellular coat in orchestrating intracellular signalling, regulating CD44 activity and stabilising the myofibroblast phenotype. Targeting the HA pericellular coat may be one way to reverse the myofibroblast phenotype and limit or prevent progressive fibrosis.

e) 4MU Treated Fibroblasts – Inhibition of HA synthesis has proven to be detrimental to HA pericellular coat formation and cell function [244, 245], resulting in the failure of differentiation. The data reported here suggest that HA can modify CD44 membrane motility. Therefore, 4MU removal of HA synthesis was used to further test this hypothesis. The results showed CD44 diffusion rate and mobile fraction decreased. The loss of CD44 movement may primarily be a consequence of the loss of HA binding regions that CD44 could move between.

This research highlights CD44, lipid rafts; and the HA-pericellular coat/hyaladherin network, as potential targets for intervention of fibrosis or promotion of efficient wound healing. It also advances our understanding of specific receptor function and behavioural modifications driving cellular change. CD44 functions as a co-receptor, with indications of specialised actions, e.g. association with lipid raft proteins in a HA- and acylation-dependent manner [424, 425]. Therefore, defining the mechanism involved in the acylation of CD44, following TGF-β1 stimulation, would be an appropriate course for future investigation, as the data showed CD44 association with lipid rafts was required to activate intracellular signalling cascades involved in promoting differentiation. Although the application of CD44 dynamics would be limited in a clinical scenario, assessing the movement potential of CD44 using

FRAP and Confocal Microscopy could be an effective way of elucidating whether or not live *ex vivo* cells from tissue biopsies have either progressed to a fibrotic or protomyofibrotic state, or whether the cell is senescent or near to senescence.

When considering the targeting of lipid rafts, it would be important to consider their overall function. Depletion of cholesterol from lipid rafts may have a preventative effect on myofibroblast differentiation. However, it would not be a feasible option for targeting, due to their importance in regulating signalling, endocytosis and structural properties of the cell membrane [284, 287, 298, 299, 311]. Additionally, reports have suggested that the forced release of EGFR from cholesterol rich lipid rafts may result in ligand independent activation [289]. Thus, the effects of nystatin depletion of cholesterol may be in the short-term. Therefore, blocking CD44 movement into lipid rafts may be a favoured alternative. Furthermore, identification of the structural features of CD44 and how it activates EGFR would help target specific regions of the protein, without disrupting major functions (such as endocytosis [279]) important for cell survival. One recently described interaction of CD44 that may be involved in mediating EGFR association is the transmembrane glycoprotein, emmprin (basigin/CD147) [426]. This is a protein involved in the induction of HA synthesis in tumour cell lines [427], through the increase of HAS2 expression [428]. Inhibition using targeted siRNA to emmprin may provide insight into whether it has functional significance in myofibroblast development. Additionally, if a specific CD44v is involved in the activation of EGFR, then its variable exon coding region and resultant function (e.g. CD44v3 “handle receptor” GAG-site and binding of EGF/HB-EGF or driving cell invasiveness [262, 429]), could be targeted directly.

This thesis also explored the differences in phenotypic expression between young fibroblasts and *in vitro* aged fibroblasts, to identify key differences to explain the loss of EGFR protein

and the reduction in TGF-β1-stimulated, HA upregulation that were previously found [160, 244]. With each proliferation, cells approach the phenomenon known as cellular senescence, by which point normal diploid cells cease to divide and lose phenotypic qualities and functions. The number of cellular divisions depends on cell type and source [430-432]. Senescent cells remain metabolically active and generally adopt an irregular, flattened morphology; and altered gene expression and secretion profiles [433]. In one study, the eradication of senescent cells by drug-induced apoptosis in mice, led to resistance against age-associated diseases [434]. Cellular senescence is causally implicated in generating age-related phenotypes. As such the reversal of lost function in near senescent cells could prevent or delay tissue dysfunction.

The accumulation of senescent fibroblasts within tissues has been suggested to play an important role in mediating impaired wound healing in the elderly. As fibroblasts near senescence, their responsiveness to extracellular signals diminish [435] and they exhibit a decreased ability to divide in response to damage or cell loss [436, 437]. Such alterations are thought to be responsible for the physiological deterioration and limited tissue regeneration observed in ageing individuals. Reversing the resistance to TGF-β1-driven differentiation in near senescent cells could provide a valid approach to promoting the efficient wound healing, that is required in elderly patients with chronic non-healing wounds.

The inhibitory effect of miR-7 on EGFR expression has been documented in several instances, including its dysfunctional regulation of EGFR in cancers [332-334, 401]. As a potent inhibitor of EGFR mRNA, miR-7 was chosen for in-depth investigation in order to determine whether it had a role in the dysfunction of differentiation, arising from cellular ageing.

Category	Term	Count	Percent	P-Value
miR-7 Targets	Phospho-protein	247	59.5%	6.60e-21

Table 6i. *In silico* analysis of TargetScan database for miR-7 targets cross-referenced with GoDAVID target analysis software. The majority (59.5%) of known/predicted miR-7 targets of repression are proteins involved in activation and signalling pathways (phospho-proteins). The Fisher Exact P-value is displayed (lower value = more enriched gene-analysis; represents the certainty of *in silico* accuracy).

Table 6i demonstrates the involvement of miR-7 in the regulation of biochemical pathways, with the majority of predicted miR-7 targets (59.5%) implicated in protein signalling pathways. The pathways with the most targets included are shown below in table 6ii.

Pathway	Count	Percent	P-Value	Notable Targets
Cancers	14	3.4%	5.20e-2	EGFR, FGF11, IGF-1R, PI3Kδ, PI3K3γ, PKCβ
Focal Adhesion	13	3.1%	3.20e-3	COLIa2, COLIIa1, EGFR, IGF-1R, integrin-α9, integrin-β8, PI3Kδ, PI3K3γ, PKCβ, vinculin
Actin Cytoskeleton Regulation	11	2.7%	3.40e-2	PI3Kδ, PI3K3γ, FGF11, EGFR, Ras, Raf, integrin-α9, integrin-β8,
ErbB/EGFR Signalling	8	1.9%	4.80e-3	CaMKIIδ, EGFR, PI3Kδ, PI3K3γ, PKC, Raf, Ras, ERK1/2, c-Myc, Akt, mTOR
Insulin Signalling	8	1.9%	4.40e-2	ERK1/2-S/TK1, IRS1, IRS2, PI3Kδ, PI3K3γ, Raf
mTOR Signalling	7	1.7%	1.50e-3	EGFR, Akt, mTOR, PI3Kδ, PI3K3γ, ERK1/2, PKCβ

Table 6ii. In-depth GoDAVID software analysis of precise pathways that contain targets for miR-7. Included are counts, percentage of total phospho-proteins (Table 6i) involved in each pathway, The Fisher Exact P-value is displayed (lower value = more enriched gene-analysis; represents the certainty of *in silico* accuracy).

The *in silico* analysis of miR-7 target pathways indicates predicted suppression of myofibroblast differentiation, changes to cell morphology (FA upregulation), actin

cytoskeleton reorganisation; and EGFR and mTOR signalling. Therefore, the upregulation of miR-7 in aged cells could impact on several pathways, involved in differentiation and proliferation [5, 365, 438, 439] (summarised in Figure 6ii). The observed effects of miR-7 overexpression on myofibroblast differentiation have helped in detailing the intricacies of the pathway, reinforcing the importance of the EGFR-HAS2-HA-CD44 relationship. EGFR is the initiating receptor in many of the miR-7 targeted pathways (particularly ErbB and mTOR). Therefore, the inhibition of EGFR by miR-7 is likely a major factor in the decrease of HAS2 expression, lowering HA synthesis and diminishing CD44 membrane movement and co-localisation with EGFR, following TGF-β1 stimulation. Additionally, other signalling proteins are notable targets of miR-7 and may be involved in driving HAS2 transcription (PI3K/Akt/mTOR [440]), or CD44 modulation (PKC [420, 421]).

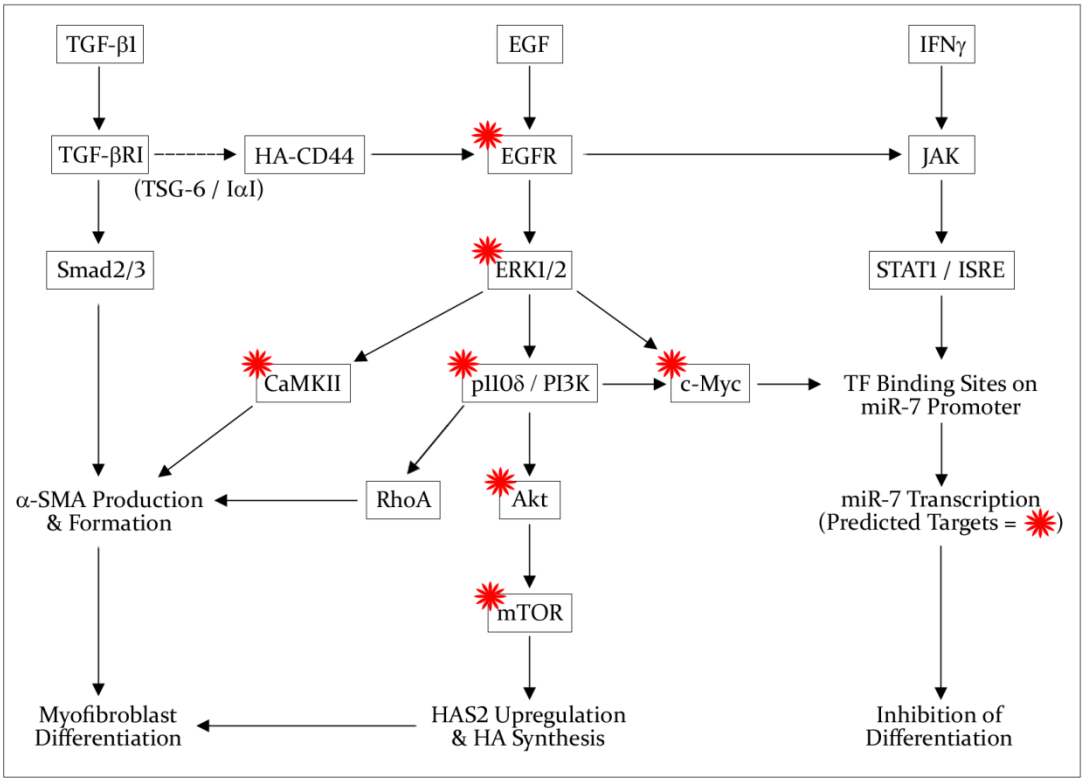

Figure 6ii. Summary of the pathways investigated in this thesis, known/predicted miR-7 targets are indicated by a red star. Adapted from GoDAVID software analysis for miR-7 targets of the ErbB/EGFR signalling pathway.

Since c-Myc is a predicted target of miR-7 and is also downstream of EGFR activity, an alternative pathway for miR-7 transcriptional activation was proposed. The *in silico* analysis of the miR-7 promoter fragment indicated several STAT binding sites. The data show that EGFR and IFNγ upregulation of miR-7 was prevented when the JAK/STAT pathway was inhibited. The increased miR-7 expression was only seen at 72 hours, post-TGF-β1 stimulation, leading to the conjecture that this mechanism may be in place to prevent excessive EGFR pathway signalling; a dysfunctional occurrence that seems to present in many cancers [333, 441-443].

The persistence of miR-7 expression in aged fibroblasts may be due to an over-active STAT pathway, but this was not investigated in detail here. The reported increase of IL-6 (a potent STAT activator) with ageing [408, 410, 444] may be responsible. The concise regulation of miR-7 (i.e. transient transfection of inhibitors or through blocking the IL-6 pathway) could reverse age-associated loss of differentiation and promote wound healing in chronic non-healing wounds. Alternatively, the detected expression of miR-7 in wound biopsies could serve as indication of the prognosis of rate of recovery.

Furthering the investigation into potential suppressors of miR-7, and in light of reports of E2 upregulation of EGFR [397-399] and beneficial effects on wounds [386], E2 treatment of aged fibroblasts was performed to examine the potential for enhancing wound healing or fibroblast function. The results shown here suggest a potentially viable role for E2 as a promoter of fibroblast differentiation, in the presence of TGF-β1. Preliminary data indicated that IL-6 and STAT1/3 are upregulated by TGF-β1; and E2 had the opposite effect. Since STAT1/3 are targets of downstream IL-6 and EGFR signalling, the current hypothesis is that E2 acts independently of EGFR signalling in fibroblasts and has direct effects via transcriptional activation (EGFR, HAS2) or repression (IL-6, STAT1, STAT3). The effects

on miR-7 could, therefore, be a result of this proposed mechanism of action (summarised in figure 6iii).

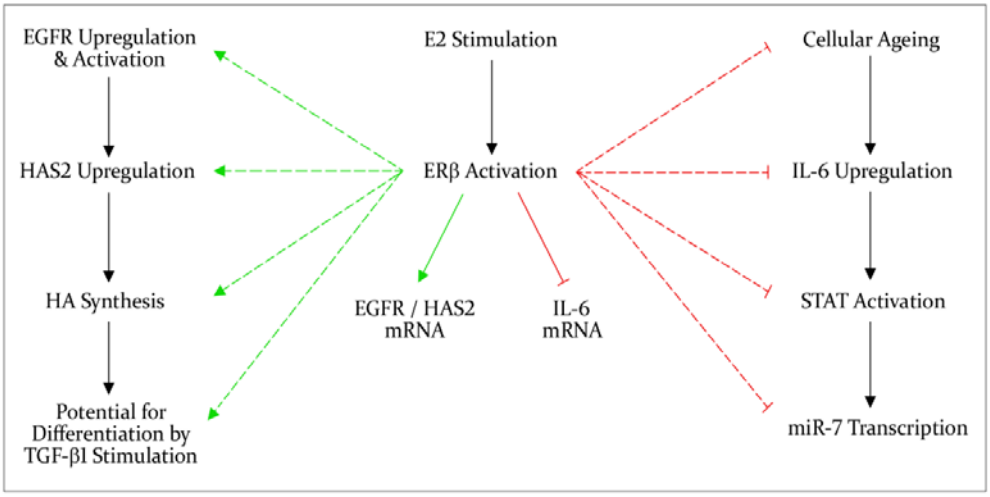

Figure 6iii. Proposed mechanism of actions resulting from E2 stimulation in fibroblasts. Full lines are hypothesised direct effects and dashed lines are hypothesised indirect effects (green; stimulatory, red; inhibitory).

E2-dependent suppression of inflammation could contribute to its pro-healing properties, as chronic inflammation can cause failure of wound resolution and chronic non-healing wounds [445, 446]. E2 has been noted to have beneficial effects on wound healing through ERβ [390, 393]. The actions of ERα have been described as having the opposite effect [387, 394]. The proposed mechanism of action for ERβ in fibroblasts is through its suppression of IL-6, a function shown in various cell types [404-407, 447]. Through this inhibitory mechanism, the downregulatory effects on miR-7 could be explained. Interestingly, during *in silico* analysis, it was noted that a site for ER binding was predicted to be present on the miR-7 promoter fragment used for investigation in this thesis. This site overlapped with STAT/ISRE sites and analysis of suppression of miR-7 promoter activity by E2 would be worth examining in future experiments. Additionally, the upregulatory effects of E2 on EGFR and HAS2 would also require investigation, whether this action is primarily down to miR-7 inhibition or through E2 responsive sites within the promoter regions of both EGFR and HAS2. Elucidating which of

the ERs, ERα or ERβ is active in fibroblasts and their precise actions, could highlight a novel target to exploit in order to promote wound healing *in vivo*.

By targeting miR-7, multiple potential routes of inhibition have been identified to drive EGFR and HAS2 upregulation, and myofibroblast differentiation in the presence of TGF-β1. These data also help explain why there is limited clinical success when treating non-healing wounds, application of antibiotics and growth factors may go some way in helping improve the wound environment, but without treating the underlying reason for inherent impaired cellular activity (fibroblast resistance to growth factors), limited success would be expected. The data provided here indicate targets for therapeutic intervention, that when targeted singularly or in combination, could provide a valid form of therapy for chronic non-healing wounds. The aberrant expression of miR-7 in aged cells could be a marker of age-associated resistance to differentiation, significantly changing the fibroblast cell proteome expression. Whether miR-7 upregulation is purely a senescence-associated mechanism or a result of the persistent expression of inflammatory factors (IFNγ, IL-6) and primarily through a STAT dependent pathway, or whether the two scenarios are causative or coincidental, remains to be clarified. Accordingly, the results clearly demonstrated the possibility of reversing the aged phenotype to the functionally active young phenotype, by restoration of EGFR, HAS2 and HA-dependent, CD44 motility.

What are the actual ramifications of these findings for age-related wound healing? One must be careful in applying the results of the findings from *in vitro* experiments to *in vivo* clinical problems. However, the implications of this study are that interventions to improve healing in the elderly need to be targeted toward improving cell responsiveness, by enhancing signalling and augmenting the cell response. The data support the use of a) inhibiting miR-7 activity through miR-7 LNA transfer to non-healing wounds in the elderly, or b) counter-acting the

actions of miR-7 directly, through the use of E2 treatment as a more rationale therapy than the application of growth-factors, since the rate limiting step is the EGFR pathway and downstream signalling, as opposed to the availability of TGF-β1 and Smad phosphorylation. That being said, investigation into additional effects arising from treatment concerning E2 and TGF-β1 pathways should be performed, as both have been reported as being implicated and have excessive expression in many cancers [381, 382, 448, 449].

Progression of the research toward clinical scenarios would need to involve intermediate stages: 3D cell cultures or collagen gels can be used to effectively measure and quantify the physical activity of myofibroblasts [450], required to support the actions of miR-7 inhibition on aged fibroblasts. Fibroblast isolation from chronic wound biopsies has been deemed safe and does not hamper the wound-healing outcome [451]. Therefore, the next stage would be using cells acquired *ex vivo*; from healthy control patients and a varying range of biopsies from non-healing wound edges. Beyond the context of wound healing, 3D culture models may provide useful in studying associations between receptor function and behavioural changes which indicate innate function e.g. ECM co-ordinated intracellular signalling induced through HA (in an *in vivo*-like environment, not possible in 2D plate cultures); and successful incorporation of miR-7 inhibitors (miR-7 LNA or E2) into cells in a 3D culture, optimisation of technique before transferring into animal models.

The work outlined in this thesis identified several novel and functional relationships between HA, CD44, EGFR and miR-7. These included cellular localisation and functional significance of the cellular location, the importance of transcriptional regulation, and routes of intervention. One implication of this system is the capacity for HA to regulate cellular phenotype. The data suggests this may be achieved through direct association and driven function with CD44, as highlighted in figure 6i. Additionally, with replicative ageing the

increase in miR-7 by increased secretion of inflammatory factors (the upregulated secretion of factors, such as IL-6, IFNγ; their receptors may be a direct result of cellular ageing; and loss of transcriptional control of these proteins), indicated changes at the genetic level that contribute to the regulation of myofibroblast differentiation. The proposed pathway of E2 action in figure 6iii illustrates potential mechanisms of counteractive measures to miR-7 transcription and its EGFR-suppressing activity. In conclusion, this work demonstrated that in the cellular ageing of fibroblasts, EGFR was lost due to a steady and persistent increase in miR-7 expression, resulting in the loss of downstream EGFR responses, including HAS2 expression, HA synthesis and a loss of CD44 membrane motility. This ultimately resulted in the loss of CD44-EGFR co-localisation in lipid rafts and the loss of the EGFR-mediated branch of the differentiation response, i.e. a resistance to myofibroblast differentiation. The figures provided here are starting points to be built upon for future investigation. Further studies to elucidate details of the interactions between CD44 and EGFR in lipid rafts, the relation between STAT activation and the resultant miR-7 transcription; and the extent of the effects of E2 on this relationship and the differentiation pathway, should provide new opportunities for modifying the wound healing response and for ameliorating clinical conditions that involve age-related complications or alternatively, progressive fibrosis.

References

1. Andl, C.D., et al., *EGFR-induced cell migration is mediated predominantly by the JAK-STAT pathway in primary esophageal keratinocytes.* Am J Physiol Gastrointest Liver Physiol, 2004. **287**(6): p. 1227-37.
2. Corcoran, R.B., et al., *EGFR-mediated re-activation of MAPK signaling contributes to insensitivity of BRAF mutant colorectal cancers to RAF inhibition with vemurafenib.* Cancer Discov, 2012. **2**(3): p. 227-35.
3. Cordero, J.B., et al., *Non-autonomous crosstalk between the Jak/Stat and Egfr pathways mediates Apc1-driven intestinal stem cell hyperplasia in the Drosophila adult midgut.* Development, 2012. **139**(24): p. 4524-35.
4. Catto, J.W., et al., *MicroRNA in prostate, bladder, and kidney cancer: a systematic review.* Eur Urol, 2011. **59**(5): p. 671-81.
5. Dobashi, Y., et al., *EGFR-dependent and independent activation of Akt/mTOR cascade in bone and soft tissue tumors.* Mod Pathol, 2009. **22**(10): p. 1328-40.
6. Hashimoto, A., et al., *Shc regulates epidermal growth factor-induced activation of the JNK signaling pathway.* J Biol Chem, 1999. **274**(29): p. 20139-43.
7. Murphy, P.S. and G.R. Evans, *Advances in wound healing: a review of current wound healing products.* Plast Surg Int, 2012. vol. **2012**(Article ID 190436): p. 8.
8. Vileikyte, L., *Stress and wound healing.* Clin Dermatol, 2007. **25**(1): p. 49-55.
9. Bitar, M.S., *Insulin and glucocorticoid-dependent suppression of the IGF-I system in diabetic wounds.* Surgery, 2000. **127**(6): p. 687-95.
10. Werner, S. and R. Grose, *Regulation of wound healing by growth factors and cytokines.* Physiol Rev, 2003. **83**(3): p. 835-70.
11. Whaley, K. and A.D. Burt, *Inflammation, healing and repair*. 13th ed. In Muir's Textbook of Pathology, ed. R.M.N. MacSween and K. Whaley, London, Arnold, 1996.
12. Hackam, D.J. and H.R. Ford, *Cellular, biochemical, and clinical aspects of wound healing.* Surg Infect, 2002. **3**(1): p. 23-35.
13. Harding, K.G., et al., *Wound chronicity and fibroblast senescence--implications for treatment.* Int Wound J, 2005. **2**(4): p. 364-68.
14. Yamaguchi, Y. and K. Yoshikawa, *Cutaneous wound healing: an update.* J Dermatol, 2001. **28**(10): p. 521-34.
15. Witte, M.B. and A. Barbul, *General principles of wound healing.* Surg Clin North Am, 1997. **77**(3): p. 509-28.
16. Broughton, G., et al., *The basic science of wound healing.* Plast Reconstr Surg, 2006. **117**(7): p. 12-34.
17. Broughton, G., et al., *Wound healing: an overview.* Plast Reconstr Surg, 2006. **117**(7): p. 1-32.
18. Corbett, S.A., et al., *Covalent cross-linking of fibronectin to fibrin is required for maximal cell adhesion to a fibronectin-fibrin matrix.* J Biol Chem, 1997. **272**(40): p. 24999-5005.
19. Hoffman, M.M. and D.M. Monroe, *Rethinking the coagulation cascade.* Curr Hematol Rep, 2005. **4**(5): p. 391-96.
20. Knox, P., et al., *Role of fibronectin in the migration of fibroblasts into plasma clots.* J Cell Biol, 1986. **102**(6): p. 2318-23.
21. Burgers, J.A., et al., *Human platelets secrete chemotactic activity for eosinophils.* Blood, 1993. **81**(1): p. 49-55.
22. Kronemann, N., et al., *Aggregating human platelets stimulate expression of vascular endothelial growth factor in cultured vascular smooth muscle cells through a*

synergistic effect of transforming growth factor-β(1) and platelet-derived growth factor(AB). Circulation, 1999. **100**(8): p. 855-60.
23. Stadelmann, W.K., et al., *Physiology and healing dynamics of chronic cutaneous wounds.* Am J Surg, 1998. **176**(2): p. 26-38.
24. Greenhalgh, D.G., *The role of apoptosis in wound healing.* Int J Biochem Cell Biol, 1998. **30**(9): p. 1019-30.
25. Martin, P. and S.J. Leibovich, *Inflammatory cells during wound repair: the good, the bad and the ugly.* Trends Cell Biol, 2005. **15**(11): p. 599-607.
26. Knighton, D.R. and V.D. Fiegel, *Macrophage-derived growth factors in wound healing: regulation of growth factor production by the oxygen microenvironment.* Am Rev Respir Dis, 1989. **140**(4): p. 1108-11.
27. Newton, P.M., et al., *Macrophages restrain contraction of an in vitro wound healing model.* Inflammation, 2004. **28**(4): p. 207-14.
28. Willenborg, S., et al., *Chronic wounds and inflammation.* Advances in Wound Care, 2010. **1**: p. 259-65.
29. Guo, S. and L.A. Dipietro, *Factors affecting wound healing.* J Dent Res, 2010. **89**(3): p. 219-29.
30. Lamalice, L., et al., *Endothelial cell migration during angiogenesis.* Circ Res, 2007. **100**(6): p. 782-94.
31. Newman, A.C., et al., *The requirement for fibroblasts in angiogenesis: fibroblast-derived matrix proteins are essential for endothelial cell lumen formation.* Mol Biol Cell, 2011. **22**(20): p. 3791-800.
32. Urbich, C. and S. Dimmeler, *Endothelial progenitor cells: characterization and role in vascular biology.* Circ Res, 2004. **95**(4): p. 343-53.
33. Pepper, M.S., *Role of the matrix metalloproteinase and plasminogen activator-plasmin systems in angiogenesis.* Arterioscler Thromb Vasc Biol, 2001. **21**(7): p. 1104-17.
34. Sang, Q.X., *Complex role of matrix metalloproteinases in angiogenesis.* Cell Res, 1998. **8**(3): p. 171-77.
35. Andersson-Sjoland, A., et al., *Fibrocytes are a potential source of lung fibroblasts in idiopathic pulmonary fibrosis.* Int J Biochem Cell Biol, 2008. **40**(10): p. 2129-40.
36. Zeisberg, E.M., et al., *Endothelial-to-mesenchymal transition contributes to cardiac fibrosis.* Nat Med, 2007. **13**(8): p. 952-61.
37. Zeisberg, M., et al., *Fibroblasts derive from hepatocytes in liver fibrosis via epithelial to mesenchymal transition.* J Biol Chem, 2007. **282**(32): p. 23337-47.
38. Welch, M.P., et al., *Temporal relationships of F-actin bundle formation, collagen and fibronectin matrix assembly, and fibronectin receptor expression to wound contraction.* J Cell Biol, 1990. **110**(1): p. 133-45.
39. Badylak, S.F., *The extracellular matrix as a scaffold for tissue reconstruction.* Semin Cell Dev Biol, 2002. **13**(5): p. 377-83.
40. Wysocki, A.B. and F. Grinnell, *Fibronectin profiles in normal and chronic wound fluid.* Lab Invest, 1990. **63**(6): p. 825-31.
41. Eckes, B., et al., *Cell-matrix interactions in dermal repair and scarring.* Fibrogenesis Tissue Repair, 2010. **3**: p. 4.
42. Clark, R.A., et al., *Fibronectin and fibrin provide a provisional matrix for epidermal cell migration during wound reepithelialization.* J Invest Dermatol, 1982. **79**(5): p. 264-69.
43. Ruszczak, Z., *Effect of collagen matrices on dermal wound healing.* Adv Drug Deliv Rev, 2003. **55**(12): p. 1595-611.

44. Ruszczak, Z. and R.A. Schwartz, *Modern aspects of wound healing: An update.* Dermatol Surg, 2000. **26**(3): p. 219-29.
45. Clark, R.A., *Wound repair: Overview and general considerations*. The molecular and cellular basis of wound repair. New York, Plenum Press, 1996.
46. Eckes, B., et al., *Fibroblast-matrix interactions in wound healing and fibrosis.* Matrix Biol, 2000. **19**(4): p. 325-32.
47. Hinz, B., *Masters and servants of the force: the role of matrix adhesions in myofibroblast force perception and transmission.* Eur J Cell Biol, 2006. **85**(3-4): p. 175-81.
48. Grinnell, F., *Fibroblasts, myofibroblasts, and wound contraction.* J Cell Biol, 1994. **124**(4): p. 401-04.
49. Darby, I., et al., *A-smooth muscle actin is transiently expressed by myofibroblasts during experimental wound healing.* Lab Invest, 1990. **63**(1): p. 21-29.
50. Gabbiani, G., *The myofibroblast in wound healing and fibrocontractive diseases.* J Pathol, 2003. **200**(4): p. 500-03.
51. Deodhar, A.K. and R.E. Rana, *Surgical physiology of wound healing: a review.* J Postgrad Med, 1997. **43**(2): p. 52-56.
52. Eyden, B.P., *Brief review of the fibronexus and its significance for myofibroblastic differentiation and tumor diagnosis.* Ultrastruct Pathol, 1993. **17**(6): p. 611-22.
53. Mulholland, M.W. and G.M. Doherty, *Management of Surgical Complications*. 2nd ed. Complications In Surgery. Philadelphia, Lippencott Williams & Williams, 2011.
54. Noiri, E., et al., *Nitric oxide is necessary for a switch from stationary to locomoting phenotype in epithelial cells.* Am J Physiol, 1996. **270**(3): p. 794-802.
55. Saarialho-Kere, U.K., et al., *Distinct localization of collagenase and tissue inhibitor of metalloproteinases expression in wound healing associated with ulcerative pyogenic granuloma.* J Clin Invest, 1992. **90**(5): p. 1952-57.
56. Morioka, S., et al., *Migrating keratinocytes express urokinase-type plasminogen activator.* J Invest Dermatol, 1987. **88**(4): p. 418-23.
57. Bennett, N.T. and G.S. Schultz, *Growth factors and wound healing: Part II. Role in normal and chronic wound healing.* Am J Surg, 1993. **166**(1): p. 74-81.
58. Nguyen, D.T., et al., *The pathophysiologic basis for wound healing and cutaneous regeneration.* Biomaterials for Treating Skin Loss. Cambridge, Woodhead Publishing Ltd., 2009.
59. Sudo, T., et al., *Expression of Mesenchymal Markers Vimentin and Fibronectin: The Clinical Significance in Esophageal Squamous Cell Carcinoma.* Ann Surg Oncol, 2012. **20**(3): p. 324-35.
60. Chang, H.Y., et al., *Diversity, topographic differentiation, and positional memory in human fibroblasts.* Proc Natl Acad Sci USA, 2002. **99**(20): p. 12877-82.
61. De la Chapelle, et al., *The origin of bone marrow fibroblasts.* Blood, 1973. **41**(6): p. 783-87.
62. Hay, E.D., *An overview of epithelio-mesenchymal transformation.* Acta Anat (Basel), 1995. **154**(1): p. 8-20.
63. Hashimoto, N., et al., *Bone marrow-derived progenitor cells in pulmonary fibrosis.* J Clin Invest, 2004. **113**(2): p. 243-52.
64. Mori, L., et al., *Fibrocytes contribute to the myofibroblast population in wounded skin and originate from the bone marrow.* Exp Cell Res, 2005. **304**(1): p. 81-90.
65. Ogawa, M., et al., *Hematopoietic origin of fibroblasts/myofibroblasts: Its pathophysiologic implications.* Blood, 2006. **108**(9): p. 2893-96.
66. Iwano, M., et al., *Evidence that fibroblasts derive from epithelium during tissue fibrosis.* J Clin Invest, 2002. **110**(3): p. 341-50.

67. Krenning, G., et al., *The origin of fibroblasts and mechanism of cardiac fibrosis.* J Cell Physiol, 2010. **225**(3): p. 631-37.
68. Lodish, H., et al., *The Actin Cytoskeleton*. Molecular Cell Biology. New York, W.H. Freeman, 2000.
69. Tilghman, R.W. and J.T. Parsons, *Focal adhesion kinase as a regulator of cell tension in the progression of cancer.* Semin Cancer Biol, 2008. **18**(1): p. 45-52.
70. Wang, H.B., et al., *Focal adhesion kinase is involved in mechanosensing during fibroblast migration.* Proc Natl Acad Sci U S A, 2001. **98**(20): p. 11295-300.
71. Grinnell, F., *Fibroblast-collagen-matrix contraction: growth-factor signalling and mechanical loading.* Trends Cell Biol, 2000. **10**(9): p. 362-65.
72. Border, W.A. and N.A. Noble, *TGF-β in kidney fibrosis: a target for gene therapy.* Kidney Int, 1997. **51**(5): p. 1388-96.
73. Border, W.A. and N.A. Noble, *Fibrosis linked to TGF-β in yet another disease.* J Clin Invest, 1995. **96**(2): p. 655-56.
74. Desmouliere, A., et al., *Transforming growth factor-β 1 induces α-smooth muscle actin expression in granulation tissue myofibroblasts and in quiescent and growing cultured fibroblasts.* J Cell Biol, 1993. **122**(1): p. 103-11.
75. Furie, B. and B.C. Furie, *Thrombus formation in vivo.* J Clin Invest, 2005. **115**(12): p. 3355-62.
76. Desmouliere, A., et al., *Normal and pathologic soft tissue remodeling: role of the myofibroblast, with special emphasis on liver and kidney fibrosis.* Lab Invest, 2003. **83**(12): p. 1689-707.
77. Burridge, K., et al., *Focal adhesions: transmembrane junctions between the extracellular matrix and the cytoskeleton.* Annu Rev Cell Biol, 1988. **4**: p. 487-525.
78. Geiger, B., et al., *Transmembrane crosstalk between the extracellular matrix--cytoskeleton crosstalk.* Nat Rev Mol Cell Biol, 2001. **2**(11): p. 793-805.
79. Katz, B.Z., et al., *Physical state of the extracellular matrix regulates the structure and molecular composition of cell-matrix adhesions.* Mol Biol Cell, 2000. **11**(3): p. 1047-60.
80. Goldman, R., *Growth factors and chronic wound healing: past, present, and future.* Adv Skin Wound Care, 2004. **17**(1): p. 24-35.
81. Pereira, M., et al., *The incorporation of fibrinogen into extracellular matrix is dependent on active assembly of a fibronectin matrix.* J Cell Sci, 2002. **115**(Pt 3): p. 609-17.
82. Sottile, J. and D.C. Hocking, *Fibronectin polymerization regulates the composition and stability of extracellular matrix fibrils and cell-matrix adhesions.* Mol Biol Cell, 2002. **13**(10): p. 3546-59.
83. Chen, W.Y. and G. Abatangelo, *Functions of hyaluronan in wound repair*. Wound Repair Regen, 1999. **7**(2): p. 79-89.
84. Gailit, J. and R.A. Clark, *Wound repair in the context of extracellular matrix.* Curr Opin Cell Biol, 1994. **6**(5): p. 717-25.
85. Eddy, A.A., *Molecular basis of renal fibrosis.* Pediatr Nephrol, 2000. **15**(3-4): p. 290-301.
86. Bedossa, P. and V. Paradis, *Liver extracellular matrix in health and disease.* J Pathol, 2003. **200**(4): p. 504-15.
87. Chapman, H.A., *Disorders of lung matrix remodeling.* J Clin Invest, 2004. **113**(2): p. 148-57.
88. Cox, T.R. and J.T. Erler, *Remodeling and homeostasis of the extracellular matrix: implications for fibrotic diseases and cancer*. Dis Model Mech, 2011. **4**(2): p. 165-78.

89. Hinz, B., et al., *The myofibroblast: one function, multiple origins.* Am J Pathol, 2007. **170**(6): p. 1807-16.
90. Brown, R.D., et al., *The cardiac fibroblast: therapeutic target in myocardial remodeling and failure.* Annu Rev Pharmacol Toxicol, 2005. **45**: p. 657-87.
91. Spanakis, S.G., et al., *Functional gap junctions in corneal fibroblasts and myofibroblasts.* Invest Ophthalmol Vis Sci, 1998. **39**(8): p. 1320-28.
92. Tomasek, J.J., et al., *Myofibroblasts and mechano-regulation of connective tissue remodelling.* Nat Rev Mol Cell Biol, 2002. **3**(5): p. 349-63.
93. Dunkern, T.R., et al., *Inhibition of TGF-β induced lung fibroblast to myofibroblast conversion by phosphodiesterase inhibiting drugs and activators of soluble guanylyl cyclase.* Eur J Pharmacol, 2007. **572**(1): p. 12-22.
94. Hinz, B., et al., *A-smooth muscle actin expression upregulates fibroblast contractile activity.* Mol Biol Cell, 2001. **12**(9): p. 2730-41.
95. Hinz, B., et al., *The NH2-terminal peptide of α-smooth muscle actin inhibits force generation by the myofibroblast in vitro and in vivo.* J Cell Biol, 2002. **157**(4): p. 657-63.
96. Wang, J., et al., *Smooth muscle actin determines mechanical force-induced p38 activation.* J Biol Chem, 2005. **280**(8): p. 7273-84.
97. Wang, J., et al., *Multiple roles of α-smooth muscle actin in mechanotransduction.* Exp Cell Res, 2006. **312**(3): p. 205-14.
98. Schwartz, M.A., *Integrins and extracellular matrix in mechanotransduction.* Cold Spring Harb Perspect Biol, 2010. **2**(12): p. 5066.
99. Thannickal, V.J., et al., *Myofibroblast differentiation by transforming growth factor-β1 is dependent on cell adhesion and integrin signaling via focal adhesion kinase.* J Biol Chem, 2003. **278**(14): p. 12384-89.
100. Thibault, G., et al., *Upregulation of α(8)β(1)-integrin in cardiac fibroblast by angiotensin II and transforming growth factor-β1.* Am J Physiol Cell Physiol, 2001. **281**(5): p. C1457-67.
101. Carlson, M.A., et al., *Wound splinting regulates granulation tissue survival.* J Surg Res, 2003. **110**(1): p. 304-9.
102. Hinz, B., *Formation and function of the myofibroblast during tissue repair.* J Invest Dermatol, 2007. **127**(3): p. 526-37.
103. Hao, H., et al., *Phenotypic modulation of intima and media smooth muscle cells in fatal cases of coronary artery lesion.* Arterioscler Thromb Vasc Biol, 2006. **26**(2): p. 326-32.
104. Rajkumar, V.S., et al., *Shared expression of phenotypic markers in systemic sclerosis indicates a convergence of pericytes and fibroblasts to a myofibroblast lineage in fibrosis.* Arthritis Res Ther, 2005. **7**(5): p. 1113-23.
105. Abe, R., et al., *Peripheral blood fibrocytes: differentiation pathway and migration to wound sites.* J Immunol, 2001. **166**(12): p. 7556-62.
106. Direkze, N.C., et al., *Multiple organ engraftment by bone-marrow-derived myofibroblasts and fibroblasts in bone-marrow-transplanted mice.* Stem Cells, 2003. **21**(5): p. 514-20.
107. Forbes, S.J., et al., *A significant proportion of myofibroblasts are of bone marrow origin in human liver fibrosis.* Gastroenterology, 2004. **126**(4): p. 955-63.
108. Ishii, G., et al., *Bone-marrow-derived myofibroblasts contribute to the cancer-induced stromal reaction.* Biochem Biophys Res Commun, 2003. **309**(1): p. 232-40.
109. Schmidt, M., et al., *Identification of circulating fibrocytes as precursors of bronchial myofibroblasts in asthma.* J Immunol, 2003. **171**(1): p. 380-89.

110. Kim, K.K., et al., *Alveolar epithelial cell mesenchymal transition develops in vivo during pulmonary fibrosis and is regulated by the extracellular matrix.* Proc Natl Acad Sci USA, 2006. **103**(35): p. 13180-85.
111. Zeisberg, M. and R. Kalluri, *The role of epithelial-to-mesenchymal transition in renal fibrosis.* J Mol Med (Berl), 2004. **82**(3): p. 175-81.
112. Zhang, K., et al., *Myofibroblasts and their role in lung collagen gene expression during pulmonary fibrosis. A combined immunohistochemical and in situ hybridization study.* Am J Pathol, 1994. **145**(1): p. 114-25.
113. Strieter, R.M., et al., *The role of circulating mesenchymal progenitor cells, fibrocytes, in promoting pulmonary fibrosis.* Trans Am Clin Climatol Assoc, 2009. **120**: p. 49-59.
114. Kisseleva, T., et al., *Bone marrow-derived fibrocytes participate in pathogenesis of liver fibrosis.* J Hepatol, 2006. **45**(3): p. 429-38.
115. Xia, J.L., et al., *Hepatocyte growth factor attenuates liver fibrosis induced by bile duct ligation.* Am J Pathol, 2006. **168**(5): p. 1500-12.
116. Willis, B.C., et al., *Induction of epithelial-mesenchymal transition in alveolar epithelial cells by transforming growth factor-β1: potential role in idiopathic pulmonary fibrosis.* Am J Pathol, 2005. **166**(5): p. 1321-32.
117. Barth, K., et al., *Epithelial vs myofibroblast differentiation in immortal rat lung cell lines--modulating effects of bleomycin.* Histochem Cell Biol, 2005. **124**(6): p. 453-64.
118. Horowitz, J.C., et al., *Activation of the pro-survival phosphatidylinositol 3-kinase/AKT pathway by transforming growth factor-β1 in mesenchymal cells is mediated by p38 MAPK-dependent induction of an autocrine growth factor.* J Biol Chem, 2004. **279**(2): p. 1359-67.
119. Horowitz, J.C., et al., *Combinatorial activation of FAK and AKT by transforming growth factor-β1 confers an anoikis-resistant phenotype to myofibroblasts.* Cell Signal, 2007. **19**(4): p. 761-71.
120. Zhang, H.Y. and S.H. Phan, *Inhibition of myofibroblast apoptosis by transforming growth factor β(1).* Am J Respir Cell Mol Biol, 1999. **21**(6): p. 658-65.
121. Gressner, A.M. and R. Weiskirchen, *Modern pathogenetic concepts of liver fibrosis suggest stellate cells and TGF-β as major players and therapeutic targets.* J Cell Mol Med, 2006. **10**(1): p. 76-99.
122. Guyot, C., et al., *Hepatic fibrosis and cirrhosis: the (myo)fibroblastic cell subpopulations involved.* Int J Biochem Cell Biol, 2006. **38**(2): p. 135-51.
123. Bataller, R., et al., *Hepatitis C virus core and nonstructural proteins induce fibrogenic effects in hepatic stellate cells.* Gastroenterology, 2004. **126**(2): p. 529-40.
124. Weng, H., et al., *IFN-γ abrogates profibrogenic TGF-β signaling in liver by targeting expression of inhibitory and receptor Smads.* J Hepatol, 2007. **46**(2): p. 295-303.
125. Cassiman, D., et al., *Hepatic stellate cell/myofibroblast subpopulations in fibrotic human and rat livers.* J Hepatol, 2002. **36**(2): p. 200-09.
126. Ramadori, G. and B. Saile, *Portal tract fibrogenesis in the liver.* Lab Invest, 2004. **84**(2): p. 153-59.
127. Chen, Y.T., et al., *Platelet-derived growth factor receptor signaling activates pericyte-myofibroblast transition in obstructive and post-ischemic kidney fibrosis.* Kidney Int, 2011. **80**(11): p. 1170-81.
128. Owens, G.K., et al., *Molecular regulation of vascular smooth muscle cell differentiation in development and disease.* Physiol Rev, 2004. **84**(3): p. 767-801.
129. Niessen, P., et al., *Biochemical evidence for interaction between smoothelin and filamentous actin.* Exp Cell Res, 2004. **292**(1): p. 170-78.

130. Tomasek, J.J., et al., *Contraction of myofibroblasts in granulation tissue is dependent on Rho/Rho kinase/myosin light chain phosphatase activity.* Wound Repair Regen, 2006. **14**(3): p. 313-20.
131. Estes, J.M., et al., *Phenotypic and functional features of myofibroblasts in sheep fetal wounds.* Differentiation, 1994. **56**(3): p. 173-81.
132. Zhong, L., et al., *The anti-fibrotic effect of bone morphogenic protein-7(BMP-7) on liver fibrosis.* Int J Med Sci, 2013. **10**(4): p. 441-50.
133. Gurujeyalakshmi, G. and S.N. Giri, *Molecular mechanisms of antifibrotic effect of interferon γ in bleomycin-mouse model of lung fibrosis: downregulation of TGF-β and procollagen I and III gene expression.* Exp Lung Res, 1995. **21**(5): p. 791-808.
134. Xue, F., et al., *Hepatocyte growth factor gene therapy accelerates regeneration in cirrhotic mouse livers after hepatectomy.* Gut, 2003. **52**(5): p. 694-700.
135. Clement, S., et al., *The N-terminal Ac-EEED sequence plays a role in α-smooth-muscle actin incorporation into stress fibers.* J Cell Sci, 2005. **118**(Pt 7): p. 1395-404.
136. Kim, S.S., et al., *Skin regeneration using keratinocytes and dermal fibroblasts cultured on biodegradable microspherical polymer scaffolds.* J Biomed Mater Res B Appl Biomater, 2005. **75**(2): p. 369-77.
137. Venugopal, J. and S. Ramakrishna, *Biocompatible nanofiber matrices for the engineering of a dermal substitute for skin regeneration.* Tissue Eng, 2005. **11**(5-6): p. 847-54.
138. Baouz, S., et al., *Lung myofibroblasts as targets of salmeterol and fluticasone propionate: inhibition of α-SMA and NF-kappaB.* Int Immunol, 2005. **17**(11): p. 1473-81.
139. Palmes, D. and H.U. Spiegel, *Animal models of liver regeneration.* Biomaterials, 2004. **25**(9): p. 1601-11.
140. Fujita, M., et al., *Sequential observation of liver cell regeneration after massive hepatic necrosis in auxiliary partial orthotopic liver transplantation.* Mod Pathol, 2000. **13**(2): p. 152-7.
141. Murakami, T., et al., *Liver necrosis and regeneration after fulminant hepatitis: pathologic correlation with CT and MR findings.* Radiology, 1996. **198**(1): p. 239-42.
142. Andiran, F., et al., *Regenerative capacities of normal and cirrhotic livers following 70% hepatectomy in rats and the effect of α-tocopherol on cirrhotic regeneration.* J Surg Res, 2000. **89**(2): p. 184-88.
143. Kawasaki, S., et al., *Direct evidence for the intact hepatocyte theory in patients with liver cirrhosis.* Gastroenterology, 1992. **102**(4): p. 1351-55.
144. Rolfe, K.J. and A.O. Grobbelaar, *A review of fetal scarless healing.* ISRN Dermatol, 2012. **2012**: p. 698034.
145. Adzick, N.S. and M.T. Longaker, *Animal models for the study of fetal tissue repair.* J Surg Res, 1991. **51**(3): p. 216-22.
146. Lorenz, H.P., et al., *Scarless wound repair: a human fetal skin model.* Development, 1992. **114**(1): p. 253-59.
147. Ellis, I., et al., *Differential response of fetal and adult fibroblasts to cytokines: cell migration and hyaluronan synthesis.* Development, 1997. **124**(8): p. 1593-600.
148. Mast, B.A., et al., *Hyaluronic acid modulates proliferation, collagen and protein synthesis of cultured fetal fibroblasts.* Matrix, 1993. **13**(6): p. 441-46.
149. Mak, K., et al., *Scarless healing of oral mucosa is characterized by faster resolution of inflammation and control of myofibroblast action compared to skin wounds in the red Duroc pig model.* J Dermatol Sci, 2009. **56**(3): p. 168-80.

150. Wong, J.W., et al., *Wound healing in oral mucosa results in reduced scar formation as compared with skin: evidence from the red Duroc pig model and humans.* Wound Repair Regen, 2009. **17**(5): p. 717-29.
151. WHO, World Health Organization, 2008.
152. MacDonald, J.M. and T.J. Ryan, *WHO: Global Impact of the Chronic Wound and Lymphodema.* WHO Publication, 2010. **Chapter 3**: p. 13-24.
153. Ashcroft, G.S., et al., *Ageing and wound healing.* Biogerontology, 2002. **3**(6): p. 337-45.
154. Dow, G., et al., *Infection in chronic wounds: controversies in diagnosis and treatment.* Ostomy Wound Manage, 1999. **45**(8): p. 23-40.
155. Greenhalgh, D.G., *Wound healing and diabetes mellitus.* Clin Plast Surg, 2003. **30**(1): p. 37-45.
156. Freedman, G., et al., *Pathogenesis and treatment of pain in patients with chronic wounds.* Surg Technol Int, 2003. **11**: p. 168-79.
157. Baxter, C.R., *Immunologic reactions in chronic wounds.* Am J Surg, 1994. **167**(1): p. 12-14.
158. Giulian, D., et al., *The role of mononuclear phagocytes in wound healing after traumatic injury to adult mammalian brain.* J Neurosci, 1989. **9**(12): p. 4416-29.
159. Shiraha, H., et al., *Aging fibroblasts present reduced epidermal growth factor (EGF) responsiveness due to preferential loss of EGF receptors.* J Biol Chem, 2000. **275**(25): p. 19343-51.
160. Simpson, R.M., et al., *Aging fibroblasts resist phenotypic maturation because of impaired hyaluronan-dependent CD44/epidermal growth factor receptor signaling.* Am J Pathol, 2010. **176**(3): p. 1215-28.
161. Mustoe, T.A., et al., *Chronic wound pathogenesis and current treatment strategies: a unifying hypothesis.* Plast Reconstr Surg, 2006. **117**(7): p. 35-41.
162. Loot, M.A., et al., *Fibroblasts derived from chronic diabetic ulcers differ in their response to stimulation with EGF, IGF-I, bFGF and PDGF-AB compared to controls.* Eur J Cell Biol, 2002. **81**(3): p. 153-60.
163. Frank, R.N., *Diabetic retinopathy.* N Engl J Med, 2004. **350**(1): p. 48-58.
164. Friedlander, M., *Fibrosis and diseases of the eye.* J Clin Invest, 2007. **117**(3): p. 576-86.
165. Green, F.H., *Overview of pulmonary fibrosis.* Chest, 2002. **122**(6): p. 334-339.
166. Kissin, E.Y. and J.H. Korn, *Fibrosis in scleroderma.* Rheum Dis Clin North Am, 2003. **29**(2): p. 351-69.
167. Mack, C.L. and R.J. Sokol, *Unraveling the pathogenesis and etiology of biliary atresia.* Pediatr Res, 2005. **57**(5): p. 87-94.
168. Kisseleva, T. and D.A. Brenner, *Mechanisms of fibrogenesis.* Exp Biol Med, 2008. **233**(2): p. 109-22.
169. Suematsu, M., et al., *The inflammatory aspect of the microcirculation in hypertension: oxidative stress, leukocytes/endothelial interaction, apoptosis.* Microcirculation, 2002. **9**(4): p. 259-76.
170. Kosmehl, H., et al., *Molecular variants of fibronectin and laminin: structure, physiological occurrence and histopathological aspects.* Virchows Arch, 1996. **429**(6): p. 311-22.
171. Eddy, A.A., *Experimental insights into the tubulointerstitial disease accompanying primary glomerular lesions.* J Am Soc Nephrol, 1994. **5**(6): p. 1273-87.
172. Fellstrom, B., et al., *Importance of PDGF receptor expression in accelerated atherosclerosis-chronic rejection.* Transplant Proc, 1989. **21**(4): p. 3689-91.

173. Ito, Y., et al., *Expression of connective tissue growth factor in human renal fibrosis.* Kidney Int, 1998. **53**(4): p. 853-61.
174. Nikolic-Paterson, D.J., et al., *Interleukin-1 in renal fibrosis.* Kidney Int Suppl, 1996. **54**: p. S88-90.
175. Ray, P.E., et al., *bFGF and its low affinity receptors in the pathogenesis of HIV-associated nephropathy in transgenic mice.* Kidney Int, 1994. **46**(3): p. 759-72.
176. Wolf, G. and E.G. Neilson, *Angiotensin II as a renal growth factor.* J Am Soc Nephrol, 1993. **3**(9): p. 1531-40.
177. Leask, A., *Targeting the TGFβ, endothelin-1 and CCN2 axis to combat fibrosis in scleroderma.* Cell Signal, 2008. **20**(8): p. 1409-14.
178. Broekelmann, T.J., et al., *Transforming growth factor β 1 is present at sites of extracellular matrix gene expression in human pulmonary fibrosis.* Proc Natl Acad Sci U S A, 1991. **88**(15): p. 6642-46.
179. Khalil, N., *TGF-β: from latent to active.* Microbes Infect, 1999. **1**(15): p. 1255-63.
180. Shi, Y. and J. Massague, *Mechanisms of TGF-β signaling from cell membrane to the nucleus.* Cell, 2003. **113**(6): p. 685-700.
181. Chatzaki, E., et al., *Transforming growth factor β1 exerts an autocrine regulatory effect on human endometrial stromal cell apoptosis, involving the FasL and Bcl-2 apoptotic pathways.* Mol Hum Reprod, 2003. **9**(2): p. 91-95.
182. Wrana, J.L., et al., *TGF β signals through a heteromeric protein kinase receptor complex.* Cell, 1992. **71**(6): p. 1003-14.
183. Mythreye, K. and G.C. Blobe, *The type III TGF-β receptor regulates epithelial and cancer cell migration through β-arrestin2-mediated activation of Cdc42.* Proc Natl Acad Sci USA, 2009. **106**(20): p. 8221-26.
184. Schiller, M., D. Javelaud, and A. Mauviel, *TGF-β-induced SMAD signaling and gene regulation: consequences for extracellular matrix remodeling and wound healing.* J Dermatol Sci, 2004. **35**(2): p. 83-92.
185. Conery, A.R., et al., *Akt interacts directly with Smad3 to regulate the sensitivity to TGF-β induced apoptosis.* Nat Cell Biol, 2004. **6**(4): p. 366-72.
186. Edlund, S., et al., *Transforming growth factor-β-induced mobilization of actin cytoskeleton requires signaling by small GTPases Cdc42 and RhoA.* Mol Biol Cell, 2002. **13**(3): p. 902-14.
187. Lee, M.K., et al., *TGF-β activates Erk MAP kinase signalling through direct phosphorylation of ShcA.* EMBO J, 2007. **26**(17): p. 3957-67.
188. Letterio, J.J. and A.B. Roberts, *Regulation of immune responses by TGF-β.* Annu Rev Immunol, 1998. **16**: p. 137-61.
189. Mansbridge, J.N., et al., *Growth factors secreted by fibroblasts: role in healing diabetic foot ulcers.* Diabetes Obes Metab, 1999. **1**(5): p. 265-79.
190. Kingsley, D.M., *The TGF-β superfamily: new members, new receptors, and new genetic tests of function in different organisms.* Genes Dev, 1994. **8**(2): p. 133-46.
191. Wahl, S.M., et al., *Transforming growth factor-β is a potent immunosuppressive agent that inhibits IL-1-dependent lymphocyte proliferation.* J Immunol, 1988. **140**(9): p. 3026-32.
192. Willis, B.C. and Z. Borok, *TGF-β-induced EMT: mechanisms and implications for fibrotic lung disease.* Am J Physiol Lung Cell Mol Physiol, 2007. **293**(3): p. 525-34.
193. Verrecchia, F. and A. Mauviel, *Transforming growth factor-β signaling through the Smad pathway: role in extracellular matrix gene expression and regulation.* J Invest Dermatol, 2002. **118**(2): p. 211-15.

194. Sato, Y., et al., *Characterization of the activation of latent TGF-β by co-cultures of endothelial cells and pericytes or smooth muscle cells: a self-regulating system.* J Cell Biol, 1990. **111**(2): p. 757-63.
195. Meran, S., et al., *Hyaluronan facilitates transforming growth factor-β1-dependent proliferation via CD44 and epidermal growth factor receptor interaction.* J Biol Chem, 2011. **286**(20): p. 17618-30.
196. Webber, J., et al., *Modulation of TGFβ1-dependent myofibroblast differentiation by hyaluronan.* Am J Pathol, 2009. **175**(1): p. 148-60.
197. Ramirez, A.M., et al., *Myofibroblast transdifferentiation in obliterative bronchiolitis: tgf-β signaling through smad3-dependent and -independent pathways.* Am J Transplant, 2006. **6**(9): p. 2080-88.
198. Fahey, M.S., et al., *Dysregulation of autocrine TGF-β isoform production and ligand responses in human tumour-derived and Ha-ras-transfected keratinocytes and fibroblasts.* Br J Cancer, 1996. **74**(7): p. 1074-80.
199. Shah, M., et al., *Neutralising antibody to TGF-β 1,2 reduces cutaneous scarring in adult rodents.* J Cell Sci, 1994. **107**(5): p. 1137-57.
200. Bottinger, E.P., et al., *Biology of TGF-β in knockout and transgenic mouse models.* Kidney Int, 1997. **51**(5): p. 1355-60.
201. Kulkarni, A.B., et al., *Transforming growth factor β 1 null mutation in mice causes excessive inflammatory response and early death.* Proc Natl Acad Sci USA, 1993. **90**(2): p. 770-74.
202. Tang, B., et al., *Transforming growth factor-β1 is a new form of tumor suppressor with true haploid insufficiency.* Nat Med, 1998. **4**(7): p. 802-07.
203. Jarvelainen, H., et al., *Extracellular matrix molecules: potential targets in pharmacotherapy.* Pharmacol Rev, 2009. **61**(2): p. 198-223.
204. Frantz, C., et al., *The extracellular matrix at a glance.* J Cell Sci, 2010. **123**(24): p. 4195-200.
205. Turk, B., *Targeting proteases: successes, failures and future prospects.* Nat Rev Drug Discov, 2006. **5**(9): p. 785-99.
206. Toth, M., et al., *Pro-MMP-9 activation by the MT1-MMP/MMP-2 axis and MMP-3: role of TIMP-2 and plasma membranes.* Biochem Biophys Res Commun, 2003. **308**(2): p. 386-95.
207. Bode, W., et al., *Insights into MMP-TIMP interactions.* Ann NY Acad Sci, 1999. **878**: p. 73-91.
208. Walsh, K.M., et al., *Plasma levels of matrix metalloproteinase-2 (MMP-2) and tissue inhibitors of metalloproteinases -1 and -2 (TIMP-1 and TIMP-2) as noninvasive markers of liver disease in chronic hepatitis C: comparison using ROC analysis.* Dig Dis Sci, 1999. **44**(3): p. 624-30.
209. Reiss, K. and P. Saftig, *The "a disintegrin and metalloprotease" (ADAM) family of sheddases: physiological and cellular functions.* Semin Cell Dev Biol, 2009. **20**(2): p. 126-37.
210. Liu, P.C., et al., *Identification of ADAM10 as a major source of HER2 ectodomain sheddase activity in HER2 overexpressing breast cancer cells.* Cancer Biol Ther, 2006. **5**(6): p. 657-64.
211. Shen, E., et al., *Association between myocardial ADAMTS-1 expression and myocardial fibrosis in a murine model of viral myocarditis.* Zhonghua Xin Xue Guan Bing Za Zhi, 2007. **35**(9): p. 854-58.
212. Sang, Q.X., et al., *Matrix metalloproteinase inhibitors as prospective agents for the prevention and treatment of cardiovascular and neoplastic diseases.* Curr Top Med Chem, 2006. **6**(4): p. 289-316.

213. Shuttleworth, T.L., et al., *Characterization of the murine hyaluronidase gene region reveals complex organization and cotranscription of Hyal1 with downstream genes, Fus2 and Hyal3.* J Biol Chem, 2002. **277**(25): p. 23008-18.
214. Lokeshwar, V.B., et al., *Association of elevated levels of hyaluronidase, a matrix-degrading enzyme, with prostate cancer progression.* Cancer Res, 1996. **56**(3): p. 651-57.
215. Rahmanian, M. and P. Heldin, *Testicular hyaluronidase induces tubular structures of endothelial cells grown in three-dimensional collagen gel through a CD44-mediated mechanism.* Int J Cancer, 2002. **97**(5): p. 601-07.
216. Starr, C.R. and N.C. Engleberg, *Role of hyaluronidase in subcutaneous spread and growth of group A streptococcus.* Infect Immun, 2006. **74**(1): p. 40-48.
217. Zukaite, V. and G.A. Biziulevicius, *Acceleration of hyaluronidase production in the course of batch cultivation of Clostridium perfringens can be achieved with bacteriolytic enzymes.* Lett Appl Microbiol, 2000. **30**(3): p. 203-06.
218. Alberts, B., et al., *Molecular Biology of the Cell*. 4th Edition. New York, Garland Science, 2002.
219. Liu, D., et al., *Expression of hyaluronidase by tumor cells induces angiogenesis in vivo.* Proc Natl Acad Sci USA, 1996. **93**(15): p. 7832-37.
220. Girish, K.S. and K. Kemparaju, *The magic glue hyaluronan and its eraser hyaluronidase: a biological overview.* Life Sci, 2007. **80**(21): p. 1921-43.
221. van der Rest, M. and R. Garrone, *Collagen family of proteins.* FASEB J, 1991. **5**(13): p. 2814-23.
222. van der Rest, M., et al., *Structure and function of the fibril-associated collagens.* Biochem Soc Trans, 1991. **19**(4): p. 820-24.
223. Weber, L., et al., *Collagen polymorphism in pathologic human scars.* Arch Dermatol Res, 1978. **261**(1): p. 63-71.
224. Esko, J.D., et al., *Proteoglycans and Sulfated Glycosaminoglycans.* Essentials of Glycobiology, 2nd Edition. New York, Cold Spring Harbor, 2009.
225. Iozzo, R.V., *Matrix proteoglycans: from molecular design to cellular function.* Annu Rev Biochem, 1998. **67**: p. 609-52.
226. Forsberg, E. and L. Kjellen, *Heparan sulfate: lessons from knockout mice.* J Clin Invest, 2001. **108**(2): p. 175-80.
227. Ameye, L. and M.F. Young, *Mice deficient in small leucine-rich proteoglycans: novel in vivo models for osteoporosis, osteoarthritis, Ehlers-Danlos syndrome, muscular dystrophy, and corneal diseases.* Glycobiology, 2002. **12**(9): p. 107-16.
228. Iozzo, R.V. and A.D. Murdoch, *Proteoglycans of the extracellular environment: clues from the gene and protein side offer novel perspectives in molecular diversity and function.* FASEB J, 1996. **10**(5): p. 598-614.
229. Sasisekharan, R., et al., *Glycomics approach to structure-function relationships of glycosaminoglycans.* Annu Rev Biomed Eng, 2006. **8**: p. 181-231.
230. Hollander, C., et al., *Human mast cells decrease SLPI levels in type II - like alveolar cell model, in vitro.* Cancer Cell Int, 2003. **3**(1): p. 14.
231. Sasisekharan, R. and G. Venkataraman, *Heparin and heparan sulfate: biosynthesis, structure and function.* Curr Opin Chem Biol, 2000. **4**(6): p. 626-31.
232. Li, F., et al., *Neuritogenic activity of chondroitin/dermatan sulfate hybrid chains of embryonic pig brain and their mimicry from shark liver. Involvement of the pleiotrophin and hepatocyte growth factor signaling pathways.* J Biol Chem, 2007. **282**(5): p. 2956-66.
233. Funderburgh, J.L., *Keratan sulfate: structure, biosynthesis, and function.* Glycobiology, 2000. **10**(10): p. 951-58.

234. Chakravarti, S., et al., *Corneal opacity in lumican-null mice: defects in collagen fibril structure and packing in the posterior stroma.* Invest Ophthalmol Vis Sci, 2000. **41**(11): p. 3365-73.
235. Laurent, T.C., et al., *The structure and function of hyaluronan: An overview.* Immunol Cell Biol, 1996. **74**(2): p. 1-7.
236. Gibbs, D.A., et al., *Rheology of hyaluronic acid.* Biopolymers, 1968. **6**(6): p. 777-91.
237. Necas, J., et al., *Hyaluronic acid (hyaluronan): a review.* Veterinarni Medicina, 2008. **53**(8): p. 397–411.
238. Gustafson, S. and T. Bjorkman, *Circulating hyaluronan, chondroitin sulphate and dextran sulphate bind to a liver receptor that does not recognize heparin.* Glycoconj J, 1997. **14**(5): p. 561-68.
239. Balazs, E.A., et al., *Nomenclature of hyaluronic acid.* Biochem J, 1986. **235**(3): p. 903.
240. Toole, B.P., *Hyaluronan promotes the malignant phenotype.* Glycobiology, 2002. **12**(3): p. 37-42.
241. Turley, E.A., et al., *Signaling properties of hyaluronan receptors.* J Biol Chem, 2002. **277**(7): p. 4589-92.
242. Hascall, V.C., et al., *Intracellular hyaluronan: a new frontier for inflammation?* Biochim Biophys Acta, 2004. **1673**(1-2): p. 3-12.
243. Noble, P.W., *Hyaluronan and its catabolic products in tissue injury and repair.* Matrix Biol, 2002. **21**(1): p. 25-29.
244. Simpson, R.M., et al., *Age-related changes in pericellular hyaluronan organization leads to impaired dermal fibroblast to myofibroblast differentiation.* Am J Pathol, 2009. **175**(5): p. 1915-28.
245. Evanko, S.P., et al., *Formation of hyaluronan- and versican-rich pericellular matrix is required for proliferation and migration of vascular smooth muscle cells.* Arterioscler Thromb Vasc Biol, 1999. **19**(4): p. 1004-13.
246. Yamada, T., et al., *Effects of hyaluronan on cell proliferation and mRNA expression of procollagens α 1 (I) and α 1 (III) in tendon-derived fibroblasts from patients with rotator cuff disease: an in vitro study.* Am J Sports Med, 2007. **35**(11): p. 1870-76.
247. Day, A.J. and G.D. Prestwich, *Hyaluronan-binding proteins: tying up the giant.* J Biol Chem, 2002. **277**(7): p. 4585-88.
248. Toole, B.P., *Hyaluronan and its binding proteins, the hyaladherins.* Curr Opin Cell Biol, 1990. **2**(5): p. 839-44.
249. Milner, C.M. and A.J. Day, *TSG-6: a multifunctional protein associated with inflammation.* J Cell Sci, 2003. **116**(Pt 10): p. 1863-73.
250. Mindrescu, C., et al., *Amelioration of collagen-induced arthritis in DBA/1J mice by recombinant TSG-6, a tumor necrosis factor/interleukin-1-inducible protein.* Arthritis Rheum, 2000. **43**(12): p. 2668-77.
251. Baranova, N.S., et al., *The inflammation-associated protein TSG-6 cross-links hyaluronan via hyaluronan-induced TSG-6 oligomers.* J Biol Chem, 2011. **286**(29): p. 25675-86.
252. Webber, J., et al., *Hyaluronan orchestrates transforming growth factor-β1-dependent maintenance of myofibroblast phenotype.* J Biol Chem, 2009. **284**(14): p. 9083-92.
253. Frenkel, J.S., *The role of hyaluronan in wound healing.* Int Wound J, 2012.
254. Yang, C., et al., *The high and low molecular weight forms of hyaluronan have distinct effects on CD44 clustering.* J Biol Chem, 2012. **287**(51): p. 43094-107.
255. Itano, N., et al., *Three isoforms of mammalian hyaluronan synthases have distinct enzymatic properties.* J Biol Chem, 1999. **274**(35): p. 25085-92.

256. Tien, J.Y. and A.P. Spicer, *Three vertebrate hyaluronan synthases are expressed during mouse development in distinct spatial and temporal patterns.* Dev Dyn, 2005. **233**(1): p. 130-41.
257. Li, Y., et al., *Severe lung fibrosis requires an invasive fibroblast phenotype regulated by hyaluronan and CD44.* J Exp Med, 2011. **208**(7): p. 1459-71.
258. Tian, X., et al., *High-molecular-mass hyaluronan mediates the cancer resistance of the naked mole rat.* Nature, 2013. **499**(7458): p. 346-49.
259. Kim, Y., et al., *CD44-epidermal growth factor receptor interaction mediates hyaluronic acid-promoted cell motility by activating protein kinase C signaling involving Akt, Rac1, Phox, reactive oxygen species, focal adhesion kinase, and MMP-2.* J Biol Chem, 2008. **283**(33): p. 22513-28.
260. Meran, S., et al., *Hyaluronan facilitates transforming growth factor-β1-mediated fibroblast proliferation.* J Biol Chem, 2008. **283**(10): p. 6530-45.
261. Milner, C.M., et al., *The molecular basis of inter-α-inhibitor heavy chain transfer on to hyaluronan.* Biochem Soc Trans, 2007. **35**(Pt 4): p. 672-6.
262. Naor, D., et al., *CD44: structure, function, and association with the malignant process.* Adv Cancer Res, 1997. **71**: p. 241-319.
263. Lesley, J. and R. Hyman, *CD44 structure and function.* Front Biosci, 1998. **3**: p. 616-30.
264. Meyer, L.J. and R. Stern, *Age-dependent changes of hyaluronan in human skin.* J Invest Dermatol, 1994. **102**(3): p. 385-89.
265. Wong, V.S., et al., *Serum hyaluronic acid is a useful marker of liver fibrosis in chronic hepatitis C virus infection.* J Viral Hepat, 1998. **5**(3): p. 187-92.
266. Crawford, D.H., et al., *Serum hyaluronic acid with serum ferritin accurately predicts cirrhosis and reduces the need for liver biopsy in C282Y hemochromatosis.* Hepatology, 2009. **49**(2): p. 418-25.
267. Michael, D.R., et al., *The human hyaluronan synthase 2 (HAS2) gene and its natural antisense RNA exhibit coordinated expression in the renal proximal tubular epithelial cell.* J Biol Chem, 2011. **286**(22): p. 19523-32.
268. West, D.C., et al., *Fibrotic healing of adult and late gestation fetal wounds correlates with increased hyaluronidase activity and removal of hyaluronan.* Int J Biochem Cell Biol, 1997. **29**(1): p. 201-10.
269. Murillo, M.M., et al., *Involvement of EGF receptor and c-Src in the survival signals induced by TGF-β1 in hepatocytes.* Oncogene, 2005. **24**(28): p. 4580-87.
270. Wang, Y., et al., *Hypoxia promotes ligand-independent EGF receptor signaling via hypoxia-inducible factor-mediated upregulation of caveolin-1.* Proc Natl Acad Sci U S A, 2012. **109**(13): p. 4892-97.
271. Yu, X., et al., *Ligand-independent dimer formation of epidermal growth factor receptor (EGFR) is a step separable from ligand-induced EGFR signaling.* Mol Biol Cell, 2002. **13**(7): p. 2547-57.
272. Li, Q., et al., *A syntaxin 1, Gα(o), and N-type calcium channel complex at a presynaptic nerve terminal: analysis by quantitative immunocolocalization.* J Neurosci, 2004. **24**(16): p. 4070-81.
273. Axelrod, D., et al., *Mobility measurement by analysis of fluorescence photobleaching recovery kinetics.* Biophys J, 1976. **16**(9): p. 1055-69.
274. Goodison, S., et al., *CD44 cell adhesion molecules.* Mol Pathol, 1999. **52**(4): p. 189-96.
275. Banky, B., et al., *Characteristics of CD44 alternative splice pattern in the course of human colorectal adenocarcinoma progression.* Mol Cancer, 2012. **11**: p. 83.

276. Zoller, M., *CD44: can a cancer-initiating cell profit from an abundantly expressed molecule?* Nat Rev Cancer, 2011. **11**(4): p. 254-67.
277. Napier, S.L., et al., *Selectin ligand expression regulates the initial vascular interactions of colon carcinoma cells: the roles of CD44v and alternative sialofucosylated selectin ligands.* J Biol Chem, 2007. **282**(6): p. 3433-41.
278. Sackstein, R., et al., *Ex vivo glycan engineering of CD44 programs human multipotent mesenchymal stromal cell trafficking to bone.* Nat Med, 2008. **14**(2): p. 181-87.
279. Thankamony, S.P. and W. Knudson, *Acylation of CD44 and its association with lipid rafts are required for receptor and hyaluronan endocytosis.* J Biol Chem, 2006. **281**(45): p. 34601-09.
280. Rugg, M.S., et al., *Characterization of complexes formed between TSG-6 and inter-α-inhibitor that act as intermediates in the covalent transfer of heavy chains onto hyaluronan.* J Biol Chem, 2005. **280**(27): p. 25674-86.
281. Perez, A., et al., *CD44 interacts with EGFR and promotes head and neck squamous cell carcinoma initiation and progression.* Oral Oncol, 2012. **49**(4): p. 306-13.
282. Bourguignon, L.Y., et al., *CD44 interaction with c-Src kinase promotes cortactin-mediated cytoskeleton function and hyaluronic acid-dependent ovarian tumor cell migration.* J Biol Chem, 2001. **276**(10): p. 7327-36.
283. Donatello, S., et al., *Lipid raft association restricts CD44-ezrin interaction and promotion of breast cancer cell migration.* Am J Pathol, 2012. **181**(6): p. 2172-87.
284. Lee, J.L., et al., *CD44 engagement promotes matrix-derived survival through the CD44-SRC-integrin axis in lipid rafts.* Mol Cell Biol, 2008. **28**(18): p. 5710-23.
285. Neame, S.J. and C.M. Isacke, *The cytoplasmic tail of CD44 is required for basolateral localization in epithelial MDCK cells but does not mediate association with the detergent-insoluble cytoskeleton of fibroblasts.* J Cell Biol, 1993. **121**(6): p. 1299-310.
286. Bourguignon, L.Y., et al., *Hyaluronic acid-induced lymphocyte signal transduction and HA receptor (GP85/CD44)-cytoskeleton interaction.* J Immunol, 1993. **151**(12): p. 6634-44.
287. Pike, L.J., *The challenge of lipid rafts.* J Lipid Res, 2009. **50 Suppl**: p. S323-8.
288. Irwin, M.E., et al., *Lipid raft localization of EGFR alters the response of cancer cells to the EGFR tyrosine kinase inhibitor gefitinib.* J Cell Physiol, 2011. **226**(9): p. 2316-28.
289. Lambert, S., et al., *Ligand-independent activation of the EGFR by lipid raft disruption.* J Invest Dermatol, 2006. **126**(5): p. 954-62.
290. Bourguignon, L.Y., et al., *Hyaluronan-CD44 interaction with leukemia-associated RhoGEF and epidermal growth factor receptor promotes Rho/Ras co-activation, phospholipase C epsilon-Ca^{2+} signaling, and cytoskeleton modification in head and neck squamous cell carcinoma cells.* J Biol Chem, 2006. **281**(20): p. 14026-40.
291. Lu, Z. and S. Xu, *ERK1/2 MAP kinases in cell survival and apoptosis.* IUBMB Life, 2006. **58**(11): p. 621-31.
292. Mebratu, Y. and Y. Tesfaigzi, *How ERK1/2 activation controls cell proliferation and cell death: Is subcellular localization the answer?* Cell Cycle, 2009. **8**(8): p. 1168-75.
293. Roskoski, R., Jr., *ERK1/2 MAP kinases: structure, function, and regulation.* Pharmacol Res, 2012. **66**(2): p. 105-43.
294. Okamoto, K., et al., *The role of CaMKII as an F-actin-bundling protein crucial for maintenance of dendritic spine structure.* Proc Natl Acad Sci U S A, 2007. **104**(15): p. 6418-23.

295. Sanabria, H., et al., *{β}CaMKII regulates actin assembly and structure.* J Biol Chem, 2009. **284**(15): p. 9770-80.
296. Zayzafoon, M., *Calcium/calmodulin signaling controls osteoblast growth and differentiation.* J Cell Biochem, 2006. **97**(1): p. 56-70.
297. Meran, S., et al., *Involvement of hyaluronan in regulation of fibroblast phenotype.* J Biol Chem, 2007. **282**(35): p. 25687-97.
298. Tsui-Pierchala, B.A., et al., *Lipid rafts in neuronal signaling and function.* Trends Neurosci, 2002. **25**(8): p. 412-7.
299. Zhuang, L., et al., *Cholesterol-rich lipid rafts mediate akt-regulated survival in prostate cancer cells.* Cancer Res, 2002. **62**(8): p. 2227-31.
300. Takebayashi, M., et al., *Sigma-1 receptors potentiate epidermal growth factor signaling towards neuritogenesis in PC12 cells: potential relation to lipid raft reconstitution.* Synapse, 2004. **53**(2): p. 90-103.
301. Akhmetshina, A., et al., *Rho-associated kinases are crucial for myofibroblast differentiation and production of extracellular matrix in scleroderma fibroblasts.* Arthritis Rheum, 2008. **58**(8): p. 2553-64.
302. Bourguignon, L.Y., et al., *Heregulin-mediated ErbB2-ERK signaling activates hyaluronan synthases leading to CD44-dependent ovarian tumor cell growth and migration.* J Biol Chem, 2007. **282**(27): p. 19426-41.
303. Zhai, H., et al., *Honokiol-induced neurite outgrowth promotion depends on activation of extracellular signal-regulated kinases (ERK1/2).* Eur J Pharmacol, 2005. **516**(2): p. 112-17.
304. Singer, H.A., *Ca^{2+}/calmodulin-dependent protein kinase II Function in Vascular Remodeling.* J Physiol, 2012. **15**(509): p. 1349-56.
305. Spicer, A.P. and J.A. McDonald, *Characterization and molecular evolution of a vertebrate hyaluronan synthase gene family.* J Biol Chem, 1998. **273**(4): p. 1923-32.
306. Spicer, A.P. and T.K. Nguyen, *Mammalian hyaluronan synthases: investigation of functional relationships in vivo.* Biochem Soc Trans, 1999. **27**(2): p. 109-15.
307. Palyi-Krekk, Z., et al., *EGFR and ErbB2 are functionally coupled to CD44 and regulate shedding, internalization and motogenic effect of CD44.* Cancer Lett, 2008. **263**(2): p. 231-42.
308. Wang, S.J. and L.Y. Bourguignon, *Hyaluronan and the interaction between CD44 and epidermal growth factor receptor in oncogenic signaling and chemotherapy resistance in head and neck cancer.* Arch Otolaryngol Head Neck Surg, 2006. **132**(7): p. 771-78.
309. Pike, L.J. and L. Casey, *Cholesterol levels modulate EGF receptor-mediated signaling by altering receptor function and trafficking.* Biochemistry, 2002. **41**(32): p. 10315-22.
310. Nylander, N., et al., *Topography of amphiregulin expression in cultured human keratinocytes: colocalization with the epidermal growth factor receptor and CD44.* In Vitro Cell Dev Biol Anim, 1998. **34**(2): p. 182-88.
311. Liu, Y., et al., *The involvement of lipid rafts in epidermal growth factor-induced chemotaxis of breast cancer cells.* Mol Membr Biol, 2007. **24**(2): p. 91-101.
312. Roepstorff, K., et al., *Sequestration of epidermal growth factor receptors in non-caveolar lipid rafts inhibits ligand binding.* J Biol Chem, 2002. **277**(21): p. 18954-60.
313. Deng, Z.Y., et al., *Effect of oxymatrine on the p38 mitogen-activated protein kinases signalling pathway in rats with CCl4 induced hepatic fibrosis.* Chin Med J, 2009. **122**(12): p. 1449-54.
314. Ma, F.Y., et al., *Mitogen activated protein kinases in renal fibrosis.* Front Biosci, 2009. **1**: p. 171-87.

315. Knudson, C.B. and W. Knudson, *Hyaluronan and CD44: modulators of chondrocyte metabolism.* Clin Orthop Relat Res, 2004(427 Suppl): p. 152-62.
316. Poumay, Y. and V. Mitev, *Members of the EGF receptor family in normal and pathological epidermis.* Folia Med, 2009. **51**(3): p. 5-17.
317. Grande, M., et al., *Transforming growth factor-β and epidermal growth factor synergistically stimulate epithelial to mesenchymal transition (EMT) through a MEK-dependent mechanism in primary cultured pig thyrocytes.* J Cell Sci, 2002. **115**(22): p. 4227-36.
318. He, J. and H.E. Bazan, *Epidermal growth factor synergism with TGF-β1 via PI-3 kinase activity in corneal keratocyte differentiation.* Invest Ophthalmol Vis Sci, 2008. **49**(7): p. 2936-45.
319. Song, K., et al., *Novel permissive role of epidermal growth factor in transforming growth factor β (TGF-β) signaling and growth suppression. Mediation by stabilization of TGF-β receptor type II.* J Biol Chem, 2006. **281**(12): p. 7765-74.
320. Hongo, M., et al., *Distribution of epidermal growth factor (EGF) receptors in rabbit corneal epithelial cells, keratocytes and endothelial cells, and the changes induced by transforming growth factor-β 1.* Exp Eye Res, 1992. **54**(1): p. 9-16.
321. Goldkorn, T. and J. Mendelsohn, *Transforming growth factor β modulates phosphorylation of the epidermal growth factor receptor and proliferation of A431 cells.* Cell Growth Differ, 1992. **3**(2): p. 101-09.
322. Uchiyama-Tanaka, Y., et al., *Involvement of HB-EGF and EGF receptor transactivation in TGF-β-mediated fibronectin expression in mesangial cells.* Kidney Int, 2002. **62**(3): p. 799-808.
323. Lu, H.S., et al., *Crystal structure of human epidermal growth factor and its dimerization.* J Biol Chem, 2001. **276**(37): p. 34913-17.
324. Leahy, D.J., *Structure and function of the epidermal growth factor (EGF/ErbB) family of receptors.* Adv Protein Chem, 2004. **68**: p. 1-27.
325. Ono, M. and M. Kuwano, *Molecular mechanisms of epidermal growth factor receptor (EGFR) activation and response to gefitinib and other EGFR-targeting drugs.* Clin Cancer Res, 2006. **12**(24): p. 7242-51.
326. Tao, R.H. and I.N. Maruyama, *All EGF(ErbB) receptors have preformed homo- and heterodimeric structures in living cells.* J Cell Sci, 2008. **121**(19): p. 3207-17.
327. Abulrob, A., et al., *Nanoscale imaging of epidermal growth factor receptor clustering: effects of inhibitors.* J Biol Chem, 2010. **285**(5): p. 3145-56.
328. Ichinose, J., et al., *EGF signalling amplification induced by dynamic clustering of EGFR.* Biochem Biophys Res Commun, 2004. **324**(3): p. 1143-49.
329. Jo, M., et al., *Cross-talk between epidermal growth factor receptor and c-Met signal pathways in transformed cells.* J Biol Chem, 2000. **275**(12): p. 8806-11.
330. Biscardi, J.S., et al., *c-Src-mediated phosphorylation of the epidermal growth factor receptor on Tyr845 and Tyr1101 is associated with modulation of receptor function.* J Biol Chem, 1999. **274**(12): p. 8335-43.
331. Kefas, B., et al., *microRNA-7 inhibits the epidermal growth factor receptor and the Akt pathway and is down-regulated in glioblastoma.* Cancer Res, 2008. **68**(10): p. 3566-72.
332. Chou, Y.T., et al., *EGFR promotes lung tumorigenesis by activating miR-7 through a Ras/ERK/Myc pathway that targets the Ets2 transcriptional repressor ERF.* Cancer Res, 2010. **70**(21): p. 8822-31.
333. Webster, R.J., et al., *Regulation of epidermal growth factor receptor signaling in human cancer cells by microRNA-7.* J Biol Chem, 2009. **284**(9): p. 5731-41.

334. Li, X. and R.W. Carthew, *A microRNA mediates EGF receptor signaling and promotes photoreceptor differentiation in the Drosophila eye.* Cell, 2005. **123**(7): p. 1267-77.
335. Midgley, A., et al., *TGF-β1-stimulated fibroblast to myofibroblast differentiation is mediated by HA-facilitated EGFR and CD44 co-localisation in lipid rafts.* J Biol Chem, 2013. **288**: p. 14824-38.
336. Kohan, M., et al., *EDA-containing cellular fibronectin induces fibroblast differentiation through binding to α4β7 integrin receptor and MAPK/Erk 1/2-dependent signaling.* FASEB J, 2010. **24**(11): p. 4503-12.
337. Meran, S. and R. Steadman, *Fibroblasts and myofibroblasts in renal fibrosis.* Int J Exp Pathol, 2011. **92**(3): p. 158-67.
338. Wang, S.J. and L.Y. Bourguignon, *Hyaluronan-CD44 promotes phospholipase C-mediated Ca^{2+} signaling and cisplatin resistance in head and neck cancer.* Arch Otolaryngol Head Neck Surg, 2006. **132**(1): p. 19-24.
339. Bourguignon, L.Y., et al., *Hyaluronan-CD44 interaction stimulates keratinocyte differentiation, lamellar body formation/secretion, and permeability barrier homeostasis.* J Invest Dermatol, 2006. **126**(6): p. 1356-65.
340. Sherman, L., et al., *Hyaluronate receptors: key players in growth, differentiation, migration and tumor progression.* Curr Opin Cell Biol, 1994. **6**(5): p. 726-33.
341. Bernert, B., et al., *Hyaluronan synthase 2 (HAS2) promotes breast cancer cell invasion by suppression of tissue metalloproteinase inhibitor 1 (TIMP-1).* J Biol Chem, 2011. **286**(49): p. 42349-59.
342. Kultti, A., et al., *Methyl-β-cyclodextrin suppresses hyaluronan synthesis by down-regulation of hyaluronan synthase 2 through inhibition of Akt.* J Biol Chem, 2010. **285**(30): p. 22901-10.
343. Ashcroft, G.S. and A.B. Roberts, *Loss of Smad3 modulates wound healing.* Cytokine Growth Factor Rev, 2000. **11**(1-2): p. 125-31.
344. Mukku, V.R. and G.M. Stancel, *Regulation of epidermal growth factor receptor by estrogen.* J Biol Chem, 1985. **260**(17): p. 9820-24.
345. Soares, R., et al., *17β-estradiol-mediated vessel assembly and stabilization in tumor angiogenesis requires TGF β and EGFR crosstalk.* Angiogenesis, 2003. **6**(4): p. 271-81.
346. Stevenson, S. and J. Thornton, *Effect of estrogens on skin aging and the potential role of SERMs.* Clin Interv Aging, 2007. **2**(3): p. 283-97.
347. Sugiura, K., et al., *Estrogen promotes the development of mouse cumulus cells in coordination with oocyte-derived GDF9 and BMP15.* Mol Endocrinol, 2010. **24**(12): p. 2303-14.
348. Uzuka, M., et al., *The mechanism of estrogen-induced increase in hyaluronic acid biosynthesis, with special reference to estrogen receptor in the mouse skin.* Biochim Biophys Acta, 1980. **627**(2): p. 199-206.
349. Arora, A. and D.A. Simpson, *Individual mRNA expression profiles reveal the effects of specific microRNAs.* Genome Biol, 2008. **9**(5): p. 82.
350. Poller, W. and H. Fechner, *Development of novel cardiovascular therapeutics from small regulatory RNA molecules--an outline of key requirements.* Curr Pharm Des, 2010. **16**(20): p. 2252-68.
351. Schanen, B.C. and X. Li, *Transcriptional regulation of mammalian miRNA genes.* Genomics, 2011. **97**(1): p. 1-6.
352. Ozsolak, F., et al., *Chromatin structure analyses identify miRNA promoters.* Genes Dev, 2008. **22**(22): p. 3172-83.

353. Zhou, H., et al., *A tightly regulated Pol III promoter for synthesis of miRNA genes in tandem.* Biochim Biophys Acta, 2008. **1779**(11): p. 773-79.
354. Snyder, L.L., et al., *RNA polymerase III can drive polycistronic expression of functional interfering RNAs designed to resemble microRNAs.* Nucleic Acids Res, 2009. **37**(19): p. 127.
355. Jenuwein, T. and C.D. Allis, *Translating the histone code.* Science, 2001. **293**(5532): p. 1074-80.
356. Li, B., et al., *The role of chromatin during transcription.* Cell, 2007. **128**(4): p. 707-19.
357. Santos-Rosa, H., et al., *Active genes are tri-methylated at K4 of histone H3.* Nature, 2002. **419**(6905): p. 407-11.
358. Schneider, R., et al., *Histone H3 lysine 4 methylation patterns in higher eukaryotic genes.* Nat Cell Biol, 2004. **6**(1): p. 73-77.
359. Cai, X., et al., *Human microRNAs are processed from capped, polyadenylated transcripts that can also function as mRNAs.* RNA, 2004. **10**(12): p. 1957-66.
360. Lee, Y., et al., *MicroRNA genes are transcribed by RNA polymerase II.* EMBO J, 2004. **23**(20): p. 4051-60.
361. Ozsolak, F., et al., *High-throughput mapping of the chromatin structure of human promoters.* Nat Biotechnol, 2007. **25**(2): p. 244-48.
362. Yuan, G.C., et al., *Genome-scale identification of nucleosome positions in S. cerevisiae.* Science, 2005. **309**(5734): p. 626-30.
363. Spizzo, R., et al., *miR-145 participates with TP53 in a death-promoting regulatory loop and targets estrogen receptor-α in human breast cancer cells.* Cell Death Differ, 2010. **17**(2): p. 246-54.
364. Tessel, M.A., et al., *Steroid receptor and microRNA regulation in cancer.* Curr Opin Oncol, 2010. **22**(6): p. 592-97.
365. Fang, Y., et al., *MicroRNA-7 inhibits tumor growth and metastasis by targeting the phosphoinositide 3-kinase/Akt pathway in hepatocellular carcinoma.* Hepatology, 2012. **55**(6): p. 1852-62.
366. Tchernitchin, A., et al., *Correlation of estrogen-induced uterine eosinophilia with other parameters of estrogen stimulation, produced with estradiol-17β and estriol.* Experientia, 1975. **31**(8): p. 993-94.
367. Chiu, T.C., et al., *Determining estrogens using surface-assisted laser desorption/ionization mass spectrometry with silver nanoparticles as the matrix.* J Am Soc Mass Spectrom, 2008. **19**(9): p. 1343-46.
368. Schuit, S.C., et al., *Estrogen receptor-α gene polymorphisms are associated with estradiol levels in postmenopausal women.* Eur J Endocrinol, 2005. **153**(2): p. 327-34.
369. Szulc, P., et al., *Role of sex steroids in the regulation of bone morphology in men. The MINOS study.* Osteoporos Int, 2004. **15**(11): p. 909-17.
370. Quesada, A. and A.M. Etgen, *Functional interactions between estrogen and insulin-like growth factor-I in the regulation of α 1B-adrenoceptors and female reproductive function.* J Neurosci, 2002. **22**(6): p. 2401-08.
371. Gruber, H.E., et al., *Alterations in osteoclast morphology following long-term 17β-estradiol administration in the mouse.* BMC Cell Biol, 2001. **2**: p. 3.
372. Kaludjerovic, J. and W.E. Ward, *The Interplay between Estrogen and Fetal Adrenal Cortex.* J Nutr Metab, 2012. **2012**: p. 837901.
373. Kelch, R.P., et al., *Estradiol and testosterone secretion by human, simian, and canine testes, in males with hypogonadism and in male pseudohermaphrodites with the feminizing testes syndrome.* J Clin Invest, 1972. **51**(4): p. 824-30.
374. Nelson, L.R. and S.E. Bulun, *Estrogen production and action.* J Am Acad Dermatol, 2001. **45**(3): p. 116-24.

375. Levin, E.R., *Integration of the extranuclear and nuclear actions of estrogen.* Mol Endocrinol, 2005. **19**(8): p. 1951-9.
376. Wu, C.H., et al., *Free and protein-bound plasma estradiol-17 β during the menstrual cycle.* J Clin Endocrinol Metab, 1976. **43**(2): p. 436-45.
377. Roman-Blas, J.A., et al., *Osteoarthritis associated with estrogen deficiency.* Arthritis Res Ther, 2009. **11**(5): p. 241.
378. Bercovitch, F.B., *Estradiol concentrations, fat deposits, and reproductive strategies in male rhesus macaques.* Horm Behav, 1992. **26**(2): p. 272-82.
379. Shah, M.G. and H.I. Maibach, *Estrogen and skin. An overview.* Am J Clin Dermatol, 2001. **2**(3): p. 143-50.
380. Thornton, M.J., *The biological actions of estrogens on skin.* Exp Dermatol, 2002. **11**(6): p. 487-502.
381. Lyytinen, H., et al., *Breast cancer risk in postmenopausal women using estradiol-progestogen therapy.* Obstet Gynecol, 2009. **113**(1): p. 65-73.
382. Mahlck, C.G., et al., *Plasma level of estradiol in patients with ovarian malignant tumors.* Gynecol Oncol, 1988. **30**(3): p. 313-20.
383. Lepine, J., et al., *Circulating estrogens in endometrial cancer cases and their relationship with tissular expression of key estrogen biosynthesis and metabolic pathways.* J Clin Endocrinol Metab, 2010. **95**(6): p. 2689-98.
384. Emmerson, E. and M.J. Hardman, *The role of estrogen deficiency in skin ageing and wound healing.* Biogerontology, 2012. **13**(1): p. 3-20.
385. Hardman, M.J. and G.S. Ashcroft, *Estrogen, not intrinsic aging, is the major regulator of delayed human wound healing in the elderly.* Genome Biol, 2008. **9**(5): p. 80.
386. Hardman, M.J., et al., *Selective estrogen receptor modulators accelerate cutaneous wound healing in ovariectomized female mice.* Endocrinology, 2008. **149**(2): p. 551-7.
387. Gilliver, S.C., et al., *17β-estradiol inhibits wound healing in male mice via estrogen receptor-α.* Am J Pathol, 2010. **176**(6): p. 2707-21.
388. Haczynski, J., et al., *Differential effects of estradiol, raloxifene and tamoxifen on estrogen receptor expression in cultured human skin fibroblasts.* Int J Mol Med, 2004. **13**(6): p. 903-8.
389. Haczynski, J., et al., *Human cultured skin fibroblasts express estrogen receptor α and β.* Int J Mol Med, 2002. **10**(2): p. 149-53.
390. Palmieri, C., et al., *The expression of oestrogen receptor (ER)-β and its variants, but not ERα, in adult human mammary fibroblasts.* J Mol Endocrinol, 2004. **33**(1): p. 35-50.
391. Stabile, L.P., et al., *Human non-small cell lung tumors and cells derived from normal lung express both estrogen receptor α and β and show biological responses to estrogen.* Cancer Res, 2002. **62**(7): p. 2141-50.
392. Valimaa, H., et al., *Estrogen receptor-β is the predominant estrogen receptor subtype in human oral epithelium and salivary glands.* J Endocrinol, 2004. **180**(1): p. 55-62.
393. Campbell, L., et al., *Estrogen promotes cutaneous wound healing via estrogen receptor β independent of its antiinflammatory activities.* J Exp Med, 2010. **207**(9): p. 1825-33.
394. Freudenberger, T., et al., *Estradiol inhibits hyaluronic acid synthase 1 expression in human vascular smooth muscle cells.* Basic Res Cardiol, 2011. **106**(6): p. 1099-109.
395. Rock, K., et al., *Estradiol protects dermal hyaluronan/versican matrix during photoaging by release of epidermal growth factor from keratinocytes.* J Biol Chem, 2012. **287**(24): p. 20056-69.

396. Uzuka, M., et al., *Induction of hyaluronic acid synthetase by estrogen in the mouse skin.* Biochim Biophys Acta, 1981. **673**(4): p. 387-93.
397. Tsonis, A.I., et al., *Evaluation of the coordinated actions of estrogen receptors with epidermal growth factor receptor and insulin-like growth factor receptor in the expression of cell surface heparan sulfate proteoglycans and cell motility in breast cancer cells.* FEBS J, 2013. **280**(10): p. 2248-59.
398. Sukocheva, O., et al., *Estrogen transactivates EGFR via the sphingosine 1-phosphate receptor Edg-3: the role of sphingosine kinase-1.* J Cell Biol, 2006. **173**(2): p. 301-10.
399. Koibuchi, Y., et al., *Regulation of estrogen receptor and epidermal growth factor receptor by tamoxifen under high and low estrogen environments in MCF-7 cells grown in athymic mice.* Oncol Rep, 2000. **7**(1): p. 135-40.
400. Stabile, L.P., et al., *Combined targeting of the estrogen receptor and the epidermal growth factor receptor in non-small cell lung cancer shows enhanced antiproliferative effects.* Cancer Res, 2005. **65**(4): p. 1459-70.
401. Masuda, M., et al., *An induction of microRNA, miR-7 through estrogen treatment in breast carcinoma.* J Transl Med, 2012. **10**(1): p. 2.
402. Fontana, L., et al., *Antagomir-17-5p abolishes the growth of therapy-resistant neuroblastoma through p21 and BIM.* PLoS One, 2008. **3**(5): p. 2236.
403. van Solingen, C., et al., *Antagomir-mediated silencing of endothelial cell specific microRNA-126 impairs ischemia-induced angiogenesis.* J Cell Mol Med, 2009. **13**(8): p. 1577-85.
404. Girasole, G., et al., *17β-estradiol inhibits interleukin-6 production by bone marrow-derived stromal cells and osteoblasts in vitro: a potential mechanism for the antiosteoporotic effect of estrogens.* J Clin Invest, 1992. **89**(3): p. 883-91.
405. Ray, P., et al., *Repression of interleukin-6 gene expression by 17 β-estradiol: inhibition of the DNA-binding activity of the transcription factors NF-IL6 and NF-kappa B by the estrogen receptor.* FEBS Lett, 1997. **409**(1): p. 79-85.
406. Stein, B. and M.X. Yang, *Repression of the interleukin-6 promoter by estrogen receptor is mediated by NF-kappa B and C/EBP β.* Mol Cell Biol, 1995. **15**(9): p. 4971-79.
407. Wang, L.H., et al., *Activation of estrogen receptor blocks interleukin-6-inducible cell growth of human multiple myeloma involving molecular cross-talk between estrogen receptor and STAT3 mediated by co-regulator PIAS3.* J Biol Chem, 2001. **276**(34): p. 31839-44.
408. Ershler, W.B. and E.T. Keller, *Age-associated increased interleukin-6 gene expression, late-life diseases, and frailty.* Annu Rev Med, 2000. **51**: p. 245-70.
409. Tchkonia, T., et al., *Fat tissue, aging, and cellular senescence.* Aging Cell, 2010. **9**(5): p. 667-84.
410. Wei, J., et al., *Increase of plasma IL-6 concentration with age in healthy subjects.* Life Sci, 1992. **51**(25): p. 1953-56.
411. Beharka, A.A., et al., *Interleukin-6 production does not increase with age.* J Gerontol A Biol Sci Med Sci, 2001. **56**(2): p. 81-88.
412. Wang, Y., et al., *STAT3 activation in response to IL-6 is prolonged by the binding of IL-6 receptor to EGF receptor.* Proc Natl Acad Sci USA, 2013. **110**(42): p. 16975-80.
413. Shen, X.H., et al., *Interleukin-6 enhances porcine parthenote development in vitro, through the IL-6/Stat3 signaling pathway.* J Reprod Dev, 2012. **58**(4): p. 453-60.
414. Wang, Y.Z., et al., *CD44 mediates oligosaccharides of hyaluronan-induced proliferation, tube formation and signal transduction in endothelial cells.* Experimental biology and medicine, 2011. **236**(1): p. 84-90.

415. Fujisaki, T., et al., *CD44 stimulation induces integrin-mediated adhesion of colon cancer cell lines to endothelial cells by up-regulation of integrins and c-Met and activation of integrins.* Cancer research, 1999. **59**(17): p. 4427-34.
416. Okamoto, I., et al., *CD44 cleavage induced by a membrane-associated metalloprotease plays a critical role in tumor cell migration.* Oncogene, 1999. **18**(7): p. 1435-46.
417. Levesque, M.C. and B.F. Haynes, *Cytokine induction of the ability of human monocyte CD44 to bind hyaluronan is mediated primarily by TNF-α and is inhibited by IL-4 and IL-13.* Journal of immunology, 1997. **159**(12): p. 6184-94.
418. Cichy, J. and E. Pure, *Oncostatin M and transforming growth factor-β 1 induce post-translational modification and hyaluronan binding to CD44 in lung-derived epithelial tumor cells.* The Journal of biological chemistry, 2000. **275**(24): p. 18061-69.
419. Ponta, H., et al., *CD44: from adhesion molecules to signalling regulators.* Nature reviews. Molecular cell biology, 2003. **4**(1): p. 33-45.
420. Lim, J.Y., et al., *TGF-β1 induces cardiac hypertrophic responses via PKC-dependent ATF-2 activation.* Journal of molecular and cellular cardiology, 2005. **39**(4): p. 627-36.
421. Stapleton, G., et al., *Downregulated AP-1 activity is associated with inhibition of Protein-Kinase-C-dependent CD44 and ezrin localisation and upregulation of PKC theta in A431 cells.* Journal of cell science, 2002. **115**(13): p. 2713-24.
422. Bommaya, G., et al., *Tumour necrosis factor-stimulated gene (TSG)-6 controls epithelial-mesenchymal transition of proximal tubular epithelial cells.* The international journal of biochemistry & cell biology, 2011. **43**(12): p. 1739-46.
423. Zhang, M., et al., *ERK, p38, and Smad signaling pathways differentially regulate transforming growth factor-β1 autoinduction in proximal tubular epithelial cells.* The American journal of pathology, 2006. **169**(4): p. 1282-93.
424. Peterson, R.S., et al., *CD44 modulates Smad1 activation in the BMP-7 signaling pathway.* The Journal of cell biology, 2004. **166**(7): p. 1081-91.
425. Jiang, H., et al., *A requirement for the CD44 cytoplasmic domain for hyaluronan binding, pericellular matrix assembly, and receptor-mediated endocytosis in COS-7 cells.* The Journal of biological chemistry, 2002. **277**(12): p. 10531-38.
426. Grass, G.D., et al., *CD147, CD44, and the epidermal growth factor receptor (EGFR) signaling pathway cooperate to regulate breast epithelial cell invasiveness.* The Journal of biological chemistry, 2013. **288**(36): p. 26089-104.
427. Toole, B.P. and M.G. Slomiany, *Hyaluronan, CD44 and Emmprin: partners in cancer cell chemoresistance.* Drug resistance updates : reviews and commentaries in antimicrobial and anticancer chemotherapy, 2008. **11**(3): p. 110-21.
428. Maria, B.L., et al., *Targeting hyaluronan interactions in spinal cord astrocytomas and diffuse pontine gliomas.* Journal of child neurology, 2008. **23**(10): p. 1214-20.
429. Suga, N., et al., *Heparin/heparan sulfate/CD44-v3 enhances cell migration in term placenta-derived immortalized human trophoblast cells.* Biology of reproduction, 2012. **86**(5): p. 134, 1-8.
430. Ferbeyre, G., et al., *Oncogenic ras and p53 cooperate to induce cellular senescence.* Mol Cell Biol, 2002. **22**(10): p. 3497-508.
431. Muller, M., *Premature cellular senescence induced by pyocyanin, a redox-active Pseudomonas aeruginosa toxin.* Free Radic Biol Med, 2006. **41**(11): p. 1670-77.
432. Ye, C., et al., *Radiation-induced cellular senescence results from a slippage of long-term G2 arrested cells into G1 phase.* Cell Cycle, 2013. **12**(9): p. 1424-32.
433. Rodier, F. and J. Campisi, *Four faces of cellular senescence.* J Cell Biol, 2011. **192**(4): p. 547-56.

434. Baker, D.J., et al., *Clearance of p16Ink4a-positive senescent cells delays ageing-associated disorders.* Nature, 2011. **479**(7372): p. 232-36.
435. Carpenter, G., *The EGF receptor: a nexus for trafficking and signaling.* Bioessays, 2000. **22**(8): p. 697-707.
436. Campisi, J., *The role of cellular senescence in skin aging.* J Investig Dermatol Symp Proc, 1998. **3**(1): p. 1-5.
437. Stephens, P., et al., *An analysis of replicative senescence in dermal fibroblasts derived from chronic leg wounds predicts that telomerase therapy would fail to reverse their disease-specific cellular and proteolytic phenotype.* Exp Cell Res, 2003. **283**(1): p. 22-35.
438. Liang, J. and J.M. Slingerland, *Multiple roles of the PI3K/PKB (Akt) pathway in cell cycle progression.* Cell Cycle, 2003. **2**(4): p. 339-45.
439. Lawlor, M.A. and D.R. Alessi, *PKB/Akt: a key mediator of cell proliferation, survival and insulin responses?* J Cell Sci, 2001. **114**(Pt 16): p. 2903-10.
440. Kultti, A., et al., *Methyl-β-cyclodextrin suppresses hyaluronan synthesis by down-regulation of hyaluronan synthase 2 through inhibition of Akt.* The Journal of biological chemistry, 2010. **285**(30): p. 22901-10.
441. Amann, J., et al., *Aberrant epidermal growth factor receptor signaling and enhanced sensitivity to EGFR inhibitors in lung cancer.* Cancer research, 2005. **65**(1): p. 226-35.
442. Hatanpaa, K.J., et al., *Epidermal growth factor receptor in glioma: signal transduction, neuropathology, imaging, and radioresistance.* Neoplasia, 2010. **12**(9): p. 675-84.
443. Tzeng, C.W., et al., *EGFR genomic gain and aberrant pathway signaling in pancreatic cancer patients.* The Journal of surgical research, 2007. **143**(1): p. 20-26.
444. Gomez, C.R., et al., *Interleukin-6 contributes to age-related alteration of cytokine production by macrophages.* Mediators Inflamm, 2010. **2010**: p. 475139.
445. Pierce, G.F., *Inflammation in nonhealing diabetic wounds: the space-time continuum does matter.* The American journal of pathology, 2001. **159**(2): p. 399-403.
446. Trengove, N.J., et al., *Mitogenic activity and cytokine levels in non-healing and healing chronic leg ulcers.* Wound Repair and Regen, 2000. **8**(1): p. 13-25.
447. Liu, H., et al., *Estrogen receptor inhibits interleukin-6 gene expression by disruption of nuclear factor kappaB transactivation.* Cytokine, 2005. **31**(4): p. 251-57.
448. Shaker, O., et al., *TGF-B1 pathway as biological marker of bladder carcinoma schistosomal and non-schistosomal.* Urol Oncol, 2013. **31**(3): p. 372-78.
449. Kakehi, Y., et al., *Elevation of serum transforming growth factor-β1 Level in patients with metastatic prostate cancer.* Urol Oncol, 1996. **2**(5): p. 131-35.
450. Meyer-Ter-Vehn, T., et al., *p38 inhibitors prevent TGF-β-induced myofibroblast transdifferentiation in human tenon fibroblasts.* Investigative ophthalmology & visual science, 2006. **47**(4): p. 1500-09.
451. Panuncialman, J., et al., *Wound edge biopsy sites in chronic wounds heal rapidly and do not result in delayed overall healing of the wounds.* Wound Repair and Regen, 2010. **18**(1): p. 21-25.

Appendix 1: Buffers and Reagents

Solution	Contents
Blocking Buffer:	5%(w/v) Dried Skimmed Milk Powder, 0.5%(v/v) Tween-20, 20ml PBS
Reducing Buffer (3x):	62.5mM Tris, 30%(v/v) Glycerol, 6%(w/v) SDS, 0.03%(w/v) Bromophenol-blue, 25%(v/v) β-mercaptoethanol, 10ml dH_2O
Reducing Buffer (1x):	62.5mM Tris, 10%(v/v) Glycerol, 2%(w/v) SDS, 0.01%(w/v) Bromophenol-blue, 8.3%(v/v) β-mercaptoethanol, 10ml dH_2O
Running Buffer (10x):	30g/L Tris, 144g/L Glycine, 10g/L SDS, 1L dH_2O, pH8.3
Running Buffer (1x):	100ml 10x Running Buffer, 900ml dH_2O
Transfer Buffer (10x):	30g/L Tris, 144g/L Glycine, 1L dH_2O, pH8.3
Transfer Buffer (1x):	80ml 10x Transfer Buffer, 200ml Methanol, 720ml dH_2O
TAE Buffer (1x):	40mM Tris, 20mM Acetic Acid, 1mM EDTA, 1L dH_2O
PCR Loading Buffer:	30%(v/v) Glycerol, 0.1%(w/v) Orange(/Blue)-G
Phosphate Buffered Saline (PBS):	2.68mM KCl, 1.47mM KH_2PO_4, 137mM NaCl, 8.1mM Na_2HPO_4
Cytokine Buffer:	4mM HCl, 1mg/ml BSA, in PBS
Mild Stripping Buffer:	15g/L Glycine, 1g/L SDS, 1%(v/v) Tween-20, 1L dH_2O, pH2.2
Stripping Buffer:	20g/L SDS, 7.57g/L Tris, 100mM/L β-mercaptoethanol, 1L dH_2O, pH6.7
Wash Buffer (5x):	0.5%(v/v) Tween-20, 1L PBS
Wash Buffer (1x):	0.1%(v/v) Tween-20, 1L PBS

Appendix 2: Supplemental Data

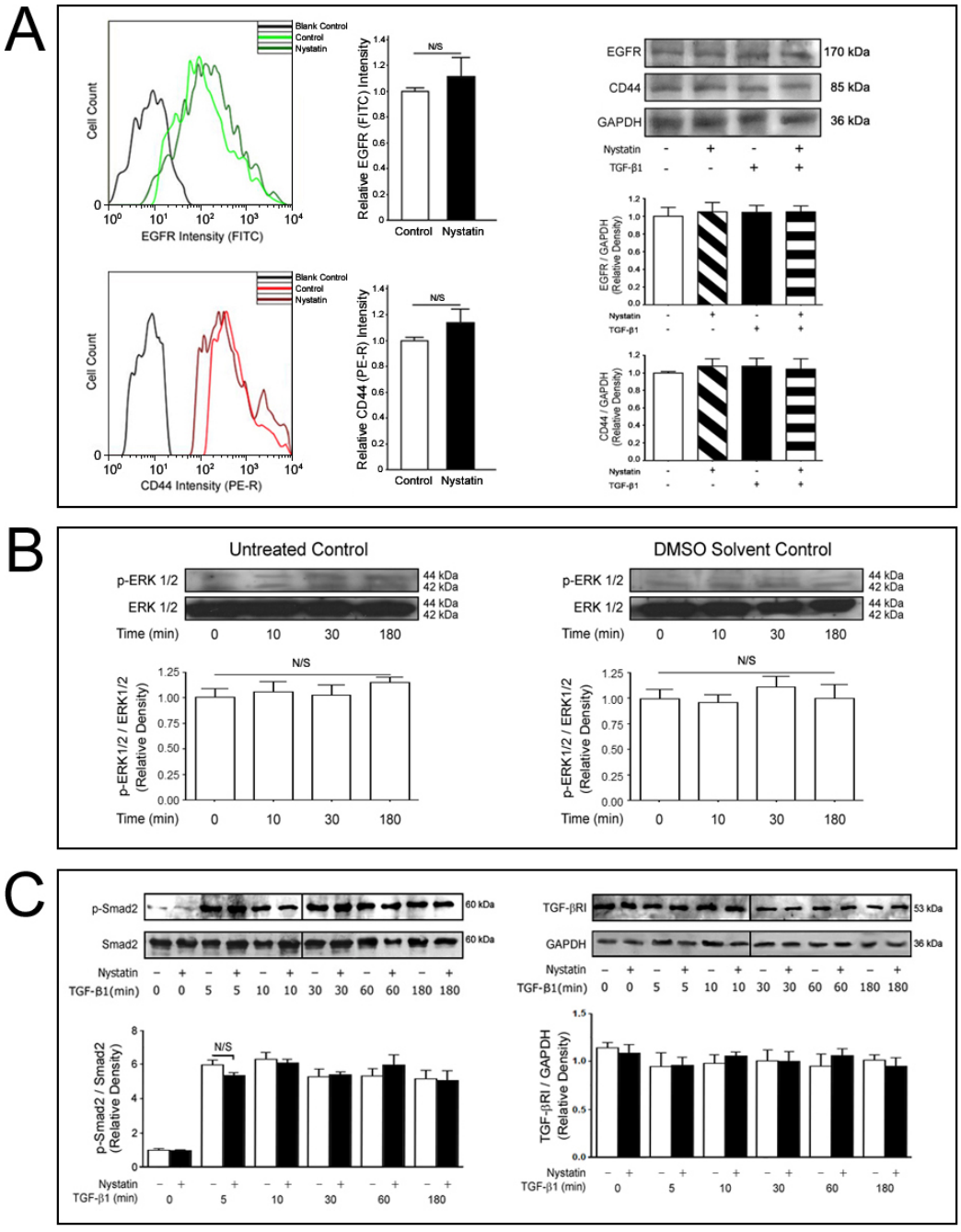

Supplementary Figure 3.S. A. Cell surface and total protein expression of EGFR and CD44 in 50µg/mL nystatin and 10ng/mL TGF-β1 treated fibroblasts. **B.** Untreated and 0.06%(v/v) DMSO solvent time-course controls for pERK1/2 / ERK1/2 signalling time-courses. **C.** Western blot analysis of p-Smad2/Smad2 and TGF-βRI/GAPDH in cells treated with 50µg/mL nystatin and 10ng/mL TGF-β1 time-courses. *N/S* = no significance.